



Ministry of National Education and Scientific Research
National Authority for Scientific Research and Innovation

NATIONAL INSTITUTE OF RESEARCH AND
DEVELOPMENT FOR MECHATRONICS AND
MEASUREMENT TECHNIQUE



THE PROFESSIONAL ASSOCIATION OF
THE ROMANIAN PATRONAGE OF PRECISION MECHANICS,
OPTICS AND MECHATRONICS



THE ASSOCIATION OF
PRECISION MECHANICS & OPTICS
OF ROMANIAN

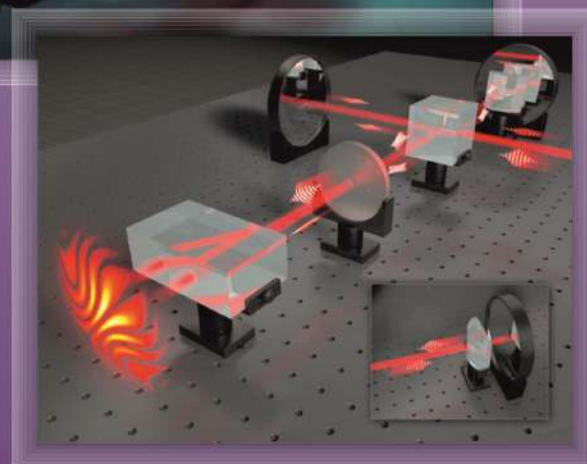
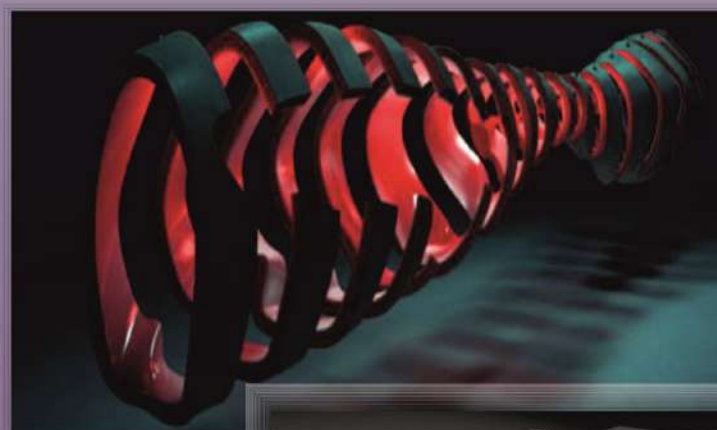


Biannual publication • INCDMTM, AMFOR, APROMECA

ROMANIAN REVIEW PRECISION MECHANICS, OPTICS & MECHATRONICS

THEMATIC:

- ⇒ Mechatronics and micro-nanomechatronics;
- ⇒ Microsystems and micro-nanomechanisms;
- ⇒ Electronics and micro-nanoelectronics;
- ⇒ Optoelectronics and holography;
- ⇒ Precision Micro-nanomechanisms;
- ⇒ Instruments engineering;
- ⇒ Measurement technique;
- ⇒ Sensors and transducers;
- ⇒ Actuators, drives and microdrives;
- ⇒ Computer - aided design;
- ⇒ Dimensional control automats;
- ⇒ Measurement devices and systems;
- ⇒ Environment quality control devices;
- ⇒ Industrial informatics;
- ⇒ Robotics and micro-nanorobotics



THE ROMANIAN REVIEW PRECISION MECHANICS, OPTICS & MECHATRONICS

Published by

The Association of Precision Mechanics & Optics of Romania – AMFOR

and

**National Institute of Research and Development for Mechatronics and Measurement
Technique – INCDMTM – Bucharest**

**The Professional Association of the Romanian Patronage of Precision Mechanics, Optics and
Mechatronics**

The Association of
Precision Mechanics &
Optics of Romania



◆ AMFOR

**National Institute of Research
and Development for
Mechatronics and Measurement
Technique**



◆ INCDMTM



The Professional Association of
the Romanian Patronage of
Precision Mechanics, Optics and
Mechatronics

◆ APROMECA



Pantelimon Road 6-8, sector
2, Bucharest

Pantelimon Road 6-8, sector 2,
Bucharest

Pantelimon Road 6-8, sector 2,
Bucharest

The Association of Precision Mechanics & Optics of Romania – AMFOR – has legal personality and unlimited duration; it has the administrative headquarters at INCDMTM and Consultative headquarters at the University of Polytechnic Bucharest – Chair of Precision Mechanics; aims at development of precision mechanics, technical optics and mechatronics; organizes internal and international session. AMFOR – represents a scientifically offer in contemporary engineering world; offers new solutions for the interpenetrating technique-social: performances of trust and economic cost; encourages development of the professional training for employees and support a highly ethical management.

National Institute of Research and Development for Mechatronics and Measurement Technique – INCDMTM – of Bucharest is a 41 years old company and with tradition concerning the relations with all customers; solves any problem emerged at: the measurement the nicks and quality engineering, the machines of measurement, integrated control, equipment for research and laboratory, precision mechanisms, special cutting tools of high work efficiency, measurement equipment and instruments for heat and pressure, specific stands and equipment, production of small series and unique products of domain, marketing, consulting, engineering, technical assistance, technical and trading services, technological transfer and representation.

The Professional Association of the Romanian Patronage of Precision Mechanics, Optics and Mechatronics – APROMECA - is a private law legal person and actions as a Patronage Professional Association, with a non-governmental status, a un-political, non-profit organization acting in the field of the Precision Mechanics, Optics and Mechatronics fields. Its basic activity profile takes into account: the stimulation and the creation of an environment that is favorable for the research-development-innovation activities as well as to those of production, distribution and use; training, personnel formation; promoting, sustaining and protecting economical, technical and judicial interest of its members.

PUBLISHING HOUSE: INCDMTM – Bucharest Year XXIII No. 49/2016

The editorial staff AMFOR – INCDMTM:

EDITOR IN CHIEF: Gh. Ion Gheorghe
☎ 021.252. 30.68/240; 241; 252.20.96
☎ Fax: 021.252.34.37
E-mail: incdmtm@incdmtm.ro,
Internet: <http://www.incdmtm.ro/publicatii>

EDITORS: Mihai Avram
Constantin Buçsan
Octavian Donțu

COVER GRAPHICS: Tudor Dragomir

MAKE – UP: Ligia Petrescu

*«Edited with support from
Ministry of National Education and Scientific Research -
National Authority for Scientific Research and Innovation »*

*↳ Romanian Review Precision Mechanics, Optics & Mechatronics is included in the
EBSCO, SCOPUS and PROQUEST International Databases.
Each paper published in this scientific journal has a **DOI** assigned*



SUMMARY

Daniel Besnea, Mihaela Constantin, Evelina Donisan, Roxana Mechno, Nicolae Băran	RESEARCHES REGARDING THE MANUFACTURING TECHNOLOGY OF A PROFILED ROTOR USED IN FLUID CIRCULATION	7
Saeed Olyae, Mahmood Seifouri and Ali Nikoosohbat	HEXAGONAL-CIRCULAR AND SQUARE-HEXAGONAL INDEX-GUIDING PHOTONIC CRYSTAL FIBERS	13
Hans Essone Obame, Rochdi El Abdî, Noureddine Benjemâa, Erwann Carvou	PLUG-IN CONNECTORS AGING AND IN SITU DIAGNOSTIC TOOL FOR FORCE MEASUREMENT IMPLEMENTATION	19
Iulian - Sorin Munteanu, Aurel Zapciu, Marian Vocurek	STUDENTS CONTESTS, COMPLEMENTARY ACTIVITY OF UNIVERSITY CURRICULA IN THE MECHATRONICS ENGINEER TRAINING	28
Wang Xin	EFFECT OF JAPANESE SMW ENGINEERING METHOD ON DEEP FOUNDATION PIT OF SUBWAY STATIONS	34
Zhang Wencai	INFLUENCING FACTORS OF FATIGUE BREAK OF ROUND SPRING FOR RAILWAY FREIGHT CAR'S BOGIE	43
Daniela Cioboata, Octavian Dontu, Daniel Besnea, Robert Ciobanu, Aurel Abalaru	INTEGRATED MECHATRONIC SYSTEM FOR BEARING RINGS CONTROL	48
Jipan Yi	RESEARCH AND APPLICATION OF OPTOMETRY RETINOSCOPY TEACHING BASED ON THREE-DIMENSIONAL SIMULATION	58
Paul-Nicolae Ancuta, Iulian Vasile, Anca-Irinel Atanasescu, Sorin Sorea	AUTOMATION OF GEAR PUMPS TESTING USING PROGRAMMABLE LOGIC CONTROLLER	62
Lei Guo, Bo Liang, Lina An	PARAMETRIC MODELING ANALYSIS OF BATTLEDORES MADE OF BRAIDED COMPOSITE MATERIALS BASED ON ANSYS	67
Youyu Hu	DESIGN AND IMPLEMENTATION OF RECRUITMENT MANAGEMENT SYSTEM BASED ON ANALYSIS OF ADVANTAGES AND DISADVANTAGES OF PHP THREE-TIER	74
Hongxia Wei	IMPROVEMENT OF ENGLISH-CHINESE TRANSLATION METHOD BY FEATURE REDUCTION AND RULE OPTIMIZATION BASED ON ROUGH SET THEORY	80
Zhijun Wu	EXPRESSION OF SERIAL ROBOT MANIPULATORS BASED ON SPACE AND STRUCTURE PARAMETERS	85
Yuanming Zhu	LOCALIZATION AND MAPPING OF MOBILE ROBOT BASED ON HUMAN KINEMATICS INFORMATION	94
Guoyang Liu	DEVELOPMENT AND DESIGN OF MANIPULATORS' POSITION MEASUREMENT SYSTEM BASED ON FIELD PROGRAMMABLE GATE ARRAY	102

Gornoava Valentin, Gheorghe I. Gheorghe	THE IMPROVEMENT OF MATERIAL'S SURFACES WITH MICRO AND NANOMETRICS COATED THROUGH INTELLIGENT MECHATRONIC TECHNOLOGIES FOR BIOMEDICAL APLICATIONS	109
Xiaole Wang	STUDY ON THE FLIGHT PATH OF PING-PANG BASED ON THE TECHNOLOGY OF ROBOT PITCHING MACHINE	112
Yanlong Hao	DESIGN AND DEVELOPMENT OF MEASUREMENT SYSTEM OF SPORTS SHOT PERFORMANCE UNDER THE GUIDANCE OF VISION MEASUREMENT TECHNOLOGY	117
Minting Wang	STUDY OF SOCCER ROBOT PATH PLANNING BASED ON SIMULATION ENVIRONMENT	123
Ruicheng Pan	NUMERICAL MODELING ANALYSIS ON AERODYNAMIC PERFORMANCE OF SAILING WINGS FROM CATIA	129
Yarong Zheng	RESEARCH ON THE APPLICATION OF PID CONTROL TECHNOLOGY COMBINED WITH FNN ALGORITHM IN INTELLIGENT WHEELCHAIR OBSTACLE AVOIDANCE FOR DISABLED ATHLETES	134
Xuelin Pang, Zhengze Zhang	STUDY AND ANALYSIS ON STRATEGY OF AI SOCCER MATCH BASED ON IMPROVED MOBILE ROBOT TECHNOLOGY	140
Pan Liu, Ariston Reis, Paulo J.S. Gonçalves	A TOOL TOWARDS EEG SEMI-AUTONOMOUS ELECTRODE PLACEMENT	147
Rodolfo A. A. Farinha, Paulo J.S. Gonçalves	KNOWLEDGE BASED ROBOTIC SYSTEM, TOWARDS ONTOLOGY DRIVEN PICK AND PLACE TASKS	152
Iulian Ilie, Gheorghe Gheorghe	EQUIPMENT FOR AUTOMATIC POSITION DETECTION OF NODAL POINT	158

RESEARCHES REGARDING THE MANUFACTURING TECHNOLOGY OF A PROFILED ROTOR USED IN FLUID CIRCULATION

Lecturer Daniel Besnea, PhD Eng., As. Mihaela Constantin PhD Eng., Evelina Donisan, PhD Student Eng., Roxana Mechno, PhD Student Eng., Prof. Nicolae Băran, PhD Eng.

Affiliation: Politehnica University of Bucharest

Post address: Splaiul Independenței nr. 313, sector 6, Bucharest

E-mail: d_bes@yahoo.com, i.mihaelaconstantin@gmail.com, evelina.donisan@yahoo.com, roxanamechno@yahoo.com, n_baran_fimm@yahoo.com

Abstract - The paper has the following objectives: The rotor constructive solution presentation, that, in conjunction with an adjacent rotor may form a reversible machine; The manufacturing technology development of a rotor in two versions:

I. By processing on C.N.C I;

II. By using quick prototyping (manufacturing technology with material addition).

The end of the paper presents the results obtained in version I and II.

Keywords: Profiled rotors, rotating pistons, 3D printer.

1. Introduction

To achieve results concerning new constructive solutions to any mechanism or machine, it must be designed, developed and built as a model in the laboratory. The theory underlying any machines are the results obtained on the model in the laboratory.

Using the similarity theory of the results obtained in the laboratory, it will be applied to the "natural model", ie the prototype.

The paper presents a rotor model which will be used to create a prototype.

The model constructive solution is original, it can be applied in the field of rotating machines in the following two model versions I and II:

If note: p_a - aspiration fluid pressure; p_r - discharge fluid pressure, then, two versions follows [2]:

Version I: $p_a > p_r$, as force machine:

- Steam engine;
- Pneumatic engine or hydrostatic motor.

Version II: $p_a < p_r$, as working machine:

- Pump;
- Fan;
- Low pressure compressor.

The concept of the reversible machine refers to the fact that the same construction can be used as:

- Pump (hydrostatic motor)
- Compressor (steam engine)

There are several possibilities to build the rotor model:

- By machining
- By working on a numerical control center (C.N.C.)
- Using quick prototyping

2. The rotor framing in a fluid circulation system

The papers [2] [3] presented a mathematical model for calculating the rotor contour, ie specifying the coordinates (x_i , y_i) in xOy orthogonal system of the rotor profile contour.

If now, the two rotors are assembled in a case, a fluid circulation system (fig. 1) or a metering fluid volume system results.

The fluid is transported to the discharge and after a 90° rotation of both rotors, the situation in Figure 1. b and thereafter in Figure 1. c is reached.

After a 180° rotation the fluid contained in the useful volume V_u (Fig. 1. b.), ie in the space between the pistons 3' and 4', will be transported to discharge.

The two rotors are identical, tangent and rotates in reverse.

Each rotor is symmetrical to Ox and Oy axis.

In order that the rotating pistons (1) and (2) of the upper rotor (5) to enter into the cavities (1') and (2') of the lower rotor (6), a cylindrical gear was performed outside the machine comprising two gear wheels with the same division diameter.

This cylindrical gear ensures a synchronous rotation of the two rotors.

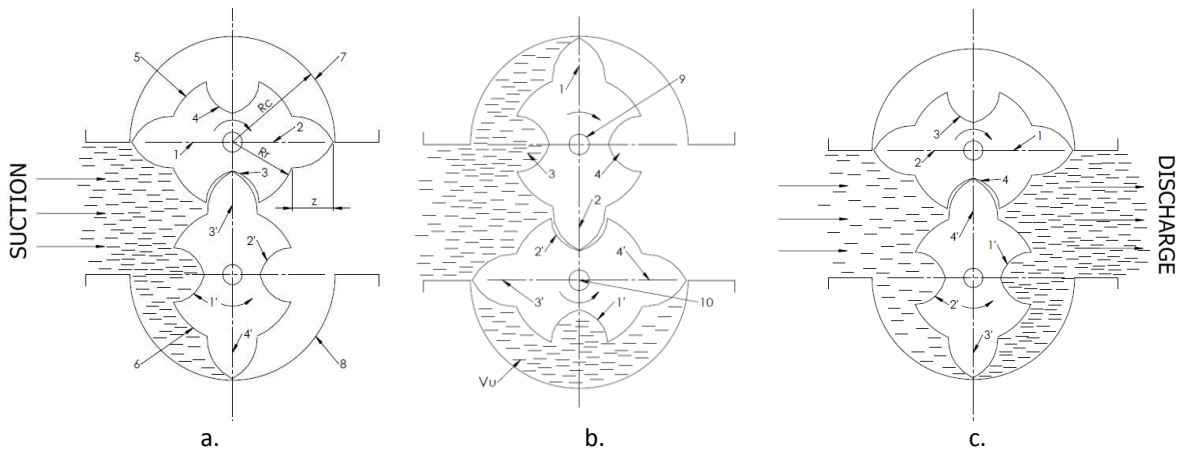


Figure 1. The operating principle of the volumetric meter

1, 2, 3', 4'- rotating pistons; 1', 2', 3, 4- cavities in which the rotating pistons enters; 5-upper rotor; 6-lower rotor; 7- upper case; 8- lower case; 9-upper shaft; 10-lower shaft

2. The manufacturing technology of the profiled rotor

In this situation two constructive solution are distinguished:

- 2.1. The rotor construction using a C.N.C.
- 2.2. The rotor construction with a manufacturing technology with material addition.

Further, the two versions will be analyzed:

2.1. The rotor construction using a C.N.C.

CAD designing and execution CAM for numerically controlled machines having 3 to 5-axis was performed using the CATIA V5 software package which features a powerful post –processing engine that allows the coverage of the entire manufacturing process, from the machining tool trajectory generation up to NC Code software generation [4] [5]. Based on the coordinates, using the Sketcher mode in the Profile toolbar Point by Using Coordinates is selected and the points are inserted into sketch by entering the Cartesian coordinate's Figure 2. The rotor execution precision on C.N.C. is 0.01 mm [6].

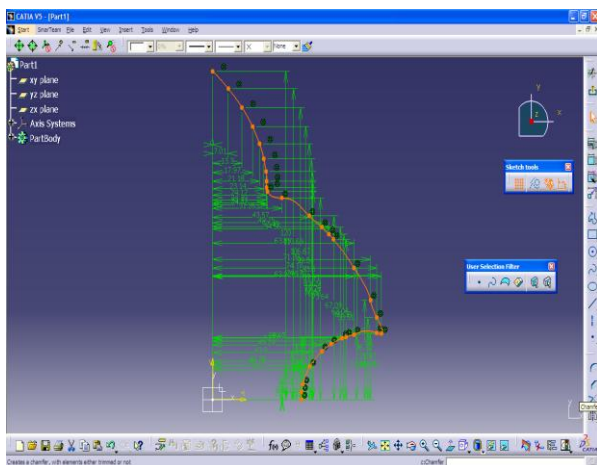


Figure 2. The profile defining through Cartesian coordinates and the Spline application use

The defined points are merged with the Spline toolkit and by Transformation tool using the Symmetry controls the full rotor profile is defined (Figure 3).

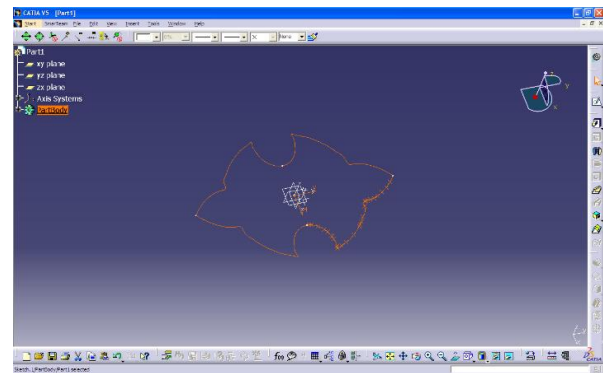


Figure 3. The rotor profile defining

The extrusion on the Z axis can be achieved using a drawn profile (Sketcher) in closed contour and by activating the Pad Definition command enables the extrusion on a normal direction to the drawing plan or, by activating the Mirrored extend option, the extrusion can be done in both senses of the normal, figure 4.

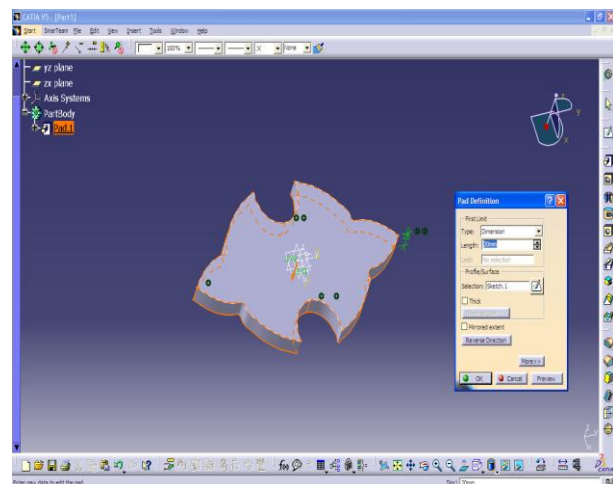


Figure 4. The rotor three dimensional model created with the Pad option

After defining the rotor geometry, the working area opens for the NC manufacturing process in a document CAT Product that will determine the initialization of a new executions within the manufacturing process and the addition of a new entity to the Operation Part structure (Figure 4).

The access to the operation parameters can be done through the Part Operation dialog box where the machine tool type can be choose (Machine - editor) and

where the specific parameters of the processing machine can be defined (numerical command parameters, the rotation parameters, the changing tool parameters, etc.) [7] [8].

The Axis Machine icon activates to assign a reference axis to the processing system in operation, the Product icon is presses to associate an existing product to a certain operations [9] (Figure 5):

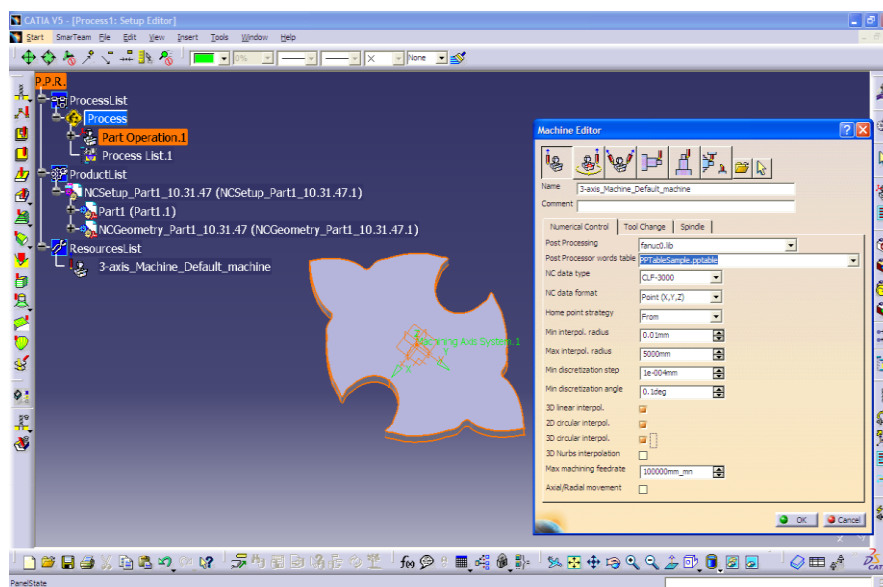


Figure 5. Selecting the processing machine depending on the axes number

The Manufacturing Program mode allows the distinct and different technological operations defining on surfaces categories and according to the processing type, roughing respectively finishing.

Depending on the rotor geometrical particularities the ZLevel option is choose (processing a vertical surface) with an end mills (Figure 6).

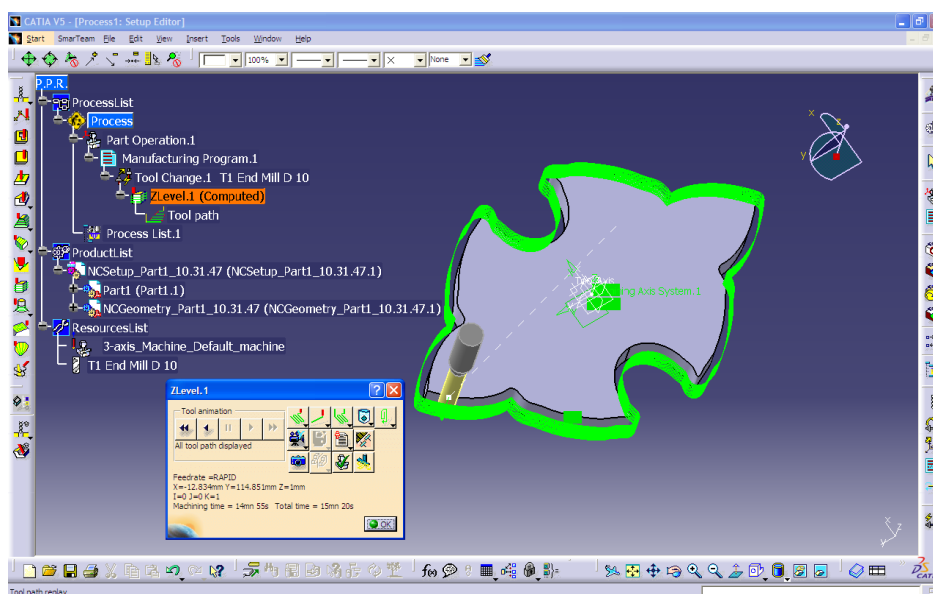


Figure 6. Milling operation simulation using the Video Mode

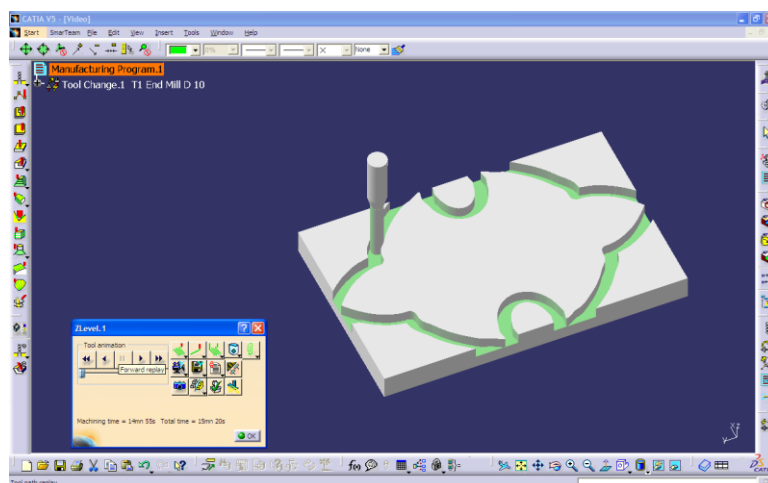


Figure 7. The machining tool trajectories in Photo Mode

The code language software generation, the machine is achieved by activating the Generate NC Code icon opening the active window in Figure 7 and, on the page IN / Out The Document CAT Process is selected; the file path that will be generated is specified, Output File,

in the NC date Type menu, the NC Code is selected (Figure 8), and in the NC Code page the appropriate postprocessor type corresponding to the numerical control machining center (Fanuc 0) is selected.

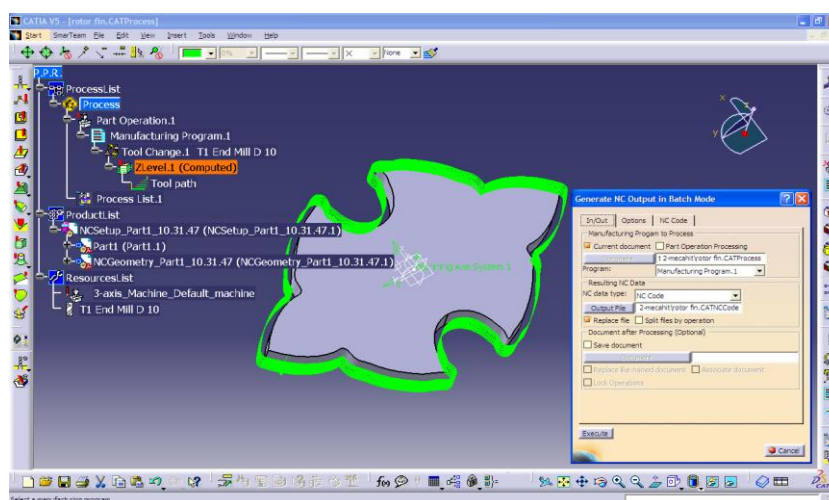


Figure 8. The NC Code software generation

The rotors were constructed of duralumin, on C.N.C. Figure 9, 10.



Figure 9. Plan view of a profiled rotor



Figure 10. . Plan view of the two profiled rotors

From Figure 10 one observes that the seal between the two rotors is provided by:

- A contact between the lower rotor piston top and the upper rotor cavity;
- Two contacts between the curved sides of the lower rotor piston and the upper rotor cavity.

2.2. The rotor construction with a manufacturing technology with material addition

Rapid Prototyping technology (Rapid Prototyping - R. P.) is used for prototypes achievement or a reduced number of parts, their architecture is given as CAD (Computer Aided Design). The first rapid prototyping machines development was due to Charles W. Hull, who made the first machine SLA (Stereo Litographic Apparatus).

Rapid prototyping stages, in order to achieve a rotor prototype are [10]:

- Step 0: Creating a CAD file;
- Step 1: Creating STL file (Standard Triangulation Language To Layer);
- Step 2: STL files processing;
- Step 3: Building the prototype layer by layer;
- Step 4: Post processing operations

Rapid prototyping process for manufacturing the profiled rotor, essentially, consist of the following:

The thermoplastic material (PLA), in filament form, \varnothing 1.75 mm, is heated to a temperature of 215°C and it is deposited on the work surface using an extrusion head which has at the top, a dose with \varnothing 0.2 mm.

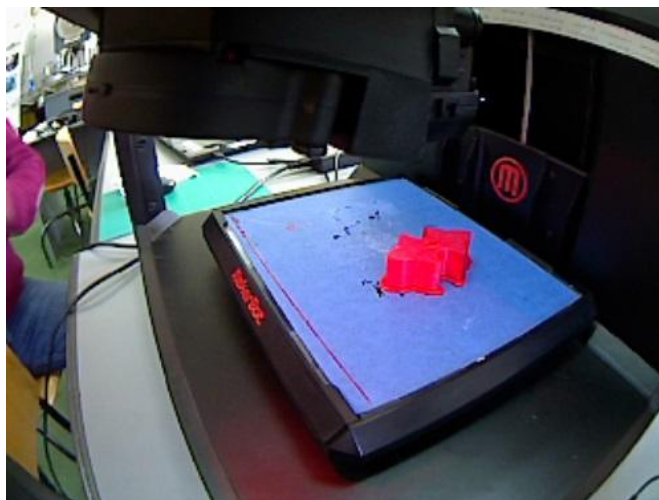


Figure 11. The rotor of the Maker Bot Replicator machine platform

The dose is able to perform movements on all three axes, above the rotor fixed on the machine platform (Figure 11).

Unlike the conventional manufacturing processes, the R.P. processes is based on building prototypes by adding material; a prototype can be considered as consisting of a sequence of layers of very small thickness.

The prototype is built layer by layer; the material is deposited on the previous layer at the calculated level position, by the computer.

The construction of each layer, first, begins through submitting thermoplastic material on the rotor contour.

Figure 12 shows the two rotors constructed of plastics materials.

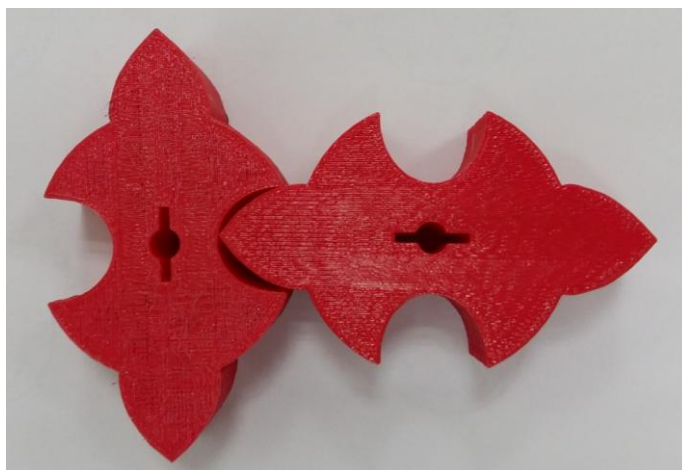


Figure 12. Rotors built with the R.P. technology

3. Conclusions

- For the rotor manufacturing, a computing program specifying the coordinates (xi, yi) of the rotor profile contour must be achieved; subsequently, this program is used to achievement of the profiled rotor.
- The rotor can be easily constructed because the execution technology of the rotor and the case is based on a numerical command program and their execution is performed using a C.N.C. or rapid prototyping.
- The C.N.C. accuracy ensure a satisfactory sealing between the two rotors and between the rotors and the case.
- The execution accuracy of the rotors is:
 - I. By processing on C.N.C.: - 0.01 mm;
 - II. By using Rapid prototyping: 0.1 mm.Obviously, the first method is more advantageous.
- In operation, at the speed of 300 rpm and assuming that warm fluids circulates, version I is preferred, within which the rotors are built of duralumin, not plastics.

4. References

- [1] A. Motorga, „Influența parametrilor constructive și funcționali asupra performanțelor mașinilor rotative cu rotoare profilate”, Teză de doctorat, Facultatea Inginerie Mecanică și Mecatronică, Universitatea, POLITEHNICA din București, București, 2011.
- [2] A. Detzortzis, „Influența arhitecturii rotoarelor asupra performanțelor compresoarelor volumice rotative cu rotoare profilate” Teză de doctorat, Teză de doctorat, Facultatea Inginerie Mecanică și Mecatronică, Universitatea POLITEHNICA din București, București, 2014.
- [3] N. Băran, D. Besnea, A. Motorga, „Elements of computing the architecture and manufacturing technology for a new type of profiled rotor”, PROCEEDINGS International Conference, 6th Workshop on European Scientific and Industrial Collaboration on promoting Advanced Technologies in Manufacturing, WESIC'08 Bucharest 25-26, 2008, pp. 233-241.
- [4] N. Băran, O. Donțu, D. Besnea, A. Costache, „Constructive elements and technological procedures used in the construction of a new type of rotating compressor”, Romanian Review Precision Mechanics, Optics & Mechatronics, nr. 2/2004, București, pp. 261-268.
- [5] D. Besnea, N. Băran, A. Costache, „Manufacturing Technology for a New Type of Profiled Rotor Used in the Construction of Rotating Machines”, Proceedings of the 2nd International Conference on Innovations, Recent Trends and Challenges in Mechatronics, Mechanical Engineering and New High-Tech Products Development MECAHITECH 10, ISSN 2068-648x, Bucharest, 23-24 September 2010, pp. 18-27.
- [6] V. Tcacenco, Centre de prelucrare cu ax vertical „Alzmetall” Rev. Tehnică și Tehnologie nr. 4, 2005, pp. 16-17.
- [7] A. Zaid, N. Băran, D. Duminiță, „Research Regarding the construction of a new type of profiled rotor” Romanian Review Precision Mechanics, Optics & Mechatronics”, Nr.30, 2006, București, pp.721-724.
- [8] N. Băran, D. Besnea, A. Detzortzis, A. Bărăscu, „Manufacturing technology of a new type of profiled rotor used by a rotating volumetric pump”, Proceedings in Manufacturing Systems, Vol. 7, Iss.2, 2012, pp. 105-110.
- [9] N. Băran, D. Besnea, A. Detzortzis, C. Cărnaru, „Manufacturing Technology for a new type of a new type of Profiled Rotor”, Trans Tech Publications, Switzerland, Advanced Materials Research, Vols. 655-657, 2013, pp. 235-240.
- [10] P. Bercea și col., „Tehnologii de fabricație prin adăugare de material și aplicațiile lor”, Editura Academiei Române, București, 2015.

HEXAGONAL-CIRCULAR AND SQUARE-HEXAGONAL INDEX-GUIDING PHOTONIC CRYSTAL FIBERS

Saeed Olyaei, Mahmood Seifouri and Ali Nikoosohbat

Nano-photonics and Optoelectronics Research Laboratory (NORLab), Faculty of Electrical Engineering, Shahid Rajaei Teacher Training University (SRTTU), 16788-15811, Tehran, Iran.

Email: s_olyaei@srttu.edu

Abstract - Optical fibers are widely used in optical communication systems as waveguides with low confinement loss, low chromatic dispersion, and low nonlinear effects. Besides conventional optical fibers, photonic crystal fibers can be also used in transmission media for optical communication systems. In this paper, we present two new designs of index-guiding photonic crystal fiber (IGPCF) with characteristics appropriate for optical communications. In the first proposed design with a hexagonal-circular structure (HC-IGPCF), the chromatic dispersion and the confinement loss at the wavelength of 1550 nm are 0.4 ps/(nm.km) and 1.2×10^{-10} dB/cm, respectively. In the second design with a square-hexagonal structure (SH-IGPCF) having air holes with unequal diameters, nearly zero dispersion at the wavelength range of 1540 to 1550 nm is achieved. For the latter design, at the wavelength of 1550 nm, the chromatic dispersion slope is -0.05 ps/(km.nm), the confinement loss is less than 10-12 dB/cm and the nonlinear coefficient reaches 8.380 w-1.km-1.

Keywords: Optical communication systems; index-guiding; chromatic dispersion; confinement loss; photonic crystal fiber; nonlinear coefficient.

1. Introduction

Over the last decade, photonic crystal fibers (PCFs) [1, 2] which enjoy some excellent properties like low chromatic dispersion, low confinement loss, reasonable effective mode area, and low nonlinear effects, have attracted much attention amongst various research groups. Nanostructured PCFs with large effective mode area can strongly confine light in their hollow cores, while PCFs with nearly zero and flat dispersion over a wide range of wavelengths are suitable media for applications in wavelength-division-multiplexing (WDM) systems. It is imperative to maintain a uniform response at different wavelength channels. This requires for transmission to occur within both very low chromatic dispersion and confinement loss regions. Consequently, PCFs perform very well in both telecom and non-telecom applications. As chromatic dispersion plays an important role in optical communications, therefore, it becomes very important to study the chromatic dispersion properties of PCFs. Also the control of chromatic dispersion in PCFs is a crucial issue for other practical applications in dispersion compensation and nonlinear optics [3-6].

Usually, PCFs are constructed from silica glass which contains very tiny air holes. The air holes running through the length of the structure act as the cladding of the fiber and a defect at the center (done by removing the hole at the center of the structure) acts as the core [7]. Since the average refractive index of the area surrounding core is lower than that of the core in the index-guiding photonic crystal fiber (IGPCF), the

transmission in this type of PCFs is due to the total internal reflection (TIR).

Up until now, several designs for PCFs have been proposed to achieve a very low chromatic dispersion and low confinement loss. For example, various designs such as different core geometries and multiple air-hole diameters in different rings have been studied to achieve both ultra-flattened chromatic dispersion and ultra-low confinement loss over a wide wavelength range [8-14]. However, the fabrication technology of realizing such complicated structures of PCFs remains truly challenging. To achieve similar performance, filling the air holes with liquid crystals, polymers, water, and ethanol can be utilized [15-21]. Tunable photonic bandgap (PBG) effect and long-period fiber grating have been successfully realized with liquid-filled PCFs [22].

As mentioned above, optical parameters such as chromatic dispersion, confinement loss and nonlinear effects are highly important in PCFs designing. However by tuning physical parameters including the diameter of the air holes, the shape of the holes, the defect at the center of the fiber or surrounding the core, the number of hole rings in the area surrounding the core, and the spacing between the adjacent air holes, one could design PCFs with desired properties [23].

In this paper, we design and simulate two IGPCFs with improved optical parameters. In the first proposed design with a hexagonal-circular structure, the chromatic dispersion at the wavelength of 1550 nm is less than 0.4 ps/(nm.km). In the second design with a square-hexagonal structure having air holes with

unequal diameters, zero dispersion, low nonlinearity, and very low confinement loss are obtained.

2. PCF characteristics

PCFs have some important optical characteristics and each of which is crucial for high-speed optical communications. These important characteristics are chromatic dispersion, confinement loss, mode effect area, and nonlinear effects.

An important parameter for designing PCFs is the total dispersion. The chromatic dispersion, $D(\lambda)$, is the sum of the material dispersion and the waveguide dispersion. Unlike conventional fibers, in PCFs both of material dispersion and confinement loss are controllable via suitable design of the cladding, core, and their air-holes. The chromatic dispersion of PCF is computed from the real part of the effective mode index, n_{eff} , by using the following equation [24]:

$$D(\lambda) = -\frac{\lambda}{c} \frac{d^2 \text{Re}[n_{eff}]}{d\lambda^2} \quad (1)$$

where, λ is the operating wavelength in μm , c is the velocity of light in free space, and $\text{Re}[n_{eff}]$ is the real part of the effective refractive index. Therefore, the unit of chromatic dispersion is $\text{ps}/(\text{nm}\cdot\text{km})$. For a given wavelength, the effective mode index of a guided mode is obtained by solving the Maxwell's equations [25] using the FDTD method as explained in Eq. (2):

$$n_{eff} = \frac{\beta}{k_0} \quad (2)$$

where, β and k_0 are the propagation constant and the free space wave number, respectively.

The confinement loss, L_c , is the light confinement ability within the core region. Increasing the number of air hole rings can strengthen the confinement of light in the core region. This in turn results in smaller losses than those with less air hole rings. The confinement loss is calculated as [23-27]:

$$L_c = \frac{(20 \times 10^6)}{(\ln 10)} k_0 \text{Im}[n_{eff}] \quad (3)$$

where, $\text{Im}[n_{eff}]$ is the imaginary part of the n_{eff} and the unit of L_c is dB/m .

Another important parameter is mode effective area, A_{eff} , which in units of mm^2 is given by:

$$A_{eff} = \frac{(\iint |E|^2 dx dy)^2}{(\iint |E|^4 dx dy)} \quad (4)$$

Here, E is the electric field distribution which is derived from the eigenvalue problem drawn from the Maxwell's equations [28]. By changing the geometric characteristics of the fiber cross-section, such as using large effective area, it is possible to obtain PCFs with various properties [29].

If one chooses the air hole diameter and lattice constant properly, the confinement loss in highly nonlinear PCFs can be lower than that in PCFs with low nonlinearity. However, such PCFs are not used in long-haul communications. Therefore, the nonlinearity in PCFs must be minimized. Large mode area of PCFs can prevent unwanted nonlinear impairments [30]. On the other hand, low confinement loss or small effective mode area is required for some special applications including the nonlinear based phenomena. The nonlinear effects can be written as [31]:

$$\gamma = \left(\frac{2\pi n_2}{\lambda A_{eff}} \right) \times 10^3 \text{ w}^{-1} \cdot \text{km}^{-1} \quad (5)$$

where, γ and n_2 are the nonlinear coefficient and nonlinear refractive index of PCFs, respectively [31].

3. Design and simulation results

3.1 The HC-IGPCF design

In this paper, to analyze the proposed PCFs, finite-difference time-domain (FDTD) method with the perfectly matched layers boundary conditions is used. The first proposed IGPCF is made up of pure silica with a refractive index of 1.45. It has a triangular array of air holes formed along its length. This PCF consists of 6 air hole rings with two different structures. The inner structure is circular lattice with 3 rings of air holes and the outer structure is hexagonal lattice also with 3 rings of air holes. The diameter of the holes and the pitch of the lattice, Λ_1 (the spacing between the centers of two adjacent holes), in the three inner rings with circular structure PCF are respectively chosen to be $d_1=900$ nm and 2200 nm. The diameter of the holes and the pitch of the lattice, Λ_2 , in the three outer rings with hexagonal structure are respectively considered as $d_2=1750$ nm and 2000 nm. We have two structures in this PCF with unequal diameters and lattice constant in order to enable us to control both the chromatic dispersion and confinement loss. The transverse cross-section of the PCF is demonstrated in Fig. 1.

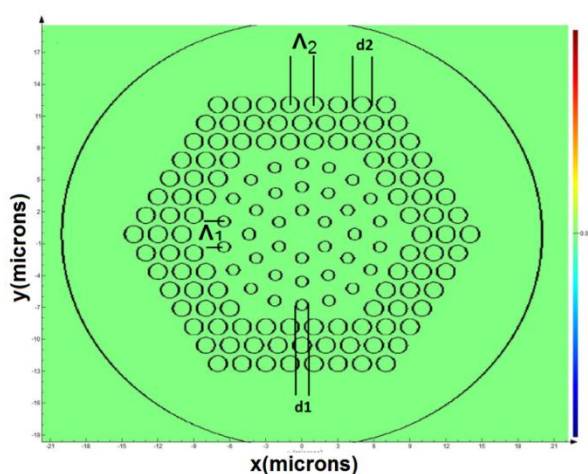


Fig. 1. The cross section of the HC-IGPCF with $d_1=900$ nm, $\Lambda_1=2200$ nm, $d_2=1750$ nm, and $\Lambda_2=2000$ nm.

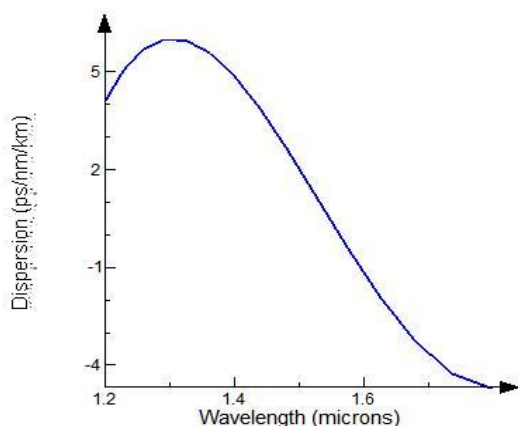


Fig. 2. The chromatic dispersion curve of the HC-IGPCF as a function of wavelength.

For the HC-IGPCF design, the pitch and the diameter of holes in the three inner rings and the three outer rings are not chosen to be constant. Therefore, the chromatic dispersion, confinement loss, and the nonlinearity can be changed by either increasing or decreasing the d_1/Λ_1 and d_2/Λ_2 .

The chromatic dispersion curve of HC-IGPCF design is illustrated in Fig. 2. The measured values of the chromatic dispersion over the wavelength range 1200-1800 nm are acceptable. The chromatic dispersion of the first proposed IGPCF is 0.4 ps/(nm.km), at the wavelength of 1550 nm. The minimum chromatic dispersion which is zero is related to the wavelength of 1580 nm. In the other ranges of wavelengths, the IGPCF has a less positive dispersion and in longer wavelengths, the positive dispersion decreases and reaches some negative values. The best results are achieved with $\Lambda_1=2200$ nm and $\Lambda_2=2000$ nm.

The loss characteristic of the proposed IGPCF within the wavelength range of 1200-1550 nm is plotted in Fig. 3. The PCF shows the losses of $0.01 \times 10^{-10} \sim 1.2 \times 10^{-10}$ dB/cm in the wavelength range of 1200-1550 nm and the loss of the PCF is 1.2×10^{-10} dB/cm at the wavelength of 1550 nm.

Fig. 4 illustrates the variation of the n_{eff} with respect to the wavelength in the first proposed IGPCF. As shown in Fig. 4, the effective index decreases with increasing wavelength. In the suggested design, a strong confinement of light is obtained in the core. The mode field is mainly distributed and guided in the silica core region. The light is well trapped at the center of the structure and the mode effective area of $26.52 \mu\text{m}^2$ is achieved at 1550 nm. In order to visualize and confirm our results, we then calculated the nonlinear coefficient of HC-IGPCF design which is a relatively low value of $4.580 \text{ w}^{-1} \cdot \text{km}^{-1}$, as shown in Fig. 5.

The effective mode area of about $26.52 \mu\text{m}^2$ is calculated at 1550 nm wavelength. Because of the obtained mode field distribution, the maximum optical power is at the center of the HC-IGPCF core. In addition, a PCF with small effective mode area is useful for nonlinear optical applications. It is appropriate to couple the proposed PCF to an index-guiding fiber.

This structure due to its symmetry is simple and also easy to fabricate.

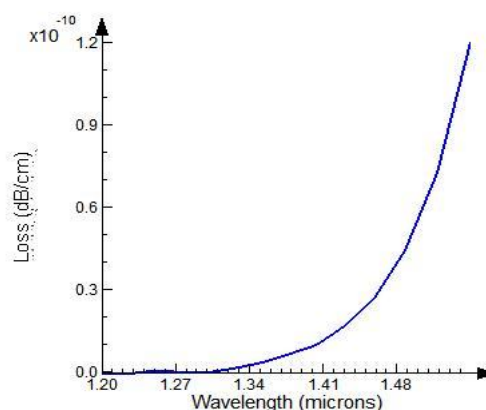


Fig. 3. The confinement loss curve of the HC-IGPCF as a function of wavelength.

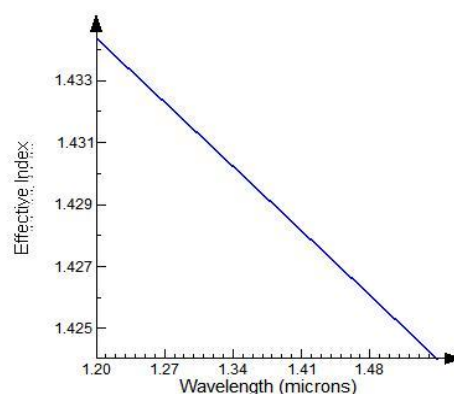


Fig. 4. The effective index curve of the HC-IGPCF as a function of wavelength.

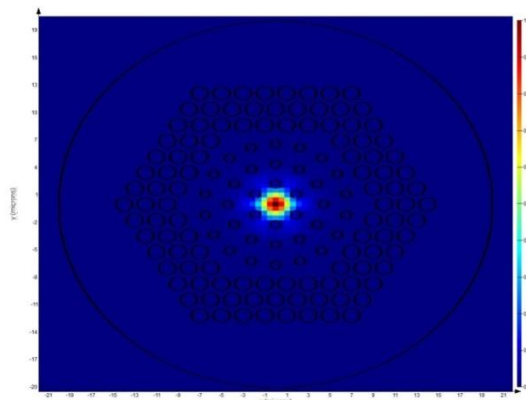


Fig. 5. The field distribution of the first-order mode for the HC-IGPCF at $\lambda=1.55 \mu\text{m}$.

3.2 The SH-IGPCF design

In IGPCF with square-hexagonal structure, the holes that are closer to the core have stronger impacts on dispersion, although their effects on confinement loss are quite negligible. To improve the characteristics of our first SH-IGPCF structure, we designed our second IGPCF as shown in Fig. 6. The air hole diameter-to-pitch ratio, (d/Λ), plays a critical role in the design of

IGPCF. By decreasing the d/Λ value in the cladding, the chromatic dispersion reduces. But on the other hand, increasing the d/Λ reduces the confinement loss.

To better control the chromatic dispersion, the confinement loss, and nonlinearity, unequal d/Λ for air holes structures can be selected. Hence, larger d_2/Λ_2 for holes in the outer rings is necessary. In order to have both low dispersion and low confinement loss, the d_2/Λ_2 of the outer rings is made bigger. Therefore, the d_1/Λ_1 of the holes in the internal rings is selected to be smaller, whereas the d_2/Λ_2 of the holes in the external rings is chosen to be larger, as illustrated in Fig. 6.

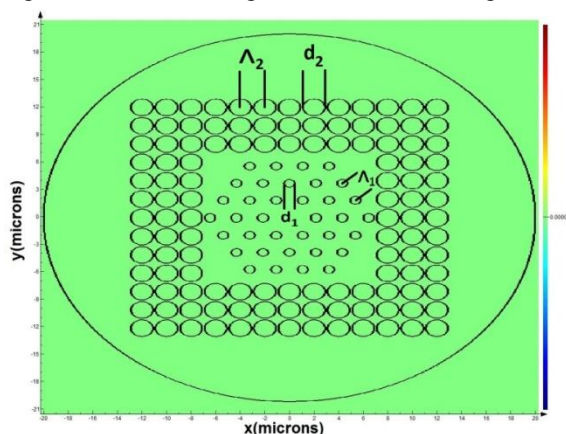


Fig. 6. The cross section of the SH-IGPCF with $d_1=847$ nm, $\Lambda_1=2150$ nm, $d_2=1800$ nm, and $\Lambda_2=2000$ nm.

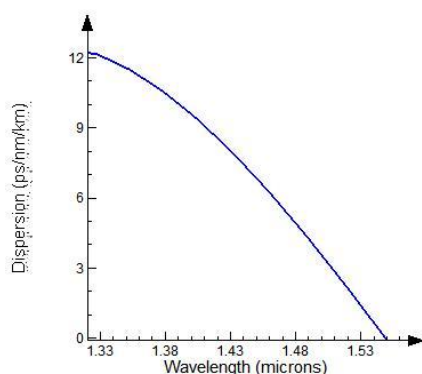


Fig. 7. The chromatic dispersion curve of the SH-IGPCF as a function of wavelength.

In this design, the PCF consists of 6 air hole rings with two different structures. In the inner structure of the proposed PCF which is hexagonal with three air holes rings, the diameters of the holes in the first three inner rings are chosen to be $d_1=847$ nm and the pitch of the holes is $\Lambda_1=2150$ nm. In the outer structure of the PCF that is squared lattice with three air holes rings, the diameters are chosen to be $d_2=1800$ nm and the pitch is selected $\Lambda_2=2000$ nm.

The dispersion curve of the second design is shown in Fig. 7. At the wavelength of 1550 nm, the chromatic dispersion of the structure is -0.05 ps/(nm.km). The zero chromatic dispersion occurs at the wavelength of 1545 nm. The average chromatic dispersion is 5.5 ps/(nm.km) over the wavelength range of 1200-1560 nm, which is fairly low. Below this wavelength range, the structure has even lower positive dispersion and

above that, the negative dispersion increases. The best chromatic dispersion is achieved with $\Lambda_1=2150$ nm and $\Lambda_2=2000$ nm.

The loss characteristic of the second proposed PCF within the wavelength range of 1200-1560 nm is plotted in Fig. 8. As it can be seen from the figure, an ultra-low loss is achieved at the wavelength of 1550 nm. Moreover, the PCF shows the losses of $0.2 \times 10^{-13} \sim 2.2 \times 10^{-13}$ dB/cm over the wavelength range of 1460-1560 nm and less than 10^{-12} dB/cm over the other wavelengths.

Fig. 9 illustrates the variation of the n_{eff} with respect to the wavelength in the SH-IGPCF. The effective index decreases at a smaller rate with increasing wavelength. In the SH-IGPCF design, a strong confinement of light in the core of the IG-PCF is obtained. The mode field is mainly distributed and guided in the silica core region. We have calculated the first-order mode for the SH-IGPCF at $\lambda = 1550$ nm. The light is well trapped at the center of the structure and the mode effective area of $14.51 \mu\text{m}^2$ is achieved, as shown in Fig. 10.

In this proposed structure, with such a large mode area, the unwanted nonlinear impairments are prevented and hence the nonlinear effects are decreased. We have calculated the nonlinear coefficient for the SH-IGPCF as small as $8.380 \text{ w}^{-1} \cdot \text{km}^{-1}$. Table 1 compares our proposed PCFs with other PCFs in the literature at the wavelength of 1550 nm.

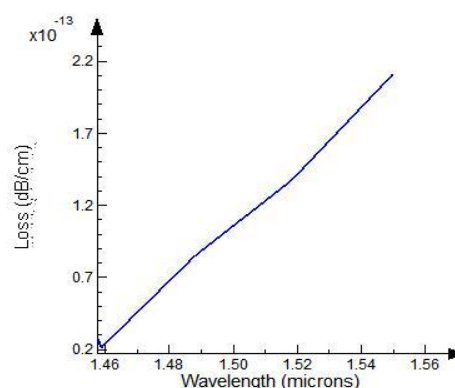


Fig. 8. The confinement loss curve of the SH-IGPCF with respect to the wavelength.

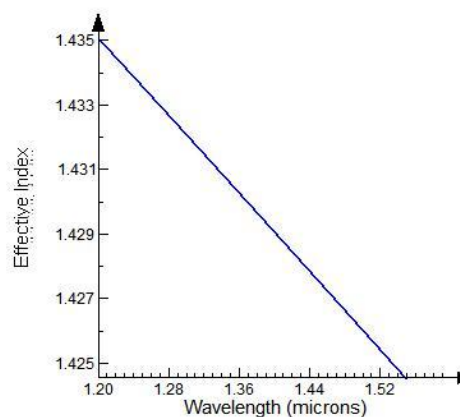


Fig. 9. The effective index curve of the SH-IGPCF with respect to the wavelength.

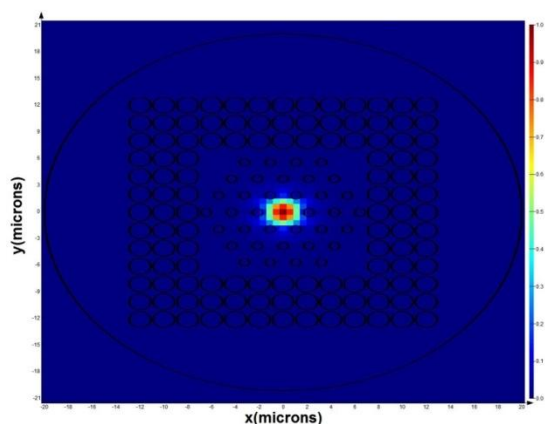


Fig. 10. The field distribution of the first-order mode for the SH-IGPCF at $\lambda=1.55\mu\text{m}$.

4. Conclusions

In this paper, two new index-guiding photonic crystal fibers based on pure silica have been designed and simulated. According to the results, lower values for chromatic dispersion, nonlinear effects, and confinement loss can be acquired by reducing the size of the holes (d/Λ) in the inner rings and increasing the d/Λ of the holes in the outer rings. These PCFs have two different structures of air holes array having unequal d/Λ . In these IGPCFs, the results show that both ultra-low negative dispersion and nearly zero dispersion can be obtained. The main advantages of these PCFs are zero chromatic dispersion, very low confinement loss, and low nonlinear effects.

Table 1. Comparison results amongst the presented PCFs and other PCFs in the literature at the wavelength of $1.55\mu\text{m}$.

	Dispersion (ps/nm.km)	Loss (dB/cm)	Effect mode area (μm^2)	Nonlinearity ($\text{w}^{-1}.\text{km}^{-1}$)
Primary design (HC-IGPCF)	0.4	1.2×10^{-10}	26.52	4.58
Secondary design (SH-IGPCF)	-0.05	2.1×10^{-13}	14.51	8.38
Ref. [20]	-195	0.3×10^{-5}	-	-
Ref. [24]	2.7	0.3×10^{-10}	61.2	-
Ref. [29]	3	10^{-10}	7.7	18
Ref. [30] PCF ₁	0.002	10^{-11}	-	-
Ref. [30] PCF ₂	8.2	2×10^{-12}	-	-
Ref. [31]	0.24	--	1.764	72.6
Ref. [32]	0.22	10^{-13}	8-15	--
Ref. [33]	0.42	--	5.3	--

5. References

- [1] J. Broeng, D. Mogilevstev, S.E Barkou, A. Bjakle, Photonic crystal fibers: a new class of optical waveguides, *Opt. Fiber Technol.*, Vol. 5 pp. 305–330, 1999.
- [2] G. J. Pearce, J. M. Pottage, D. M. Bird, P. J. Roberts, J. C. Knight, and P. S. Russell, Hollow-core PCF for guidance in the mid to far infra-red, *Opt. Exp.*, Vol. 13, pp. 6937–6946, 2005.
- [3] T. A. Birks, J. C. Knight, and P. St. J. Russell, “Endlessly single-mode photonic crystal fiber,” *Opt. Lett.*, Vol. 22, pp. 961-963, 1997.
- [4] J. C. Knight and P. St. J. Russell, “Applied optics: new ways to guide light,” *Science*, Vol. 296, pp. 276-277, 2002.
- [5] J. Noda, K. Okamoto and Y. Sasaki, “Polarization-Maintaining Fibers and Their Applications,” *J. Lightwave Technol.*, Vol. 4, pp. 1071-1089, 1986.
- [6] P. St. J. Russell, “Photonic-Crystal Fibers,” *J. Lightwave Technol.*, Vol. 24, pp. 4729-4749, 2006.
- [7] N. H. Hai, Y. Namihiray, S. F. Kaijage, T. Kinjo, F. Begum, S. M. A. Razzak and N. Zou, “Multiple defect-core hexagonal photonic crystal fiber with flattened dispersion and polarization-maintaining properties,” *Opt. Review*, Vol. 15, pp. 31-37, 2008.
- [8] K.P. Hansen, Dispersion flattened hybrid-core nonlinear photonic crystal fiber, *Opt. Express*, Vol. 11, pp. 1503-1509, 2003.
- [9] K. Saitoh, N.J. Florous, M. Koshiba, Theoretical realization of holey fiber with flat chromatic dispersion and large mode area: an intriguing defected approach, *Opt. Lett.*, Vol. 31 pp. 26–28, 2006.
- [10] N.J. Florous, K. Saitoh, M. Koshiba, The role of artificial defects for engineering large effective mode area, flat chromatic dispersion and low leakage losses in photonic crystal fibers: towards high speed reconfigurable transmission platforms, *Opt. Express*, Vol. 14, pp. 901–913, 2006.
- [11] K. Saitoh, M. Koshiba, Highly nonlinear dispersion-flattened photonic crystal fibers for supercontinuum generation in a telecommunication window, *Opt. Express*, Vol. 12, pp. 2027–2032, 2004.
- [12] K. Saitoh, M. Koshiba, T. Hasegawa, E. Sasaoka, Chromatic dispersion control in photonic crystal fibers: application to ultra-flattened dispersion, *Opt. Express*, Vol. 11, pp. 843–852, 2003.
- [13] F. Poletti, V. Finazzi, T.M. Monro, N.G.R. Broderick, V. Tse, D.J. Richardson, Inverse design and fabrication tolerances of ultra-flattened

- dispersion holey fibers, *Opt. Express*, Vol. 13, pp. 3728–3736, 2005.
- [14] T.-L. Wu, C.-H. Chao, A novel ultraflattened dispersion photonic crystal fiber, *IEEE Photonics Technol. Lett.*, Vol. 17, pp. 67–69, 2005.
- [15] C. Zhang, G. Kai, Z. Wang, T. Sun, C. Wang, Y. Liu, W. Zhang, J. Liu, S. Yuan, and X. Dong, Transformation of a transmission mechanism by filling the holes of normal silica-guiding microstructure fibers with nematic liquid crystal, *Opt. Lett.*, Vol. 30, pp. 2372–2374, 2005.
- [16] T.T. Alkeskjold, J. Laegsgaard, A. Bjarklev, D.S. Hermann, J. Broeng, J. Li, S.Gauza, S.-T. Wu, Highly tunable large-core single-mode liquid-crystal photonic bandgap fiber, *Appl. Opt.*, Vol. 45, pp. 2261–2264, 2006.
- [17] J. Eggleton, C. Kerbage, P.S. Westbrook, R.S. Windeler, A. Hale, Microstructured optical fiber devices, *Opt. Express*, Vol. 9, pp. 698–713, 2001.
- [18] J. Martelli, K. Canning, N. Lyttikainen, Groothoff, Water-core Fresnel fiber, *Opt. Express*, Vol. 13, pp. 3890–3895, 2005.
- [19] S. Yiou, P. Delaye, A. Rouvie, J. Chinaud, R. Frey, G. Roosen, P. Viale, S. F'evrier, P. Roy, J.-L. Auguste, J.-M. Blondy, Stimulated Raman scattering in an ethanol core microstructured optical fiber, *Opt. Express*, Vol. 13, pp. 4786–4791, 2005.
- [20] S. M. Nejad and N. Ehteshami, “Novel design to compensate dispersion for index-guiding photonic crystal fiber with defected core,” 2nd International Conference on Mechanical and Electronics Engineering, IEEE, Vol. 2, pp. 417-421, 2010.
- [21] S. Olyae and F. Taghipour, “Doped-core octagonal photonic crystal fiber with ultra-flattened nearly zero dispersion and low confinement loss in a wide wavelength range,” *Fiber and Integrated Optics*, Vol. 31, pp. 178-185, 2012.
- [22] C. Yu, J. Liou, Selectively liquid-filled photonic crystal fibers for optical devices, *Opt. Express*, Vol. 17, pp. 8729–8734, 2009.
- [23] S. M. A. Razzak, M. A. G. Khan, Y. Namihira and M. Y. Hussain “Optimum design of a dispersion managed photonic crystal fiber for nonlinear optics applications in telecom systems”. Fifth Int. Conf. Electrical and Computer Engineering ICECE 2008, Bangladesh, pp. 570-573, 2008.
- [24] S. Olyae and F. Taghipour, “Ultra-flattened dispersion hexagonal photonic crystal fiber with low confinement loss and large effective area”, *IET Optoelectronics*, Vol. 6, No. 2, pp. 82-87, 2012.
- [25] S. Olyae, F. Taghipour, and M. Izadpanah, “Nearly zero-dispersion, low confinement loss, and small effective mode area index-guiding PCF at 1550nm wavelength”, *Frontiers of Optoelectronics in China*, Vol. 4, No. 4, PP. 420-425, 2011.
- [26] Naraghi, S. Olyae, A. Najibi, and E. Leitgeb, “Photonic crystal fiber gas sensor for using in optical network protection systems”, 18th European Conference on Network and Optical Communications and 8th Conference on Optical Cabling and Infrastructure, Graz, Austria, 10-12 July 2013.
- [27] S. Olyae and F. Taghipour, “Ultra-flattened dispersion photonic crystal fiber with low confinement loss”, 11th International Conference on Telecommunications, ConTEL, Graz University of Technology, Austria, June 2011, PP. 531-534, 2011.
- [28] W. H. Reeves, J. C. Knight, P. S. J. Russell, and P. J. Roberts, “Demonstration of ultra-flattened dispersion in photonic crystal fibers,” *Opt. Express*, Vol. 10, pp. 609-613, 2002.
- [29] M. Chen, S. Xie, “New nonlinear and dispersion flattened photonic crystal fiber with low confinement loss”, *Opt. Commun.*, Vol. 281, pp. 2073–2076, 2008.
- [30] S. Olyae and F. Taghipour, “Design of new square-lattice photonic crystal fibers for optical communication applications”, *Int. J. Phys. Sci.*, Vol. 6, pp. 4405–4411, 2011.
- [31] Yashar. E. Monfared, A. Mojtahednia, A. R. Malekijavan, A. R. Monajatikashani, “Highly nonlinear enhanced-core photonic crystal fiber with low dispersion for wavelength conversion based on four-wave mixing” *Optoelectron*, Vol. 6(3), pp. 297–30, 2013.
- [32] N. Hoang Hai, N. Hoang Dai, H. Tuan Viet, N. T. Tien, “A Nearly-Zero Ultra-Flattened Dispersion Photonic Crystal Fiber: Application to Broadband Transmission Platforms” *IEEE*, Vol. 6(3), pp. 341–347, 2010.
- [33] P. S. Maji, P. R. Chaudhuri, “Super continuum generation in ultra-flat near zero dispersion PCF with selective liquid infiltration”, *Optik*, Vol. 125, pp. 5986–5992, 2014.
-

PLUG-IN CONNECTORS AGING AND IN SITU DIAGNOSTIC TOOL FOR FORCE MEASUREMENT IMPLEMENTATION

Hans Essone Obame¹, Rochdi El Abdi², Nouredine Benjemâa², Erwann Carvou²

¹Ecole Normale Supérieure, BP:17009, Libreville-Gabon,

²Université de Rennes- Institut de Physique de Rennes- Campus de Beaulieu, 35042 Rennes Cedex France

hans.essone@gmail.com; relabdi@univ-rennes1.fr; benjemaa@univ-rennes1.fr;

erwan.carvou@univ-rennes1.fr

Abstract - This paper concerns the study of plug-in connector used in low level (a few Amperes). In this case, the application fields are instrumentation and control (I&C) installations.

The long service duration of these semi-permanent contacts throughout their lifetime relies on having a stable force. The objective of this study is to know the main mechanical parameters which impact on the connector's lifetime.

The main results are that insertion force and friction coefficient of contact change after thousands of insertion-extraction cycles. To avoid these parameters (insertion force and friction coefficient μ) that change during mating cycle, an innovative diagnostic tool has been investigated, to directly measure, in situ, the contact force of each spring of the connector.

Keywords: Contact force, contact resistance, connector, diagnostic tool, force sensor.

1. Introduction

For most interconnection systems a pin in the male half of the connector will make contact with spring beams inside the female half of the connector. As the pin is inserted, it will slide across and deflect the spring beams, which generate the normal force necessary for good electrical contact.

Reducing insertion force and wear are among the goals of optimization of pin and socket connectors [1-3]. Insertion and extraction force also called mating and unmating force are respectively the necessary force for establishment and cut of electric contact [4 - 6].

Once the beams are fully deflected and are touching only the flat contact area of the pin, the contact force will be perpendicular to the insertion direction. The insertion force then will simply be equal to the normal force multiplied by the coefficient of sliding friction and the number of contact points. However, before this steady state condition is reached, the insertion force shows very complex behavior [7- 9].

If the force required to insert to the connector is easily measured and most manufacturers publish specification limits for their products routinely, the normal force with which the connector contact pushed on male part is more difficult to measure. Normal force measurement of plug in connector contacts is complicated by the enclosing geometry of the connector body. The connector body can be cut in half to provide direct access to the contact springs. Another described technique utilizes a friction probe to obtain an indirect measurement of normal force. Unfortunately, each of these techniques are either destructive or do not measure the whole intact connector system [10]. There is a need

for non-destructive normal force measurement techniques, for quality assessment, for product characterization, and for failure analysis [10].

2. Studied connector's mechanical parameters

The male part of the studied connector consists of a printed circuit board (PCB) of 1.6 mm thickness, made of a fibre material (FR4), and covered by a strip of copper with a second layer of nickel with a thin cobalt-gold layer on top. The female part is composed of spring beams of beryllium- copper (in the shape of a tulip) inside a receptacle that is often located on the backplane of a computer rack [10] (Fig. 1). Regarding the design, a stop was placed to maintain the initial gap at 600 μm and to reduce the insertion peak.

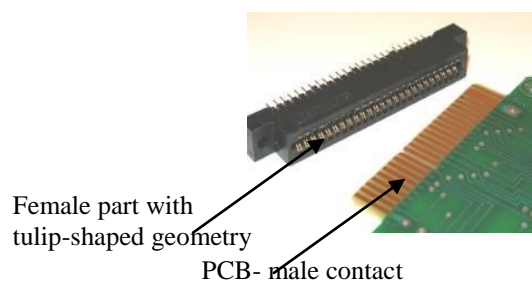


Figure 1: HE9 female part with tulip-shaped geometry and PCB (Printed Circuit Board) contact

Figure 2 illustrates a standard insertion phase of a pair of contact (tulip) of the connector [11]. Insertion of the male contact in the receptacle engenders deflection

of springs that are going to exercise a normal contact force in return on the contact PCB.

The phase 1 (Figure 2 a, and Figure 3, part a.) corresponds to spring flexion: insertion force passes by a maximal value (insertion peak). The maximal value of insertion force will depend at the same time on the geometry of the spring and on chamfer of the PCB and on friction coefficient μ of the contacts [11].

During the phase 2 (Figure 2 b, and Figure 3, part b), the insertion is made in constant deflection (that is the movement obtained in a point of a body under the influence of a force). It depends on friction between both contacts.

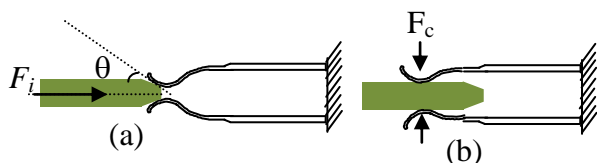


Figure 2: Insertion phase: a) before and b): after complete insertion

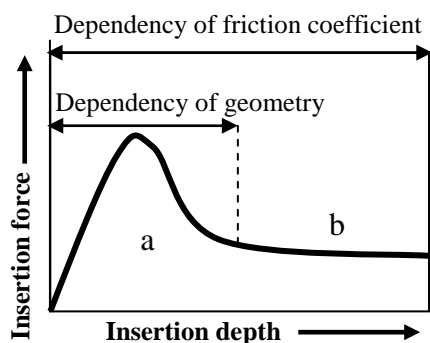


Figure 3: Insertion force versus insertion depth

Insertion force of contact pair during insertion (Fig.2) is written according to simplified equation [2, 3]:

$$F_i = F_c \left(\frac{\sin \theta + \mu \cos \theta}{\cos \theta - \mu \sin \theta} \right) \quad (1)$$

Once the contact is established ($\theta = 0$, Figure 2b):

$$F_i = \mu F_c \quad (2)$$

where F_i is the insertion force, F_c is the contact force, θ is the incidence angle as shown in Figure 2a, μ is the friction coefficient [12].

3. Analysis of state of contact surface by (SEM/EDX) technique

The nature and thickness of contact areas of the two coatings play an important role, especially when called to suffer mechanical or tribological stress, for example during the operations taking place for maintenance [13].

For their characterization, connectors pass in a first time through coatings analysis. Technical EDX (energy-dispersive X-ray spectroscopy) coupled to SEM (scanning electron microscope) is used to determine the nature of the elements in the sample.

A first EDX analysis was conducted on springs as shown on Figure 4 below, to determine the thicknesses of the various coatings. According to the measurements made by a scanning electron microscope, the thickness of gold layer is about $0.5 \mu\text{m}$ and that of the under-layer of nickel is $3 \mu\text{m}$.

For male contact (Fig. 5), present on PCB, the thickness of gold layer is about $3 \mu\text{m}$, that of the sub-layer of nickel is about $10 \mu\text{m}$ and copper is about $55 \mu\text{m}$ thick.

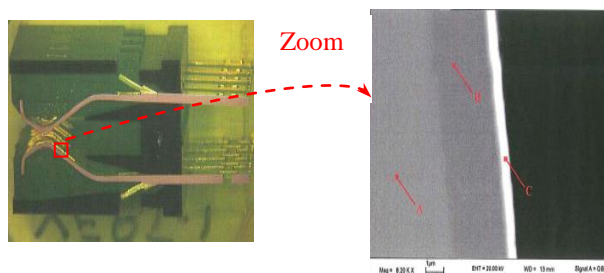


Figure 4: Cut of HE9 connector tulip

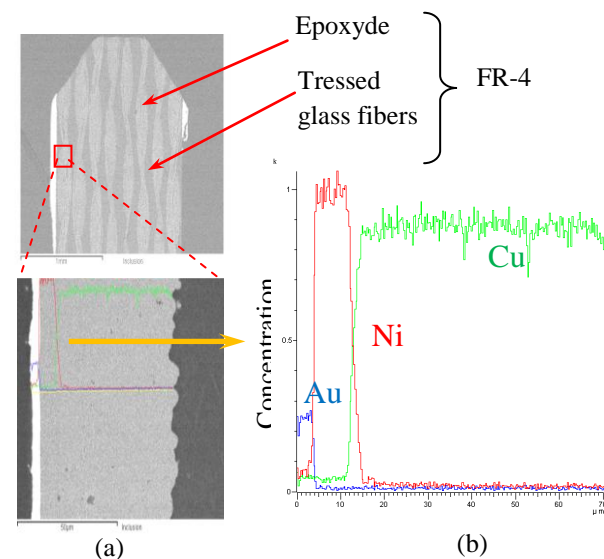


Figure 5: a) Detail of PCB contact materials and b) Profile of existing chemical elements

4. Implementation of insertion bench and insertion force and contact resistance measurement

The experimental bench that allows us to estimate the influential parameters of insertion of plug-in connectors is represented on Figure 6. A track of PCB contact was isolated so as to measure only the force on a "tulip" (Fig. 4). The male and female parts are aligned thanks to micrometric tables. We define x-axis as being

the axis of insertion. This operation is realized by means of the micro-engine (1 μm of precision). The characteristics of the micro-engine were fixed to ensure a constant speed of insertion in the case of insertion-extraction cycles.

A force sensor (0.01 N of precision), positioned on the same axis, allows measurement of force during insertion and extraction. Two displacement sensors (Laser) with a precision of 0.1 μm , aiming deflection measurement (Fig. 6).

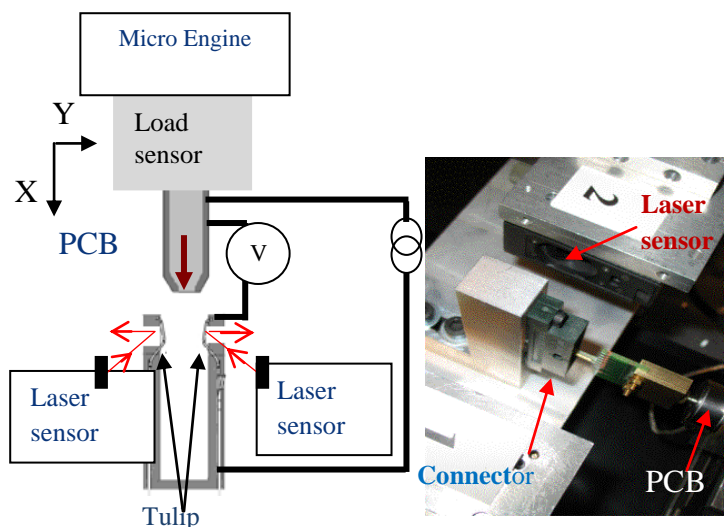


Figure 6: Sliding wear bench and detail of laser sensor

a) Influence of the number of cycle

The graph in Figure 7 shows the evolution of the insertion force on a pair of contacts of a connector, from 1 to 2000 insertions, with one measurement every 50 mating cycles.

Overall, the insertion force increases with the number of insertions and then tends to stabilize. The non-smooth form of the insertion force, as seen in Fig. 3, both on the first and on the second phase when inserting, is mainly due to friction between the contacts. We clearly observe the effect of aging on the contacts by increasing of the insertion force.

For different tested contacts, we determined a change in the value of the peak of the initial insertion force of 1.5 N and 2 N (lower than 2.7 N set by the connector manufacturer as the maximum force per contact).

This insertion peak increases with the extraction and insertion operations tending to stabilize.

Contact resistance drops rapidly at first contact and then stabilizes upon insertion (Figure 9). For the 2000 insertion - extraction cycles, the contact resistance was between 5 and 9 m Ω . It can be concluded that mechanical phenomena that have led to an increase in the contact force, have not altered the currents crossing points. This would mean that the contact materials and contact force are unchanged. For the tests, it does not depend on the number of operations or the kinetics of insertion.

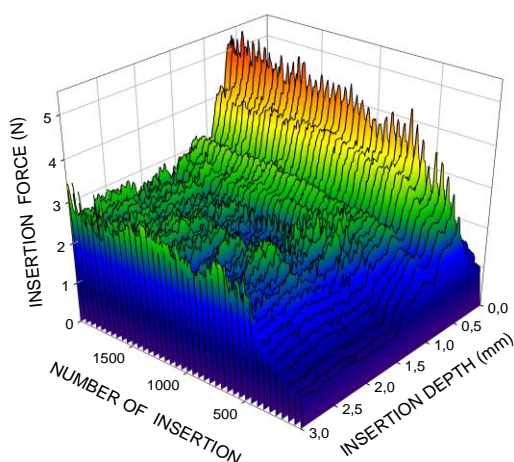


Figure 7: Change of insertion force in comparison with insertion number

The Figure 8 gives the change of the insertion peak obtained from the curve in Fig. 7. The initial value of the insertion spike is 1.75 N.

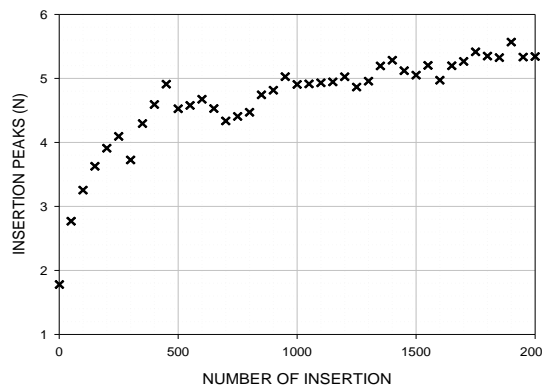


Figure 8: Change of insertion peak versus insertion Number

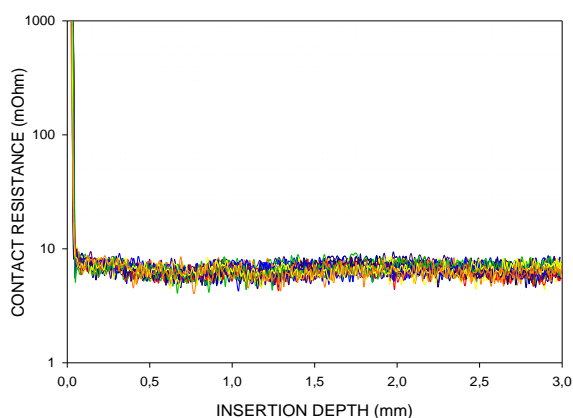


Figure 9: Change of contact resistance during multiple insertions

b) Influence of insertion velocity

During insertion-extraction operations, operators will not have the same velocity of insertion of the card used in these tests. We wanted to know the influence of velocity on the insertion force.

Three velocities were chosen: 0.6 mm/s; 1.5 mm/s and 3 mm/s (Fig. 10). We observed that the insertion rate strongly influences the evolution of the insertion force. An increase of 55% of the value of the insertion peak and an increase of approximately 53% of the sliding force after 2000 cycles between a velocity of 0.6 mm/s and a velocity of 3 mm/s.

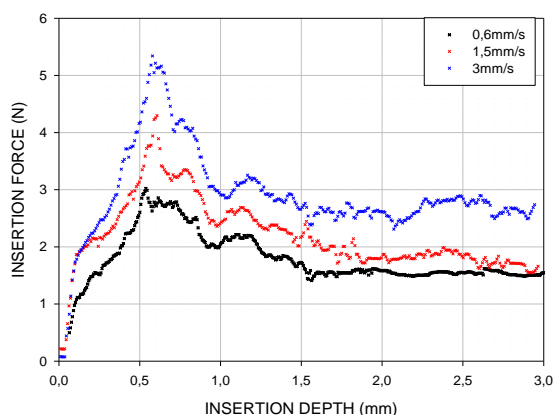


Figure 10: Change of insertion force versus insertion velocity (after 2.000 insertion-extraction cycles)

Another phenomenon observed is an increase of the amplitude of the variations in the insertion force δF_i with the velocity (Fig. 11). From these results it can be concluded that increasing the insertion velocity will generate more debris that will create resistance during insertion. This resistance translates concretely small insertion force peaks observed on the curve.

The first experiment performed was the measurement of insertion force vs. insertion depth for a new and aged contact (2000 sliding cycles) without the contact force sensor. The 2000 sliding wear cycles were applied on 3 mm aged zone of the insertion depth and the measurement was made on 4 mm intact zone.

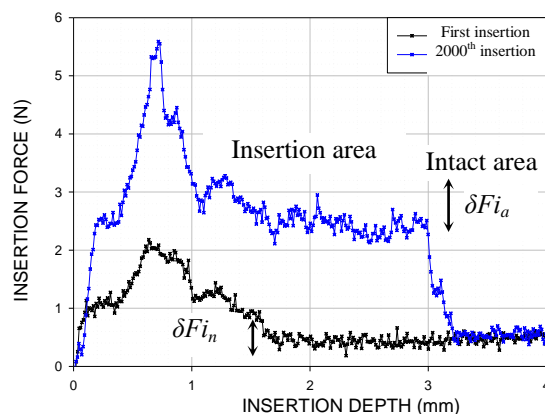


Figure 11: Insertion force vs. insertion depth for new and aged contacts

We notice that insertion force at the final stage finds its initial value (0.5N) on the “intact zone” while in the “ageing zone”; the insertion force is about 2.5N (Fig. 11).

In the sliding part, the amplitude of the insertion force (F_i) variation in the aged zone $\delta F_{i_a}=1N$ is greater than the F_i variation for the new contact $\delta F_{i_n}=0.4N$.

If we take a constant value of friction parameter $\mu =0.2$, the calculation of the contact force gives:

- At first insertion $F_c=0.5N/0.2=2.5N$
- After 2000 insertion/extractions: $F_c=2.5N/0.2=12.5N$

5. Synthesis on insertion force study

These results show that insertion force depends on normal force, contact geometry and on friction coefficient.

Maximum insertion force (insertion peak) depends on three factors: normal force, size of pin tip and receptacle entry and μ (friction coefficient).

All parameters, together consisting of in the order of ten individual dimensions, need to be in tight control in order to keep the insertion force within its design limits.

The profilometer used [14] to determine the profile of the contact zone is an apparatus enabling contactless measurement of topographies of the different surfaces cited previously. These are measured using a confocal laser. A DC motor controls the laser. The resolution of the profilometer sensor is adjustable between 0.001 μm and 10 μm . The studied profiles of spring are obtained after a measurement by scanning with a resolution of 2 $\mu m \times 2 \mu m$ on a window of 0.6 mm x 1.32 mm.

Profile measurements of contact area by profilometer show that wear cannot be uniform in view of the concave shape of spring in both longitudinal (Fig. 12) and transverse view (Fig. 13). Asperities of about 30 μm were observed on contact areas of spring. The shape of the contact area of spring allows that nickel will appear firstly on high rough that would be highly constrained (with the loss of their gold layers) while on the little constraint area (located valley), always gold coating sufficient to maintain a low contact resistance.

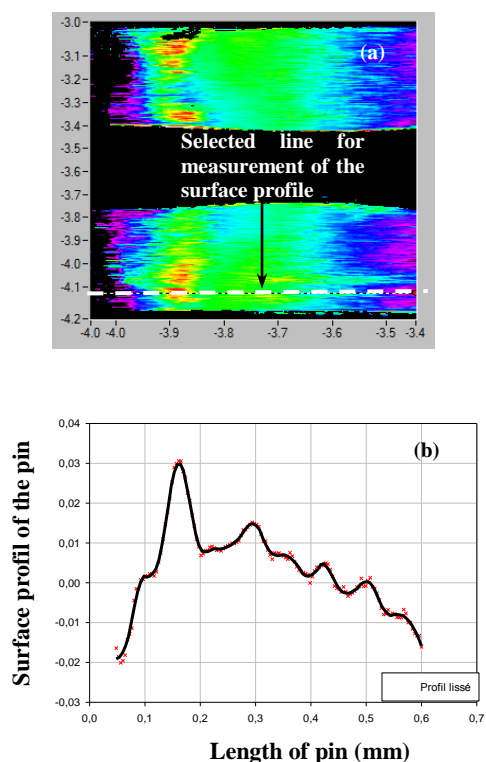


Figure 12: a) Wear track of the two parts of spring and b) Longitudinal profile of spring from laser profilometer

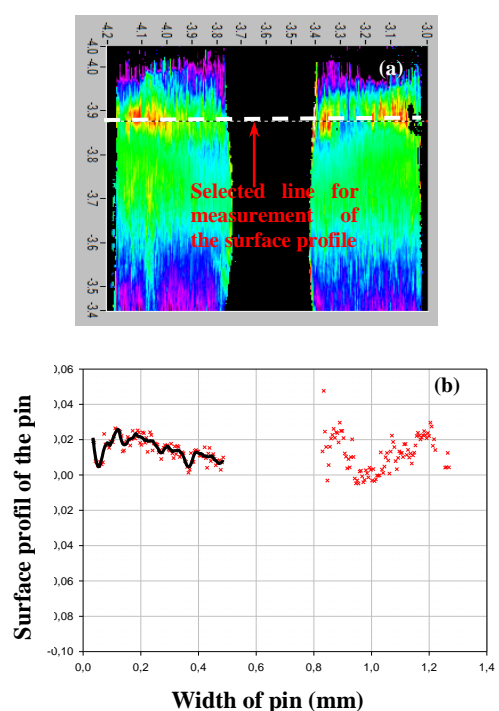


Figure 13: a) Wear track of the two parts of spring and b) Transversal profile of spring from laser profilometer (Confocal Taicaan profilometer)

The conclusion that can be drawn from this study is that, because of its small thickness (0.5 μm), the gold layer of the spring is removed faster than the one on

PCB (3 μm), meanwhile, simply distorted. This degradation will deeply on the morphology of the spring at the contact area.

For some springs, after 1000 sliding cycles, we observed the presence of copper on the surface. The presence of oxygen may cause a rapid oxidation and create an insulating layer.

The deterioration of the contact surface changes the coefficient of friction. The aim will then be to determine the evolution of this parameter.

6. Analysis synthesis

EDX study of spring has enabled to highlight emergence of nickel from 400 wear cycles in laboratory conditions. Copper onset occurs early in 1000 wear cycles for some springs. Non-coplanarity of contact zones in same spring causes wear disproportionate in both parts of spring.

A difference of degradation of the springs was observed for the same number of cycle's friction, probably due to lack of control during the deposition process. Severity of wear will depend jointly on number of friction cycle and topography of contact areas.

Wear of contact areas during frictions tests showed appearance of nickel in contact area. Consideration of gold friction coefficient (deposited on both parts of contact) during calculation of contact force cannot be valid anymore because the contact is not 100% Au-Au (nickel presence on a part of the contact surface with friction coefficient of 0.5).

In order to overcome μ this uncertainty on (friction coefficient), we worked on developing a non-destructive measurement and portable system, which would measure directly normal force on each contact after insertion into the connector.

7. Innovative on insertion force study

To avoid the influence of the friction coefficient during contact force determination, an innovative ultra-thin piezoresistive sensor, for a direct measurement of contact force, was developed for plugging it into the connector [15]. The contact forces of these terminals, however, could decay gradually due to the stress relaxation effect under the high temperature conditions [16].

The purpose is to set up a sensor which, once fixed to the contact PCB, will have the same thickness as the standard contact PCB in order to facilitate its insertion into the HE9 connector.

Piezoresistive sensors have found widespread use in the field of pressure and force sensors due to their low cost, good stability, and high response. Piezoresistance or piezoresistive effect is a change in resistivity of a material due to mechanical stress [17, 18]. In semiconductors such as silicon that exhibit a strong piezoresistive effect, electrical resistivity changes

significantly when the material is subjected to a stress/strain, which leads to a measurable resistance change with overlaid single-element strain gages.

The sensor used in this study, developed by Mescan®, is made of two substrate layers.

The substrate is composed of a polyester film. On each layer, a conductive material (silver) is deposited, followed by a layer of pressure-sensitive ink (doped silicon) as can be observed on Fig. 14.

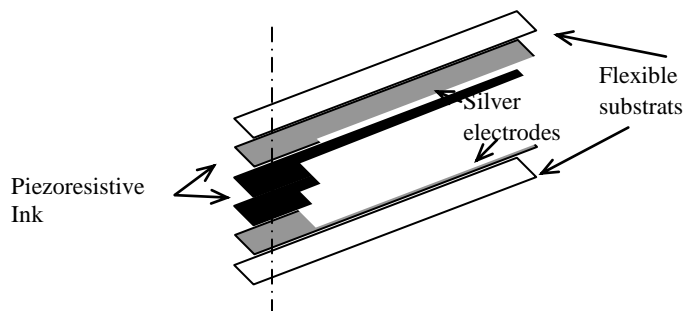


Figure 14: Piezoresistive sensor composition

With a fixed DC voltage applied across the sensor, output voltage corresponds to contact force, as illustrated in Figure 15. As the contact PCB undergoes mating, voltage measured will change accordingly.

A calibration test has been carried out to quantify the relationship between measured voltage and force (Figure 15)

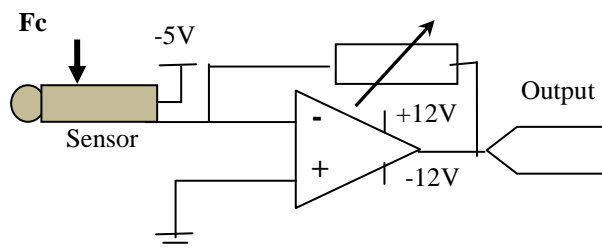


Figure 15: Drive circuit of one sensor

The output voltage expression was given by:

$$V_{out} = - \frac{R_s}{R_{sensor}} V_{in} \quad (3)$$

where V_{in} is the input voltage (equal to -5V), V_{out} is the output voltage, R_{sensor} is the sensor resistance and R_s is the gain resistor. R_s is chosen so as to obtain a sensitivity of 1V/N.

The Figure 16 represents the sensor's calibration curve obtained by the driver circuit of sample; the reference force is the one measured by the reference sensor. The sensitivity of each sensor was found to be approximately 1N/V ($\pm 3\%$) (Fig. 16).

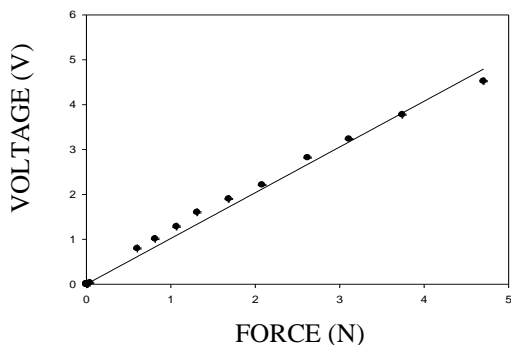


Figure 16: Calibration curve of the piezoresistive sensor

8. Final prototype

The prototype was improved so as to measure contact force of each spring beam pair. It consists of twelve separate active parts with a force range of 4.4N (1 Pound). Each active part of sensor corresponds to one PCB track (Fig. 17).

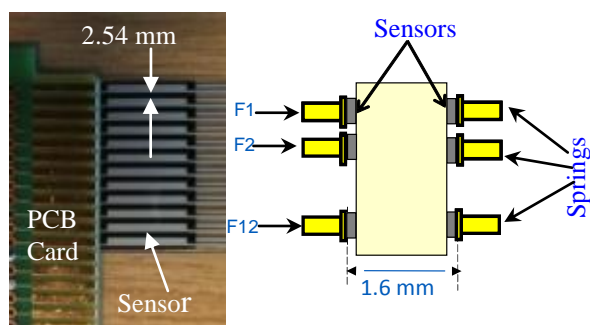


Figure 17: a) A photograph of sensor with PCB card, b) shape of sensor fixation

Conditioning cards with piezoresistive sensors were assembled as shown in Fig. 18. The cards are double-sided, with a sensor placed on each. The total thickness of the card with the two sensors is 1.6 mm \pm 0.2 mm, decomposed as following: 1.18 mm (one card) + 2 x

0.208 mm (piezoresistive sensor) + 2 x 0.104 mm (extra thick Mylar®).

It is estimated that losses in the mechanical properties of the Mylar® negligible in the measurement of force.

The two sensors have been chosen in particular to correct the defects of non-symmetrical insertion of the card into the connector axis when measuring. Each sensor measures the force exerted by the pair of springs.

The 24 analog outputs of the card, treated separately, were transferred via a multiplexer (MUX) 8 differential channels (DG407 model) to an analog digital (USB Redlab 1008 model, 4 channels in differential, 12 bit, 5 V, 1.2 kS / s) controlled by a computer with the software Labview® as can be seen on Fig. 18. This approach greatly simplifies the acquisition and processing data from the sensor.

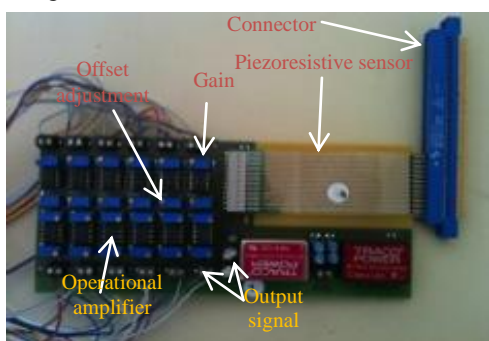


Figure 18: Conditioning card of the prototype

The architecture used is shown schematically in Figure 19. It is possible to access to analogue signals by a data acquisition system (DAQ).

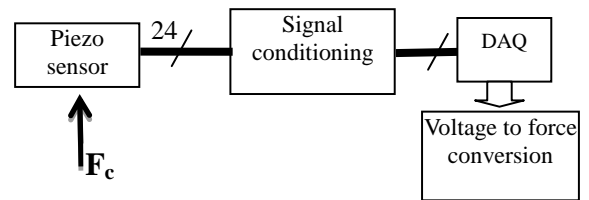


Figure 19: Schematic representation of sensor's conditioning principle [19, 20]

9. Requirements for contact force

a) Tolerance for connector

In order to maintain a contact force at the end of life properly, the contact must be manufactured to provide greater initial force than minimum required to maintain the minimum and stable contact resistance (integrity of the electrical signal) [21] as shown in Fig. 20.

Studies of the influence of the dimensional tolerance of a connector socket on the contact force were also made by Grill et al [22]. It shows that in the worst case sizing, loss of strength may be 40% and force gain of 20% compared to the required force (Fig. 20).

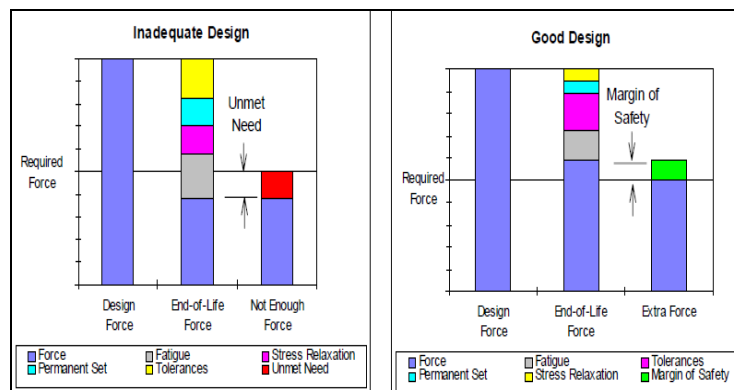


Figure 20: Contact force at end of life and reliability

b) Contact force for different tulips

The Figure 21 gives the contact forces for 12 tulips in new and aged connectors. The vertical bar chart represents contact force for a pair of contacts. The contact force varies significantly from one tulip to another in the same connector. This difference in contact force is observed for a new contact (Figure 21.a) and for used one (Figures 21.b, c and d). However, standard deviation σ of the contact force is less for new connector (0.22 for Fig. 21.a) than for three used connectors (0.35 for Fig.21.b, 0.38 for Fig. 21.c and 0.47 for Fig. 21 d).

These results indicate that there is an influence due to the dimensions of the parts used.

Variations in these dimensions can accumulate and lead to variations in the measured contact force.

For HE9 connector, two parameters must be taken into account: the nominal contact force which is 2 N (per contact pair in contact and a contact resistance <10 mΩ) and the minimum contact force contact which is 0.1 N (for a contact resistance of about 20 mΩ).

In most cases, results showed higher contact forces at 2 N (except for the tulip # 5 of Figure 27.d whose value is 1.6 N).

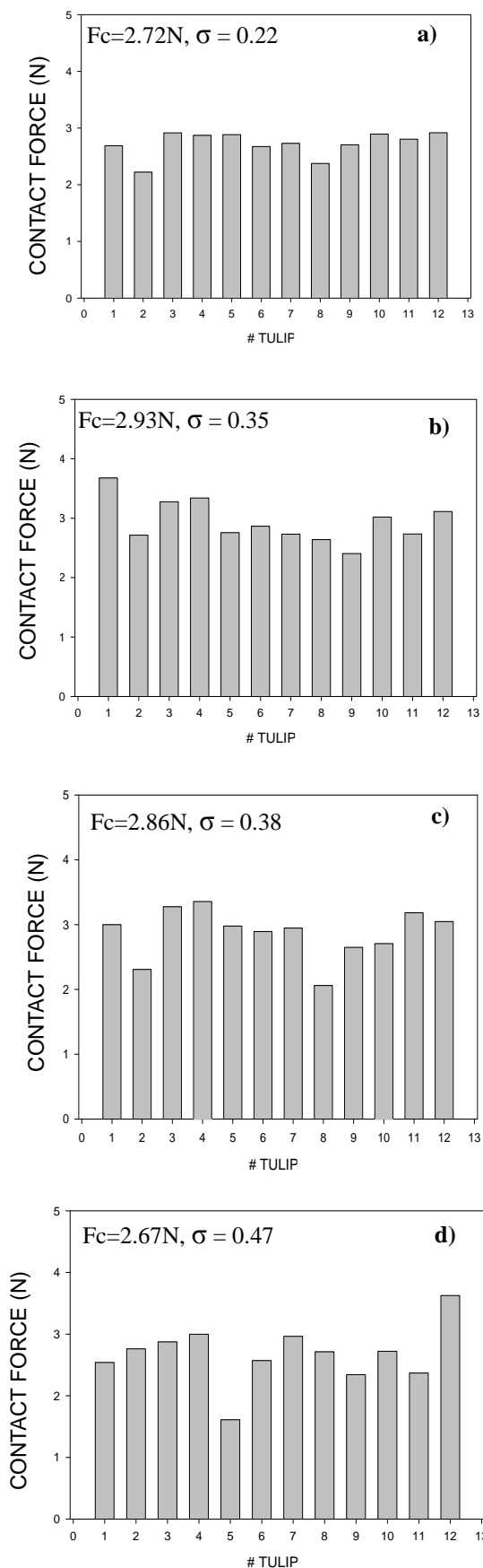


Figure 21: Contact force values on a new connector (a) and aged connectors (b, c, d)

10. Global synthesis

A novel in-situ force system measurement has been proposed using an innovative sensor using the piezoresistive effect.

- The EDX study of spring highlights nickel appearance at the surface of the contact from 400 cycles of friction in laboratory conditions.
- Copper appearance occurs from 1000 cycles of friction for certain springs.
- Coplanarity of contact of the same spring results in a disproportionate wear of both parts in spring.
- A difference of spring's degradation is observed for the same number of friction cycles. Shape of wear track depends on surface profile of each spring. This profile varies according to shape of spring during its manufacturing.
- The severity of wear is going to depend jointly on the number of friction cycles and on topography of contact zones.

11. Conclusion

The conclusion that can be drawn from this study is that, because of its small thickness ($0.5\ \mu\text{m}$), the gold layer of the spring is removed faster than the one on PCB ($3\ \mu\text{m}$), meanwhile, simply distorted. This degradation will deeply on the morphology of the spring at the contact area.

For some springs, after 1000 sliding cycles, we observed the presence of copper on the surface. The presence of oxygen may cause a rapid oxidation and create an insulating layer.

The deterioration of the contact surface changes the coefficient of friction. The aim will then be to determine the evolution of this parameter.

Wear of contact areas during frictions tests of the contact showed the appearance of nickel in contact area.

The insertion force depends on the insertion velocity: it increases when the insertion velocity increases and this can produce more debris which can lead to an increasing of the contact resistance.

Acknowledgments

The author expresses his gratitude to EDF for the material supplies and also the electrical contact laboratory and the SEM Center of the Rennes1 University for the technical assistance.

12. References

- [1] J. Horn, Shape optimization of connector contact for reduced wear and reduced insertion force. AMP Journal of Technology. 1992; 2, 42.
- [2] S. Aujla and B. Wilshire, Connector insertion force characteristics. Proceedings of the 31st IEEE Holm Conference on Electrical Contacts. 1985.
- [3] I. Sawchyn, E. S. Sproles Jr., Optimizing force and geometry parameters in design of reduced insertion

- force connectors. Proceedings of the 38th IEEE Holm Conference on Electrical Contacts. 1992.
- [4] L. H. Yang, The characteristic research of contact insertion and separation force in connector. Proceedings of the 36th IEEE Holm Conference on Electrical Contacts. 1990.
- [5] R. I. Jackson, W. R. Ashurst, G. T. Flowers, S. Angadi, S. Y. Choe, M. J. Bozack, The Effect of initial connector insertions on electrical contact resistance. Proceedings of the 53rd IEEE Holm Conference on Electrical Contacts. 2007; 17.
- [6] A. El Manfalouti, N. Benjema, R. El Abdi and T. Reiss, Experimental and theoretical investigations on connector insertion phase. Proceedings of the 49th IEEE Holm Conference on Electrical Contacts. 2003.
- [7] R. El Abdi and N. Benjema, Experimental and analytical studies of the connector insertion phase. IEEE Transaction on Components and Packaging Technologies. 2008; 31, 751.
- [8] M. Gedeon, Connector insertion force. Edition of Technical Tidbits. Vol.5, N°2, March-April 2004.
- [9] H. Essone Obame, L. Cretinon, R. El Abdi, N. Benjemâa and E. Carvou, Spring stiffness investigation for long lifetime connectors. Proceedings of the 55th IEEE Holm Conference on Electrical Contacts. 2009.
- [10] Connectors for printed circuit boards series 254 double side, Norm NFC/UTE 93-423 HE901 HE902.
- [11] P. V. Dijk, Critical aspects of electrical connector contacts. Proceedings of the 21st International Conference on Electrical Contact (ICEC). 2002.
- [12] B. Willman Engineered Materials, Connector insertion force. Technical Tidbits. 2004; Vol. 5, N°2.
- [13] J. Moran, M. Sweetland, N. P. Suh, Low Friction and Wear on Non- Lubricated Connector Contact Surfaces. Proceedings of 50th IEEE Holm Conference on Electrical Contacts. 2004.
- [14] TaiCaan Technologies Ltd website, also available at <http://www.taicaan.com>.
- [15] H. Essone Obame, E. Carvou, N. Ben Jemaa, B. Cousin, R. El Abdi, Implementation of a diagnostic tool for semi-permanent electrical contacts for a direct contact force measurement. Proceedings of the 59th IEEE Holm Conference on Electrical Contacts. 2013.
- [16] K.C. Liao and Wei-Chong Chiu, Investigation of relaxation behavior for terminals of CPU Socket. Proceedings of the 54th IEEE Holm Conference on Electrical Contacts. 2008.
- [17] C.S. Smith, Piezoresistance effect in germanium and silicon. Physics Review, Springer. 1954; 94, 42-49.
- [18] Y. Kanda, Piezoresistance Effect of Silicon. Sensors and Actuators A: Physical. 1991; 28, 83-91.
- [19] M. Gedeon, Reliability and end-of-life contact force. Technical Tidbits. 1999; 5.
- [20] A. Permuy, Capteurs microélectroniques. Techniques de l'Ingénieur. Traité Electronique. 1993; E2315 (3-1993).
- [21] A. Boukabache, Microcapteurs de pression. Techniques de l'Ingénieur. Traité de Mesure et de Contrôle. 2001; 016577, R2 070, 1-10.
- [22] R. Grill, R. Kösters, F.E.H. Müller, P. Stenzel, Material optimized design of contact-tulips. Proceedings of the 21st international conference on electrical contacts (ICEC), 2000.

BRAND:
«SMART MECHATRON - Competitiveness,
performance and high quality through
HIGH-TECH MECHATRONIC PRODUCTS »

STUDENTS CONTESTS, COMPLEMENTARY ACTIVITY OF UNIVERSITY CURRICULA IN THE MECHATRONICS ENGINEER TRAINING

Iulian-Sorin Munteanu, Aurel Zapciu, Marian Vocurek
National Institute of Research and Development in Mechatronics and Measurement Technique
munteanu75@gmail.com, zapciu.aurel@yahoo.com, marian_vocurek@yahoo.com

Abstract - In the strategic documents in the field of research are proposed three themes of reflection and action for the immediate future, namely prioritization of real sector R & D and innovation, install a climate of integrity, predictability and transparency of decision making and improved linkage between education and research and innovation. The overall objective of the students contest is to create the framework for student expression and creative skills of young people, namely to promote, support and enhancement of the results achieved by boosting the efficiency of the educational and extracurricular activities, achieved by implementing the principle of "learning by practice and research. For the students contest, students teams must prepare a innovative project for a product developing, (hardware or software) or a new technology. The subjects of the projects for the contests must be chosen by the team of students, but in their endeavors design and drafting the report that shows the contest, students can be guided by one or more teachers or researchers, with the role of specialized consultants. The subjects for the competition were from the field of robotics, mechatronics, IT, hydraulics. The most representative projects were awarded with money, diplomas and technical books.

Keywords: students contests, curricula, mechatronics, research, robotics.

1. Introduction. About an education system connected to global realities and scientific developments

By huge intellectual potential, resources and ambition inventiveness, creative ability and professional excellence in country and overseas, Romania has all the prerequisites to leave the perpetual delay and to build their own place in on the European scene and in the global research.

By developing the research, Romania will be able to respond sustainable in the context of global challenges - economic, demographic, security and climate. The field of RDI is the only area of the economy which has exceeded the 100% as the level of absorption of structural funds, a possible solution is redirecting a significant part of unspent funds from other areas to research, along with prioritizing real this area, from the perspective of public funding.

Also in the idea of sustainable development, Romania needs a prioritization of areas in the strategic research and innovation, in which the real connections with the economy and scientific areas are encouraged consistently performance. The policies in this field should be related to economic and education. Strengthening the link between research and education is essential in a democratic society. A good education system, connected to global realities and scientific developments can not exist without research as advanced research any sustainable system can not exist

without young people have contact with the latest news research, at all education levels.

By type, POSDRU projects is done a full correlation between research and development institutes, technical universities and the manufacturing industry, which is the ultimate aim of preparing young specialists, namely finding faster a job and integrating the graduates into employment.

2. Project ID 141 251 – an important linkage between education and research and innovation

A The project with the significant title "**By practice you have future**" - ID 141 251, Major Intervention Field 2.1 - "Transition from school to active life" reveals the importance of student practice, in training as specialists of the future graduates of technical education.

According to its mission, the technical universities prepare the students for careers that require the application of scientific knowledge and methods to develop products and technologies demanded by society. To this end, students must learn the knowledge and skills appropriate to the scope and specialization training program. The contest for Students Creativity and Innovation is addressed to students of higher technical education and aims to stimulate the application of theoretical and practical knowledge to concrete achievements, while developing skills and creative skills, innovative or enhancement of the

technical thinking analytical originality and flexibility in scientific and technical concepts, the practical skill, imagination and inventiveness in the developing process of new products and technologies.

Since the the majority of students participate in training competitions are enrolled in the technical profile: mechatronics and related sciences as electronics and informatics, we should mention which was the course of mechatronics concept.

There are a large variety of ways to present mechatronics. In this sense it is interesting views of the NSF - National Science Foundation, the fundamental role in orienting the organization and financing of the American academic system. A summary of the way NSF study concerns the necessity introducing of the mechatronics in higher technical education is able to be continued.

Along with the explosive growth of computing efficiency, the mechatronic systems have become common in any engineering discipline that relates to application control which applies physical strength. From this point of view, mechatronic systems are physical systems for component computing has a primordial role. This formulation is a generalization of the older definitions of mechanical systems mechatronics according to which the decisions are managed based on the provided by analogical and digital electronic systems.

With the spread of the universal mechatronics engineering products and systems of all kinds, it is imperative that future engineers to be aware of the principles and practices in this area. Regardless of where are preparing, engineers must meet mechatronic systems in their professional practice.

For engineers, full participation is essential at all stages of design, from conceptualization to final product mechatronic design. A key role is played in mechatronic systems need a complex calculation that defines real-time nature of most engineering systems. The successful implementation of a mechatronic system [1, 3] requires an organized approach to software system design.

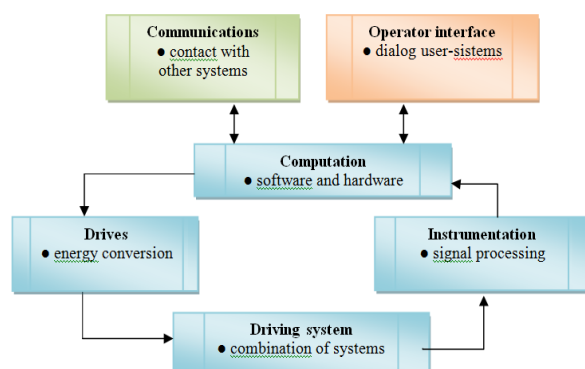


Figure 1 Component of a mechatronic system

The purpose of field of competitions in training in mechatronics is to ensure all students familiarization with the elements mentioned above (Figure 1), for them to be able to use mechatronics principles into practical applications.

We can say that Mechatronics is an interdisciplinary field of science and technology dealing with in general problems in mechanics, electronics and informatics. However, it includes several areas that form the basis of mechatronics, and covering many known disciplines, such as: electrical, energy, encryption technology, information microprocessing technology, and other technical adjustment

With time, the notion of mechatronics has changed the meaning and has expanded its definition: mechatronics engineering science based disciplines become classics for engineering, electrical engineering, electronics and computer science. The purpose of this science is improving the functionality of the equipment and technical systems by merging the disciplines in one unit. Mechatronics technology was born and became a philosophy which has spread worldwide. In recent years, mechatronics is simply defined: the science of intelligent machines.

Mechatronic systems are assemblies that integrates components that fulfill different functions, acting on the basis rules. Their main task is mechanical operation, thus producing useful work, and their essence is able to react intelligently, through a system of sensors to external stimuli acting on device taking appropriate decisions for every situation.

Apart from specialized technical training, each student must be trained to develop teamwork ability. The main Individuals competent concerns:

- ✓ the team spirit;
- ✓ willingness to cooperate;
- ✓ ability to learn;
- ✓ initiative;
- ✓ organizational qualities.

The existence and development of these skills is a key factor in individual professional career, regardless of professional skills of technical education graduates.

Another important educational component linked to stimulate scientific and technical creativity of students is to develop own models for exploration, investigation and expression, in the context of assuming decisions on technical solutions adopted as a result of collaboration and defining responsibilities within a working team.

Students competitions was an important part of POSDRU "By practice you have future" - ID 141 251, Priority 2 - "The correlation of long learning with the labor market", Key Area of Intervention 2.1 - "Transition from school to active life ". The project had like beneficiary "The Professional Association of Romanian Employers of Precision Industry Mechanics, Optics and Mechatronics – APROMECA" and partners were INCDMTM Bucharest, UPB - FIMM and the Lumina University.

Students Contests are a way to put into practice the theoretical knowledge accumulated in technical universities. If mechatronics is required to constitute groups of students from several people, even if only reason is that as mechatronics consists of three scientific components: mechanics, electronics and informatics.

The working group will be the main way in which students will put into practice the knowledge accumulated college.

The participants of the creativity and innovation student contest must be members of the target group of POSDRU ID 141 251 "By practice you have future" grouped in teams of minimum 3 students. Thus, eligible students belong from the University POLITEHNICA of Bucharest, with License specializations in: Mechatronics, Precision Mechanics and Nanotechnologies, Optometry, Hydraulic Machines, Economic Engineering, Medical Engineering. This was recommended, but not mandatory, they form part of different study programs, namely from different years of study, order to cover the specific working tasks of various technical fields, differentiated complexity respectively.

By this project, we have organized two student contests attended by students of universities Lumina and UPB - FIMM, members in the target group.

The first contest, according to the planning, between 8 – 9 January, 2015 at the headquarters of the Faculty of

Mechatronics and Precision Mechanics, Department of Mechanical Engineering and Mechatronics at the University Politehnica of Bucharest, has been the public presentation and judging the projects. Participants are students from years 1 to 4 of two universities participating in the project generally mixed teams, reflecting the concept of good practice on equality of chances.

The students enrolled in the contest are part of different study programs from different years of study, and so they have been able to cover specific working tasks of various technical fields, respectively of differentiated complexity. The setting up teams of students was the result of a mature assessment of the workload required for the project and the individual competence of their members.

It was attended 11 teams, 5 from University UPB, 6 from Lumina University, 2 teams outside of contest from UPB (2nd year students, FIMM).

We provide, further, some information about the winners of the two contests, as follows:

Table 1 – 1st Contest – Award 1

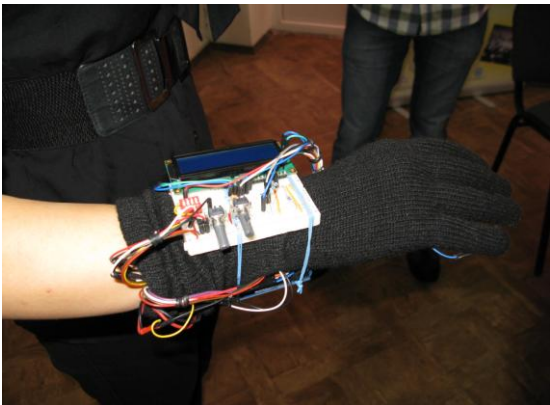

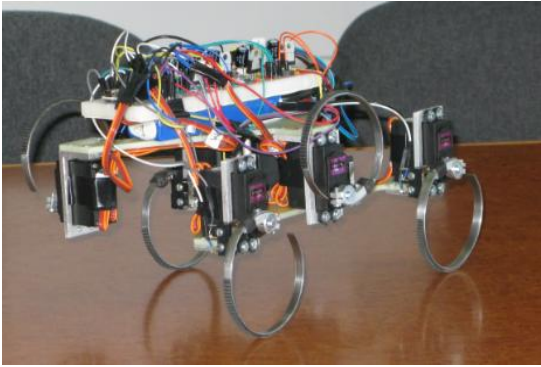
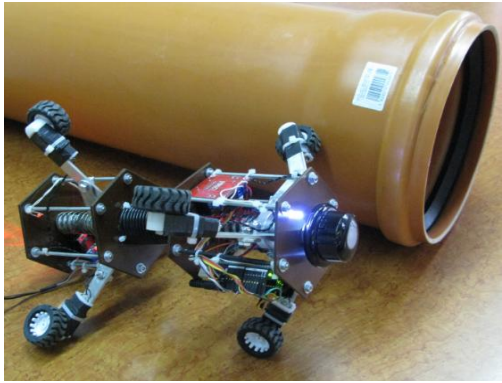
<p style="text-align: center;">Mechatronic system for improving communication and socialization skills of people affected by disability</p>  <p>Authors: Luca Vasile Răzvan, Petre Alina Stefania, Neagu Cătălin Ionuț, Dinu George Dragoș Scientific consultants: S.I. Dr. Ing. Bogdan Gramescu, As. Dr. Ing. Adrian Laurențiu Cartal, Dr. Ing. Iulian - Sorin Munteanu, Mat. Victor Dunca. Mechatronic system aimed at improving communication of people with disabilities by using the transmission of words using coded language with the help of contacts located on the fingertips</p>	<p style="text-align: center;">Humanoid Robot</p>  <p>Authors: Voiniciuc Constantin, Mărcoianu Ingrid, Văduva Andreea, Petre Floriana Scientific consultants: Conf. Dr. Ing. Lucian Grigore, Lector Dr. Ing. Alexandru Cioacă, Conf. Dr. Ing. Anton Soloi, Prof. Dr. Ing. Ticușor Ciobotaru, Dr.ing. Iulian- Sorin Munteanu. Humanoid robots are developed to perform human tasks, such as personal assistant, sick and old people, became increasingly popular in entertainment events.</p>
---	--

Table 2 – 2nd Contest - Award 1

<p>Mechatronic system for hazardous and radioactive exploration areas</p>  <p>Authors: Vasile Răzvan Luca, Alina Ștefania Petre, George Dragoș Dinu, students IV, FIMM, specialization Mechatronics and Robotics.</p> <p>Scientific consultants: S.l.dr.ing. Bogdan Gramescu, As.dr.ing. Adrian Laurențiu Cartal</p> <p>It is a mechatronic system that enables a robot locomotion on difficult terrain, with high humidity levels, within radioactive or corrosive potentially for inspection and analysis of the environmental conditions in which its visit.</p>	<p>Pipe Inspection Robot</p>  <p>Authors: Severin Andrei, Tudor Bogdan, Mihalea Bogdan, students II Mechatronics, FIMM</p> <p>Scientific consultants: Prof.dr.ing. Constantin Nițu, S.l.dr.ing. Lucian Bogatu, S.l.dr.ing. Bogdan Grămescu, Ing. Marian Vocurek, Dr.ing. Aurel Zapciu, Dr.ing. Iulian- Sorin MUNTEANU</p> <p>The robot is intended to inspect pipe inside diameter range between 250 and 350 mm. The robot is useful both in case of technical quality control as well as in the pipe verification for water, gas, oil, etc.</p>
--	--

The second competition took place between 7 to 8 May 2015, with a total of 9 teams, 8 from UPB and 1 from Lumina University, first award is presented in Table 2.

Summarizing the presented two charts can be drawn representing the students participation in competitions from UPB and Lumina, year of study and number of students. (Figure 2 and Figure 3).

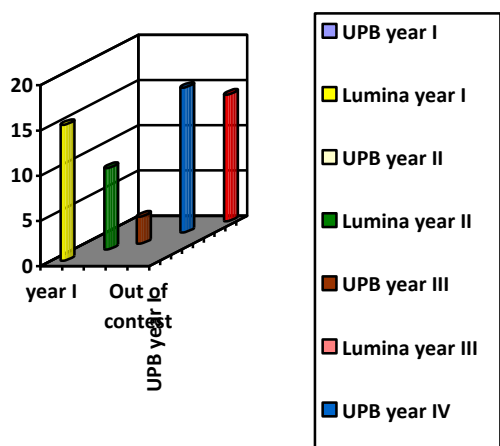


Figure 2 Distribution of students in the first contest

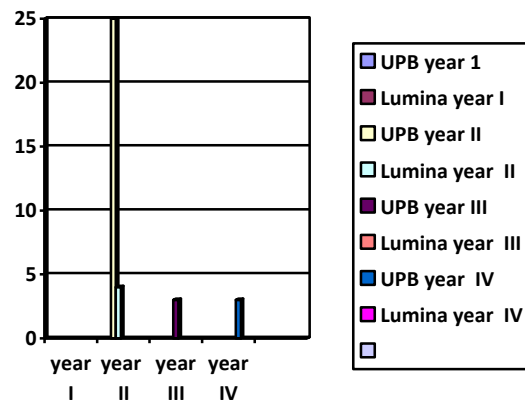


Figure 3 Distribution of students in the second contest

All the knowledge in the field of mechatronics curriculum can be capitalized only if they are put into practice [1, 2].

As a student, one of the methods of the practical use of technical knowledge acquired is the practical training. Another method, as necessary and useful technical development of students is the *students competitions*, in which students are required to appeal directly to specialized technical knowledge acquired, to technical creativity and also to realize the available combinations.

Practical Training objectives include developing the ability to:

- analysis of functional relationships in mechatronic systems;
- to understand the stages / operations of the manufacturing processes of mechatronic components;
- plan and organize manufacturing processes;
- put into operation the mechatronic systems;
- find and fix the defects of mechatronic systems;
- communicate using data processing systems;
- to monitor and perform corrective to electrical sub-systems, to pneumatic sub-systems, and to hydraulic sub-systems, within complex mechatronic systems.

Practice-oriented training is ideal preparation for work. Learning to workplace (job in production) is not feasible due to risks of damage production systems.

A specialized system of learning – oriented on practice – is optimal alternative for the qualification and specialization of future technicians and engineers who will work in production field. With such a system of learning, professional training can be done gradually and thoroughly, without pressure of time and without the risk of stopping production.

In daily practice, a team of mechatronics technicians (or specialized technicians as mechanical, electrical, etc.) must be able to assemble, to put into operation, operate and maintain the production capacity of a factory, as well to eliminate any malfunction in the production system. Often, they (mechatronics technicians) are asked all of this in the shortest time possible (Figure 4).



Figure 4 – Aspects of practical training

Professional performance of a mechatronics specialist is based on two types of skills:

- professional;
- individual;

Mechatronics specialist must have the following professional skills:

- planning and control of production processes, control and evaluation of results, and the use of quality management systems;
- mechanical parts processing, assembly of parts and components in mechatronic systems;
- installing electrical subassemblies and components;
- measuring and checking electrical quantities;

- installation and testing of hardware and software components;
- construction of electric actuators, pneumatic and hydraulic and checking them;
- programming of mechatronic systems;
- assembly, disassembly, transport and maintenance of safety machines, systems and installations;
- adjust and check the mechatronic systems;
- commissioning of mechatronic systems and customer training;
- making intretinereii mechatronic systems;
- work with documents in English and communication in English.

The vocational training must secure adequate means for acquiring the skills and knowledge of mechatronics, including design, execution and individual control. The following skills and knowledge of basic and supplementary underlying the preparation of the work program [1,2, 4,7]:

- safety and health protection at work;
- environmental protection;
- technical and professional communication;
- quality management;
- assembly of parts and components in machines and systems;
- installation, demounting and safe maintenance for machines, systems and installations;
- verification and regulation functions in mechatronic systems;
- installing electrical/ mechanical subassemblies and components;
- measuring and checking electrical quantities;
- planning and control of production processes, control and evaluation of results;
- verification, marking and labeling;
- manual or mechanical operations like compression, separation and deformation;
- installation and testing of hardware and software components;
- start-up / carrying into action and servicing of mechatronic systems;
- assembly and control devices (mechanic, electric, pneumatic and hydraulic);
- programming of mechatronic systems;

3. Conclusions

Contests for students is a way of putting into practice the theoretical knowledge gained in technical universities, these providing students with complex situations to be solved, which requires original and innovative solutions, and the need to synthesize and appeal to specific technical knowledge previous acquired with the aim of create a whole complex and competitive mechatronic assembly/ product, with higher innovative technical performance (a good example, in this respect, it may be the POSDRU project ID 141 251: "By practice you have future").

Thus, mechatronics requires that into the important contests for students to form groups of students with more individual specializations, because mechatronics is

made up of three major scientific fields: electro-mechanics, electronics and programming. These mixed working groups will ensure successful realization of systems /complex mechatronic assemblies, by various technical expertise of its members.

It can be pointed out that to obtain exceptional technical projects presented in contests for students an important role in finalizing the optimal creative processes - scientific undertaken by participants a heavy responsibility rests upon formers with over 5 years of real technical experience, such as university lecturers or trainers (scientific researchers with relevant experience in technical projects R&D) from research and development institutes (NIRD). [1]

Romanian students often prove inventiveness, the desire to create original projects, but like any young people involved still in the process of university technical training feel the need for technical discussions with technical experts, need confirmation and expert mentoring throughout the stages of development the original projects for competitions. [1]

Only a creative effort properly directed, can bring full satisfaction of students and at the same time for trainers with role of *Scientific consultants* in technical contests for students, each of those involved gained multiple rewarding (personal and scientific satisfaction) at the end of the Mechatronics contests and at the end of practical period in manufacturing, and prospects subsequent for new researches at the superior technical parameters into new advanced R&D projects [1, 2].

4. References

- [1] Project POSDRU/161/2.1/6/141251, "By practice you have future", Priority Axis 2 - "Linking lifelong learning and labor market", Major Domain 2.1 - "Transition from school to work"
- [2] Project POSDRU/90/2.1/S/62144 , "Dezvoltarea educației pentru viabilizarea pieței muncii prin vectori inovatori mecatronică –integronică"
- [3] Maluf, N., Williams, K. "An Introduction to Micro-electromechanical Systems Engineering", Second Edition Artech House, Inc., Boston, London, 2004
- [4] <http://www.unitbv.ro/il/Studenti/Concursuristudentesti.aspx>
- [5] <http://robotx.baiasu.ro/en/robotx-robomovies-2015/>
- [6] <http://www.wroromania.ro/>
- [7] <http://editie.ro/articole/actualitate/concurs-regional-de-mecatronicasi-robotica-la-universitatea-din-craiova.html>
- [8] <http://www.ziare.com/brasov/articole/concursul+national-de+mecatronicahttp://www.gds.ro/Educatie/2014-06-14/Prima+competitie+de+robotica++si+mecatronicain+Craiova/>

BRAND:
«SMART MECHATRON - Competitiveness,
performance and high quality through
HIGH-TECH MECHATRONIC PRODUCTS »

EFFECT OF JAPANESE SMW ENGINEERING METHOD ON DEEP FOUNDATION PIT OF SUBWAY STATIONS

Wang Xin

School of Foreign Languages, Dalian Jiaotong University, Dalian, Liaoning, 116028

wangxx056@163.com

Abstract - On the basis of requirements on retaining and protection of deep foundation pit in subway stations, this study analyzes deformation laws of deep soil horizontal displacement, ground settlement and axial load of bracing of foundation pit. Through changing relevant parameters of soil mass and space enclosing structure, this study also explores effect of different physical properties of soil, different types and layout forms of fashioned iron and different pre axial forces on deformation of retaining structures of soil mixing wall (SMW), as well as put forward relevant measures for predicting and controlling of foundation pit deformation. Besides, numerical modeling is also performed during excavation process of subway stations and effects of different parameters on structure of foundation pit deformation are obtained.

Keywords: SMW engineering method; subway; deep foundation pit; pre axial force; horizontal displacement.

1. Introduction.

Soil mixing wall (SMW) method derives from a new-type construction method called MIP which was developed in late World War II in America [1-3]. In 1955, SMW method was introduced to Japan and column-type underground walls were constructed on the basis of MIP method. In 1971, the production of multi-axis mixing and drilling machines solved various problems of traditional drilling machines, which created favorable conditions for wide application of steel reinforced concrete composite mixing piles. Since then, SMW method became mature gradually [4-8] and was widely used in many developed countries in the 1990's.

SMW pile construction method is also called steel reinforced concrete composite mixing pile method, which usually adopts multi-axis drilling and mixing machines for drilling at construction sites as well as construction of soil-cement piles through mixing foundation soil with cement paste sprayed from drills; overlap and overlap joint are performed on each element during construction, and H-beams or steel plates are inserted between soil-cement columns to form rigid and seamless soil-blocking and waterproof structures. Development of foundation pit in stations is closely related to diverse and functional development of enclosing structure. Reasonable choice of enclosing structural forms on the basis of project profile of foundation pit can not only ensure safety and stability of excavation work, but can also lower construction costs. With the growing requirements on construction

environment of foundation pit as well as foundation pit deformation, the development of enclosing structure in the future should have high strength, multifunction and easy operation. Due to engineering application and promotion of foundation pit as well as diversified foundation pit forms and complicated environmental conditions [9-10], traditional calculation methods can not meet needs of current complicated engineering needs. Therefore, the development of numerical methods provides foundation pit engineering calculation with new methods and ways. However, numerical simulation is not truly developed and applied until realization of development and popularization of calculation; meanwhile, theoretical researches of foundation pit engineering is further developed on the platform of numerical simulation.

2. Project Profile

The station is in two-layer, double-column and three-span structure, and it has an island-type platform. Burial depth of station is 17~18 m; overall size of standard paragraph is 20.5 m × 13.21 m (width × height); thickness of covered soil on top is about 3.5 m. Mileage between the starting point and terminal point is designed as Y (Z) DK31 + 654.698 ~ Y (Z) DK31 + 888.98; available center mileage of station is YDK31 + 736.473; available center rail surface elevation is 391.475, and length of the station is 233.7 m. Plan sketch of the subway station is as shown in figure 1.

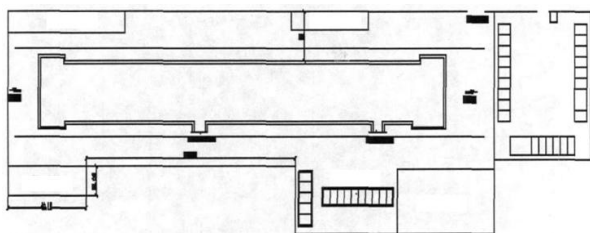


Figure 1. Plan sketch of the subway station

Open cut method was adopted in the construction of major structures [11-12]. Depth of the foundation pit was 14.364 ~ 14.978 m; 850@600 cemented soil was used in the space enclosing structure using three stalk agitation stake; HN700 × 300 fashioned iron was inserted for supporting. P.O32.5 Portland cement was adopted and cement-mixing ratio was 18.2%. Interpolated fashioned iron was arranged using “insert two jump one” and “intensive splice” these two methods according to foundation pit depth as well as geological data. Fashioned iron was recycled after the construction was finished. Fashioned iron should be derusted and brushed with anti friction agent before insertion;

reinforced concrete top beam in 900 × 800 (width × height) was set on pile top.

The station was arranged in plane direction and was mainly designed in diagonal bracing. Corners of foundation pit were set up with appropriate amount of diagonal bracing to stabilize the foundation pit; the foundation pit was excavated symmetrically in two sides and depths excavated in each layer were controlled at about 3 m; the excavation was stopped after the excavated depth was 0.3 m below the supporting, and waist beams were erected. 609 steel tubes were used as internal bracing and t=14 mm (the first line of supporting as well as accessory structure bracing were both 12 mm). Main part of the foundation pit was vertically set with four lines of bracing; vertical intervals were 4.1 m, 3.0 m and 4.1 m while horizontal intervals were 3.5 m. Details are shown in figure 2.

Pre-applied force was exerted during installation of steel tube bracing [13-15] and pre-applied force was 50% ~ 80% of designed axial force. The number of steel waist-beams was 2 ~ 3 and they were combined with batten plates; waist beams were fixed on steel supports and supports were welded on H-fashioned iron.

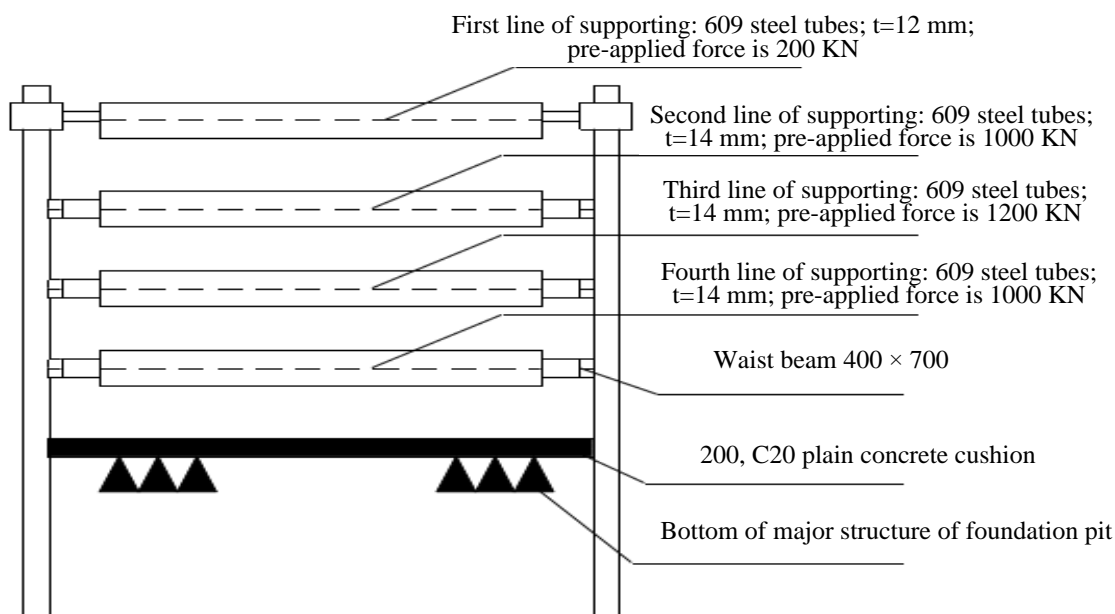


Figure 2. Sketch map of foundation pit supporting

3. Effect of physical properties of soil mass on supporting structure deformation

Effect of Elasticity Modulus of Soil Mass on Supporting Structure Deformation

Model simulation scheme in this study is as follows [16-18]: parameters of soil mass were taken as 0.8 and 1.2 times respectively of original elasticity modulus for calculation to analyze rules of elasticity modulus of soil mass to deep soil horizontal displacement, ground settlement and bottom heave of foundation pit supporting structure. Figure 3, figure 4 and figure 5 show changing curves of horizontal

displacement, ground settlement and bottom heave of supporting structure under different elasticity modulus of soil mass.

Results show that when intensities of the soil are the same (c and are the same), the increase of modulus of soil will significantly reduce deformation of supporting structure, which can be explained from two aspects: firstly, increase of modulus of soil will enhance restraint effect of unexcavated soil on deformation of supporting structure, thus deformation of foundation pit is decreased; secondly, increase of modulus of soil can improve self stability of soil outside the pit, which also decreases deformation of foundation pit.

Therefore, modulus of soil is the main parameter that affects deformation of foundation pit supporting

structure, and increase of modulus of soil can greatly control deformation of foundation pit.

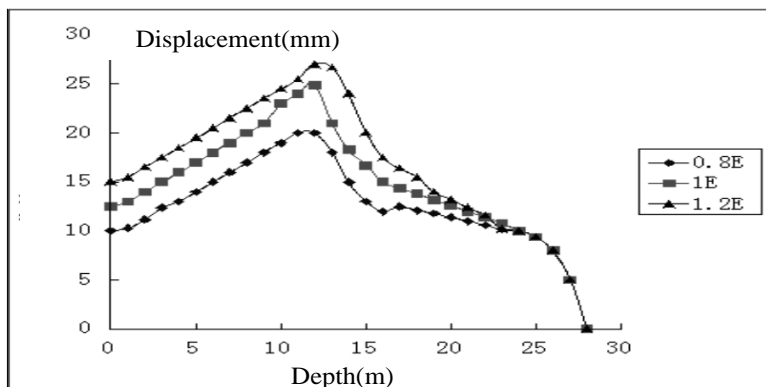


Figure 3. Changing curves of deep soil horizontal displacement

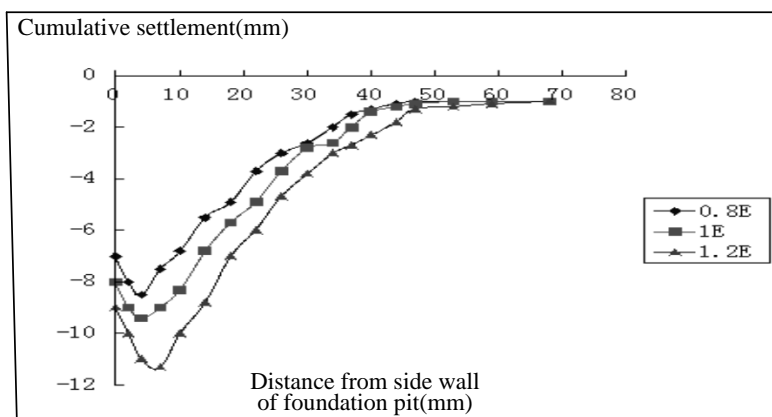


Figure 4. Changing curves of ground settlement

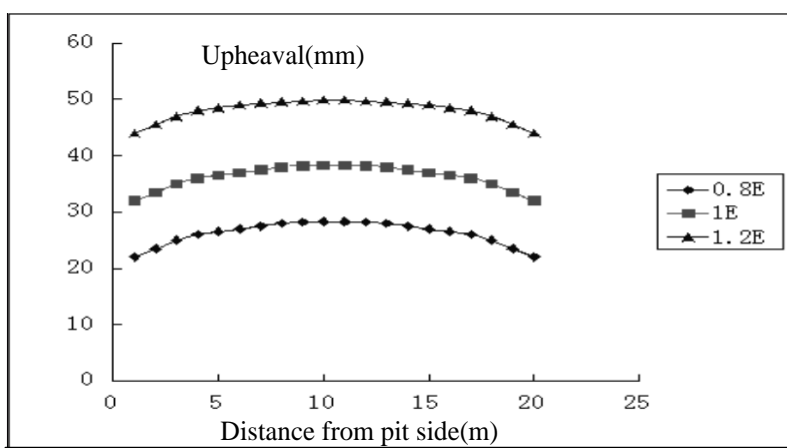


Figure 5. Changing curves of bottom heave

Effect of Cohesive Force of Soil Mass on Deformation of Supporting Structure

Soil mechanical parameters were taken as 0.8 and 1.2 times of original cohesive force respectively for calculation;

rules of elasticity modulus of soil mass to deep soil horizontal displacement, ground settlement and bottom heave of foundation pit supporting structure were obtained.

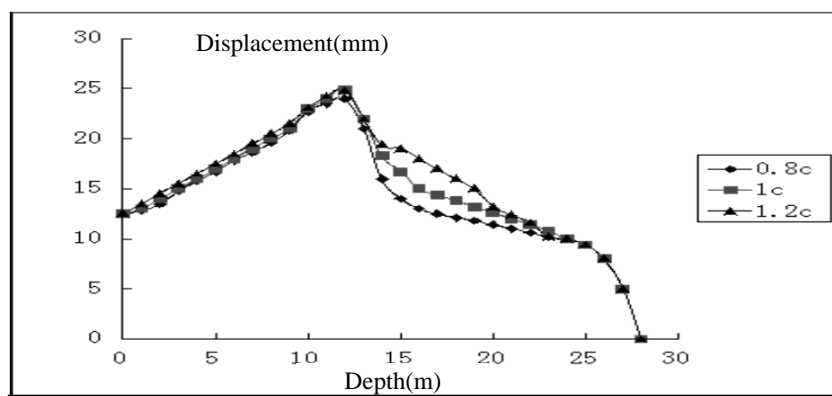


Figure 6. Curves of deep soil horizontal displacement

Figure 6 shows changing curves of horizontal displacement of supporting structure with different cohesive force of soil mass, which indicates that cohesive force of soil mass has little effect on deformation of supporting structure, and with the increase of cohesion of soil mass, the maximum horizontal displacement of supporting structure decreases gradually. The reason can be explained by following active earth pressure equation:

$$\sigma_a = \gamma Z t g^2 \left(45^\circ - \frac{\varphi}{2} \right) - 2c \cdot t g \left(45^\circ - \frac{\varphi}{2} \right)$$

The equation shows that with the increase of soil cohesion, active earth pressure is decreasing, which results in decrease of deformation of supporting structure and soil mass. As shown in figure 6, changes of c values of first, second and third layer (excavation depth is 12 m) have little effect on horizontal displacement of supporting structure, while changes of c value of the fourth layer (11 m excavation depth to the bottom of pit) have the biggest effect on horizontal displacement of supporting structure, which means this layer has the biggest effect on stability of foundation pit. In the scheme, changes of each layer are considered to be the same to study the effect of cohesion on deformation of foundation pit, and the fourth layer has big cohesion value as well as cohesion changes. The equation of active earth pressure shows that in corresponding positions, decreasing extent of horizontal displacement is obvious, which provides a basis for how SMW method guarantees stability of foundation pit excavation: the key soil layer which affects stability is calculated through numerical modeling before foundation pit excavation; then reinforcement treatment is performed on corresponding soil layers, thus to obtain satisfying results with a small cost, which saves engineering costs as well as guarantee safety of foundation pit excavation.

4. Effect of buried depth of support pile on deformation of supporting structure

Buried depths of supporting structure were taken as 0.5 H, 1.0 H, 1.5 H, 2 H and 2.5 H of excavation depth, and length of fashioned iron was the same as support pile. In order to analyze effect of buried depth of support pile in vertical force and deformation of foundation pit, suppose physical conditions, displacement boundary condition and load boundary conditions as well as geometric model are the same as basic example model [25-27]. When buried depth of support pile is 0.5 H and the excavation depth is close to the pit bottom, numerical results indicate that the foundation pit is damaged. Therefore, buried depth of foundation pit should be ensured, or the increase of supporting structure displacement will lead to instability of foundation pit. Figure 7 shows horizontal displacement curves of supporting structure with different buried depths. When the buried depth is 1 H, the maximum value of horizontal displacement of soil mass is 25.2 mm, which indicates big deformation. When the buried depth is 1.5 H, the buried depth can effectively decrease horizontal displacement of support pile, and the maximum value of horizontal displacement is 23.7 mm. When the buried depth is over 1.5 H, the effect becomes insignificant. Therefore, the maximum horizontal displacements all occur at around 12 m depth of foundation pit.

Figure 7 shows that depth of supporting structure should meet certain requirements, and increase of depth can reduce lateral displacement of supporting structure. However, when the buried depth already meets needs of supporting structure stability, the increase of buried depth will lead to unsatisfying results. Literature [19-20] indicate that on the promise that the bottom of foundation pit shows no upheaval or instability, that is to say the buried depth meets the minimum value requirement, the buried depth of supporting structure has little relation with lateral displacement and deformation of foundation pit.

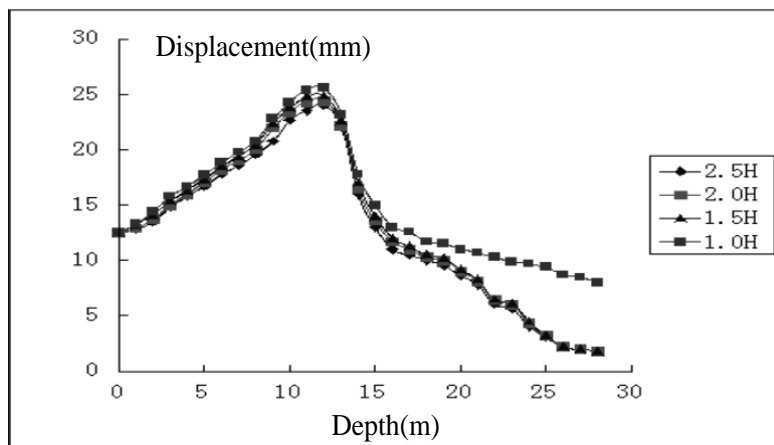


Figure 7. Curves of lateral displacement of supporting structure under different buried depths

Figure 8 reveals relationship between surrounding earth surface and different buried depths. Results indicate that changes of surrounding earth surface are basically the same as different buried depths and lateral displacement. When the buried depth of supporting structure is over 1.5 H, changes of surrounding earth surface become insignificant. Buried depth of support

pile is the important content in supporting structure design. Shallow buried depth will lead to life danger. However, controlling deformation of supporting structures through increasing depth only has insignificant effect, which will also increase engineering cost. Thus, these factors should be considered comprehensively to maintain stability of pit bottom.

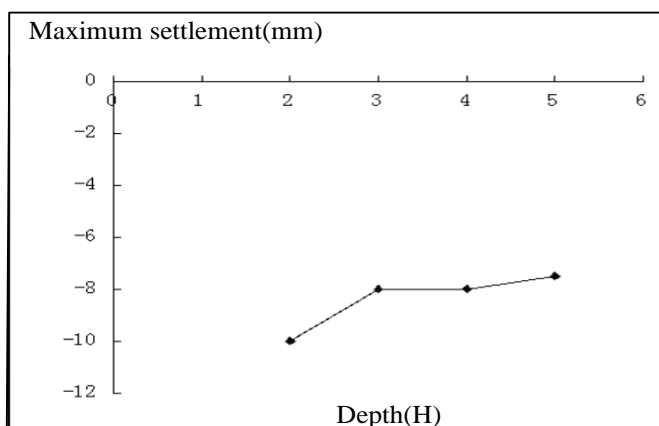


Figure 8. Relationship between surrounding earth surface and different buried depths

5. Effect of fashioned iron arrangement on deformation of supporting structures

Suppose fashioned iron arrangement is designed as in figure 9 to analyze deformation of supporting structure like horizontal displacement and surrounding earth surface changes. Displacement boundary conditions and load boundary conditions of surrounding soil mass and cement soil as well as geometric model are the same as basic example model. Parameters are shown in table 1.

Table 1. Parameters of fashioned iron in different arrangement

Arrangement forms	Thickness of soil-cement pile	Excavation depth
Intensive splice		
Insert one jump one	0.6 m	14 m
Insert two jump one		

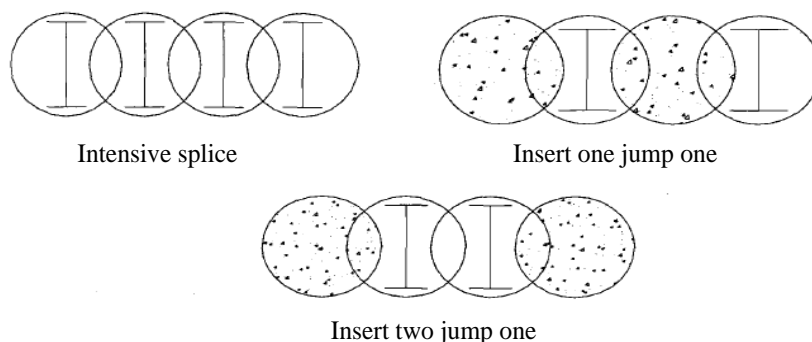


Figure 9. Sketch map of fashioned iron in different arrangement

Curves of horizontal displacement of supporting structures of fashioned iron in different arrangement are as shown in figure 10 [21-22]. It can be seen from figure 10 that horizontal displacement curves of soil-cement piles in different arrangement are roughly the same;

horizontal displacement of the supporting structure used intensive splice is the smallest, and biggest displacement occurs at 12 m depth and horizontal displacement amount is 23.5 mm.

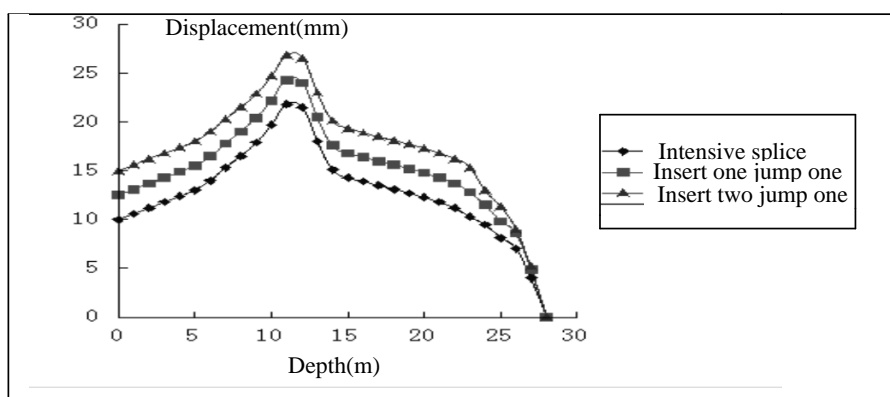


Figure 10. Curves of horizontal displacement of fashioned iron in different arrangement

6. Effect of horizontal intervals of supporting on support deforming

Horizontal intervals of supporting in the engineering are about 3.5 m. In order to analyze effect of horizontal intervals of supporting on deformation of foundation pit, horizontal intervals of foundation pit are simulated as 3 m and 4 m respectively while other parameters are the same.

It is an important method to control deformation of supporting structures through adjusting support intervals. When intervals are 4 m, the biggest displacement is 28.8 mm, which is within the alarm value; however, when intervals are 3 m, it is inconvenient for excavators to operate normally, and it also brings extra costs to engineering. Therefore, it is appropriate to set support intervals as 3.5 m ~ 4 m, which has little influence on deformation of foundation pit.

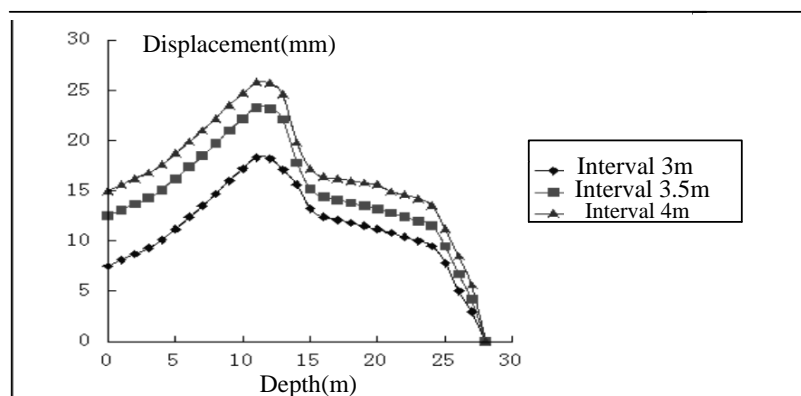


Figure 11. Changing curves of horizontal displacement of supporting structures with different support intervals

7. Effect of axis force of braces on support structure deformation

In order to explore effect of axis force of braces on support structure deformation [23-24], 10%, 50%, 80% and 100% of design value are taken, as shown in table

2, and the relationship between brace pre axial force and deformation and displacement of foundation pit supporting is obtained, thus to further obtain effect laws of brace pre axial force to structure of foundation pit supporting.

Table 2. Parameters of support in advance and axial force of steel

Parameters	Design axial force (KN)	Pre axial force (KN)				Note
		Design value 10%	Design value 50%	Design value 80%	Design value 100%	
First line of support	215.6	21.56	107.8	172.48	215.6	Other parameters are the same
Second line of support	1960	196	980	1568	980	
Third line of support	2303	230.3	1151.5	1842.4	2303	
Fourth line of support	1568	156.8	784	1254.4	1568	

Figure 12 shows curves of horizontal displacement of space enclosing structure with different support in advance and axial force [31-34]. Axis force of brace increases from 10% of design value to 100% of design value, and horizontal displacement of pile top of support structure decreases 112.3 mm and horizontal displacement of deep soil mass decreases 8.9 mm.

Figure 12 indicates that increase of pre axial force of foundation pit can effectively decrease deformation of support structure, but changes of support structure become insignificant below excavation face. When the support in advance and axial force is 100% of design value, increase of axis force of brace will make pile top of foundation pit gradually move to outside of foundation pit, and horizontal displacement of deep soil mass decreases significantly.

Therefore, increase of support in advance and axial force can effectively control support structure deformation, especially support structure deformation above the excavation face. However, too much support in advance and axial force can lead to excessive retrocession of support pile as well as worsen stress conditions of support pile, thus affect strength of support pile.

Therefore, in projects which are strict with deformation of supporting structures, it is effective to decrease deformation through increasing rigidity of support as well as accordingly increasing sections of piles to improve bending moment. 50% ~ 80% of axial force is suggested.

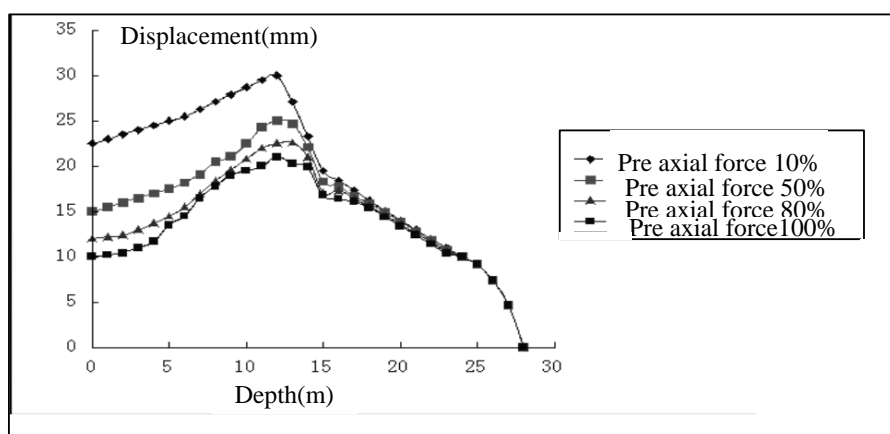


Figure 12. Curves of horizontal displacement of space enclosing structure in different support in advance and axial force

8. Conclusion

Analysis of effect of influencing factors on deformation of foundation pit supporting show that when buried depth of support pile is 5 H, foundation pit

capsizes due to insufficient buried depth of soil-cement piles; when buried depth of support structure is over 1.5 H, deformation of surrounding earth surface becomes insignificant; when buried depth meet stability requirements, increase of buried depth has little effect

on decreasing horizontal displacement of support structure. Besides, in different arrangement of fashioned iron, soil mass of soil-cement piles using intensive splice method has the smallest horizontal displacement, and it also has certain control effect on settlement of surrounding earth surface. Therefore, increase of density of fashioned iron can significantly increase stress and deformability of support structure. However, increase of fashioned iron will increase costs of construction as well as make construction become difficult, thus factors should be considered comprehensively. Space effect law of foundation pit should be paid attention to and Hold Before Digging method should be adopted; appropriate support intervals are 3.5 m ~ 4 m and decrease of support intervals can effectively reduce displacement. The first line of support plays an important role in controlling displacement of pile top, because improvement of first line of support in advance and axial force can effectively control displacement of pile top. Numerical modeling indicates that the first line of support in advance and axial force should be 80% ~ 100% of axial force. Increase of pre axial force can effectively reduce the maximum horizontal displacement of pile top of foundation pit and supporting structure; however, too much pre axial force will lead to excessive retrocession of support pile; pre axial force is usually 50% ~ 80% of axial force.

9. Reference

- [1] Iijima Y., Kawanabe A., Yoshida Y. Statistical Analysis of Current State of Regional Wood Use in Wooden House in Akita Prefecture (2): Current State and Recognition of Material Use[J]. Wood Industry, 2008, 63:602-607.
- [2] Horiuchi M. A Study of the German Roof Frame in Japan in Comparison with the Purlin Roof Construction Method in Germany [J]. Journal of Architecture Planning & Environmental Engineering, 2001:221-227.
- [3] Wei X., Jin M., Chi Y. Prevention Measures of Sand Soil Liquefaction and Construction Method in Japan [J]. Journal of Heilongjiang Hydraulic Engineering College, 2001, (2):76-78.
- [4] Song J. L., Gong X. N., Ri-Qing X. U. Analysis on Inner Force of Circular Working Shaft with SMW Method [J]. Coal Geology & Exploration, 2004, 32(6):42-44.
- [5] Huang W D, Zhang M, Lan Y J, et al. Practice of SMW Method and Reaming Anchors in Deep and Large Foundation Pits[J]. Chinese Journal of Geotechnical Engineering, 2010:261-264.
- [6] Hao Y. Application Research on Deformation Monitoring of SMW Method H Steel Pile Using BOTDA[C]// Multimedia Technology (ICMT), 2011 International Conference on IEEE, 2011:3862-3865.
- [7] Gu S T, Wang C Q. Interface Stress Distribution Law of SMW Method Section Steel-cemented Soil[C]// Mechanic Automation and Control Engineering (MACE), 2011 Second International Conference on IEEE, 2011:2263-2266.
- [8] Yin G J, Xiao-Dong H E, Qin L. Applications of SMW Method in Deep Pit Protection Engineering Under Complex Conditions [J]. Journal of Hebei University of Technology, 2009, 38(4):111-114.
- [9] Xia J T, Zhang S F, Shen H R, et al. Monitoring and Analysis for the Deformation of SMW Retaining Structures in Subway Station[J]. Applied Mechanics & Materials, 2014, 580-583:1249-1253.
- [10] Sun B, Zeng S, Ding D X, et al. Finite Element Analysis of Heave Deformation in Deep Foundation Pit with SMW Retaining Structure[J]. Journal of Disaster Prevention & Mitigation Engineering, 2008, 28(3):319-324.
- [11] Hisatake M, Ohno S. Effects of Pipe Roof Supports and the Excavation Method on the Displacements above a Tunnel Face [J]. Tunnelling & Underground Space Technology, 2008, 23(2):120-127.
- [12] Budney C J, Lucey P G. Basalt Thickness in Mare Humorum: The Crater Excavation Method [J]. Journal of Geophysical Research Atmospheres, 1998, 103(E7):16855-16870.
- [13] Shen Y P, Wang H H, Jing P, et al. Orthogonal Analysis of Influence Factors for Foundation Pit Support Approaching Existing Railway Line[J]. Journal of Traffic & Transportation Engineering, 2014, 14(2):14-20.
- [14] Hong M A, Cong J I, Yang R G, et al. Numerical Simulation Analysis of Foundation Pit Support Using FLAC 3D[J]. Global Geology, 2013, 32(4):857-861.
- [15] Fang D S, Yao S. Foundation and Application of Optimization Model for Foundation Pit Support Scheme [J]. Journal of Yangzhou University, 2007, 10(4):71-74.
- [16] Shen Z L, Liu W W. Effect of Elastic Modulus of Foundation Soil on Seawalls with Thin-walled Tubular Piles [J]. Advances in Science & Technology of Water Resources, 2011, 31(2):77-80.
- [17] Sall O A, Fall M, Berthaud Y, et al. Influence of the Elastic Modulus of the Soil and Concrete Foundation on the Displacements of a Mat Foundation[J]. Open Journal of Civil Engineering, 2013, 03(4):228-233.
- [18] Hany Farouk, Mohammed Farouk. Effect of Elastic Soil Structure Interaction on Modulus of Subgrade Reaction[C]// Recent Advances in Material, Analysis, Monitoring, and Evaluation in Foundation and Bridge Engineering ASCE, 2014:111-118.
- [19] Qi H U, Si-Fa X U, Chen R P, et al. Influence of Soil Disturbance on Metro Tunnel in Soft Clay Due to Excavation of Deep Foundation Pit[J]. Chinese Journal of Geotechnical Engineering, 2013, 35(zk2):537-541.
- [20] Li H, Zhao P, Li G, et al. Time-Effect Analysis Of Deep Foundation Pit Excavation And Support In Soft Clay Soil Areas[C]// Remote Sensing, Environment and Transportation Engineering (RSETE), 2011 International Conference on 2011:4689-4693.
- [21] Shaw A, Roy D. A Novel Form of Reproducing Kernel Interpolation Method with Applications to Nonlinear Mechanics [J]. Computer

Modeling in Engineering & Sciences, 2007, 19(1):69-98.

[22] Aguado F, Isasi F, Hernando J M, et al. Interpolation Techniques for Ray-tracing Models[J]. Microwave & Optical Technology Letters, 2000, 25(5):343-346.

[23] Azar B F, Hadidi A, Khosravi H. Effect of the Height of SCSW on the Optimal Position of the Stiffening Beam Considering Axial Force Effect[J]. Structural Engineering & Mechanics, 2012, 41(2):299-312.

[24] Li Q Y, Wang Y. Research on Deformation Law of Deep Excavation Supporting Structures in Beijing Metro Station [J]. Advanced Materials Research, 2011, 243-249:2338-2344.

[25] Comisel H, Hategan C, Ionescu R A. The Boundary Condition Displacement for Weakly Bound and Quasistationary States[J]. Romanian Reports in Physics, 2011, 63(4):1120-1132.

[26] Huang L X, Shuang-Bei L I, Zhou X J, et al. Effects of Boundary Conditions at Fixed-end on Displacement of a Uniformly Loaded Orthotropic Cantilever Beam [J]. Fiber Reinforced Plastics/composites, 2007, 27(4):6-10.

[27] Chen Tao, Mo Rong, Wan Neng, Gong Zhongwei. Imposing Displacement Boundary Conditions with Nitsche's Method in Isogeometric Analysis[J]. Chinese Journal of Theoretical & Applied

Mechanics, 2012, 44(2):369-381.

[28] Yao S, Lin L. Measurement and Analysis on Supporting Axial Force in Deep Foundation Pit[J]. Building Structure, 2012, 42(1):112-114.

[29] Li S, Li S, Wei Z. Regularity of Supporting Axial Forces of Deep Foundation Pit with Semi-top-down Method in Soft Ground[J]. Chinese Journal of Underground Space & Engineering, 2012, 8(4):732-736.

[30] Zhang M J, Feng-Jun S I, Xin-Feng Y E, et al. Internal Force and Deformation Monitoring Analysis on Mixed-supporting System for Supporting Structure of Some Deep Foundation Pit[J]. Journal of Beijing University of Technology, 2010, 36(11):1496-1503.

[31] Wu C, Li C, Bi X, et al. Study on Distribution of Axial Force in Prestressed Anchor for Deep Foundation Pit[J]. Building Structure, 2011, 41(8):134-123.

[32] Zhang X, Yao A. Monitoring and Numerical Simulation of Structure Behaviour of Supporting Piles in a Deep Foundation Pit [J]. Chinese Journal of Underground Space & Engineering, 2011, 7(6):1138-1142.

[33] ZHANG You-jie, DING Wen-qi, LIU Xue-zeng, WANG Xiao-xing, WU Jun-don. Internal Force and Deformation of Deep Foundation Pit under Asymmetric Water Pressure[J]. Chinese Journal of Geotechnical Engineering, 2013, 35(zk2):107-112.

BRAND:
«SMART MECHATRON - Competitiveness,
performance and high quality through
HIGH-TECH MECHATRONIC PRODUCTS »

INFLUENCING FACTORS OF FATIGUE BREAK OF ROUND SPRING FOR RAILWAY FREIGHT CAR'S BOGIE

Zhang Wencai

Jilin Railway Technology College, Jilin, 132200, China

E-mail: wencaizh22@163.com

Abstract - Round spring is one of the main components of a railway freight car's bogie and its performance and service life determine the security and stability of bogie's operation. Due to the effect of alternating stress, the breakage of spring is mainly fatigue break, thus the fatigue strength of spring is a critical index to evaluate the performance of spring. Influencing factors of spring's fatigue break is various, such as factors of spring's steel raw materials and manufacturing techniques. Therefore, systematical analysis of influencing factors of spring's fatigue strength (service life) is necessary. Taking round spring (type K2 round spring was used for example) of railway freight car's bogie as research object, this study firstly discussed various performance indexes of type K2 round spring and analyzed the manufacturing technique and parameter indexes of type K2 round spring. Then, based on influencing factors of type K2 round spring's fatigue break, this study took broken round springs of railway freight cars' bogies for fatigue tests to study the reasons of spring's breakage, thus to further study various influencing factors and mechanism of spring's fatigue break.

Keywords: Round spring; fatigue break; type K2 spring; fatigue test.

1. Introduction

In recent over ten years, Chinese economy is highly developing, and as a main type of transportation, railway no longer meets the needs of economic development. Under such circumstances, railway is sped up several times and strategic target of great-leap-forward development of railway has been put forward to meet the needs of development of national economy [1]. Bogie technology is improving and developing fast, which is upgraded from 8A to 8G, type K2, type K6, etc., thus requirements on quality and reliability of all accessories of bogies as well as their service life significantly increases. At present, as a critical component of railway freight car's bogie, spring's service life increases to three million times from one million times [2], and quality guarantee upgrades from one shed repair period to one shop repair period. Steel raw materials of springs upgrade from 60Si2Mn hot rolled materials to 60Si2CrVAT surface grinding materials [3-4], thus physical and chemical properties, grain sizes [5], occluded foreign substance level and surface quality of materials all increase significantly. In recent years, product quality supervision and inspection center of China's Ministry of Railway spot checked springs produced by railway spring manufacturers for fatigue tests, and the phenomena of unqualified service life of springs were very common [6].

Some specialists and scholars did fatigue life analysis on elastic side bearing of type K2 bogie as well as used energy method and S-N curve (stress-life curve) method to calculate the fatigue life of elastic side bearing of type K2 bogie. The comparison between calculation results and fatigue testing results indicated that results from energy method were close to results from tests [7-8]. Therefore, this study analyzed influencing factors of round spring's fatigue break of railway freight car's bogie, summarized main influencing factors of spring's service life as well as analyzed reasons of spring breakage and process of crack extension.

2. Manufacturing process of springs and requirements of fatigue break test

Manufacturing Process of Springs

Types of springs have developed from type 8A to other various types, such as type K2, type K4, type K6 and MT-3 bumper, etc. So far, more and more manufacturers begin to produce railway freight car springs and the total production capacity increases year by year. The manufacturing process of railway freight car's spring has been shown in figure 1.

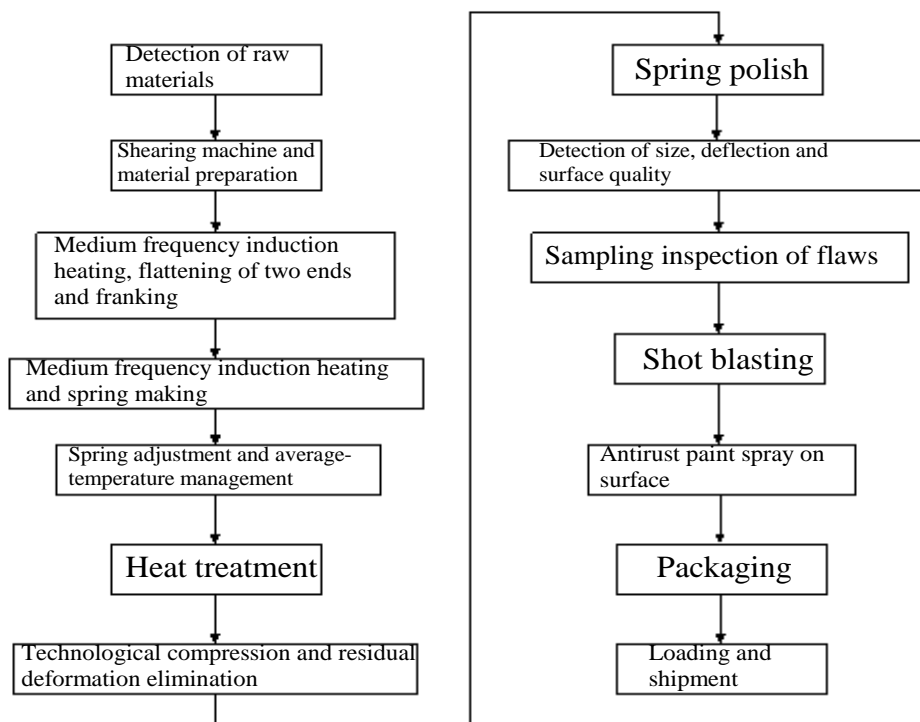


Fig 1. Manufacturing process of spring of railway freight car's bogie

Fatigue Test of Springs

Fatigue test is an effective method of testing spring's fatigue life and reliability of usage, that a testing spring is put on a testing workbench and is tested under a certain extent, maximum and minimum deformation quantity (or average load, maximum or minimum load) as well as a certain frequency (1~6 Hz) and continuous cycle effect. The aims of spring's fatigue test can be mainly divided into three kinds: first is to test fatigue life and stability of spring products or designed spring

parts [9]; second is to determine the fatigue limits of spring materials or S-N curve to provide basis for spring design; third is to determine the effect of external factors on spring's fatigue strength or fatigue life, which is mostly applied to comparison experiments to provide basis for spring design and quality improvement. The fatigue tests of railway freight car springs are mainly to verify fatigue life and evaluate reliability of springs. Experimental parameters of research object type K2 spring have been shown in table 1.

Table 1. Parameters of type K2 springs' fatigue tests

Type	Static deflection /mm	Dynamic deflection /mm	Dynami c factors	Maximum load /kN	Maximum stress /MPa	Test frequency (times/min)	Fatigue life (ten thousand times)
Outer helical spring	46.7	37.4	0.4	31972	754	180-240	300 (Normal temperature)
Inner helical spring	24.7	19.8	1.4	13457	583		
Damping outer spring	69.7	55.76	2.4	13894	762		
Damping inner spring	69.7	55.8	3.4	7582	879		

After using dynamic stress test to calculate type K2 springs' fatigue life, analyzing cycle indexes of springs under fatigue loading conditions and referring to relevant research results, we can draw following conclusions [10-11]: 500 thousand times fatigue life of spring equals to one-year normal operation of the spring, and when fatigue life reaches 3 million times,

the fatigue life tend to be stable, thus the probability of 5 million times fatigue life is high. Therefore, overall considering various factors, 3 million times fatigue life is enough for a warranty period which is one shop repair period (9 years).

Checking of Fatigue Strength and Static Strength of Type K2 Spring

The operation of type K2 spring is affected by variable load, thus the following is the checking of fatigue strength and static strength of type K2 spring.

Checking of fatigue strength:

Calculation formula of fatigue strength safety factor S is . $S = (\tau_0 + 0.75\tau_1) / \tau_2 \geq S_p$

In the formula, S is fatigue strength safety factor; τ_0 is pulsating fatigue limit of spring material; τ_1 is shear stress MPa under working load P_1 ; τ_2 is shear stress MPa under working load P_2 ; S_p is allowable safety factor and $S_p = 1.3 \sim 1.7$;

$$\tau_1 = 8C_w P_1 D / \pi d^3 \text{ and } \tau_2 = 8C_w P_2 D / \pi d^3 .$$

In the following equation, D is the pitch diameter of spring (mean diameter) in mm, and d is the diameter of material in mm:

$$C_w = \tau_{\max} / \tau = (4C - 1) / (4C - 4) + 0.615 / C ;$$

$$C = D / d$$

C_w is the theoretical stress concentration factor (stress modifying factor) and C is spring index. Material of type K2 spring is 60Si2CrVA and its strength of extension $\sigma_b = 1900$ MPa. Therefore, the fatigue strength safety factor of type K2 spring can be calculated according to above formula.

Checking of static strength

Calculation formula of static strength safety factor is $S = \tau_s / \tau_{\max} \geq S_p$.

In the formula, τ_s is yield limit of spring material; S_p is allowable safety factor which is the same as the checking of fatigue strength. The yield limit of type K2 spring material is 1700 MPa.

3. Influencing factors of fatigue life of spring

Occurrence and Classification of Breakage

Under the cyclic loading effects, metals or components will break even the stress is under yield strength, which is called fatigue break. Breakage is a very complicated phenomenon that occurs on components or materials. In different mechanics, physical and chemical environments, high temperature and lasting stress effect will cause creep break and corrosion environment will cause stress corrosion or corrosion fatigue break, etc. In engineering applications, breakage can be divided into brittle break and tenacity break, and in different situations, different terms are used to describe characteristics of breakage.

Fatigue Break

In general conditions, fatigue fracture consists of fatigue source, crack extension area (smooth area) and the final instant break area. Fatigue source can be obvious or unknown, thus crack extension area and instant break area are two main parts of fracture.

Main characteristics of crack extension area are that the surface is smooth, and it is the result from friction of crack surfaces in the extending process of cracks. However, the characteristics of instant break area are that when fatigue cracks extend to a certain extent, effective loading area is reducing and relevant operating stress is increasing. Thus when stress is bigger than breaking stress of the material, spring will have instance breakage, and the fracture is rough and irregular.

When spring surface has no macroscopic defects, fatigue cracks mostly occur at grain boundaries, phase boundaries, foreign substances and brittle carbide, etc., and then gradually extend inwards. Microscopic characteristics of fatigue fracture mainly show in the crack extension area, and main microscopic characteristics of crack extension area are fatigue striations, which can only be observed under high-power microscope. Shapes of striations are fluctuated and rippled, and every striation stands for one loading cycle. The leading edge line of cracks can be determined by striations, and striations have plasticity and brittleness.

Generally speaking, fatigue break process of metal materials has following stages: slippage, nucleation, microcosmic crack extension, macroscopic crack extension and instant breakage. Metal materials have multiple ways to have fatigue cracks: some fatigue cracks occur at the surface of metallic crystal, crystal boundaries or the connection part of nonmetal foreign substances inside metal; some occur at congenital defect areas of metal, such as mechanical scratch on surface, pitting, manufacturing defects, decarburization, etc; Some are due to the stress concentration caused by the component's structure and thus occur at component's inner or outer circular bead, gap, etc.

Fatigue Curve (S-N Curve)

Traditional fatigue design is based on fatigue curve of material or S (stress)- N (life) curve. Because actual data have big discreteness, statistical adjustment method is used for curve plotting. As for varying stress, damage accumulation hypothesis should be used to estimate fatigue life of components [12].

The resistivity of materials to varying stress is presented by maximum stress σ_N that will not cause damage under certain cycle indexes N . σ_N is called the limiting stress under certain cycle indexes N as well as conditional fatigue limit. The limiting stress of a material under cycle indexes N can be obtained through experiments. Taking abscissa as cycle indexes N and ordinate as limiting stress to draw a fatigue curve (S - N curve) of the material. As shown in figure 2, higher stress will result in less cycle indexes. When varying stress is lower than a certain value, the material stops producing fatigue damage, and the stress at that time is called the limiting stress of material. The cycle indexes at the time that limiting stress occurs is called cycle cardinal number N_0 , and the cycle cardinal number of general steels was about 106-107.

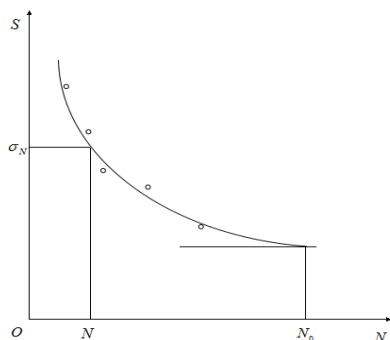


Fig 2. Fatigue curve of spring

Theoretical Analysis of Influencing Factors of Spring's Fatigue Life

Springs work under high stress. Material surface has the maximum stress, thus comprehensive performance and surface quality of spring material directly influence the quality, performance and fatigue (service) life of the spring.

Fatigue break of springs often starts from tiny surface defects, and then become small cracks under the effect of alternating load, and finally the extension of cracks results in breakage. Fatigue is a gradual, partial and permanent structural change. Such change happens when spring's maximum stress value is smaller than yield strength of materials, and also due to the effect of varying stress. Small cracks can result in fatigue break after a certain stress cycle indexes. The fatigue life of railway freight car bogie's spring is $3 \cdot 10^6$ times.

Because spring fatigue is a partial damage that often

starts from the weakest part of spring material and then extends to the whole section. Thus spring's geometrical shape, discontinuity of section, surface status of material and uniformity of organizational structure are all critical factors that determine spring's fatigue performance [13]. Stress conditions of spring also have effects on fatigue performance, such as chemical components, nonmetal foreign substances, noxious gas, mechanical property, metallurgical defects, surface status, size and shape, heat treatment quality, etc.

4. Reason analysis of early breakage of spring during operation

Seven type K2 round springs of railway freight cars' bogies that broke on the road were collected. The broken parts were mainly at 1~1.5 circles and a few were at other parts. Most parts broken into two sections (broke at one end) and a few parts broke into three sections (broke at both ends). The operation time of spring was about one shed repair period, which is shorter than one shop repair period. Broken springs were numbered and the break reasons of spring samples were analyzed.

Hardness Test

First, lateral end face samples of number 1~7 broken springs were taken using wire-electrode cutting. Then samples had hardness test on Rockwell hardness tester, and the results have been shown in table 2.

Table 2. Rockwell hardness (HRC) test results of spring samples

Samples	Standard hardness value	Edge hardness value (distance from surface was about 2mm)	Average value	Center hardness value	Average value
1	42-48	44.8 45.5 45.2	45.2	46.5 46.0	46.25
2		44.2 45.0 47.0	45.4	46.0 46.8	46.4
3		42.0 47.5 46.6	45.3	47.0 47.2	47.1
4		44.0 46.9 46.2	45.7	47.0 47.0	47.0
5		45.1 47.5 45.5	46.0	48.0 48.0	48.0
6		42.0 47.5 46.5	45.3	48.5 47.5	48.0
7		45.2 47.0 46.0	46.0	45.0 45.6	45.3

Decarburized Layers Checking

After the lateral end faces of number 1~7 broken springs were burnished, polished and had corrosion process, their decarburized layer depths were observed

under metallographic microscope. The results have been shown in table 3.

Table 3. Testing results of decarburized layers (mm)

Sample numbers	Standard value	1	2	3	4	5	6	7
Decarburized layer depths	≤ 0.2	0.11	0.06	0.18	0.09	0.17	0.22	0.12

Results showed that number 2 and number 4 had small decarburized layer depth values; number 1 spring sample was a half decarburized layer; other samples were decarburized layer combined with half

decarburized layer; the decarburized layer depth value of number 6 sample was bigger than 0.2 mm, which passed standard value, and other samples all met the requirements.

Detection of Nonmetal Foreign Substances

Longitudinal samples of number 1~7 springs were taken, and they were polished but had no etching.

Then they were observed under metallographic microscope and evaluated according to ASTM-E45 rate

of GB/T10561-2005 Rating Map of Microscopy Evaluating Methods of Nonmetal Foreign Substances in Steels. Results have been shown in table 4

Table 4. Evaluation results of microscopy detection of nonmetal Foreign Substances

Sample numbers	Types of foreign substances							
	A		B		C		D	
	Thin	Thick	Thin	Thick	Thin	Thick	Thin	Thick
1	0.5	1.0	0.5	0.5	0.5	0.5	0.5	0.5
2	0.5	0.5	1.0	0.5	0.5	0.5	0.5	0.5
3	0.5	0.5	0.5	0.5	0.5	0.5	0.5	0.5
4	0.5	0.5	0.5	0.5	0.5	1.0	0.5	0.5
5	0.5	0.5	0.5	0.5	0.5	0.5	0.5	0.5
6	0.5	0.5	0.5	1.0	0.5	0.5	0.5	0.5
7	1.0	0.5	0.5	0.5	0.5	0.5	0.5	0.5

Besides, this study also did metallographic structure test, fluorescence test, macroscopic test, fracture test, etc., and no more detailed description here.

All results showed that the breakage of number 1~7 spring samples were all fatigue break and cracks all started from cracks of surfaces. However, the occurrences of cracks were due to the formation of surface open grain structure during heating process, thus causes early fatigue break of springs.

5. Conclusion

The analysis of type K2 spring design and breakage during operation shows that the influencing factors of fatigue break are different. However, it is a systematic, long-term and complicated work to analyze influencing factors of spring fatigue break. Because fatigue break of spring is the result from combined action of multiple factors, different life areas have different decisive factors. At present, it is a great challenge to guarantee the fatigue life of springs to be longer than standard. Therefore, the researches on spring's fatigue break need further discussion, thus to enhance the reliability of railway freight car bogie spring's fatigue life and service life.

6. References

[1] Zeng L, Yun Pu, Rui M A. Automatic detection for the casting defects of railway freight car based on industrial CT [J]. China Railway Sci. 2009, 30(4): 76-80.
 [2] Yang B, Zhao Y X. Fatigue reliability research on RD2 axle of railway freight car[J]. Key Eng. Materials. 2007, 353-358: 62-65.
 [3] Naderi M. On the thermodynamic entropy of fatigue fracture[J]. Proceedings of the Royal Society A-Mathematical Physical & Eng. Sci. 2010, 466(2114): 423-438.

[4] Zeng L, Gao Y, Bi B I. Recognition method for the slanted DR image of casting workpiece characters for railway freight car[J]. China Railway Sci. 2012, 33(2): 95-99.
 [5] WANG. Overall evaluation of the effect of residual stress induced by shot peening in the improvement of fatigue fracture resistance for metallic materials[J]. Chinese J. Mechanical Eng. 2015, 28(2): 416-421.
 [6] Zeng L, Hong D, Liu L. Defect extraction method for the casting of railway freight car based on multiple and fast segmentation of DR image[J]. China Railway Sci. 2012, 33(1): 103-107.
 [7] Furuya Y, Abe T. 1129 mean stress effects on fatigue properties of spring steel developing fish-eye fracture[J]. The Japan Society of Mechanical Engineers. 2010, 2010: 1156-1158.
 [8] Sun S, Ding J, Huang Y, et al. Simulation study on the effect of railway freight car parameters on wheel wear[J]. China Railway Sci. 2013, 34(5): 100-107.
 [9] Furuya Y, Abe T, Matsuoka S. 1010-cycle fatigue properties of 180065MPa-class JIS-SUP7 spring steel [J]. Fatigue & Fracture of Eng. Materials & Structures. 2003, 26(7): 641-645(5).
 [10] Gardin C, Courtin S, Bezine G, et al. Numerical simulation of fatigue crack propagation in compressive residual stress fields of notched round bars [J]. Fatigue & Fracture of Eng. Materials & Structures. 2007, 30(3): 231-242.
 [11] FU Shu-hong, Hui W J, Liu Z H, et al. Fatigue fracture behaviour of a medium-carbon 2000 MPa level high strength spring steel [J]. J. Iron & Steel Res. 2006, 18(10): 30-35.
 [12] Furuya Y, Matsuoka S. Validity of inclusion inspection conducting fatigue tests for an inclusion-controlled valve spring steel [J]. Transactions of the Japan Society of Mechanical Engineers A. 2004, 70(696): 1058-1065.
 [13] Ktari A, Haddar N, Ayedi H F. Fatigue fracture expertise of train engine crankshafts [J]. Eng. Failure Analysis. 2011, 18(3): 1085-1093.

INTEGRATED MECHATRONIC SYSTEM FOR BEARING RINGS CONTROL

Daniela Cioboata¹, Octavian Dontu², Daniel Besnea², Robert Ciobanu², Aurel Abalaru¹
¹The National Institute of Research and Development in Mechatronics and Measurement Technique;
²University POLITEHNICA of Bucharest;
E-mail:d_bes@yahoo.com

Abstract - This paper presents a method for multi-parametric control of the dimensional and geometric features of the surfaces of ball and rollers bearing rings by using a mechatronic, flexible equipment, with open hardware and software architecture

Keywords: bearings rings control, form deviations, mechatronic equipment, dimensional control.

1. Introduction

This article aims to integrate the full control of the bearing rings in manufacturing technology to ensure quality growth, providing information about processes, process control by providing a mechatronic, flexible equipment with open architecture, designed to dimensional and geometric multi-parametric control of ball and rollers bearing rings surfaces.

This equipment must meet the following requirements: rapid and precise calibration; rapid adaptation to the requirements of the manufacturing process; safe and precise detection of parameters deviations resulting in processing for multi-parametric control of a wide range (shape and size) of bearing rings; decisional capacity based on predetermined criteria; statistical calculation program for control and streamlining of manufacturing process. [2]

Considering the global technological progress, the bearings are still a challenge for further research and development, as evidenced by the fact that many engineers and researchers are currently engaged in research projects in this area to develop new materials, extending the life and field of application.

The main elements that contribute to optimizing the quality of the bearings are shown in Fig. 1. [3] According to the diagram presented in Fig. 1, the development of inspection technologies, closely related to evolution of processing technologies is an important factor for improving the quality and accuracy of bearings rolling surfaces and a decisive factor in increasing the accuracy and reliability of mechanisms with bearings. Studies have indicated the need to improve the bearing components inspection technologies rings on production flow to reduce inspection costs simultaneously with increasing the accuracy. Quality requirements of precision bearing components are becoming more stringent. Manufacturing costs and processing accuracy can be improved considerably by integrating automatic control equipment.

Before developing a performance measurement system it is necessary to understand the technology of bearing components processing, sources of errors in manufacturing process, requirements regarding to measurable characteristics. Such information shall serve as a basis for developing a control system in optimal quality cost. [2] [3]

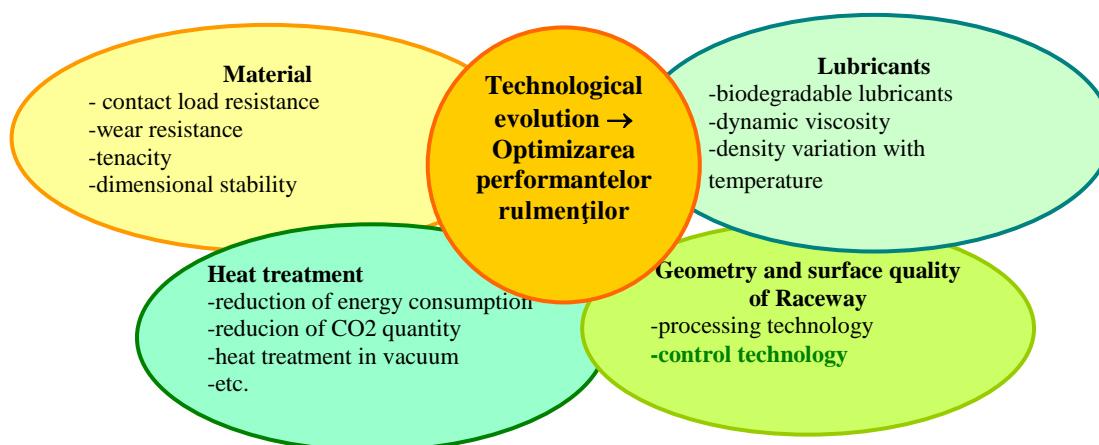


Fig.1 Trends in technological development for increasing quality of rolling bearings

The accuracy of rotation of the shafts supported on bearings depends on a number of factors. The most important factors are the position and form accuracy of the raceways of the bearing rings. DIN and ISO standards as well as the norms of national standard developing organizations, prescribe values of the dimensional, form and position deviations, which refers to the bore of the inner ring, the outer diameter of the outer ring, fillet radii or chamfers of both rings, width of rings, rotational accuracy (radial and axial runout, perpendicularity deviation, tilt). Amount of these deviations, for different bearing sizes, fit the bearings into various classes of precision. DIN ISO 620 and 492/199/582 define the dimensional tolerances of bearing fitting them into 6 accuracy classes. [5]

Dimensional and geometric deviations and raceway surfaces quality is fundamental to the level of vibration and noise, quality of rotary motion, lubrication, uniform distribution of forces on the contact line, the fatigue strength of the bearing. The quality of raceway surfaces is determined by the parameters of the cutting process, cutting tool geometry, the nature of the material being machined, the rigidity of technological system, cutting environment, etc. (fig.2) [2]

2. Dimensional and geometric measurable features of the bearing rings

The main measurable dimensional feature of the inner and outer rings of the bearings are: the inner diameter of inner ring, the outer diameter of outer ring, and the width of the rings. For the operation of the bearings, very important is the geometry of the raceways.

For ball bearings, the geometry of the raceway is defined in addition to the rolling diameter (diameter of an imaginary circle extent in a plane perpendicular to the axis of symmetry, in the deepest portion of the track of the inner or outer ring – Fig. 3) by the rolling radius (radius of the circular arc profile, in a plane which intersect the axis of symmetry - fig.3). These two parameters are very important because they influence the axial and radial clearance of bearing, contact angle and precision of the rolling movement. Rolling radius is not equal to the radius of rolling elements. The difference between these radii defines the curvature of the raceway (Fig. 3).

The main geometrical deviations of the bearing rings are: deviation of mean bore diameter, deviation of mean outside diameter, variation of rings width, radial runout of inner ring, radial runout of outer ring, axial runout.

The measurement principles for the main measurable characteristics of rolling bearings rings gauging according to ISO 1132 are shown in the table 1 [7].

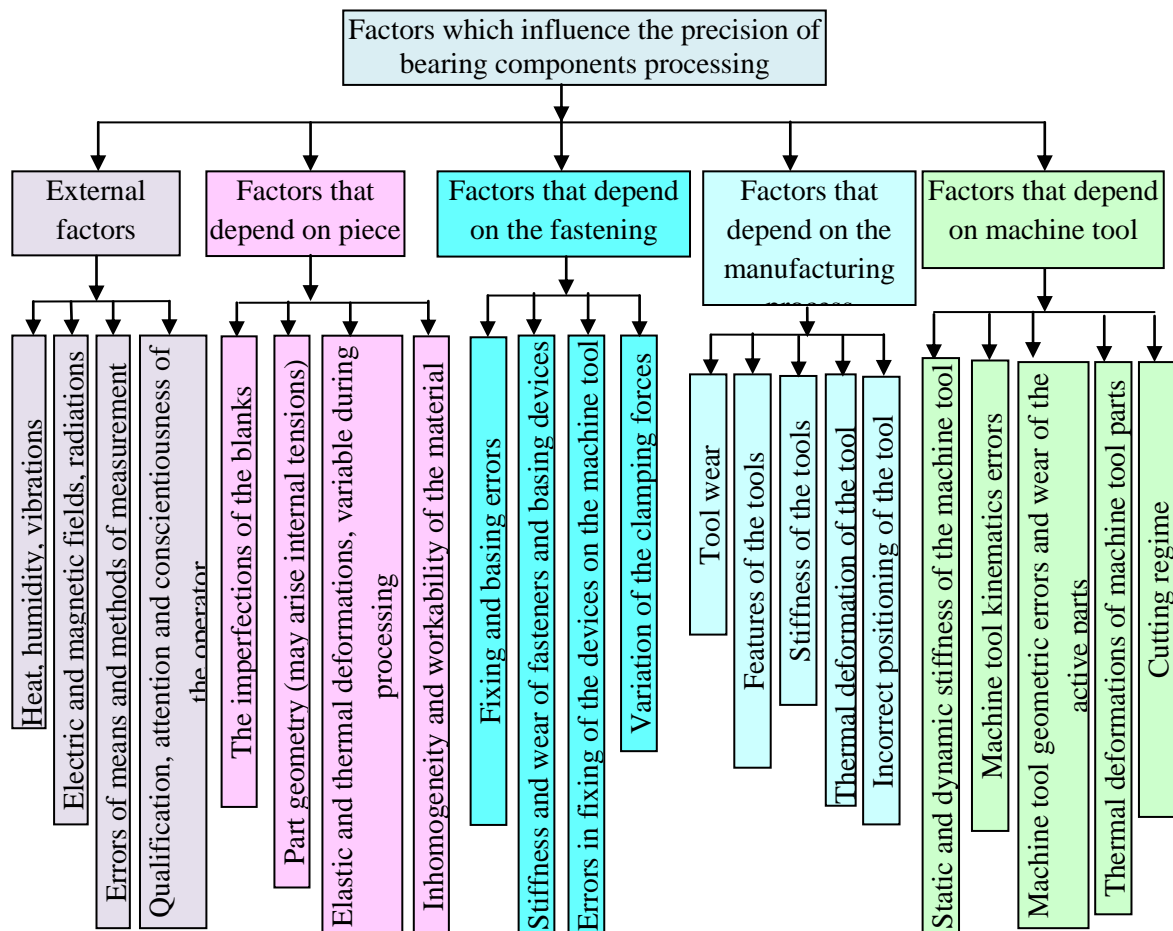


Fig.2 Factors which influence the precision of processing on machine tools

Rolling bearing rings measuring and gauging principles and methods

Table 1

	Measured feature	Measurement principle		Measured feature	Measurement principle
Dimensional features of inner ring	Inner diameter measured in a single plane d = nominal diameter (small diameter for tapered bore); d_1 = nominal large diameter for tapered bore; a = measurement distance $\Delta_{ds} = d_s - d$ = Deviation of bore diameter from nominal dimension		Geometric features	Deviation of bore diameter $\Delta_{dmp} = d_{mp} - d$ = Deviation of mean diameter from nominal dimension in a radial plane $V_{dp} = d_{ps\ max} - d_{ps\ min}$ = Variation of bore diameter in a radial plane = 2 x roundness (ISO 1132) a = measured distance	
	Inner diameters measured in multiple planes $V_{dmp} = d_{mp\ max} - d_{mp\ min}$ = variation of mean bore diameter in various radial planes a = Measured distance			Deviation of the outside diameter $D_{mp} = D_{mp} - D$ = Deviation of mean outside diameter from nominal dimension in a single radial plane $V_{Dp} = D_{ps\ max} - D_{ps\ min}$ = Variation of outside diameter in a radial plane = 2xroundness (ISO 1132) a = measured distance	
	Width measurement B = nominal width of the ring $B_s = B_s - B$ = Deviation of inner ring width from nominal dimension			Deviation of inner ring width $VB_s = B_{s\ max} - B_{s\ min}$ = Variation of inner ring width (axil runout)	
Dimensional features of outer ring	Outside diameter measured in a single plane D = Nominal outside diameter $D_s = D_s - D$ = Deviation of single outside diameter from nominal dimension a = Measured distance		Geometric features	Deviation of outer ring width $V_{Cs} = C_{s\ max} - C_{s\ min}$ = Variation of outer ring width (axil runout)	
	Outside diameters measured in multiple planes $V_{Dmp} = D_{mp\ max} - D_{mp\ min}$ = Variation of mean outside diameter in various radial planes a = Measured distance				<p>Track radius (R)</p> <p>Ball diameter (D_w)</p>

Fig. 3 Raceway curvature

3. Roundness measurement methods

For roundness measurement is required a reference. The roundness is usually assessed by measuring the radial deviation relative to a reference axis. This axis remains fixed and becomes the reference for all measurements. This requires a very precise rotary table to appreciate properly the deviations of measured parts.

According to the way to materialize the reference axis there are several ways to measure form deviation of circular profiles. The most popular method applied to measure circularity is:

V-block measurement method (three points method)

The part is placed on a V-block and is rotated manually while the workpiece surface is in contact with the probe of an indicator. The pieces should be rotated carefully to keep the contact with V-block (in two points) and with the probe of the indicator. This measurement method is very simple but has its limitations. Results may vary according to the angle of the V-block, spacing and phase of profile irregularities.

The obtained results may not accurately reflect how the part will function may not provide useful information for correction the manufacturing process. This method is only suitable for regular odd lobed profiles.

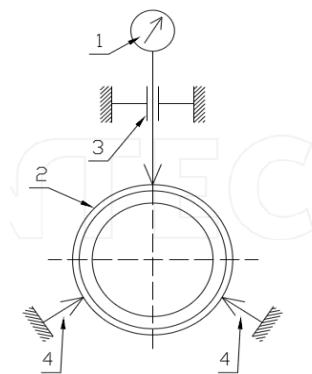


Fig.4 Three points method for the outer diameters measurement: 1. Comparison measurement instrument, 2. Measured part 3. Guiding element for ensuring measuring direction, 4. Fixed supports

Measurement method with rotary table

The method consists in positioning, centering, and leveling the piece on a rotary table and measuring the radial deviation relative to the axis of the table. Rotation table is supported on precise air bearings, oil bearings or rolling bearings. This universal method is used for small and medium parts. There are however limits related to the capacity of rotary table loading and centering precision.

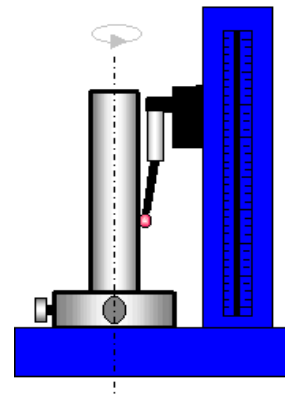


Fig. 5 Measurement equipment with rotating table

Measurement method with rotating probe

Another option for circular profiles measurement is to keep the part fixed while rotating the probe. This method is used in particular for large parts. This type of measurement systems tend to become more accurate due to continuous and constant loading of the work table, allowing better error correction.

In both measuring methods, with rotary table as well with rotary stylus, the rotary moving element must describe a "perfect" circle, taken as a reference.

The method with rotating stylus has some advantages [4]: the rotating shaft carries a relatively light and constant weight; there are no limitations of weight and shape of the piece (asymmetrical construction being allowed) because the part is placed on a fixed and stiff table; tracing an arc with fixed length can be better controlled with switches than in the case of the rotary table equipment.

The main disadvantages of this measurement method are: sizes of the pieces are limited by probe adjustment range; it is more difficult to position the probe in the grooves.

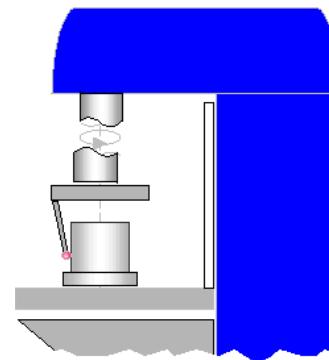


Fig. 6 Measurement equipment with rotating stylus

Analysis and interpretation of data is a complex process which often requires dedicated software for separation the deviations of concentricity between part and reference axis on one hand and shape deviations on the other had.

4. The reference elements, in relation to which is evaluated roundness

To assess the roundness, must be defined the reference element. Four reference figures are internationally accepted for roundness measurement. They are:

1. Least squares circle (LSC)
2. Minimum radial zone circles (MZC);
3. Minimum circumscribed circle (MCC);
4. Maximum inscribed circle (MIC).

The most commonly used as a reference is the **circle of least squares (LSC)**. It is defined as a line or circle where the sum of areas placed inside and outside is equal and kept to minimum separation. Roundness is then expressed as the maximum deviation from the LSC.

Minimum radial zone circle (MZC) is defined as two concentric circles positioned to enclose the measured profile such that their radial departure is a minimum. The roundness value is given by the radial departure between the two circles.

The minimum circumscribed circle (MCC) is defined like the smallest circle that totally encloses the profile. Out of roundness is the largest deviation of the profile from this circle.

Maximum inscribed circle (MIC) is the largest circle that is totally enclosed by the profile. Out of roundness is given by maximum radial deviation away this reference circle. Sometimes it refers to the reference circle of the plug gauge.

It is important to understand that using different reference circles for the same profile are obtained different results. This is not always evident, especially in the case of round parts.

5. Filters

To enable the operator to separate the desired from the undesired forms is necessary to use filters. The filters separate the different harmonic of the achieved profile. Circularity filters attenuate any undulation over a selected number allowing visibility of the desired component. Internationally accepted filters are: 1 - 15 u.p.r., 1 - 50 u.p.r., 1 -150 u.p.r., 1 -500 u.p.r. (U.p.r. = undulations per revolution). Reducing the number of undulations per revolution, are eliminated from diagram the peaks and valleys display with selected frequency. There are two types of filters: Gaussian and 2CR.

2CR filter (ISO 2CR) is an electronic filter used by early measuring instruments. It contains two capacitors and two resistors (hence the name 2CR). ISO 2CR removed first two cut-offs from analyzed profile. This filter is steel accepted still accepted and recognized by international standards despite the fact that it suffer from phase distortion caused by the nature of their electronic components. To minimize this effect, there was developed another type of filter called a 2CR PC filter. This filter removes first and last cut-off. This type of filter suffers from less distortion than the 2CR but is

still an electronic filter and, thus, still suffers from some distortion.

Modern instruments use *phase correct filters*, such as the *Gaussian filter*. Gaussian filter is a mathematically filter. These types of filters drastically reduce filter distortion, although they can only be implemented where filtering is done by mathematical algorithms: computer based processing. A property of this filter is its ability to account for the data obtained - equally - before and after the actual position of the probe when is calculated the average line. The value cut-off (UPR) is determined by the width of the Gaussian distribution curve. The effect from the selected filter is 50% of the maximum bandwidth. Gaussian filter removes half of the first cut-off of the analyzed profile and half of the last cut-off. [6]

6. Presentation of own solution

The constructive solution presented in this article is designed to measure the inner and outer diameters of the bearing rings. The fixing System allows precision rotating and centering of bearing rings. The part rotates and measurement system captures data from points on the outer or inner surfaces in the same horizontal plane. The measurement system can be moved vertically for measurement of circular profiles into different planes. Can be made measurements in as many plans.

The measurement system presented in figure 7 consists in:

- Specialized software TopGage for data acquisition;
- Transducer type TESA 03230200, equipped with USB interface (1) (it ensures the same precision in any place where is adjusted the zero position);
- Modular system manufactured by Horst-Witte (2);
- Positioning system on X, Y, Z axes, manufactured by Newport company (3);
- Computing system (4);
- Measuring bearing ring (5).

The Characteristics of the roundness measurement system by measuring the radius variation:

- The revolution axis of the measured part must be aligned with the reference (rotation) axes of the equipment; part revolution axis must be parallel to the rotation axis to avoid errors that occur due to the tilt;
- The measurement direction shall be concurrent and perpendicular to the rotation axis;
- Between the stylus and the part there is relative rotational movement;
- To facilitate interpretation of results, by reducing the influence of roughness, are used digital or electronic filters (generally low pass filters);
- The speed of the probe must ensure the necessary response time and it should not favor the loss of contact with the workpiece surface.

The measurement process consists in continuously scanning of workpiece profile, measurement of radius deviations in polar coordinates and comparison of the actual profile with a reference circular profile.

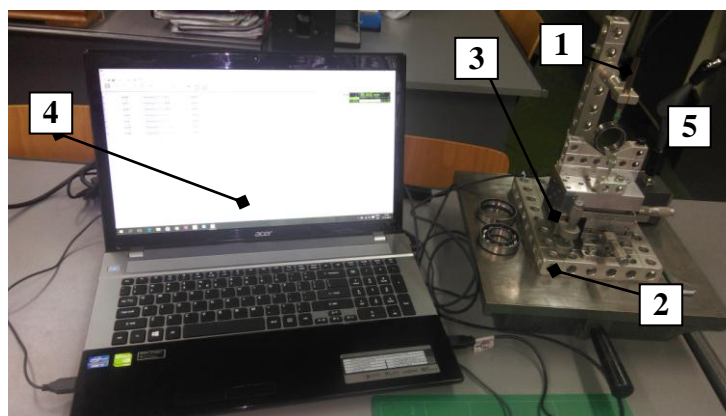


Fig.7 Hardware and software configuration of bearing rings system

Depending on the kinematics of the measurement system, there are two possibilities of measurement:

- Part is fixed and the transducer and probe are rotated around the reference axis;
- Part rotates and transducer and probe are maintained fixed.

The element with rotating movement must describe a "perfect" circle, taken as a reference. These devices use very sensitive transducers for measuring the roundness.

Distance between the axis of rotation and the contact point on the workpiece surface is considered to represent the instantaneous radius of the contact surface. Variation of the circumferential radius, determine the deviation from a perfect circle.

By its own design, the equipment shown in the above figures do not measure the nominal value of the radius, but only variation of the radial profile in a cross section of the workpiece relative to a perfect circle. Intelligent metering systems may determine also the radius / diameter of the circular profile.

Positioning the workpiece on the V blocks is using the gravitational force, measurement mass having an inclination of 20 °. This has the advantage of easily placing the piece in measurement position.

7. Experimental results

TopGage specialized software is versatile, being able to satisfy both quality control tasks and statistical processes evolution, easily configurable and it can work with a wide range of measuring instruments such as multi-parametric measuring devices with inductive or pneumatic transducers. [11]

In figure 8 is shown the windows for adding the part. In figure 9 is presented the window for setting the measurement instrument and in figure 10 is presented the window for setting the interface of the measurement probe.

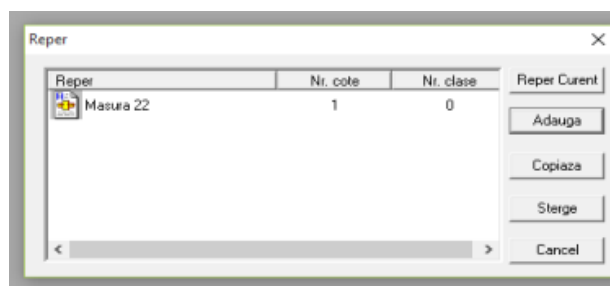


Fig. 8 Adding the part

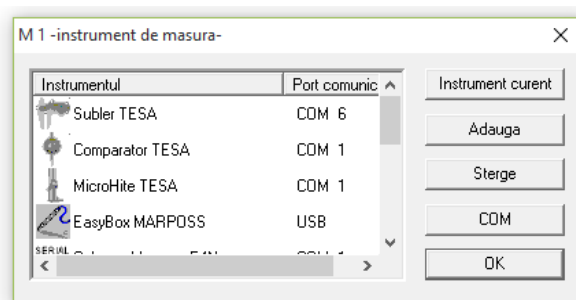


Fig.9. Adding the measurement instrument

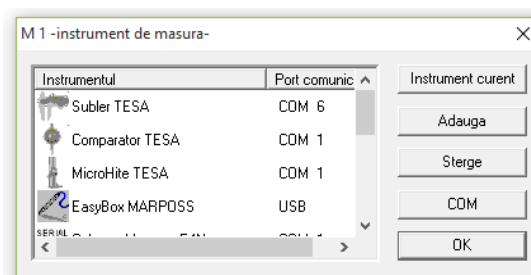


Fig.10 Setting the instrument interface - TESA USB PROBE

The resulting data from measurements are interpreted considering the limits of tolerances with the possibility of sorting the parts in precision classes. When performing a measurement there is the possibility of introducing comments about events that may occur during processing (tool wear, corrections etc.).

All this data, together with information on the person who made the measurement, date, time, are recorded in a document that constitutes measurement report. The program works under Windows operating system. Data acquisition from measurement instruments is done through standard interfaces: RS232 or USB. [11] [12].

According figure 11 the nominal value of the measured diameter is 36 mm. The measured values can be listed in a table such as in Figure 12. The measured values out of tolerance limits are marked with red and yellow color (figure 13). The measured data can be exported in xls format (figure 14).

The data in the measurement report are interpreted statistically and displayed in charts, putting into evidence parameters as X-R (Fig. 14), X-S (Fig. 15), Cp, limit control, with which the process can be analyzed and kept under control in order to obtain maximum stability.

The data in the measurement report are interpreted statistically and displayed in charts, putting into evidence parameters as X-R (Fig. 14), X-S (Fig. 15), Cp, limit control, with which the process can be analyzed and kept under control in order to obtain maximum stability.

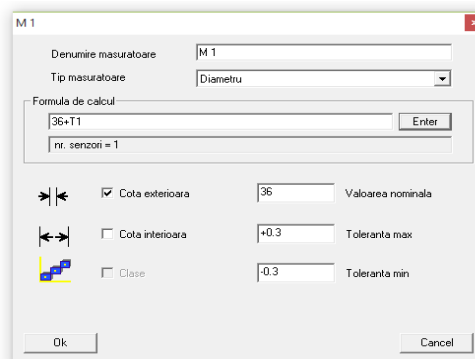


Fig.11 Introducing the nominal value of the dimension, the maximum and minimum tolerance an calculating formula

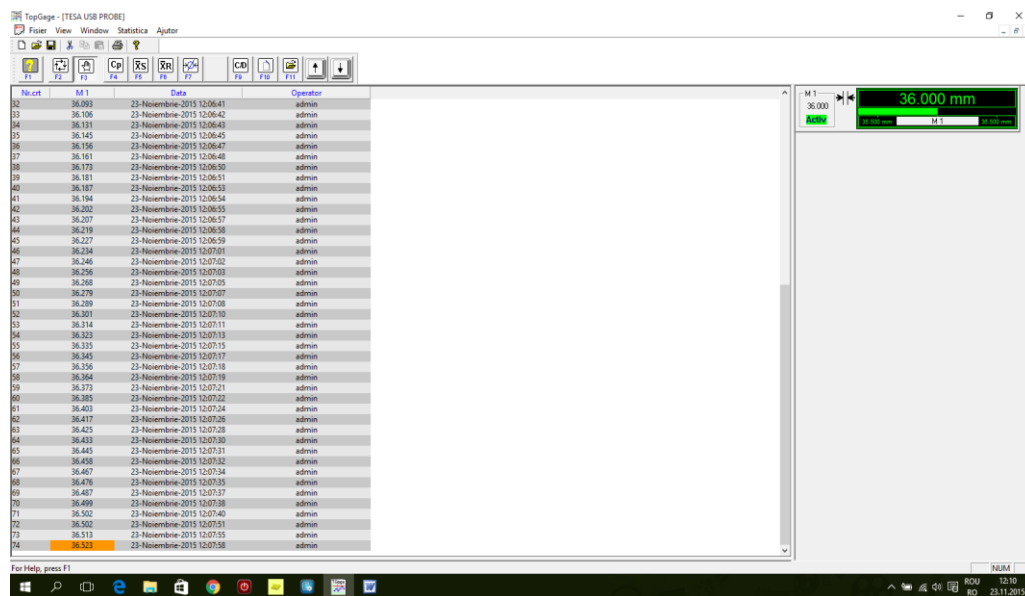


Fig. 12 Measured values

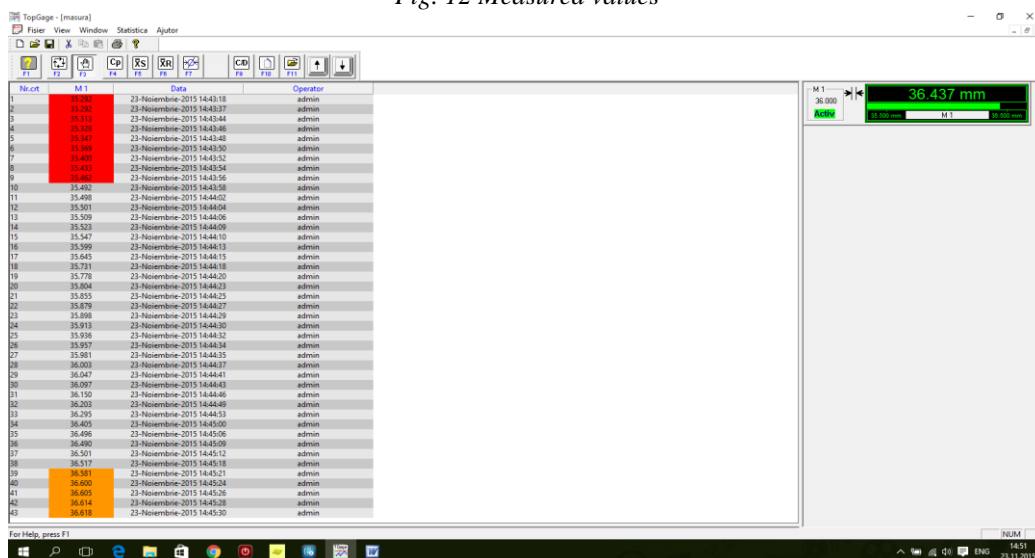


Fig. 13 Marking values are out of tolerance limits

Microsoft Excel - MASURA2

Nr.Crt.	M 1	Data	Operator
1	36	27.11.2015 12:06	admin
2	35.981	27.11.2015 12:06	admin
3	35.972	27.11.2015 12:06	admin
4	35.973	27.11.2015 12:06	admin
5	35.967	27.11.2015 12:06	admin
6	35.977	27.11.2015 12:07	admin
7	35.981	27.11.2015 12:07	admin
8	35.959	27.11.2015 12:07	admin
9	35.957	27.11.2015 12:07	admin
10	35.962	27.11.2015 12:07	admin
11	35.959	27.11.2015 12:07	admin
12	35.959	27.11.2015 12:07	admin
13	35.965	27.11.2015 12:07	admin

Fig.14 Data exported in xls format



Fig.15 X-S chart – for bearing ring with nominal value of outer diameter 36 mm

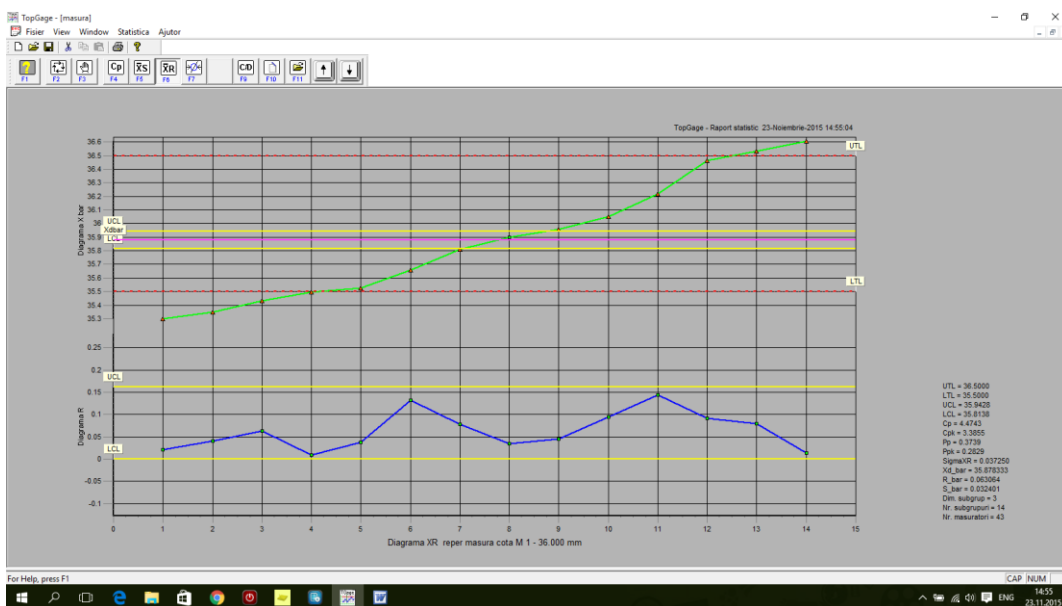


Fig.16 X-R chart - for bearing ring with nominal value of outer diameter 36 mm

8. Conclusions

When the range of products manufactured is very diverse, a more effective solution is the modular measurement systems. The control (inspection) equipments and devices with standard elements, with one or more measuring stations have a higher degree of universality and can be used for inter operational or final control, statistical control or for sorting parts in accuracy classes.

The evolution of multi-parametric control (inspection) equipment and devices was influenced by productivity growth and measurement accuracy increasing as a result of increasing manufacturing precision.

The main requirements of manufacturers refer to: conditions relating to productivity, autonomy in unsupervised operation, the degree of automation in measurement operations and decision on product quality (framing all measured parameters in tolerance limits and prescribed conditions).

Among the advantages of using installations and devices formed from standard elements may be listed:

- Qualitative improvement construction;
- Simultaneous checking of several parameters with the possibility of aggregation of results, thereby substantially decreasing time control compared to conventional control methods;
 - Reduce the duration and cost of design and execution;
 - Type the possibility of reuse elements in new combinations.
- The concept of "modularity" has emerged as a necessity to increase the flexibility of equipment. Modern modular systems combine the flexibility of a general device with the speed and accuracy of dedicated solutions.
- Are known several modular elements made of standardized functional and dimensional wider application in mechanical engineering, but they do not cover all situations specific control.
- Modular control, especially electronic ones, are intended to control more than two variables, simple form $\pm A$ and / or $\pm B$, AB or differential $-A + B$, $A + B$ or additive $-A -B$ and control functions for these deviations from the geometric shape or position. Among the advantages of using installations and devices formed from standard elements may be listed:
 - Qualitative improvement construction;
 - Simultaneous checking of several parameters with the possibility of aggregation of results, thereby substantially decreasing time control compared to conventional control methods;
 - Reduce the duration and cost of design and execution;
 - Type the possibility of reuse elements in new combinations.
 - The concept of "modularity" has emerged as a necessity to increase the flexibility of equipment. Modern modular systems combine the flexibility of a

general device with the speed and accuracy of dedicated solutions.

- Are known several modular elements made of standardized functional and dimensional wider application in mechanical engineering, but they do not cover all situations specific control.

- Modular control, especially electronic ones, are intended to control more than two variables, simple form $\pm A$ and / or $\pm B$, AB or differential $-A + B$, $A + B$ or additive $-A -B$ and control functions for these deviations from the geometric shape or position. Among the advantages of using installations and devices formed from standard elements may be listed:

- Qualitative improvement construction;

- Simultaneous checking of several parameters with the possibility of aggregation of results, thereby substantially decreasing time control compared to conventional control methods;

- Reduce the duration and cost of design and execution;

- Type the possibility of reuse elements in new combinations.

- The concept of "modularity" has emerged as a necessity to increase the flexibility of equipment. Modern modular systems combine the flexibility of a general device with the speed and accuracy of dedicated solutions.

- Are known several modular elements made of standardized functional and dimensional wider application in mechanical engineering, but they do not cover all situations specific control.

- Modular control, especially electronic ones, are intended to control more than two variables, simple form $\pm A$ and / or $\pm B$, AB or differential $-A + B$, $A + B$ or additive $-A -B$ and control functions for these deviations from the geometric shape or position. Partea superioară a machetei

Among the advantages of using equipment and devices with modular architecture, containing standard elements may be listed:

- improving the quality of the construction;

- simultaneous checking of several parameters, decreasing considerably control time compared to conventional control methods;

- reducing the duration and cost for design and execution;

- increasing equipment flexibility by rapid reconfiguring modular construction; modern modular systems combine the flexibility of a general device with the speed and accuracy of dedicated solutions.

Are known several modular elements made of functional and dimensional standardized wider application in machine building, but they do not cover all specific control cases.

Modular control systems, especially electronic ones, are designed to control more than two variables, simple form $\pm A$ and / or $\pm B$, differential $A-B$ or $A + B$, additive $A+B$ or $- A - B$ as well as other functions with these for form and position deviation measurement.

The use of the modular electronic configurations for measuring and taking decisions on part quality, offers the possibility of complex functions for calculation and correlation. They are characterized by versatility, high speed response, high speed for measuring and decision making, large possibility for automation and informational centralization of decision, remote control, etc.

Acknowledgement

This mechatronic equipment is developed under Partnerships in Priority Areas Programme - PNII supported by MEN-UEFISCDI, in the project PN II-PT-PCCA-2013-4-1671 – “Innovative mechatronic system for inspection of the bearing rings machined on CNC machines, as optimisation factor of processed surfaces quality – BeQuCon”, for experimental testing.

9. References

- [1] Cioboata D., Dontu O., Besnea D., Ciobanu R., Soare A., Equipment for bearing ring surface inspection, Romanian Review Precision Mechanics, Mhecatronic Optics & Mechatronics, Vol. 48 (2015), pg. 262-266, ISSN 1584-5982
- [2] Innovative mechatronic system for control rings bearings machined on CNC as a factor in optimizing the quality of machined surfaces – BeQuCon, Phase 1. Preliminary analyzes on the process of manufacturing bearing rings for define constructive functional requirements of control equipment. Financing contract no. 268 of 07.01.2014

BRAND:
«SMART MECHATRON - Competitiveness,
performance and high quality through
HIGH-TECH MECHATRONIC PRODUCTS »

RESEARCH AND APPLICATION OF OPTOMETRY RETINOSCOPY TEACHING BASED ON THREE-DIMENSIONAL SIMULATION

Jipan Yi

Zhejiang Industry and Trade Vocational College, Wenzhou, Zhejiang, 325000, China

E-mail: yijipan056@sina.com

Abstract - As the reform of optometry teaching gets thorough and developed, the educational technology based on computer technology has played an important role in optometry teaching. The application of three-dimensional simulation in conventional retinoscopy has great significance for improving teaching quality, stimulating learning interest and realizing teaching interaction. This paper analyzed the development, design and realization principle of teaching model of retinoscopy based on three-dimensional simulation together with its application in retinoscopy and suggested that the method was direct and vivid, had strong stereoscopic impression and optimized the teaching of key and difficult points.

Keywords: three-dimensional simulation; retinoscopy; teaching; optometry.

1. Introduction

This article aims to integrate the full control of the Three-dimensional simulation is a multimedia technology of generating a virtual environment with multiple sensations such as visual sense, auditory sense, tactile sense and gustation etc by applying computer technology. This technology allows people to interact with the entity in the virtual environment and it has been widely applied in military, medical science, architecture and entertainment etc [1-3]. Three-dimensional simulation with the vivid visual virtual reality technology has attracted extensive attention in medical education meanwhile provides a new development platform for the education and teaching of optometry [4].

Our optometry is a medical specialty of modern science and technology which combines conventional optometry and ophthalmology organically [5]. Eye is the work object of this specialty and vision the work objective which is to say the goal of the work is to improve eyesight and visual function; light is the most important method of the work and treatment, the light refers to optics instruments, optics medicine, laser, chemicals and operation etc [6]. Due to the peculiarity of the specialty design, the development of the subject depends on the interaction and infusion of many subjects including foundation medicine, clinical medicine, physical optics, geometrical optics, ophthalmic optics, materials science, instrumental science, ophthalmology and vision science etc, which make optometry difficult to teach well or learn well. Optometry technique is a highly practical and applied specialty, which demands proficient practical skills and problem solving ability besides the necessary basic

theory knowledge. Hence, during the cultivation, importance should be attached to the training of practical ability and the acquisition of vocational experiences and skills.

Retinoscopy is a most applied, most practical and most accurate objective optometry [7]. All the time, the teaching of retinoscopy is performed by the teacher observing with naked eyes through optical lenses and then dictating the results to the students. There was no way for direct comparison between optometry results of the teacher and the students, meanwhile the images and video could not be recorded. Students could only comprehend the teacher's result subjectively; the student's mistake of the optometry results could not be pointed out, which affected the effect of retinoscopy teaching. Even the application of multimedia information such as images, flash and video didn't work well. One of the solutions to the problems mentioned above is applying three-dimensional simulation. The teaching and research office of optometry of our hospital applied three-dimensional simulation into the radiology teaching for the first time, which had great significance for improving teaching quality, stimulating learning interest and realizing teaching interaction.

2. Technological realization of teaching model of retinoscopy based on three-dimensional simulation

2.1 Pre-phase analysis

Pre-phase analysis is the basis of the realization of the teaching model and the analysis of the teaching materials and parsing of model and flash. Our model analysis included the spatial structure of eyeball, the composition of skiascope and flash parsing which was composed by optical principle of skiascopy, image

motion under different refraction conditions and the relation between image motion and refraction condition.

2.2 Model making

The foremost task of three-dimensional simulation is to present experimental phenomenon faithfully and the accurate virtual model provides students the real three-dimensional feelings [8]. The model which mainly included eyeball, roles and skiascope was made by using Maya2014 software. Eyeball making: (1) firstly, lead in clinical eyeball vertical plane and striograph of cross section for reference and build Nurbus eyeball model combining eyeball dissection data. (2) Then shift into the level of model editing and perform precise adjustment. (3) At last, create virtual environmental light and apply different material for different tissue according to retinoscopy knowledge of ophthalmology. For example, we made cornea and crystalline lens with transparent materials and adjust relevant refraction and reflection coefficient to simulate the effect of real eyes. The character role model and ophthalmoscope were built applying polygon modeling.

2.3 The application of texture and map

Divide the model when the eyeball model is done, and make UV map for sclera, iris and retina

respectively. We drew the maps referring to clinical photos and applying Photoshop CS6.0 software. The maps were drawn and applied to relevant model in three-dimensional software and then the UV distribution was arranged to resemble the clinical performance. The maps application of character role was the same as above.

2.4 Flash and render output

The flash was made using Maya2014 software. Firstly, light (light from skiascope) was needed besides environmental light and the light source was moved to position which made it look like light given out from skiascope; adjust the light margin, distance and attenuation etc to make it more real. What's more important is the knowledge of retinoscopy principle is mainly about the performance of light which made light fog effect needed when we render the flash. The light fog made the light path more visible and the presentation of optical principle more direct, for example it expresses as smooth motion when the far point of the light reflected by retina rests behind the skiascope and it expresses as reverse motion when the far point rests between tested eye and skiascope, as shown in figure 1.

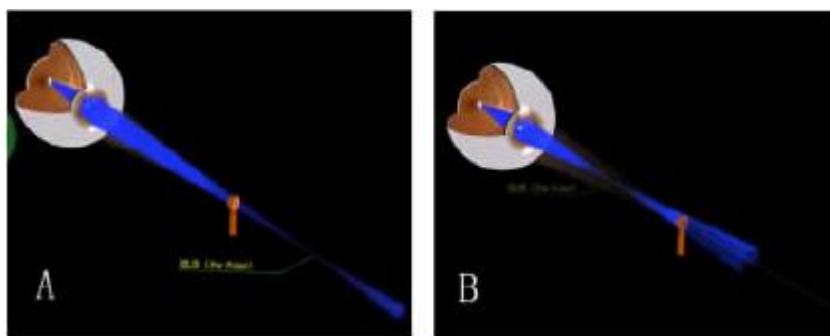


Figure 1 (in figure A, the far point rest behind ophthalmoscope; in figure B, far point rest before ophthalmoscope)

As the image motion of retina reflective strip is hard to be realized faithfully during skiascopy, we set a simulative reflective strip behind the pupil and

meanwhile adjust the light ray of skiascope to stripped light so as to simulate the real condition, as shown in figure 2.

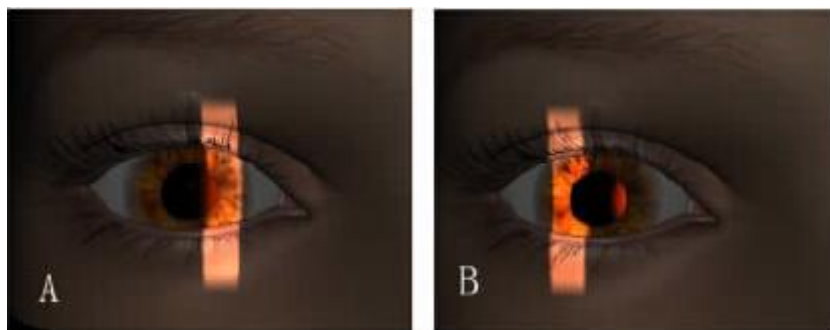


Figure 2 (image motion in A shows as smooth motion; image motion in B shows as reverse motion)

When analyzing the images, we should comprehensively consider the image motion speed, luminance and light band width to reach the correct conclusion [9]. Though the speed of smooth move and

reverse motion should be the same, the patient's pupil was filled with light during inverse motion and light band appeared when it was smooth motion. Thus, the shadow motion speed of smooth motion was thought

faster than reverse motion. Flash made applying three-dimensional simulation reflects those features vividly and benefits optometry teaching.

3. Teaching application effects

3.1 Direct and vivid teaching effect

At present, multiple media network interactive teaching based on three-dimensional simulation gets the teaching process lively and vivid with innovation, configuration of content, high teaching efficiency and has become an important teaching method which applied in medical education. Conventional retinoscopy theory teaching focuses on the analysis of optical principle and light path graph [10]. Teacher could only dictate the skiascopy images of the experimental lesson to the students while demonstration using synchronous flash was not accessible. Similarly, the student's skiascopy results could only be checked by another experiment. Optometry retinoscopy teaching applying the flash developed through three-dimensional simulation technology improves the teaching with real-time and dynamic skiascopy video. These methods syncs the expression of images, flash health card and literal data, and demonstrates abstract teaching contents which is barely described literally with synchronous flash [11]. We applied this method in the teaching and training of undergraduates admitted in 2010 and 2011. With synchronous expression of literal data, this method enabled the students to receive the knowledge directly and profoundly and provided a platform for the students to combine perceptual and conceptual knowledge together. Meanwhile, the students could better understand the basic principle of retinoscopy, eyeball refraction structure and operating points of skiascopy etc. The interest was stimulated to the best and study enthusiasm and initiative aroused.

3.2 Optimization of the teaching of the key and difficult points

Multimedia teaching combined with three-dimensional simulation applying network resource focuses on the student and transforms the central position of the teacher. It attracts the students with lively and vivid graphics and text information and arouses study interests, encourage the students to learn and explore positively. Conventional optometry retinoscopy teaching can not describe the complex image motion feature clearly or method of image motion feature interpretation [12], while the development and application of model and flash above can vividly explain the abstract theory of retinoscopy teaching and the changing process of multiple dynamic conditions, especially peculiar conception of retinoscopy such as "neutralization judgment", opened image moving and "shear effect" etc [13,14]. The demonstration applying three-dimensional simulation and combining with images, characters, audio and flash can directly and clearly explain the key and difficult points, elevate the students' cognition from abstract conception to the perceptual level, which helps them

with the comprehending and handling of the key and difficult points.

4. Conclusions

In a word, during the teaching of optometry retinoscopy theory, we should make full use of three-dimensional simulation model and the development and application of flash along with physical advantage of conventional teaching. Body language such as sound, gesture and expressions along with tidy and beautiful blackboard-writing activates classroom climate. The method guides students think positively and initiatively meanwhile trains their study skills. Optometry retinoscopy teaching based on three-dimensional simulation prevails in directness, vivid, strong stereoscopic impression and optimization of key and difficult points teaching. With the development of computer science, the medical inspection equipment renews continuously and the digitized transformation of medical equipment has become a tendency of modern medical development. Sufficient and reasonable application of new technology assisting medical teaching will promote the thorough teaching reform of each medical subject and accelerates the renewal of conception and methods of conventional teaching.

5. References

- [1] Ying Zhang, Yuanjun Xia, Lei Wan, Qingshui Yin. Computer Aid Designed Operation of Tibial Plateau Fracture by 3D Simulation Technique. *J. Chinese Journal of Bone and Joint Injury*. 25(8): 686-688. 2010.
- [2] Zhenhua Du, Chengxing Liu, Jianguo Xu, Lei Li. Application of 3D Simulation Technology into the Assembly Procedure of Paralleled Rings of Large-size Generators. *J. Electrical Machinery Technology*, (4): 29-32. 2014.
- [3] Yi Pan. Study on Virtual Dispatching of Logistics Port Activities Based on 3D Simulation Technology. *J. Logistics Technology*. 33(3): 439-441. 2014.
- [4] Keedy AW, Durack JC, Sandhu P, Chen EM, O'Sullivan PS, Breiman RS. Comparison Of Traditional Methods With 3D Computer Models in the Instruction of Hepatobiliary Anatomy. *J. Anatomical Sciences Education*. 4(2): 84-91. 2011.
- [5] Yunzhuo Bian, Lei Wang, Qiangqiang Guo, Yi Dong. Exploration of the Integration Teaching Model of "Teaching, Study and Practice" of Optometry. *J. Education Teaching Forum*, (37):84-85. 2012.
- [6] Xinyu Hou. Analysis of Information-based Instructional Design of Optometry Retinoscopy in Secondary Vocational School. *J. Occupation*, (35): 102-102. 2013.
- [7] Bo Liu, Zhigang Liu, Yan Fang. Application Study of Skiascopie in Screening and Diagnosis of Suspected Keratoconus. *J. Journal of Dalian Medical University*. 34(3): 252-256. 2012.
- [8] Yufeng Tuo, Wei Wang, Kai Qiu, Fenghua Song, Feifei Yu, Yao Wang, Yongsheng Wang. Application of

3D Simulation Technology of AWX Format Infrared Satellite Cloud Image Based on OpenGL. J. Journal of Meteorology and Environment. 27(2): 25-31. 2011.

[9] Dan Sun. The Application of Multimedia in Optometry Teaching. J. Medical Forum in Basic, 14(28): 942-943. 2010.

[10] Liang Ye, Xiaoxing Wang, Meixiao Shen. Application of Retinoscopy Theory Based on Digital Technology Transformation in Teaching. J. Health Research. 30(2): 159-161. 2010.

[11] Ke Tang, Xinhua Pan, Shouwang Cai, Yuan Gao. Application of 3D Stereoscopic Display Technology in

Simulation Training System for Liver Surgery. J. China Medical Education Technology. 25(5): 522-525. 2011.

[12] Lihui Chen, Guorong Shi. Exploration of Open Experiment Teaching Method of Optometric Technique in Five-year High-graded Vocational School. J. Examination Weekly, (15): 151-152. 2014.

[13] Junfeng Si, Jing Liu. Exploration of Double-center Teaching Model of Optometry Experimental Teaching. J. Researches in Medical Education. 26(2): 92-93. 2014.

[14] Wei Yan, Shichao Yan. Construction and Practice of Practical Teaching System of Optometry. J. Vocational Education Research, (5): 126-127. 2012.

BRAND:
«SMART MECHATRON - Competitiveness,
performance and high quality through
HIGH-TECH MECHATRONIC PRODUCTS »

AUTOMATION OF GEAR PUMPS TESTING USING PROGRAMMABLE LOGIC CONTROLLER

Dr.Ing. Paul-Nicolae Ancuta, Dr.Ing. Iulian Vasile, Ing. Anca-Irinel Atanasescu, Ing. Sorin Sorea
National Institute of Research and Development in Mechatronics and Measurement Technique, Bucharest,
E-mail: incdmtm@incdmtm.ro

Abstract - Industrial process automation typically involves high costs for design and maintenance. Changes and modifications in the system throughout its life cycle are significant. PLC programmable controller is a digital computer used for automation of industrial processes. Using PLC requires less electrical design and more software design and implementation. The paper shows the main steps in making conceptual model for equipment dedicated to gear pumps testing. It analyzes the relationship between the costs of the automation system's configuration effort and software involved.

Keywords: Gear pump automation, PLC (programmable logic controller), debugger, PC computer vs PLC equipment

1. Introduction

The main purpose of PLC automation is replacing old cabinets containing relays, switches, mechanical timers and sequencers. Digital input signals processed by PLC are generated by push buttons, sensors and transducers, smart cameras and others. PLCs generate digital output signals who can operate electric motors, pneumatic, hydraulic, magnetic relays, indicator and warning light signals and other. PLC may include analog signal processing modules (pressure, temperature etc.) for closed-loop control systems.

The operating principle of a PLC consists of three sequential processes which run permanently:

- read input data from the hardware physical devices
- proceed with the software logic which is embedded in the PLC program memory
- update internal data and send output values to output devices accordingly

In order to get overall accurate results, automation systems made with PLC are real-time systems, as output values must be delivered within a well-defined time period.

PLC incorporate physical communication ports, usually RS485. Their architecture can also embed other various communication modules to accomplish data communication protocols.

2. Summary of activities

The first phase is planning and configuration. A project containing hardware configuration and user interface device will be created. Also, input and output signals will be defined.

A simple system may use buttons and signaling lamps for user interaction, but usually automation system are using a Human Machine Interface HMI device. That kind of device provides an easy and

intuitive interaction with the system for configuration, alarm reporting, message archiving, logs and routine control procedures of process automation. Another possible option is using a PC computer as operator panel. These two methods will be detailed below.

It will also determine the floor plan of the according to beneficiary demands.

The second phase is software implementing and testing. Automation state machines, logic software as well as data visualization functions, messages, state will be implemented and tested. Offline testing program will be carried out using simulation software.

The third phase is commissioning. At the very beginning, diagnosis pattern tests will be operated by the PLC itself. PLC status is shown by colored LEDs in a green-yellow-red manner. In case of Diagnostics software modules will show up the details of the errors. If everything works correctly, software modules will be tested using the integrated debugger.

The fourth phase is current operation and maintenance. Software tools provided by Siemens SIMATIC can remotely monitor system operation.

3. Hardware design

In terms of automation, the stand will feature two levels:

- PLC device, using modules from Siemens S300 CPU family, comprising an operator panel, optionally, and the following hardware modules:

- 0..24 V digital inputs
- 0..24 V digital outputs
- ADC channels - current and voltage
- DAC channel
- counter
- data communication modules - RS232, Ethernet

PC computer

It will be used for data storage, operating diagrams and programming environments.

Optionally, the computer can be used as operator panel PLC.

The stand for measuring the pump's pumps will contain the following main elements:

-an electrical engine of 20 kW .

Operation will be done at two speeds , 1500 rpm and 3000 rpm . Ensuring these rotational speeds can be done either by switching relays or by equipping the engine with a servo equipment. Either the relay or the servo controller will be connected to the PLC. In manual operating mode, the engine can be turned on/off using buttons START-STOP.

- A proportional valve which acts as an oil pressure regulator. Pressure range will be about 0-350 Bar.

Pressure will be set and maintained at a certain value as described in the operating diagrams.

- Temperature, pressure, speed, flow and torsion transducers [1] .

These transducers will be connected to the analog input module in the PLC rack and will be used to measure the actual values taken from the measurement process. Special attention should be paid to speed transducer. The size of the output is a pulse train which must be counted somehow by a dedicated module of the PLC.

This module must have a proper working frequency. We can use an intelligent transducer, capable of delivering proper counting values as data streams.

4. Software Component of the automation system**Programming Environments**

PLC will be programmed with Simatic STEP7 software package [2] . Operator Panel will be programmed with the software package WinCC Flexible [3] . PC computer programming will be done using a universal programming language, eg C ++ [4] . Programming the actuator controller of the servo equipment will be accomplished using a dedicated software supplied by the company producing the actuator .

Software

PLC program will implement two operator modes: automatic and manual.

Special attention will be given to the identification and treatment of the errors occurred during the testing pumps process. Safety measures will be implemented , both for the operator and stand, using software sequences or hardware security barriers. The operational flow is depicted in Table 1

Table 1- Operational flow

Nb	PC computer	PLC equipment
1	Power on	Power on
2		Display the ID of the active operating diagram
3	Operator selects the type of the mechanical part which will be mounted on mechanical stand	
4	Operator enters the ID of the part	
5	Operatorul enters the ID of the operating diagrams that will be used and send these three data to the PLC	
6		PLC software compares the local ID of the active operating diagram with the ID of the data received from PC. If they are noth equal, it request the PC to send the whole operating diagram data set.
7	I fit is required, operator will send the operating diagram's data to the PLC.	
8	Software enters WAIT state in order to obtain the final values from PLC.	Waiting fron START button to be pressed.
9		Testing as active operating diagraeme states.
10		Calculus is performed. The values of volumetric , mechanical and total efficiency are displayed on the operator panel and are being sent to the PC
11	The results are stored in database tables. A report may be delivered	
12	Renter at step nb. 3	

5. Data structures

The set of parameters that uniquely defines a measuring cycle is known as an operating diagram.

In our acceptance, there are two types of operating diagrams: -testing diagrams (Fig. 1)

They involve alternating and pulsing equipment operation.

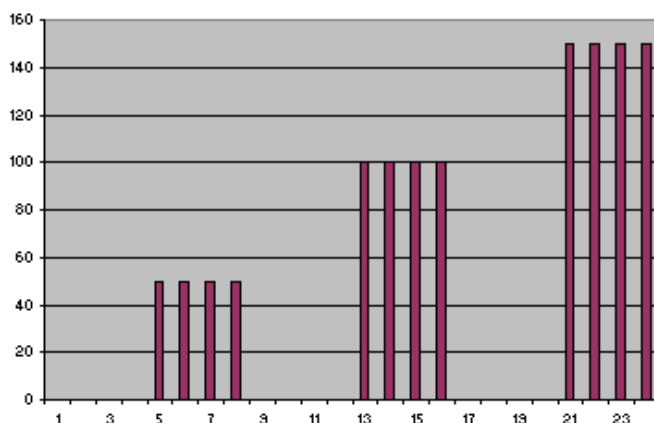


Fig. 1 Example of Testing operating diagram

- operating diagrams used for whole range measuring report WRMR

The engine speed is maintained constant and the pressure is constantly increased up to an imposed limit value.

Both operating diagrams types will be stored in tabel form database –Table #2. The operating diagrams will be uniquely identified by an ID. The operating diagram must be loaded into the PLC memory before the measuring cycle cam proceed.

Table 2- Operating diagrams’s data structure

ID	Type	Parameters			
		P1	P2	...	Pn
CT1	Testing				
CT2	Testing				
...					
CTn	Testing				
CB1	Whole range measuring report WRMR				
CB2	Whole range measuring report WRMR				
...					
CBm	Whole range measuring report WRMR				

Each pump type will be associated with a data set characteristics: volume , the maximum values of efficiency a.s.o. A table containing types of existing pumps manufactured by the customer will be created -Table 3 .

Table 3 – Set of pump’s types

Pump type	Characteristics				
	Volume -cm 3	Other	Mechanical efficiency η_m	Volumic Efficiency η_v	Total Efficiency η_t
Type 1					
Type 2					
...					
Type n					

A table of association between pump type and identification for each pump will be provided- Table 4.

There will be also a table of association between pump type and sets of possible operating diagrams- Table 5 .

The relationship between columns is “one to many”.

Type-Serial ID association Type-Operating diagram association.

Table 4

Pump type	Pump Serial ID		Pump Type	Operating diagrams	
				Testing	WRMR
Type 1	12345		Type 1	CT 1	CB 1
	23456			CT 2	CB 2
...	...			CT 3	
Type 2	QAZ12345		Type 2	CT 4	CB 3
	QAZ23456			CT 5	CB 4
...
Type n	QW12345		Type n	CT 20	CB 15

Using all these normalized tables, the pump having its unique ID will be tested using the selected operating diagram – Table #6. That pieces of data will be loaded into the memory of the PLC.

Table 5 – Pump ID – operating diagrams associations

Pump Serial ID	Type of the operating diagram	ID of the PLC operating diagram	Operating diagram parameters				Pump type characteristics				
			P1	P2	...	Pn	Vol.	...	η_m	η_v	η_t
12345	Testing	CT 2									
12345	WRMR	CB 1									

A measuring report will be issued.

Possible implementation of operator panel

As mentioned above, the operator panel can be freestanding or one may use the same PC that stores operating diagrams, constant data tables and tables with calculated results.

Nr.	POSSIBLE APPROACH	PROS	CONS
1	PLV has got its own operating panel	<ul style="list-style-type: none"> Creating user screens, tags, alarms and warning is easier by using a robust programming environment WinCC Flexible The PLC can operate independent of the PC when the actual diagrams are loaded into the memory 	The cost involved with the operator panel
2	PLC uses the PC computer as an operating panel	<ul style="list-style-type: none"> Creating user screens, tags, alarms and warning is easier by using a robust programming environment WinCC Flexible Reducing costs 	<ul style="list-style-type: none"> Changing between two software application-sending/receiving data to/from PLC and operating panel-could be annoying.
3	PLC uses the PC computer as an operating panel, but with a custom made software application	<ul style="list-style-type: none"> Reducing costs 	
3.1	PLC and PC computer are connected using RS232 interface	<ul style="list-style-type: none"> That piece of software has already been developed. 	<ul style="list-style-type: none"> A RS232 hardware module must be bought for the PLC.
3.2	PLC and PC computer are connected using PROFIBUS Protocol	<ul style="list-style-type: none"> That piece of software has already been developed, using OPC server 	<ul style="list-style-type: none"> A PROFIBUS card module must be bought for the PC. An OPC Server license for the PC must be bought
3.3	PLC and PC computer are connected using Ethernet Protocols	<ul style="list-style-type: none"> That piece of software has already been developed, using either OPC server or an open-source software library 	<ul style="list-style-type: none"> A Ethernet hardware module must be bought for the PLC. Optionally An OPC Server license for the PC must be bought.

6. Results

Carrying out a test operating diagram is as follows: the speed and pressure outputs are imposed and maintained for a few seconds as in the operating diagrams, then for a few seconds the pressure is zero. The engine speed is maintained and the pressure increases to another value. After a while, the engine speed is increased and the alternating pressures cycle is resumed. The output actual values are acquired all the time for monitoring purposes. The last set of transducers values are used for calculus.

The purpose of the test operating diagram is delivery of three final values, ie volumetric efficiency, mechanical efficiency and total efficiency.

As for the other type of diagram, the actual output values are acquired all the time, both for monitoring and for calculation. In this way, a chart with three curves to represent the evolution of the three rates will be obtained.

Future works

Research and experiments will be conducted for remote monitoring of the equipment.

7. References:

- [1]*** Catalogues edited by the following companies:Siemens,Omron,Schneider,ABB,Horner
- [2]*** SIMATIC Programming with STEP 7 Manual Edition 03/2006 A5E00706944-01
- [3]*** SIMATIC HMI WinCC flexible 2008 Compact / Standard / Advanced User's Manual, Edition 07/2008 A5E01024750-02
- [4] Wilkey,Steve Gary,Sangeeta Meyyammai, Subramanian MFC Development using Microsoft Visual C++ 6.0, Microsoft Press, 2000, ISBN 0-7356-0925-X.

BRAND:
«SMART MECHATRON - Competitiveness,
performance and high quality through
HIGH-TECH MECHATRONIC PRODUCTS »

PARAMETRIC MODELING ANALYSIS OF BATTLEDORES MADE OF BRAIDED COMPOSITE MATERIALS BASED ON ANSYS

Lei Guo¹, Bo Liang¹, Lina An²

¹ Department of physical education, Shandong institute of business and Technology, Shandong, 264005, China

² Dalian Medical University sports research department, 116044, China

Correspondence to Author: Lina An

E-mail: anlina23@163.com

Abstract - Braided composite materials by virtue of their good mechanical properties, such as high strength and modulus, are widely applied to the manufacture of battledores. In this study, battledores were taken as the research objects, and finite element parametric models of two-dimensional biaxial and two-dimensional triaxial composites battledores were constructed on the basis of ANSYS software; moreover, the battledore models in two kinds of braided forms were given overall mechanics analysis as well as invalidation discrimination analysis, which provided the structural design of battledores with a comprehensive theoretical basis. In addition, the performance prediction of the shaft of battledore was carried out, and results showed the enforceability of finite element regional method of superposition. At the present stage, researches on composite materials mainly focus on a representative unit cell model, while integral components of braided composite materials are rarely studied. Therefore, the finite element parametric modeling and numerical simulation analysis of the integral components of battledores made of braided composite materials are particularly important.

Keywords: ANSYS; braided composite materials; battledores; parametric modeling.

1. Introduction

Composite materials refer to a material system formed by two or more than two kinds of materials that have different physical and chemical properties in different structural levels through complex spatial organization [1-2]. Such kind of materials obtains new properties that none of the components have; besides, strength, rigidity and other mechanical properties of composite materials can be improved through changing categories and proportions of the component materials [3-4].

Braided structural composite materials are obtained by the combination of preforms and matrix phase materials, in which the preforms have integral structural properties and are formed by different braiding methods, especially the two-dimensional or three-dimensional braiding methods. Thus braided structural composite materials usually have different prominent mechanical properties [5-6]. Since 1970, braided composite materials have given full play to their superiorities with the rapid development of weave machinery [7]. Carbon fibers are widely used in production of fishing poles, golf rods, complete carbon battledores, tennis rackets, running machines and other sports and exercise machines made with braided composite materials, which account for about 35% of the total application amount of carbon fibers worldwide [8-9]. In recent years, a lot of experts and scholars in

China and abroad have carried out researches on this. In 2014, Wang WB, Cheng K and Cheng L et al. [10] constructed a micro-structural model based on braiding technique rules of braided composite materials; changes of yarn packing factors and distortion of the cross-section caused by different tightened conditions of yarns were considered in the model. In 2015, Boukellal A, Boumrar K and Mokdad R et al. [11] discovered the integrity of fiber bundles in braided composite materials as well as the intricate chiasmic structures of fibers in space; besides, they also predicted the elasticity modulus and shear modulus, etc., on mechanical models constructed based on finite elements.

On the basis of method of superposition of regional finite element, this study constructed an overall parametric finite element model of battledores, carried out relevant mechanical analysis as well as evaluated the battledores from the aspects of overall equivalent stress, strain and inherent frequency [12], which provided a theoretical basis for overall component design and optimizing of battledores and even other relevant braided composite materials in the future, instead of only relying on experience and expensive experiments.

2. ANSYS software and finite element analysis of braided composite materials

2.1 Brief introduction of ANSYS software

ANSYS, as a mature kind of software of finite element analysis, is a combination of structures and various kinds of physical field researches, which is mainly composed of pre-processing module, analytical calculation module and post-processing module. The pre-processing module is mainly responsible for setting of properties, units and mesh densities of different materials for construction of a finite element model of the whole structure model; the analytical calculation module mainly applies correct boundary conditions and loads according to the actual stress state on the basis of previously constructed finite element model, thus to perform statics and dynamics solution computation; the post-processing module is mainly responsible for final computation results display in diagrams, isoplethic

curves or other forms, such as equivalent stress distribution and equivalent strain distribution, etc. [13].

2.2 Finite element analytical model of braided composite materials

Boolean operations were used in ANSYS. Real braided composite material model could be obtained by subtracting constructed matrix phase model using fiber reinforcing phase model, and the finally obtained two-phase finite element model had no crossing or overlapping in spatial structures; moreover, special elements were added at the junction of two-phase model. Finally, pre-processing preparatory works were completed by adding periodic boundary conditions in the constructed model [14].

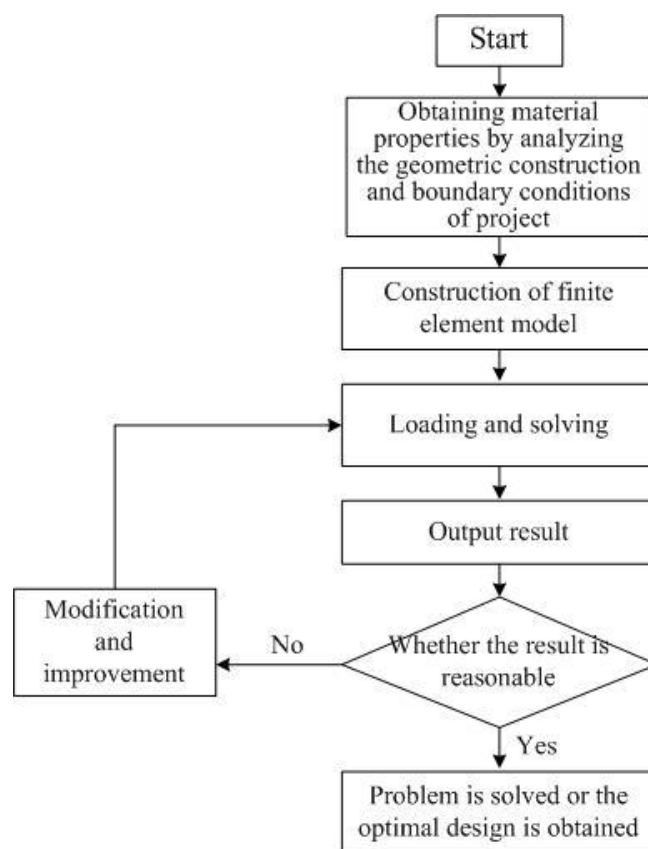


Fig.1 Flow chart of finite element analysis

2.3 Periodic boundary conditions

Under the loading effect, the modification of boundary surfaces of adjacent unit cells of braided composite materials should be the same, and the modification of any point on the surface and its corresponding node should stay the same.

For any pair of parallel surfaces, their displacement fields can be expressed by the following equations:

$$\mu_i^{j+} = \varepsilon_{ik} X_k^{j+} + \mu_i^* \quad (1)$$

$$\mu_i^{j-} = \varepsilon_{ik} X_k^{j-} + \mu_i^* \quad (2)$$

The positive signs and negative signs in above equations refer to the positive direction and negative direction of X axis respectively, and the combination of above two equations generates the following equation:

$$\mu_i^{j+} - \mu_i^{j-} = \varepsilon_{ik} (X_k^{j+} - X_k^{j-}) = \varepsilon_{ik} \Delta X_k^j \quad (3)$$

The realization of algorithmic processor description language (APDL) programming requires one-to-one correspondence of coupling nodes, and coupling relationships of correspondent nodes are realized through equation (3), thus to determine the periodic boundary conditions.

2.4 Merits and demerits of traditional modeling method of braided composite materials

Merits: traditional modeling method of braided composite materials can veritably simulate the spatial structure and material property of wild phase and matrix phase, thus the stress results and strain results obtained by traditional method have high precision.

Demerits: (1) spatial models of fiber bundle are entwined and two phase models are crossed and overlapped inevitably, thus the modeling process of traditional braiding method is time-consuming and energy-consuming.

(2) The process of handling contract issue and non-linear elements using ANSYS consumes plenty of time.

(3) Due to the limitation of its model, the traditional method can not simulate the model of the whole prefabricated part, thus the prefabricated part can not be mechanically analyzed or optimized.

3. Parametric modeling analysis of battledores

3.1 Size design of the battledore

Diameter, thickness and length of the shaft of battledore were designed as 7.2 mm, 1.6 mm and 450 mm respectively, and the shaft was a hollow pole with a circular cross section. The frame of racket was oval and the lengths of major semi axis and minor semi-axis were 138 mm and 108 mm respectively, while the thickness was 14 mm and diameter of bracing wires was 0.6 mm.

The battledore was made of carbon-epoxy composites, in which the fiber reinforcing phase material was M40 carbon fibers and the material of matrix phase and bracing wires was bisphenol A epoxy resin (details are shown in table 1).

Table 1 Material property of carbon fibers and resin matrix

Classification	E1(GPa)	E2(GPa)	G12(GPa)	G23(GPa)	V12	V23
Carbon fiber	391	25.57	25.57	11.94	0.21	0.24
Resin	3.62	3.62	--	--	0.35	0.35



Fig. 2 Physical model of battledores

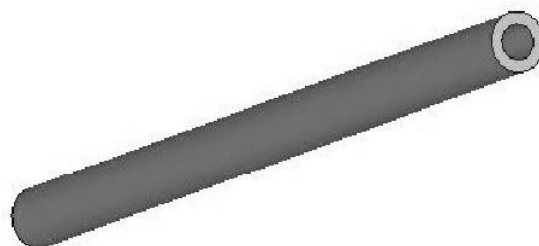


Fig. 4 The matrix finite element model of the shaft of battledore

3.2 The finite element model of two-dimensional triaxial braided battledores (figure 3 and figure 4)



Fig. 3 The finite element model of two-dimensional triaxial braided battledore

3.3 Stress analysis of two-dimensional triaxial braided battledores

According to the actual stress state of battledore and on the basis of regional method of superposition, full constraint was applied to one side of the ANSYS model of the shaft of battledore while a vertical force was applied to the other side. The average speed of badminton was around 250 km/h, the quality of badminton was about 9 g, and the time of contact of badminton and battledore during the whole process was only about 5/1000 s. Thus the stress of battledore hitting the badminton can be calculated according to above data as well as the momentum theorem. After that, an important step which followed the construction of finite element parametric model was the application of regional method of superposition. The load and constraint state of model at the moment when battledore hits the badminton is shown in figure 5.

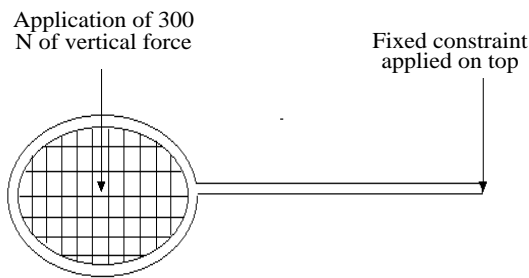


Fig. 5 Finite element model of constraint and load mode of battledore hitting the badminton

The maximum value of the overall equivalent stress of two-dimensional triaxial braided battledore is 155 MPa, while the maximum values of equivalent stress of racket frame and shaft are 73 MPa and 155 MPa respectively. Shape changes of the conjunction part can lead to concentration of stress, which can result in fracture of the joint part of racket frame and shaft. Fiber bundle plays a main load-bearing role in braided composite materials and it also plays an important role in design of the whole battledore.

3.4 Stress analysis of two-dimensional biaxial braided type battledores

Because the additional axial fiber of two-dimensional triaxial braided type battledore bore a partial load, its overall bearing capacity was obviously better than that of two-dimensional biaxial braided type battledore. The maximum value of equivalent stress of the frame of racket was 117.01 Mpa, and position of the maximum stress was at the cross of fiber and matrix. The same as the two-dimensional triaxial braided battledore, the overall equivalent stress value of fiber bundle of two-dimensional biaxial braided battledore was significantly higher than the overall equivalent stress value of matrix. The overall stress distribution of the fiber bundle was uniform except for the local stress concentration on the restrained end. Considering the effect of fiber volume ratio on design of battledore, different fiber volume ratios were chosen for ANSYS calculation of the battledore, and results are shown in figure 6.

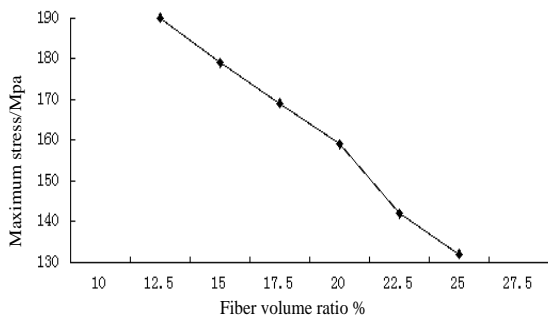


Fig. 6 Variation curve of the maximum equivalent stress of battledore with the change of fiber volume ratio

Figure 6 shows that, the maximum stress of battledore decreases gradually with the increase of fiber volume ratio. When the fiber volume ratio is small, the equivalent stress of battledore is big; on the contrary, when fiber volume ratio increases, the maximum equivalent stress decreases while the application amount of fiber materials increases gradually. However, sometimes the hitting point is off-centered or even on the frame, thus the stress of battledore is much more affected under such circumstances. Four side angle positions on the frame were selected as eccentric positions for force test; results indicated that the influence rules of these four positions on the whole racket were basically the same (figure 7).



Fig. 7 Distribution of eccentric force bearing points on the frame

3.5 Elastic property prediction of battledore shaft (analytical model is shown in figure 8)

On the basis of regional method of superposition, full constraint was applied to one side of the finite element model of battledore shaft while an axial displacement load was applied to the other side. After the calculation using ANSYS software, $X=L$, the mean strain ϵ_y and the mean stress δ_x were obtained. After that, the elasticity modulus E_y , Poisson's ratio μ_{xy} and shear modulus G_{xy} could be obtained according to constitutive relation and definition equation of Poisson's ratio.

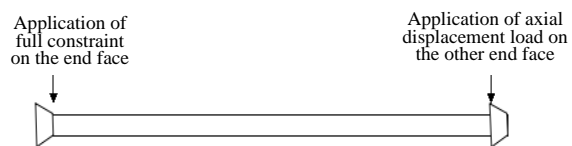


Fig. 8 Elastic property prediction of battledore shaft and constraint adding and displacement load model

During the process of finite element regional method of superposition, the application of finite element regional method of superposition saved plenty of time of analysis of overall components of the battledore; moreover, accurate results could be obtained only with the application of sparse finite element meshes, which also significantly reflected the effectiveness and high efficiency of finite element regional method of superposition. Elastic property prediction results are shown in table 2.

Table 2 Results of elastic property prediction

	Two-dimensional biaxial	Two-dimensional triaxial
E_x / GPa	40.37	61.77
E_y / GPa	6.38	9.29
E_z / GPa	6.36	9.27
μ_{xy}	0.31	0.35
μ_{xz}	0.31	0.37
μ_{yz}	0.92	0.96
G_{xy} / GPa	13.6	15.3
G_{xz} / GPa	13.4	15.3
G_{yz} / GPa	3.4	4.8

As shown in table 2, two-dimensional triaxial braided battledore was a lot better than two-dimensional biaxial braided battledore, which was because that the additional axial fibers bore a partial load. The difference of two kinds of battledores in weight was insignificant; moreover, the hand feeling and overall anti-bending and twist-resistance capacity of two-dimensional triaxial braided battledore were also better than that of the two-dimensional biaxial braided battledore. Therefore, two-dimensional triaxial braided battledores are favored more by people.

4. Dynamics analysis of battledores

4.1 Definition of modal dynamics analysis

Mode dynamics analysis is an important part of analyzing dynamic characteristics of the whole component as well as the extension of systematic resolution method in the field of vibration. Mode is the vibration characteristic of objects. Each mode has its corresponding inherent frequency, damping ratio and modal shape, and modal values of the above three modes can be obtained by calculation or experimental research. The whole process of obtaining parameters using above methods is called modal analysis.

4.2 Theoretical basis of modal analysis

When the elastic system kinematic equation contains restricting degree of freedom, it can be expressed using dynamic load principle of virtual work:

$$Ma + Cb + Kx = F \tag{4}$$

Notes: M refers to the general mass matrix of structure; C is the total damping matrix; K is the stiffness matrix; x is the nodal displacement array; a refers to the node acceleration array; b is node speed array and F is null matrix.

Because the damping of null matrix F was low, its contribution value to the modal analysis results of the overall component was small and the exciting force

array was not taken into consideration. Therefore the zero damping oscillation equation is:

$$Ma + Kx = 0 \tag{5}$$

The solution of equation (5) was:

$$x = x_0 \sin(\omega t + \varphi) \tag{6}$$

Note: ω refers to natural angular frequency of oscillation; φ refers to the initial phase of oscillation.

Equation (6) was substituted into the equation (5), thus the system of homogeneous linear equations was

$$K - \omega^2 Mx = 0 \tag{7}$$

The following condition should be met for solution of equation (7):

$$K - \omega^2 M = 0 \tag{8}$$

When matrix K and M were n-order matrixes, the equation turned into a n-real coefficient equation of ω^2 , and the final modal analysis solving problem became the problem of solving matrix eigenvalue ω and feature vector x.

4.3 Finite element modal analysis results and vibration chart

Statical analysis model was selected for finite element model of modal analysis; statics properties were selected for material properties, and fixed constraint was applied to one end of the shaft (figure 9).

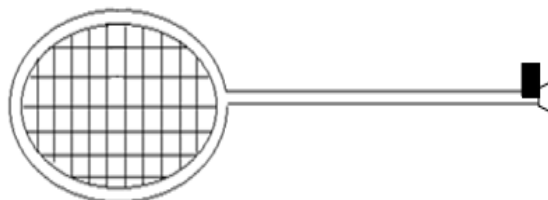


Fig. 9 Finite element model of the battledore

The contribution value of high order modal to response was low and rate of decay was fast. In common modal analysis, only low order modal was considered, thus the first four order inherent frequency was chosen (table 3).

Table 3 The first four order inherent frequencies and vibration modes of two-dimensional triaxial braided battledore

Order	Inherent frequency (Hz)	Vibration mode
1	34	X-Z in-plane vibration
2	57	X-Y in-plane vibration
3	76	X-Z in-plane vibration
4	121	X-Y、X-Z in-plane composite vibration

5. Discussion

Firstly, theoretical methods of finite element analysis were introduced and ANSYS software was introduced and described in detail in this study. After that, finite element modeling methods of traditional braided composites were expounded to solve problems of traditional braided composites in finite element, and finite element regional method of superposition was introduced. Then battledores were designed integrally, including designs of fiber phase model and matrix phase model and determination of overall size of the battledore; after that, on the basis of finite element regional method of superposition, parametric finite element models of two-dimensional biaxial and two-dimensional triaxial braided battledores were constructed [15], and two kinds of models received statics analysis. Results showed that, the two-dimensional triaxial braided battledore was better than the two-dimensional biaxial battledore, which was greatly favored by a lot of badminton amateurs [16-17]. At last, the two-dimensional biaxial battledore was taken as the research object and its modal dynamics was analyzed; in addition, theoretical basis and calculation methods of modal analysis were analyzed in detail; block Lanczos method was adopted for extraction of inherent frequencies and vibration modes of the first four order battledores, thus to provide design of the structure and size of battledore with theoretical basis [18-19].

6. Conclusions

In conclusion, we obtained the equivalent stress of battledores using ANSYS software [20]; on the basis of whole finite element model, elasticity moduli of two kinds of braided composites were predicted by mechanical analysis and elastic property parameters of two braided forms were obtained [21-22]; on the basis of finite element regional method of superposition, the overall structure of the battledore received modal analysis and the inherent frequency of the whole battledore was obtained, which could provide a powerful theoretical guarantee for design of more comfortable battledores.

7. References

[1] Ewart P, Verbeek J. Using micro-mechanical modelling to predict short-fibre composite properties in computer-aided design of sporting equipment[J]. *Sports Engineering*, 2011, 13(2):73-81.
 [2] Fragoso S (2011). Understanding links: Web Science and hyperlink studies at macro, meso and micro-levels. *New Review in Hypermedia & Multimedia*, 17(2):163-198.
 [3] Jamshidi A, Hamzah MO, Aman MY (2012). Effects of Sasobit® content on the rheological characteristics of unaged and aged asphalt binders at high and intermediate temperatures. *Materials Res*,

15(15):628-638.

[4] Bisschop A, Mullender M G, Kingma I, et al. (2012). The impact of bone mineral density and disc degeneration on shear strength and stiffness of the lumbar spine following laminectomy. *J of Comparative Neurology*, 21(3):530-536.
 [5] Fang W Z, Chen L, Gou JJ, et al. (2016). Predictions of effective thermal conductivities for three-dimensional four-directional braided composites using the lattice Boltzmann method. *International J of Heat & Mass Transfer*, 92:120-130.
 [6] Yan J, Liu K, Zhou H, et al. (2015). The bending fatigue comparison between 3D braided rectangular composites and T-beam composites. *Fibers & Polymers*, 16(3): 634-639.
 [7] Jia CY, Cui L, Gao FY (2015). The Topology Optimization Design of the Main Hand Component of Tele-operation Based on Hyper Works. *Development & Innovation of Machinery & Electrical Products*, 18(1):7-12.
 [8] Kondric M, Sekulic D, Petroczi A, et al. (2011). Is there a danger for myopia in anti-doping education? Comparative analysis of substance use and misuse in Olympic racket sports calls for a broader approach. *Substance Abuse Treatment Prevention & Policy*, 6(11):1-13.
 [9] Thien Trung L, Jelena M, Tuyet Mai N, et al. (2011). Improved solvent extraction procedure and high-performance liquid chromatography-evaporative light-scattering detector method for analysis of polar lipids from dairy materials. *J of Agricultural & Food Chemistry*, 59(19):10407-13.
 [10] Wang W B, Cheng K, Cheng L (2014). Parametric modeling and analysis of self-loading container vehicle based on ANSYS. *Applied Mechanics & Materials*, 620:137-142.
 [11] Boukellal A, Boumrar K, Mokdad R, et al. Micro-particle localization by parametric modeling analysis of digital holograms. *J of Optics*, 2015:1-7.
 [12] Fazelzadeh SA, Varzandian GA (2010). Minimum-time Earth-Moon and Moon-Earth orbital maneuvers using time-domain finite element method. *Acta Astronautica*, 66(s 3-4):528-538.
 [13] Shi W, Wang D, Atlar M, et al. (2013). Flow separation impacts on the hydrodynamic performance analysis of a marine current turbine using CFD. *Proceedings of the Institution of Mechanical Engineers Part A J of Power & Energy*, 227(8):833-846.
 [14] Carr R, Comer J, Ginsberg MD, et al. (2011). Microscopic Perspective on the Adsorption Isotherm of a Heterogeneous Surface. *J of Physical Chemistry Letters*, 2(14):1804-1807.
 [15] Kasaragod DK, Lu Z, Jacobs J, et al. (2012). Experimental validation of an extended Jones matrix calculus model to study the 3D structural orientation of the collagen fibers in articular cartilage using polarization-sensitive optical coherence tomography. *Biomedical Optics Express*, 3(3):378-387.
 [16] Fang WZ, Chen L, Gou JJ, et al. Predictions of effective thermal conductivities for three-dimensional four-directional braided composites using the lattice

Boltzmann method. *International J of Heat & Mass Transfer*, 2016, 92:120-130.

[17] Williams RD, Brasington J, Hicks M, et al. (2013). Hydraulic validation of two-dimensional simulations of braided river flow with spatially continuous aDcp data. *Water Resources Research*, 49(9):5183–5205.

[18] Liu YC, Loh CH, Ni YQ (2013). Stochastic subspace identification for output-only modal analysis: application to super high-rise tower under abnormal loading condition. *Earthquake Engineering & Structural Dynamics*, 42(4): 477–498.

[19] Campozano L, Célleri R, Trachte K, et al. (2016). Rainfall and Cloud Dynamics in the Andes: A Southern Ecuador Case Study. *Advances in Meteorology*, 2016(3):1-15.

[20] Cui X, Guo J, Zhao J, et al. (2015). Analysis of PCBN tool failure mechanisms in face milling of hardened steel using damage equivalent stress. *International J of Advanced Manufacturing Technology*, 80(9-12):1-10.

[21] Hambli R (2012). A quasi-brittle continuum damage finite element model of the human proximal femur based on element deletion. *Med & Biological Engineering*, 51(1-2):219-231.

[22] Hinz B, Seidel H, Hofmann J, et al. (2008). The significance of using anthropometric parameters and postures of European drivers as a database for finite-element models when calculating spinal forces during whole-body vibration exposure. *International J of Industrial Ergonomics*, 38(9):816–843.

BRAND:
«SMART MECHATRON - Competitiveness,
performance and high quality through
HIGH-TECH MECHATRONIC PRODUCTS »

DESIGN AND IMPLEMENTATION OF RECRUITMENT MANAGEMENT SYSTEM BASED ON ANALYSIS OF ADVANTAGES AND DISADVANTAGES OF PHP THREE-TIER

Youyu Hu

QingDao Vocational and Technical College of Hotel Management

E-mail: hyyjdim@126.com

Abstract - The purpose of this text is to design the three-tier architecture based on PHP to realize enterprise recruitment management system. The recruitment system was designed and implemented considering new features in the current recruitment work and according to the understanding of recruitment. The advantages and disadvantages of the PHP language were analyzed, and system design and implementation methods were discussed based on the analysis on the advantages and disadvantages of the three-tier architecture of PHP and researches on driver models. On the basis, we choose the most reasonable design drive way. According to the features of the current recruitment management system in enterprise, we design and realize a recruitment management system for enterprise. According to the actual recruitment work, the system is divided into four modules, recruitment system, talent recruitment database system, examination database system and access control system. This study introduces functions and function implementation of the four modules as well as functions and function implementation of their submodules. The system can normalize and systemize recruitment process, greatly reduce working load of workers, improve working efficacy, shorten recruitment time and lower cost spending on recruitment work.

Keywords: Recruitment system; PHP; three-tier architecture.

1. Introduction

With the rapid development and popularization of the Internet and personal computers, more and more job seekers are inclined online job-seekers, while many urban labor markets and the company's human resources department have also used online recruitment, and each set up their own human resources databases, these changes bring out great changes in the traditional job market management and informatization work and has taken on new characteristics. These changes also put forward new requirements for job recruitment, making network-based job recruitment work become necessary means of advertisement [1-3]. As a kind of open source software, PHP has many obvious advantages in aspect of webpage development, such as high security, cross-platform, supporting for a wide range of databases, fast implementation, and many other advantages [4]. Three-tier architecture development mode is the mature development way of the current Internet, namely in the program development and design, the system of the whole business application is divided into three layers: presentation layer, business logic layer and data access layer. Through layer development, functions in various levels become clear and all layers have adapted to strong independent development, which is beneficial for development, maintenance, deployment and expansion of system [5]. This study simplified the process based

on theory to design and realize recruitment system in enterprise. We realized a system involving establishment of recruitment requirements, examination and approval, information release, sorting, screening, hiring, and tracking according to recruitment process of an enterprise. We attempt to set up a recruitment system that meet personalized needs of internal recruitment, and recruiting process in enterprise, thus to realize office automation in enterprise. Moreover, the influence scope of recruitment information was expanded through the large online intermediary platforms and school forums and information of recruiters were collected. Then we screened recruiters as well as arranged written examination, interview and admission work. After the recruitment, we tracked and analyzed the candidates, including the current job and work within half a year and one year of recruiters. Moreover, talent analysis database was built to analyze these data, aiming to provide data references and recommendations for future recruitment.

2. Overview of PHP

PHP as a kind of open source software has many obvious advantages in Web page development [4].

(1) High safety: PHP belongs to open source software, that is to say, PHP core architecture and the source code is open to the public and programmer can view all of

source file content through the corresponding software compile tools. As the utilization rate of Apache server software is very high, most of the developed PHP software or web sites are used with the Apache service. Programs or software compiled by PHP can run on most platforms in the world. Therefore, flexibility and safety of combined use of them has been confirmed by users.

(2) Cross-platform: PHP support almost all of the operating system platforms (such as Win32 or UNIX/Linux/Macintosh/FreeBSD/OS2, etc.), as well as Apache, IIS and various Web server.

(3) Support for a wide range of databases: PHP can be compiled into a function connected to many database and can manipulate a variety of mainstream and non-mainstream database, such as MySQL, Access, SQL Server, Oracle, DB2, etc.

(4) Fast exertion: procedure code compiled using PHP is characterized by high operation efficiency and less data utilization, thus it operates fast.

(5) Easy to learn: the writing of PHP code is similar to HTML, elements on the page is composed of HTML. Page elements composing of HTML are embedded with code. At the same time, JS script language is used to do interactive operation. It is easy to learn as long as there is the basis of HTML code.

(6) Low cost: in the enterprise application scheme based on PHP, the use of the related tools and deployment environment is free, saving a lot of unnecessary spending for the enterprise.

(7) Template: separate application logic and user interface.

(8) Stable and rapid performance: embedded Zend acceleration engines.

(9) Support object-oriented: object orientation is the most popular and common development way of today's software development and PHP also provides a good support for it, such as creating a class or class libraries and closing up public partially. Using object-oriented idea for PHP application development will play a very important significance role in the application architecture design.

To sum up, PHP, a small and medium sized application system characterized by easy to learn, multiple development tools, fast development cycles and highly portable, is suitable for low-cost and short-development and construction period medium and small application system [6-8].

3. The whole system module design

System design is another important stage in the information development process. In this phase, we will design the new system according to logic analysis results in the last stage and based on requirement of logic model. System architecture design is the design of specific physical models. The main goal of this phase is to change system logic programming that reflects the information needs of users into something that can be implemented by computer-based physical scheme, and

provide the necessary technical information for the next phase of the system.

This system uses the structured design method to realize the system's overall function, improve each indicators of the system, reasonable divided whole system into each function module, correctly process relationships between modules, relationships inside modules as well as the invocation relationship and data link, define the internal structure of each module, and achieve the function of the whole system through design of module and correlation between modules. Figure 1 is overall function module structure of system.

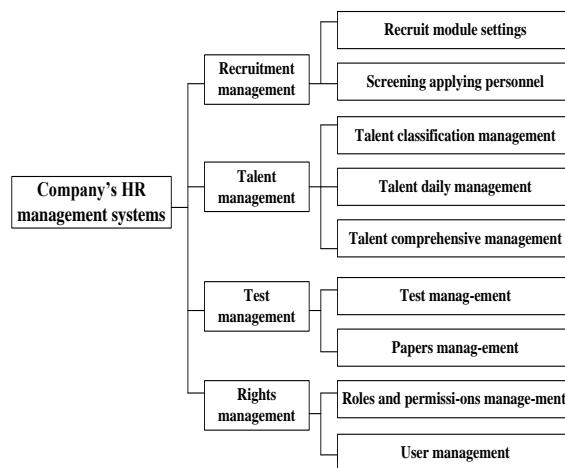


Fig.1 Overall function module structure of the system

4. System design and implementation in detail

4.1 Database connection configuration

Operating and managing database composing recruitment information is very important. It can be regarded as the foundation of recruitment management system in enterprise. Realization of the other functions is built on these bases. In this system, in order to make configuration of database connection, we put the database creation connecting process in a separate header file (web.config), hence it is easy to realize the information sharing between databases. In addition, ADO.NET technology applied in the system operates conveniently, only concise sentences are enough. For example, in Web config file, we only need to create a ConnectionStrings object responsible for the connection to the system database. Only the following connection parameters are needed to complete the operation.

1. DSN: data source.
2. UID: user name to access the database.
3. PWD: UID and the corresponding password.

The system also uses the MYSQL database connection. When using this connection method, we should first add a data source named job in the MYSQL Control Panel of the system (the corresponding user name is "jj", password is "123456"). Afterwards, we can access to database through three parameters.

Features: database connection management.
Code is as follows:

```
<%  
  
set  
corm=Server.CreateObject("ADODB.Connection")  
  
conn.open "dsn=job;uid=jj;pwd=123"  
  
%>
```

In other pages of the system, we can access to database using connection object by adding statements of the head of the page (`--##include file="corm/Web.Config"-->`).

4.2 Detailed design and implementation of system login

Any management personnel in the business module of system management before operation are required by system validation. Login function will initialize system management pages according to corresponding counterpart of different landers, i.e., hide the unprivileged operation functions and display the relevant operational menu items. This system adopts the safe way to log in. Login box appears once user enters the website. The next step is to fill user name and password and then click on the login button. Back-stage management page will come up after the information is verified. If login authentication failed, the corresponding error message will come up. The following shows the flow chart of function implementation.

Key code:

4.3 Detailed design and implementation of recruitment management module

Recruitment management module design is mainly divided into two levels, level 1 for classification and level 2 for template option under specific classification. This data structure design is reasonable in data business operations and the front desk page display. Moreover, the display is clear and offers good experience for users. The difficult point of this module lies in how to traverse template options which display based on two-level classification. Here two circular list controls will be used. One is as a container displaying all level 1 category in system and the other one is applied to display template item under that category. Circular list of level 1 category is traversed first. Then all items chosen by user under circular list of the level 1 category is acquired and temporarily stored in complex. It

continues until the last list of level 1 category is traversed. Here are the function key codes:

Key codes:

```
try  
  
{ // Select list box, get the selected item ArrayList  
list=new ArrayList()  
  
for (int j=0;j<rptOption.Items.Count; j++)  
  
{ // CheckBoxList  
cklRight=(CheckBoxList)rptOption.Items[j]  
.FindControl("cklOption"); cklRight.Enabled=true;  
  
for (int x=0; x<cklRight.Items.Count; x++)  
  
{  
  
if (cklRight.Items[x].Selected=true)  
  
{ list.Add(cklRight.Items [x]. Value); } } }  
  
catch (CMMException cmmex)  
  
{ // Business exceptions, picture processing  
  
SPUtils.CMMErrorTeardown(cmmex,1blError, imgError); }  
  
catch (Exception ex)  
  
{ // System exceptions, common exception handling  
  
SPUtils.ErrorTeardown(Session, Response, ex); }
```

The release of recruitment information and the reception of resumes from interviewees are the premises for realizing talent screening. The first step of logic process of talent screening is to select out talents whose conditions conform to the position description and test them with written examination. Then a certain proportion of talents who participate in written examination were selected out for interview. Finally talent who is suitable for the position can be confirmed. In the process of implementation, the operations are not complex.

Following code is the key to realize the function:

Key codes:

The release of recruitment information and the reception of resumes from interviewees are the premises for realizing talent screening. The first step of logic process of talent screening is to select out talents whose conditions conform to the position description and test them with written examination. Then a certain proportion of talents who participate in written examination were selected out for interview. Finally talent who is suitable for the position can be confirmed. In the process of implementation, the operations are not complex.

Following code is the key to realize the function:

Key codes:

```

Protected void btnDelete_Click(object sender,
ImageClickEventArgs e)

    {try

    {
CMMLog.BeginMethod(MethodBase.GetCurrentMethod());

    int row=((GridViewRow)((ImageButton)sender)
.NamingContainer).RowIndex;

    int InfoID=(int)this.gvwBSMG0301.DataKeys
[row].Value;

    DABBstRoleinfo bean=new DABBstRoleinfo();
    bean.InfoID=InfoID;

    BLLB SMG0301.DeleteInfo(bean);

    //GridView rebindng
this.gvwBSMG0301.DataBindQ;

    CMMLog.EndMethod(MethodBase.GetCurrentMethod());

    catch (CMMException cmmex)

    { // Business exceptions, picture processing
SPUtils.CMMErrorTeardown(cmmex, lblError,
imgError);}

    catch (Exception ex)

    { // System exceptions, common exception
handling
SPUtils.ErrorTeardown(Session,
Response, ex); }}
    
```

4.4 Detailed design and implementation of talent management module

Talent management module design is mainly divided into personnel information management, daily management, and integrated query.

Personnel information management is an indispensable part of recruitment system. Recruitment system's main function is to provide the talented person for enterprise. This function module is used to manage talent information in enterprise. As a result, talent information has multiple attributes such as basic information, opinion, the current position, and so on. There are a lot of properties under each large point, leading to large information amount. In addition, there are two main sources of talent information in the system. One way is the direct delivery of applicant into talent database, which should be reviewed by relevant department of and the other way to input by relevant staff.

Following is the function implementation key code:

Key code:

```

if (e.File.FileName!="")

    { string path="@~"+SPConstants.UPLOAD_
PICTURE_DIRECTORY; // Randomly generated
file names

    string
Folder=DateTime.Now.ToString("yyyyMM"); //
File names are generated according to the date

    string
newImgName=DateTime.Now.ToString("yyyyMM
ddhhmmssffff")+e.File.FileName;

    string
SavePath=HttpContext.Current.Server.MapPath(pat
h + Folder); // Gets the absolute path

    if (!Directory.Exists(SavePath))// Determine if
the path exists, if it does not exist, created it {
Directory.CreateDirectory(SavePath); } // Upload
pictures

    e.File.SaveAs(SavePath + "/" + newImgName); //
Save the file }
    
```

Talent management means managing and maintaining the current state of talents based on basic talent information. Taking the recruitment of talents as an example, this section explained the implementation of the function. The first step is to enter the page of talents list which demonstrates all talents information page by page. After entering into the page, users can select check box in front of every record according to demand. After selection, users can enter into relevant business operation page by right clicking operation button on the right corner of the list and fill in and save information. Following is the key code to realize this feature:

Key codes:

```

// Pop up talent selection box

function ShowUploadPic(){ var
selectInfo=ShowModulePage

    (../ShowPage/
SELECTEDInfo.aspx?selectType=1

    &rnd='+Math.randomQ, "500", "300","talent
select");

}

// receive the returned talents information

Function ReceiveParams()

// Hide frame information

HidModulePageQ;

// Update page control value

document.getElementById("<%=btnRefresh.ClientI
D %>").click();

}
    
```

Due to years of accumulation, the amount of information will increase; hence how users find the needed talent information in such a large amount of information is also an important problem. Therefore, personnel information query function is set up to facilitate the user to find talent information which they need among massive information. The implementation process is as follows. First, information input or selected by users in query page is acquired. Then the information is combined in system page background. After that, the information is transmitted to pre-defined talent comprehensive query and storage process as parameters.

Then the information set is returned back to the page to fill data source of list control of the page. Finally, the list will demonstrate talent information page by page. The Following is the key core for the implementation of the function.

Key codes:

```
@PageIndex int, -- What page, the first page is 1;
@PageSize int, -- Page size;
@ TotalCount int OUTPUT, -- Total number
output parameters;
DECLARE @ StartRowNum int;
DECLARE @EndRowNum int;
SET @StartRowNum=(@PageIndex-
1)*@PageSize+1;
SET @EndRowNum=@PageIndex*@PageSize;
SELECT
    @TotalCount =COUNT (1)
FROM tableName
WITH Temp AS
    ( SELECT TOP ( @ PageSize* )@ PageIndex)
ID, ROW_ NUMBER() OVER (ORDER BY ID
DESC) AS RowNum
FROM tableName )
SELECT *
FROM Temp AS T
INNER JOIN tableName tb ON T.Id=tb.Id
WHERE T.RowNum BETWEEN @StartRowNum
AND
@ EndRowNum
ORDER BY RowNum
```

4.5 Detailed design and implementation of examination database management module

Examination database management module design is mainly divided test question information management and test paper information management.

As the basis of test, the test information management is also very important. At present, the system mainly provides three type question categories, multiple-choice question, single-choice question and essay question. The three categories are the most common in the perspective of the question category in current test. So in the process of adding questions, the first thing is to select question category, because only after question category is chosen can the system display test question items and answer elements. Elements showed in page are different according to different question category. Next is question categorization. Corresponding management module in value system of the field will be responsible for it. The classification system will fill based on categories that have been added into the database. The last step is to fill the basic information of the question such as category, title and answer.

Test information management module is mainly used for written examinations during recruitment and internal performance assessment. Before written examination, recruiters can generate a set of test paper according to the position and print it out. The difficult point during the generation of test paper is the selection of test questions. Currently, the system provides two kinds of test question selection means. One is to randomly extract test questions using the system and the other is adding test questions by staffs. A test question selection page which demonstrates information of all test questions will come up and then operators only need to test questions they needed. But as it is a cross-page operation, how to send the selected test question information to the generation page is the key of the implementation of the function.

4.6 Detailed design and implementation of permission management module

Rights management module is divided into the following two main points: roles and permissions management, user management.

Roles and permissions management is considered playing a crucial role in ensuring the security of the whole system. Target system realizes the function by connecting right, role and user together. That means, right is not directly corresponding to user; a role is added between them. Role connects user and right. Right function can be implemented in this way. Moreover, the flexibility is large, which is beneficial for expansion of right demand afterwards.

User management refers to managing system operators. The settlement of role, i.e., the settlement of permission is the most important. Here the settlement of permission is realized by role. Role connects permission and moreover user connects role; as a result, user indirectly connects permission.

Using such a mechanism, the maintenance of user information becomes simple. When adding or maintain user information, we only need to select the role which is added in the system in advanced.

5. Conclusion

This study analyzes the technology used and advantages and disadvantages of programming language, servers and database, explores PHP three-tier structure in detail, discusses over several development patterns and compares their advantages and disadvantages. Based on the above, we make a design research on systematic structure, data mode and right model.

After the basic research work and design work are over, we implement and verify the system. Procedures of recruitment are verified in detail. Finally, advantages and disadvantages of the system are compared and analyzed. Then various functions of the recruitment system are prospected.

Recruitment as the main source of human resources in enterprise, directly affects the quality of employees and development potential. An excellent staff will play an important role for development of enterprise. A good recruitment system also will play a good role in screening excellent talent. Besides recruitment system, a set of good evaluation system and employee incentive mechanism is also needed to full play the employee's supervisor initiative and create greater value for enterprise. At the same time a good set of personnel flow statistical analysis and staff growth plan is also essential. Timely knowing the staff flow and understanding employee's demand can ensure the loyalty of staff to enterprise. Human resource structure composing of good recruitment system, outstanding job evaluation systems, sensitive staff flow analysis and potential employee growth plan can ensure rapid and high-efficient development of enterprise on the basis of stable operation.

Meanwhile, it can improve competitiveness of enterprise and enhance development potential of enterprise. Thus, a good recruitment and human resource management system can not only reduce recruitment costs and increase efficiency in the recruitment process but also can ensure stable operation and constant development of enterprise.

6. Reference

1. Zhefeng An. Research progress of internet recruitment at home and abroad. *Journal of Shanghai Business School*. (1): 75-78, 2010.
2. Yanli Ma. Analysis of advantages and disadvantages of internet talent. *Science*. 10 (18): 25-26, 2008.
3. Xing Li. Analysis of talent recruitment status and tendency of middle and small-sized enterprises. *Journal of Jilin Huaqiao Foreign Languages Institute*. 15 (2): 135-139, 2011.
4. Haibo Jin. Aspect-Oriented Programming in PHP. *Computer Development & Applications*. 22 (10): 23 - 25, 2009.
5. Qi Wang, Qinmin Zhang, Li Yuan. The implementation of human resource management system with three-tier architecture based on PHP technology. *e-Education Research*. 11 (8): 27-29, 2005.
6. Yifan Zhu, Xi Chen. Different Plan on Inputting and Outputting to MySQL Database based on PHP. *Wireless Internet Technology*. (8): 58-58, 2013.
7. Gaojie Li. Discussion on safety and encryption techniques of PHP website. *Digital Technology & Application*. (8): 182-1821, 2013.
8. Huilan Liu, Maofeng Li. Research and design of PHP site security strategy. *Popular Science & Technology*. 15 (8): 4-7, 2013.

BRAND:
«SMART MECHATRON - Competitiveness,
performance and high quality through
HIGH-TECH MECHATRONIC PRODUCTS »

IMPROVEMENT OF ENGLISH-CHINESE TRANSLATION METHOD BY FEATURE REDUCTION AND RULE OPTIMIZATION BASED ON ROUGH SET THEORY

Hongxia Wei

Foreign Languages School of Anhui Polytechnic University, Wuhu, Anhui 241000, China

E-mail: whxahgf@163.com

Abstract - Traditional machine translation algorithm faces difficulties such as low efficiency and low accuracy caused by complex grammar and multiple rules of English noun phrase. In order to improve identification accuracy of English noun phrase, a kind of noun phrase identification method based on rough set was proposed. Rough set method regarded identification of English noun phrase as a decision problem. We used rough set theory to simplify attributes and optimize rules for English noun phrase, and finally identified it. Then a stimulation experiment was carried out on English noun phrase sample on Wall Street Journal (WSJ) using rough set theory. The result of stimulation demonstrated that, the accuracy of noun phrase that was improved by rough set was higher than that of other translation methods; therefore, it is an effective machine identification method for English noun phrase, providing a basis for practical design.

Keywords: Noun phrase; machine translation; rough set; Wall Street Journal.

1. Introduction

With the constant deepening of reform and opening and foreign cooperation in China, international tourism, cultural exchange and business contacts become more and more frequent. However, language difference brings great inconvenience. Machine translation is an automatic translation that can translate texts from one natural language to another natural one using computer under the condition of meaning equivalence. Hence, machine translation is a new approach for solve communication barrier [1-3]. Noun phrase identification, a key technology in machine translation, is the basis of syntactic analysis and its identification effect directly affects the accuracy.

Rough set, a kind of machine learning method developed in recent years, has the functions of induction and decision. It can not only simplify properties and data of knowledge system and acquire decision rules from decision table, but also classify derived decision rules [4-5]. It is widely applied in various identification and classification fields since it is well suited for English noun phrase identification. In view of this, this study proposed a kind of English noun phrase

identification method based on rough set, in order to solve the low accuracy of identification of the current English noun phrase identification method. This method is to learn decision rules of English noun phrase by rough set and obtain identification results. Results of stimulation experiment demonstrated that, this method improved the accuracy of identification for English noun phrase.

2. Principle of english noun phrase identification

English noun phrase is the important constituent unit of English sentence, and meanwhile, is the unit of information transmission during speech communication. English noun phrase identification is one of the main research content in machine translation. Its purpose is to identify non-recursive noun phrase without post-modifier. Its input is English text that is labeled by participle, and the output is English text that have been identified and whose phrase have been labeled. The principle of English noun phrase identification usually is shown in figure 1.

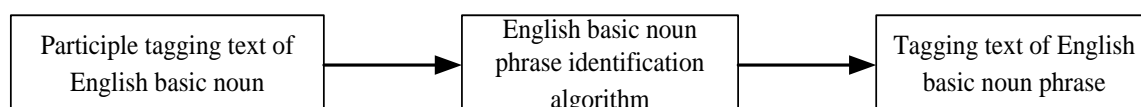


Fig. 1 The principle of English noun phrase identification

Suppose B as English noun phrase, I as internal part of noun phrase, and O as other situation. In this way, the identification of English noun phrase can be expressed in the form of {B, I, O}, we have:

$$y = f\{B, I, O\} \quad (1)$$

It can be known from formula (1) that, the identification of English noun phrase actually involved decision rules. The current identification methods for English noun phrase are not able to obtain satisfactory results since those methods have no function of decision rule analysis. Rough set is a kind of new-type method with the function of decision rule learning and is well suited for noun phrase identification; therefore, this study attempted to identify English noun phrase by rough set.

3. Design of english noun phrase identification algorithm

3.1 Reduction of noun phrase property

Definition 1: an English noun phrase decision system S was defined as a tetrad.

$$f(x): U \times R \rightarrow V \quad (2)$$

$$R = p \cup \{d\} \quad (3)$$

$$S = \{U, R, V, f\} \quad (4)$$

Where f(x) refers to information function acquired from training corpus, U stands for the set composed of every punctuation and vocabulary from the English noun corpus to be identified, R stands for attribute set, p stands for noun phrase tagging and part of speech tagging of context within certain range of the current vocabulary, d stands for noun phrase tagging of the current vocabulary, and V stands for union set of noun tagging set and part of speech tagging of context.

Definition 2: for an English noun phrase decision making system, attribute subset $B \subseteq R$ had an indiscernible relation.

$$ND(B) = \{(x, y) \mid (x, y) \in U^2, \forall b \in B(b(x) = b(y))\} \quad (5)$$

Definition 3: $a_i(x_j)$ refers to the value of x_j of the sample to be identified on attribute a_i . Then discernibility matrix of English noun phrase decision system S could be expressed as:

$$C_D: U \times U \rightarrow \rho(R) \quad (6)$$

Definition 4: suppose U as a domain of discourse, P and Q as two equivalence relation clusters on U.

If $POS_p(Q) = POS_{(p(t))}(Q)$, then r was regarded an attribute that could be omitted by Q in P; otherwise, r was regarded an attribute that could not be obligated by Q in P, that was, it could not be omitted.

If every r in P was an attribute that could not be omitted by Q in P, then P was regarded as an independent attribute of Q. For independent subset S of

Q in P, if $POS_S(Q) = POS_P(Q)$, then S was regarded an attribute reduction of Q in P. All attribute reductions of Q in P were expressed as $RED_Q(P)$. Therefore, all original relationship clusters that could not be omitted by Q in P were termed as Q cores of P, and denoted by $CORE_Q(P)$.

Procedures of simplifying attributes of English noun phrase using rough set were as follows: discernibility matrix C_D of decision table of English noun phrase decision making system was calculated; to $CORE_Q(P)$, core logical expression was:

$$L_{CORE} = a_i \varepsilon CORE_Q(p) a_i \quad (7)$$

discernibility matrix C'_D that omitted core was calculated:

$$C'_D = \begin{cases} C_D(i, j) & \text{if } CD(i, j) \cap CORE_Q(P) = \emptyset \\ 0 & \text{otherwise} \end{cases} \quad (8)$$

disjunction logical expression L_{ij} was set up for all nonempty set elements in discernibility matrix C'_D , that

$$L_{ij} = \bigvee_{a_i \in C_{ij}} (C_{ij} \neq 0, C_{ij} \neq \emptyset) \quad (9)$$

was: conjunction calculation was carried out on all

disjunction logical expression L_{ij} and L_{CORE} that were set up, and then a conjunction normal form was

$$L = \left(\bigwedge_{C_{ij} \neq 0, C_{ij} \neq \emptyset} L_{ij} \right) \wedge L_{CORE} \quad (10)$$

acquired, that was the acquired conjunction normal was converted form L into disjunctive normal form L' , that was:

$$L' = \bigvee_i L_i \quad (11)$$

finally English noun phrase attribute reduction result were output.

3.2 Set up decision making rules of noun phrase

The generation process of decision rules of English noun phrase based on rough set was as follows: T was obtained through selecting an attribute reduction result from attribute reduction table according to attribute reduction algorithm of rough set; then rule set T' was obtained through reducing attribute value and the detailed process was: value core of the rules was calculated and the rules were merged with the same value core; all rules were tested, and if the decision making rules composed by value core of the rules were

the same, then the rule remained unchanged; otherwise, a non value-core attribute was generated based on value core of the rule. Minimum rule set of English noun phrase was generated, and a minimum rule set that covered the whole information system was obtained; finally the optimal rule set of English noun phrase were output.

3.3 Tagging of English noun phrase

English noun phrase is described by using square brackets of “O+C”, that is, inserting “[” to express the starting of an English noun phrase and “]” to express the end of an English noun phrase. Tagging of English noun phrase goes on based on the decision making rules that have been generated and the context characteristics of the current words, therefore, English noun phrase, in nature, is to select a best matching rule from the decision making rule set established above, and to tagging based on decision making attribute value. The detailed procedures for tagging a noun were as follows: the first step was to confirm condition attribute value of noun phrase, i.e., obtain part-of-speech tagging information of context from English noun phrase training corpus and select noun phrase tagging

information from the results that have been tagged; then the candidate rule set was screened and the condition attribute of all rules in decision making rule set was matched with the noun phrase to be identified; rules with the least amount of inconsistent attributes were selected to make up candidate rule set; next the optimal matching rule was confirmed by classifying all the rules in candidate rule set based on decision making attribute value and selecting the first rule among the category sets with the largest number of rules.

3.4 Process of English noun phrase identification

A tagged noun was acquired through identifying English noun phrase samples by the tagging rule generated by rough set algorithm. This study adopted IOB tagging symbol sequence to obtain single word; however, an English noun phrase may be composed of one or more words. Therefore, IOB tagging symbol sequence should be converted into English noun phrase sequence. That conversion process was realized by a state transition recognizer and then the identification was carried out. Flow of English noun phrase identification algorithm is shown in figure 2.

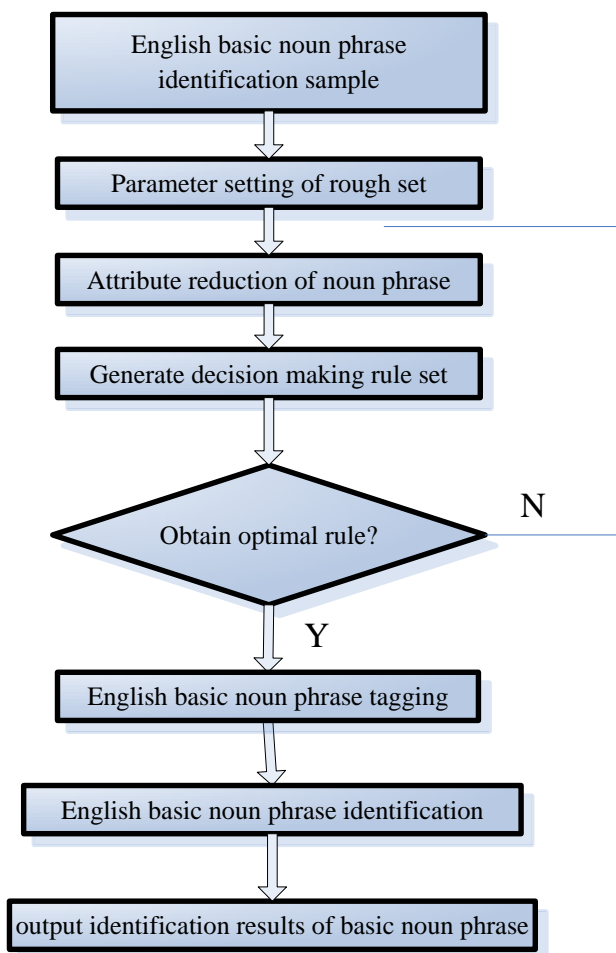


Fig. 2 Flow of English noun phrase identification

3.5 Evaluation standard of English noun phrase identification results

In order to better evaluate various identification methods for English noun phrase, this study adopted precision rate and recall rate as the evaluation standards for English noun phrase identification algorithm. The detailed definition was as follows:

Precision rate = (number of right noun phrases that have been identified / number of noun phrase that have been identified) * 100 % (12)

Recall rate = (number of right noun phrases that have been identified / number of all noun phrases in the text) * 100 %

4. Stimulation experiment

4.1 Stimulation data set

Data of the stimulation experiment came from Wall Street Journal (WSJ) corpus. WSJ corpus is the most authoritative English corpus for English phrase identification. It not only contains a large amount of texts with tagged part of speech, but also contains many tagged phrases and syntactic structure [6-9]. Training corpus samples came from the section 15-18 of the WSJ corpus. The test samples come from the section 20-22 of WSJ corpus. Hardware environment of the stimulation experiment is CPU 2.5MHz dual-core, 2Gbyte internal storage, and Windows XP operating system. The procedure is compiled under VB environment.

4.2 Identification results and analysis

First, the optimal English noun phrase identification model was obtained through training English noun phrase training set by rough set algorithm.

Then the model was adopted to identify English noun phrase test sample. The identification results are shown in table 1. From table 1, it was found that, the identification results obtained by English noun phrase identification algorithm were satisfactory and precision and recall rate were both above 90%. It illustrated that, the method proposed by this study could identify English noun phrase effectively.

Table 1. Comparison of identification precision rates of various algorithms

Test corpus	Precision rate / %	Recall rate / %
Section 20	93.84	93.53
Section 21	92.81	93.88
Section 22	92.77	92.97

4.3 Comparison with the performance of other identification methods

Advantages and disadvantages of rough set algorithm and other English noun phrase identification algorithms including Endong algorithm, Brill algorithm, TKS algorithm, TBL algorithm, Bayesian network algorithm and HMM algorithm are compared. Identification precision rates of all algorithms are shown in table 2 while recall rates of all algorithms are shown in table 3. From table 2 and 3, it could be known that the experimental results of the rough set algorithm proposed by this study were the best.

It indicated rough set was a kind of effective and accurate noun phrase identification method, and was quite suitable for solving some problems in natural language processing field.

Table 2 Comparison of identification precision rates of various algorithms

Test corpus	Brill algorithm	Endong algorithm	TKS algorithm	Bayesian network algorithm	HMM algorithm	Rough set algorithm
Section 20/%	73.91	74.93	82.25	85.76	92.67	93.84
Section 21/%	73.22	74.14	81.38	84.85	91.69	92.81
Section 22/%	73.13	74.15	81.30	84.77	91.60	92.77

Table 3 Comparison of recall rates of various algorithms

Test corpus	Brill algorithm	Endong algorithm	TKS algorithm	Bayesian network algorithm	HMM algorithm	Rough set algorithm
Section 20/%	73.57	74.61	82.98	85.48	92.37	93.53
Section 21/%	73.93	74.94	81.26	84.77	93.68	93.88
Section 22 /%	73.35	74.24	81.74	84.92	91.79	92.97

5. Conclusion

English noun phrase identification problem existing in machine translation research is the basis and key point of machine translation. Based on the discussion on the problems of the current English noun phrase

identification algorithm, this study designed an English noun phrase identification method based on rough set theory according to the characteristics of English noun phrase. This method first discovered decision making rules in training samples, then optimized learning rule in the perspective of the whole system, and finally

identified English noun phrase. Stimulation and comparison experiments suggest that the English noun phrase identification method proposed by this study is an effective method with high efficiency and recall rate; therefore, it is quite suitable for solving various natural language processing problems such as noun phrase identification, speech tagging and shallow analysis.

6. References

1. Yingjun Li. Status and Prospect of Machine Translation and Translation Technology Research — Mark Shuttleworth Bernard. *J. Chinese Science & Technology Translators Journal*. 01:24-27. 2014.
2. Yun Chen, Penghua Zhang, Lihua Ren. A Review on Machine Translation. *J. Value Engineering*. 01:174-176. 2013.
3. Ke Feng. Computer Aided Translation. *J. Brightness*. 27:289. 2014.
4. Tianrui Li, Hongmei Chen, Yan Yang. Rough Set Theory and Application. *J. International Academic Development*. 02:13-15. 2013.
5. Xiang Li, Yusheng Cheng, Meiwen Ding. The Method of Bayesian Network Based on the Rough Set. *J. Theory Journal of Anqing Teachers College (Natural Science Edition)*. 01:36-40. 2014.
6. Shuai Wang. Review of Corpus Translation Development in China. *J. Chinese Editorials*. 06:29-32. 2014.
7. Le Yin. Acquisition of Translation Knowledge in Machine Translation based on Corpus. *J. Beijing Jiaotong University*, 2014
8. Huiwen Xue. An Analysis on the Significance of Corpus to Translating Research. *J. Reading Digest*. 18:45. 2014.
9. Zhenghai Lu. Webpage Machine Translation Based on Corpus. *J. Anhui Literature (Second Half Month)*. 12:42-43. 2014.

BRAND:
**«SMART MECHATRON - Competitiveness,
performance and high quality through
HIGH-TECH MECHATRONIC PRODUCTS »**

EXPRESSION OF SERIAL ROBOT MANIPULATORS BASED ON SPACE AND STRUCTURE PARAMETERS

Zhijun Wu

Faculty of Mechanical and Electronic Engineering of West Anhui University, Liu'an, Anhui, 237012, China,
E-mail: wuzhijun230@sina.com

Abstract - Characterized by compact structure, large workspace and good flexibility, the series robots are widely used in the aided process of manufacturing. Based on the principle of centralized process, the bearing rings are made by means of lathe work by biaxial computer numerical control (CNC) machine tools. However, there were concerns about the difficulty in applying the biaxial synchronous docking technology and the high expense on equipments. The study was aimed at a research on the mechanism design and optimization of a kind of special clamping manipulator, which could replace the existing biaxial docking process. Firstly, the study analyzed the turning processing craft of bearing rings dual-axis CNC machine tools and proposed the function and performance design requirements of clamping manipulators. Secondly, forward kinematics models of clamping manipulators were established based on the D-H method. Thirdly, there was a detailed analysis of the main cross-sectional shape of clamping manipulator's workspace based on graphic method; furthermore, we analyzed the capacity of clamping manipulators to contain cuboids. On this account, an overall analysis was given about the influence that the space and structure parameters had on the serial robot manipulators.

Keywords: Series robot; Structure parameter; Kinematics analysis; The clamping manipulator; Workspace, analysis.

1. Introduction

Characterized by compact structure, large workspace, good flexibility, and good adaptability, the serial robots are widely used in the aided process of machining [1]. However, mechanism configuration [2] directly determines the performance of the robots (such as flexibility, positioning accuracy, the form of workspace and inverse kinematic), therefore, reasonable mechanism configuration is necessary in designing the robots; otherwise the robots cannot qualify for application. Kinematic analysis [3] is the precondition for the robot trajectory planning and the basis for real-time control, thus it has been a hot issue to search for a fast and accurate solution. Workspace is an important indicator to measure the performance of robots. On researching the workspace of prosthetic industrial robots, most scholars define the cross-sectional shape of workspace under the given geometric parameters, without analyzing the universality of the cross-sectional shape [4].

After the robot configuration is confirmed, robot geometric parameters need to be determined according to certain design constraints or optimal targets (such as workspace, kinematic and dynamics performance index), so that input parameter can be provided for structure design.

Quite a few scholars did research on the optimal design of geometrical parameters of prosthetic industrial robots, with workspace as optimal targets [5-7], and geometric constraint in the space was simplified into plane geometry constraint. In this study, we did research and probed into the influence that space and structure parameters had on the performance of serial robot manipulators.

2. The configuration scheme of the clamping manipulators produced by bearing rings biaxial cnc machine tools

An analysis of the design requirements of clamping manipulators.

On condition that the processing route of biaxial NC machine turning bearing rings remained the same, the research presented the clamping operation of the dynamic (not stop) cutting on the spindle end and static (stop) loading on the deputy spindle end, which could replace the non-stop synchronous docking process between the spindle and the deputy spindle so as to reduce the equipment cost and improve the processing efficiency. The total function model diagram of the clamping manipulator is shown in Fig. 1.

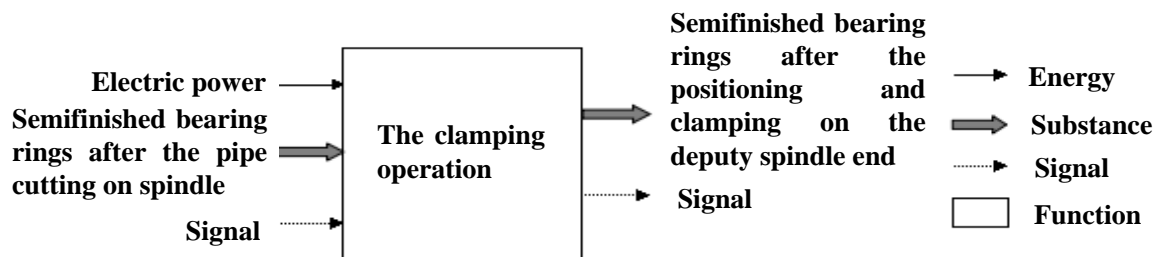


Fig.1. The total function model diagram of the clamping manipulator

Dynamic cutting on the spindle end: 1) before pipe cutting, the clamping manipulators reach the specific location on the spindle end in specified pose and wait; 2) After pipe cutting, the bearing grippers of clamping manipulators catch the semifinished bearing rings; 3) The clamping manipulators adjust the pose so that the semifinished bearing rings will be positioned by the bearing grippers on the end face; 4) The bearing grippers clamp the outer diameters of the semifinished bearing rings to finish positioning and clamping.

Static loading on the deputy spindle end: 1) the clamping manipulators move to specified stage in appointed pose; 2) The bearing grippers disengage, and the semifinished bearing rings are positioned and clamped on the stage; 3) The clamping manipulators are adjusted in specified pose; 4) The bearing grippers catch the semifinished bearing rings from the opposite direction and finish positioning on the end face. 5) The bearing grippers clamp the outer diameters of the semifinished bearing rings to finish positioning and clamping; 6) The clamping manipulators move to specific location on the spindle end and the semifinished bearing rings are positioned on the deputy spindle end; 7) After the deputy spindle fixture clamps the bearing rings, the bearing grippers disengage; 8) The clamping manipulators disengage into specified location and wait for the pipe cutting signal.

Function module decomposition of clamping manipulators

Two main functions of clamping manipulators are gripping and pose changing [8]. However, the clamping manipulator S can be decomposed into two function modules — gripping function module S1 and pose changing function module S2 (Fig. 2), both of which are equipped with their own executive system and sensor testing system. The clamping process is completed by information processing and information exchange under control system.

The gripping function module S1 — bearing gripper, takes a role in catching semifinished bearing rings as well as positioning and clamping; The pose changing function module S2 — clamping manipulator, is capable of adjusting the pose of the bearing gripper.

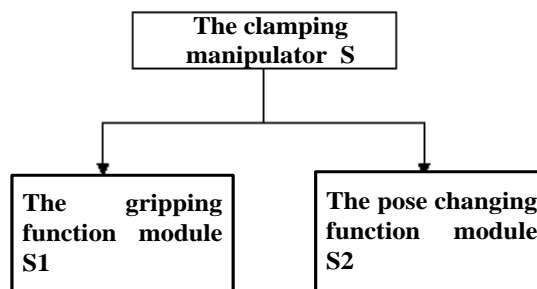


Fig.2. The function modules of clamping manipulators

Configuration scheme of the clamping manipulators

The rigid objects have six degrees of freedom (DOF), which mean the translation along three coordinate directions and rotation around three coordinates; correspondingly, the universal industrial serial robots (hereinafter referred to as robots) have six DOF that allow the robots to achieve any pose[9].

The DOF of dedicated robots need to be determined according to specified requirements. The axisymmetric structure of bearing rings only calls for five DOF to describe the spatial pose (description of the rotation around the axis is unnecessary). Correspondingly, the clamping manipulator has five DOF, three of which are aimed at adjusting the spatial location of the terminal, and another two DOF can adjust the spatial pose of the terminal.

Industrial robots have two kinds of joints: prismatic joint P and revolute joint R. There are three kinds of relations between the joint axes (Fig. 3): vertical \perp , parallel \parallel , crossed \times . Vertical includes perpendicularly intersectant (plane relation) and disjointedly vertical (spatial relation); crossed includes intersectant (plane relation) and disjointedly crossed (spatial relation); parallel includes collinear, but there is no collinear between the joints of the same kind, otherwise there is no practical application value. In the form of inverse kinematic, the robots with six DOF are typically characterized by multiple vertical or parallel joint axes; from the perspective of the parts processing and assembly, the robots are obviously superior at manufacturability when the joint axes are vertical or parallel. Therefore, the joint axes of industrial robots are vertical or parallel.

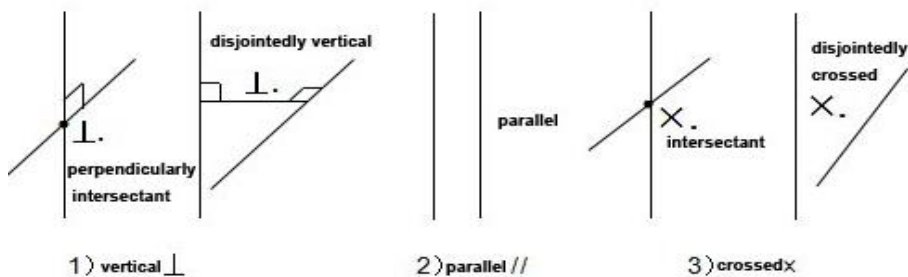


Fig.3. Three kinds of relations between the joint axes

Configuration analysis of the clamping manipulator wrist.

With three DOF, a serial industrial robot arm is composed of joint P and joint R. There are eight kinds of combinations: PPP, PPR, PRP, RPP, PRR, RPR, RRP and RRR. In each combination, there are four kinds of relations between the joint axes: ////, //⊥, ⊥⊥, ⊥// (⊥ stands for joint).

Prismatic joint P cannot adjust the pose, so the wrist joint is composed of joint R. The wrists of universal six-DOF industrial robots are made in the form of 3R (RRR) that helps the wrist achieve any pose and live up to the orthogonality condition. 3R-type wrist has three DOF, which are Roll, Pitch and Yaw around the axis. Roll can achieve 360-degree rotary, namely, Rolling R, while Pitch and Yaw are referred to as Bend B.

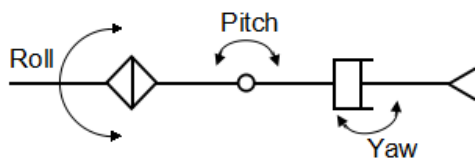


Fig. 4. The three DOS of 3R-type wrist

Due to the axisymmetric structure, it only takes two DOF to describe the pose of the bearing; the clamping manipulator has two corresponding DOF — Pitch and Yaw. The wrist with two turns is called BB-type wrist.

There are two kinds of combinations (Fig.5) for BB-type wrist of the clamping manipulator: Pitch in the front of Yaw or Yaw in the front of Pitch. The bearing rings are located at the end of the wrist, whose load force is vertically downward, and the actuator of the pitch joint needs to bear the gravity at the end.

Considering the characteristics of compact structure and dynamics, we chose the former: Pitch in front of Yaw.

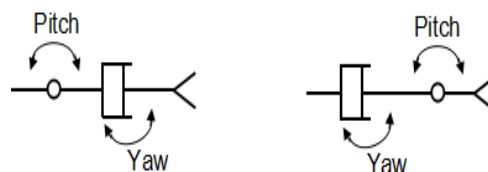


Fig.5. Two kinds of combinations for BB-type wrist of the clamping manipulator

3. Forward kinematics analysis of clamping manipulators based on d-h method

Robot kinematics is applied to the research on the transformation between joint space and Cartesian space, which covers the relations between pose, velocity and acceleration [10]. The essence of forward kinematics (pose changing) modeling is to establish the pose relations between the rigid connecting rods. First, pose description method of the rigid body was necessary, and then we established the forward kinematics model based on this method. The detailed proof of inverse kinematics that we left out could be accomplished based on the forward kinematics model.

The spatial relations between the connecting rods were described by 4×4 homogeneous transform matrix, furthermore, the homogeneous transform matrix ${}^0_T^N$ of the terminal actuator coordinate system with regard to the base coordinate system was deduced; at last, the forward kinematics equation was established. The basic flow of kinematics analysis based on D-H method is shown in Fig. 6.

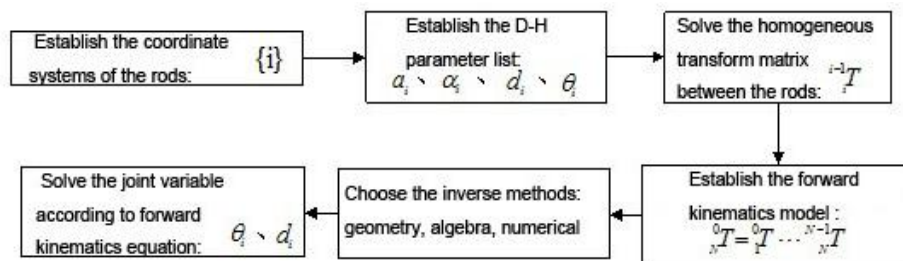


Fig.6. The basic flow of kinematics analysis based on D-H method

First, establish the clamping manipulator coordinate system, as is shown in Fig.7; next, establish

D-H parameter list (as is shown in Table 1) on the basis of the coordinate system.

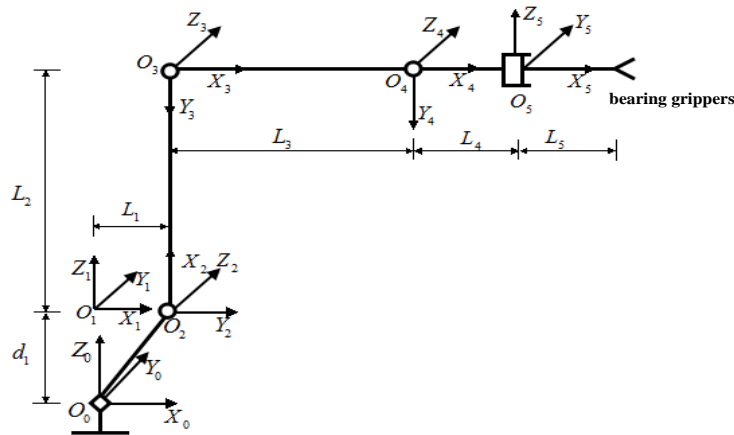


Fig.7 The coordinate system of clamping manipulator

The coordinate system i is fixed on the connecting rod i , where:

- 1) Z_i Refers to the direction (either plus or minus) of rotating or moving axis;
- 2) X_i refers to the common perpendicular between Joint i and Joint $i+1$, and the plus direction goes from Joint i to Joint $i+1$;
- 3) Right-hand rule is the determinant factor.

Table 1. D-H parameters of clamping manipulators

i	α_{i-1}	a_{i-1}	θ_i	d_i	Range of variables
1	0	0	θ_1	d_i	$-180^\circ \div 180^\circ$
2	90°	L_1	θ_2	0	$-180^\circ \div 180^\circ$
3	0	L_2	θ_3	0	$-180^\circ \div 180^\circ$
4	0	L_3	θ_4	0	$-180^\circ \div 180^\circ$
5	-90°	L_4	θ_5	0	$-180^\circ \div 180^\circ$

- 1) a_{i-1} refers to the distance measured along the X_i direction from joint axis Z_i to Z_{i+1} ;
- 2) α_{i-1} Refers to the rotation angle from the joint axis Z_i to Z_{i+1} around X_i ;
- 3) d_i Refers to the distance measured along the Z_i direction from X_{i-1} to X_i ;
- 4) θ_i Refers to the rotation angle from X_{i-1} to X_i around Z_i ;

- 5) Without considering the structural constraints, the range of variables of $\theta_1, \theta_2, \theta_3, \theta_4$ and θ_5 is $(-180^\circ, 180^\circ)$. However, the range of variables needs to be taken into consideration in practical engineering application.

The transformation matrix from connecting rod $i-1$ to i :

$${}^{i-1}T_i = \begin{bmatrix} c\theta_i & -s\theta_i & 0 & a_i \\ s\theta_i c\alpha_{i-1} & c\theta_i c\alpha_{i-1} & -s\alpha_{i-1} & -s\alpha_{i-1} d_i \\ s\theta_i s\alpha_{i-1} & c\theta_i s\alpha_{i-1} & c\alpha_{i-1} & c\alpha_{i-1} d_i \\ 0 & 0 & 0 & 1 \end{bmatrix} \quad (1)$$

$$\sin \theta_i = s\theta_i = s_i, \cos \theta_i = c\theta_i = c_i, \cos(\theta_i + \theta_j) = c(\theta_i + \theta_j) = c_{ij}$$

According to Table 1 and Formula (1), here is the transformation matrix ${}^{i-1}T_i (i=1 \div 5)$ between the connecting rods

$${}^0T_1 = \begin{bmatrix} c\theta_1 & -s\theta_1 & 0 & 0 \\ s\theta_1 & c\theta_1 & 0 & 0 \\ 0 & 0 & 1 & d_1 \\ 0 & 0 & 0 & 1 \end{bmatrix}$$

$${}^2T_3 = \begin{bmatrix} c\theta_3 & -s\theta_3 & 0 & L_2 \\ s\theta_3 & c\theta_3 & 0 & 0 \\ 0 & 0 & 1 & 0 \\ 0 & 0 & 0 & 1 \end{bmatrix}$$

$$\begin{aligned}
 {}^3_4T &= \begin{bmatrix} c\theta_4 & -s\theta_4 & 0 & L_3 \\ s\theta_4 & c\theta_4 & 0 & 0 \\ 0 & 0 & 1 & 0 \\ 0 & 0 & 0 & 1 \end{bmatrix} \\
 {}^4_5T &= \begin{bmatrix} c\theta_5 & -s\theta_5 & 0 & L_4 \\ 0 & 0 & 1 & 0 \\ -s\theta_5 & -c\theta_5 & 0 & 0 \\ 0 & 0 & 0 & 1 \end{bmatrix} \quad (2)
 \end{aligned}$$

Here is the transformation matrix of robot wrist terminal coordinate system {N} with regard to the base coordinate system {0}, namely, the forward kinematics equation of manipulators:

$${}^0_N T = {}^0_1 T {}^1_2 T \dots {}^{N-1}_N T \quad (3)$$

Substitute the transformation matrix ${}^{i-1}_i T$ (i=1÷5) and here is the forward kinematics equation of clamping manipulators:

4. An analysis on the workspace of clamping manipulators

As the basis of analysis on robot dexterity, analysis on the workspace will provide optimal target or constraint for the optimization design of geometric parameters and reference for track planning (to avoid the singular form) [11]. Here is the analysis on the

workspace of clamping manipulators by graphic method.

The workspace of prosthetic industrial robots refers to the space formed by all the points where the wrist reference points can reach. Because axes of general industrial robot wrists intersect at one point, the wrist only takes part in adjusting the pose, without couple effects on the spatial location of terminal actuators.

Clamping manipulators are equipped with BB-type wrists which make it impossible for the wrist axes to intersect at one point, and couple effects will happen when the pose adjusting on the wrists lead to position change of terminal actuators. On condition that L_4 and

L_5 live up to the structure size constraint, they are supposed to be in their minimum values in structure design. In the analysis on the workspace of clamping manipulators, only the workspace determined by the first three joints is taken into consideration, and the couple effect caused by pose changing of the wrist is not.

The workspace of clamping manipulators is mainly determined by the geometric and structural parameters of the first three joints (3R), while the clamping manipulator wrist mainly contributes to pose adjusting, so the couple effect it has on spatial position can be put aside. The sketch of the clamping manipulator arm is shown in Fig. 8. The origin O_4 of coordinate system {4} at the arm joint coincides with the arm end point P. All the points where end point P can reach form the total workspace W (P) of the clamping manipulator.

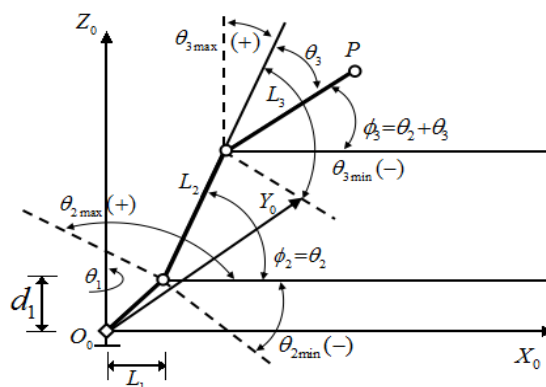


Fig.8. Sketch of the clamping manipulator arm

According to Fig.8, when $\theta_1=0$, the coordinate of point P in the base coordinate system is $P(X, Y, Z) = [X \ Y \ Z]^T$, and the analytical expression is:

$$P(X, Y, Z) = \begin{bmatrix} X \\ Y \\ Z \end{bmatrix} = \begin{bmatrix} L_1 + L_2 \cos \phi_2 + L_3 \cos \phi_3 \\ 0 \\ d_1 + L_2 \sin \phi_2 + L_3 \sin \phi_3 \end{bmatrix} \quad (5)$$

d_1 Refers to the base height that can be adjusted according to site requirements (on condition that the boundary and area of workspace are not affected), and

only the position of workspace area is affected. L_1 refers to the height of Rod 1 (offset of Joint J_1), which affects the regional boundary and cross-sectional area of the workspace; L_2 and L_3 respectively refer to the length of the upper arm and lower arm; ϕ_2 refers to the swinging angle of the upper arm with regard to the coordinate system $X_0(\phi_2=\theta_2)$, and ϕ_2 is zero in horizontal direction, minus clockwise and plus anti-clockwise, $\phi_2 \in [\theta_{2\min}, \theta_{2\max}]$; ϕ_3 refers to the swinging angle of the lower arm relative to the coordinate system $X_0(\phi_3=\theta_2+\theta_3)$, ϕ_3 is zero in horizontal direction, minus clockwise and plus anti-clockwise, $\phi_3 \in [\theta_{2\min} + \theta_{3\min}, \theta_{2\max} + \theta_{3\max}]$; likewise, the coordinate of the arm end point P in the base coordinate system {0} can be solved by means of coordinate transformation. Here is Formula (6) based on Formula (2):

$${}^0_4T = \begin{bmatrix} c_1c_{234} & -c_1s_{234} & s_1 & L_1c_1 + L_2c_1c_2 + L_3c_1c_{23} \\ s_1c_{234} & -s_1s_{234} & -c_1 & L_1s_1 + L_2s_1c_2 + L_3s_1c_{23} \\ s_{234} & c_{234} & 0 & d_1 + L_2s_2 + L_3s_{23} \\ 0 & 0 & 0 & 1 \end{bmatrix} \quad (6)$$

According to Formula (6), here is the coordinate of origin O_4 (of the coordinate system {4}) in the base coordinate system {0}:

$${}^0P_4 = \begin{bmatrix} L_1c_1 + L_2c_1c_2 + L_3c_1c_{23} \\ L_1s_1 + L_2s_1c_2 + L_3s_1c_{23} \\ d_1 + L_2s_2 + L_3s_{23} \end{bmatrix} \quad (7)$$

When $\theta_1=0$, the results of Formula (7) and Formula (5) are the same. Formula (7) is the analytical expression of the points in the total workspace W (P) of clamping manipulators.

According to graphic method, the total workspace W (P) of clamping manipulators is characterized by two cross sections:

1) The cross section of $X_0O_0Z_0$ can be denoted as the main cross section S_{XOZ} which rotates round the axis Z_0 by θ_1 , thus the total workspace W (P) is formed. The main cross-sectional area is referred to as the main work area (S_{XOZ}^1) in S_{XOZ} when $X_0 \geq 0$, and the main work area that is formed with S_{XOZ}^1 rotating around the axis Z_0 by θ_1 can be denoted as $W^1(P)$; the main cross-sectional area is referred to as the vice work area S_{XOZ}^2 when $X_0 < 0$, and the main work area that is formed with S_{XOZ}^2 rotating around the axis Z_0 by θ_1 can be denoted as $W^2(P)$. Here is Formula (8).

$$S_{XOZ} = S_{XOZ}^1 + S_{XOZ}^2 \quad (8)$$

2) The cross section of $Z_0=Z_0$ can be denoted as the vice cross section S_{XOY} ($Z_0=Z_0$), and the main cross section S_{XOZ} directly affects S_{XOY} . The main cross-sectional work area S_{XOZ}^1 rotates around the axis Z_0 by θ_1 and forms the vice work area S_{XOY}^2 of the vice cross section. Here is Formula (9):

$$S_{XOY}(Z_0=Z_0) = S_{XOY}^1(Z_0=Z_0) + S_{XOY}^2(Z_0=Z_0) \quad (9)$$

5. Optimal analysis on the geometric parameters of clamping manipulators

Analysis of the influence that rod length has on the workspace and overturning features of clamping manipulators

After the mechanism configuration of robots is confirmed, the geometrical parameters (the length of connecting rods and rotation range of the joints) of robots need to be determined according to the design constraints and the optimization targets (such as workspace, kinematic capability index and dynamic capability index) [12]. With workspace as the optimal target, a lot of scholars did relevant researches on the optimized design in geometric parameters of industrial serial robots by simplifying the space geometric constraints into plane geometry constraints.

According to the analysis above, it's obvious that the main cross section S_{XOZ} of the clamping manipulator's workspace is function of $L_2, L_3, \theta_{2\min}, \theta_{2\max}, \theta_{3\min}$ and $\theta_{3\max}$. The values of L_1 and d_1 have no effect on the shape or size (except the position) of the main cross section. Without considering the constraints of mechanical structure and so on, θ_2 and θ_3 can achieve integer rotation. Here is the area formula of the main cross section S_{XOZ} of clamping manipulator's workspace:

$$S_{XOZ} = \pi \left[(L_2 + L_3)^2 - (L_2 - L_3)^2 \right] = 4\pi L_2 L_3 \quad (10)$$

With one of L_2 and L_3 stable and the other one variable, S_{XOZ} will vary linearly along with L_2 or L_3 ; if $L_2 + L_3 = l$ is constant and $L_2 = L_3 = l/2$, the area of the main cross section is the largest.

For the second joint J_2 of industrial serial robot, there are two kinds of structure modes: non-offset ($L_1 = 0$) and offset ($L_1 \neq 0$). $S_{XOY} (Z_0 = Z_0)$ is function of L_1 when the main cross section S_{XOZ} , the position of the vice cross section ($Z_0 = Z_0$) and the range

(from $\theta_{1\min}$ to $\theta_{1\max}$) of Angle θ_1 are given. Operating assignments are usually completed in $W^1(P)$, namely, in

the vice cross section $S_{XOY}^1 (Z_0 = Z_0)$, therefore, an analysis of the influence that variation of L_1 has on

S_{XOY}^1 is more practical and beneficial. The clamping manipulator arm joint J_2 is either non-offset ($L_1 = 0$) or offset ($L_1 \neq 0$), correspondingly, the area of $S_{XOY}^1 (Z_0 = Z_0)$ is:

$$S_{XOY}^1 (Z_0 = Z_0) = \frac{\theta_{1\max} - \theta_{1\min}}{360/\pi} \times [r_1^2(z_0) - r_2^2(z_0)] \quad (11)$$

$$S_{XOY}^1 (Z_0 = Z_0) = \frac{\theta_{1\max} - \theta_{1\min}}{360/\pi} \times \{r_1^2(z_0) - r_2^2(z_0) + 2L_1[r_1(z_0) - r_2(z_0)]\} \quad (12)$$

$r_1(z_0)$ And $r_2(z_0)$ refer to the rotational radiuses from the intersection (of $Z_0 = Z_0$ and the main work area boundary curve) to the axis Z_0 , and $r_1(z_0) > r_2(z_0)$.

When Joint J_1 offsets L_1 , the increasing rate of the area of vice cross section $S_{XOY}^1 (Z_0 = Z_0)$ is $\eta_{S_{XOY}}$:

$$\eta_{S_{XOY}} = \frac{S_{XOY}^1(L_1 \neq 0) - S_{XOY}^1(L_1 = 0)}{S_{XOY}^1(L_1 = 0)} \times 100\% = \frac{2L_1}{r_1(z_0) + r_2(z_0)} \times 100\% \quad (13)$$

The area of the vice cross section $S_{XOY}^1 (Z_0 = Z_0)$ increases linearly with L_1 increasing, however, variation of L_1 also leads to the change in the overturning feature of clamping manipulators.

Contain cuboids in the target tasks of clamping manipulators

The task path of robots consists of a series of space points and space curves which can be contained by a cuboid $l \times b \times h$ (length \times width \times height), as is shown in Fig. 9. Apparently, there is an infinite variety of such cuboids on condition that they conform to the containing task path. As long as the workspace of robots contains the cuboids, task path can be completed in accord with the design requirements. The design of robots is the most reasonable when a suitable contain cuboid is given.

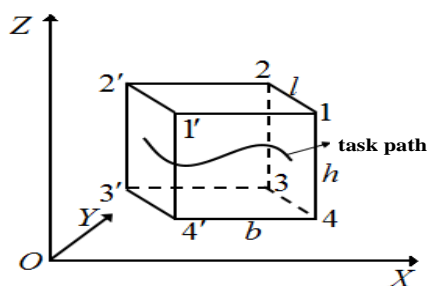


Fig. 9. The contain cuboid that contains the task path of a robot

Without considering the mechanical structure constraints of clam-ping manipulator arms, hypothesize

that θ_1 , θ_2 and θ_3 can achieve integer rotation and

$$\theta_{1\min} = \theta_{2\min} = \theta_{3\min} = -180^\circ,$$

$$\theta_{1\max} = \theta_{2\max} = \theta_{3\max} = 180^\circ;$$

suppose $l \times b \times h$ is the length of the sides of the cuboid that is formed by the clamping manipulator's work space. According to Fig. 9, the four vertexes 1, 2, 3 and 4 on the right side of the cuboid are located on the outer boundary surface of the clamping manipulator workspace, while the four vertexes

$1'$, $2'$, $3'$ and $4'$ on the left side of the cuboid are located inside the work space. Operating tasks are

usually completed in $W^1(P)$, therefore, we gave an analysis of the cuboids contained by the workspace which is formed by the ma-in cross-sectional work area

$$S_{AOY}^1 \text{ rotating by } \theta_1.$$

6. Coclusions

In this study, we researched on the bearing ring biaxial CNC machine tool clamping manipulators from the aspects of configuration design, kinematics analysis, workspace analysis and optimal design of geometrical parameters. Firstly, by analyzing the turning processing craft of bearing rings biaxial CNC machine tools, we established the total function model diagram and function structure chart of clamping manipulators based on clamping requirements; furthermore, we summarized the functions and determined the function modules of clamping manipulators as well as the functional design requirements table. Then we established the forward kinematics model of clamping manipulators by D-H method; based on graphic method, we gave a detailed analysis of the influence that the variation of joint rotating angle range has on the workspace main cross-sectional shape of clamping manipulators. At last, we analyzed the capacity to contain cuboids of clamping manipulator's workspace. There are a few deficiencies in the study; therefore, further improvements are needed to consummate the structural design of serial robot manipulators.

7. Acknowledgements

Natural Science Research Project of Anhui Province Education Office; A focused research project of natural science of Western Anhui University— Feature design of interfaces between digital controlled lathe modules based on reconfigurable mode (1.0KJ103762015B03)

An industry-university-research project of Liu'an city— Production organization of digital controlled lathe based on scale customization (2012LWB002).

Anhui Province Teaching Research Project of Engineering train teaching system based on improving the engineering practice ability. (No.2015jyxm285)

8. References

- [1] Jiang J, Zhang Y, Zhang W. Collaborative Simulation and Experimentation on the Dental Arch Generator of a Multi-manipulator Tooth-arrangement Robot [J]. International Journal of Advanced Robotic Systems, 2012, 9(4): 559-568.

- [2] Kuo Y L, Lin T P, Wu C Y. Experimental and Numerical Study on the Semi-Closed Loop Control of a Planar Parallel Robot Manipulator [J]. *Mathematical Problems in Eng*, 2014, 11(5):809-812.
- [3] Pham D T, Castellani M, Fahmy A A. Learning the inverse kinematics of a robot manipulator using the Bees Algorithm [J]. *IEEE International Conference on Industrial Infor*, 2008: 493 - 498.
- [4] Soltanpour M R, Shafiei S E. Robust Backstepping Control of Robot Manipulator in Task Space with Uncertainties in Kinematics and Dynamics [J]. *Elektronika Ir Elek*, 2009, (8): 75-80.
- [5] Liang Y W, Xu S D, Chu T C. Robust Control of the Robot Manipulator via an Improved Sliding Mode Scheme [J]. *Mechatronics & Automation .icma .international Conference on*, 2007: 1593 - 1598.
- [6] Tanev T K, Rooney J. Rotation Symmetry Axes and the Quality Index in 3D Octahedral Parallel Robot Manipulator System [J]. *Advances in Robot Kinematics*, 2002: 29-38.
- [7] Zavrazhina T V. Influence of the flexibility of links on the dynamics of a multilink robot manipulator [J]. *International Applied Mechanics*, 2007, 43(5):577-585.
- [8] Dixon W E, Moses D, Walker I D, et al. A Simulink-based robotic toolkit for simulation and control of the PUMA 560 robot manipulator [J]. *Proc.ieee/rsj Int.conf.intel.robots.syst*, 2001, 4:2202-2207 vol.4.
- [9] Tan L, Lu S Y, Li J X, et al. The Control and Simulation of the Live Washing Robot Based on the 6-DOF Manipulator [J]. *Advanced Materials Res*, 2014, 1049-1050: 1013-1017.
- [10] Chiaverini S, Siciliano B, Egeland O. Experimental results on controlling a 6-DOF robot manipulator in the neighborhood of kinematic singularities [J]. *Lecture Notes in Control & Information Sci*, 2006: 1-13.
- [11] Takahashi T, Murayama Y, Wang Z D, et al. A Control Method to Reduce the Oscillation of a Robot Manipulator with Elastic Joints and Non-Backdrivable Gear Trains [J]. *Journal of the Robotics Society of Japan*, 2000, 18(1): 142-149.
- [12] Vladimir F, Alexey K. Development of the System of Telecontrol by the Multilink Manipulator Installed on the Mobile Robot [J]. *Procedia Eng*, 2015, 100: 765-772.

BRAND:
«SMART MECHATRON - Competitiveness,
performance and high quality through
HIGH-TECH MECHATRONIC PRODUCTS »

LOCALIZATION AND MAPPING OF MOBILE ROBOT BASED ON HUMAN KINEMATICS INFORMATION

Yuanming Zhu

Basic Courses Department, Shandong University of Science and Technology, Taian, Shandong, 271019, P.R. China.

E-mail: zhuyuanming02@sina.com

Abstract - Simultaneous localization and mapping of outdoor mobile robot is a quite important research direction of autonomous mobile robot. The calculation, especially the calculation of big data, involved in localization and mapping using traditional robots, is severely restrained due to the physical factors such as airborne equipment equipped by robots, which reduces data processing efficiency and increases load. Generally, outdoor robot is localized through detecting characteristics of surrounding environment using laser scanner, visual system and sonar; however, when robots are in non-structural environment, the extraction of environmental characteristics will be difficult. To solve the problem, this study proposed a new method for the localization of mobile robot based on human kinematics information, i.e., terrain inclination characteristic. Using this method, when Global Position System (GPS) signal of robots is relatively weak or cannot be connected, self-localization can be applied based on sensors equipped by robots.

Keywords: *Human kinematics information; localization; map building; terrain inclination characteristic; Mobile robot.*

1. Introduction

To move based on the best rotation or translation matrix, traditional robots need to frequently scan surrounding environment and then match cloud point images obtained in adjacent two times through iterative closest point (ICP) matching algorithm. Simultaneous localization and mapping (SLAM) based on laser scanner becomes time-consuming because scanning and ICP matching need to be performed on the location for many times [1 ~ 3]

Therefore, this study proposed terrain inclination aided 3D localization and mapping (TILAM). The method not only can complete accurate location estimation of robots and map building, but also can save a lot of time [4 ~ 6]. The method integrates simultaneous localization and mapping based on ICP matching and terrain inclination characteristic based localization algorithm together. When moving to a new location, the robot will stop and do local scanning on surrounding environment; robot terrain inclination model can be extracted based on the obtained cloud point images [7 ~ 9]. Then local localization of robots can be realized according to terrain inclination characteristic based localization algorithm. When the mobile robot moves to another position on the path, local cloud point images will be scanned again; the location of robots and maps will be updated by matching cloud point images obtained in two times of scanning.

As to the traditional localization method, ICP matching based localization and mapping proceed simultaneously. Hence two times of continuous

scanning is needed; and the second scanning aims at estimating the location of scanning point through track estimation. When robots are in outdoor, track estimation may be biased due to the non-structural environment, which can lower the accuracy of ICP matching [10 ~ 12]. However, as human kinematics information based SLAM estimates the location of mobile robots by using terrain inclination characteristic based localization algorithm, relatively accurate estimation of initial position can be obtained in the second scanning; what is more, the spacing between two times of scanning is enlarged to reduce the times of scanning and matching.

2. Three dimensional point cloud based terrain fuzzy classification

In hypsographic maps, when local grid elevation difference of an area is larger than threshold, then the area can be determined as passable. When road surface is so uneven that there is no way to go through, it is necessary to make a terrain classification on three-dimensional point cloud more precisely and carefully. Currently, the extensively used point cloud classification method is supervised learning based outdoor scene point cloud classification method; however, the labeling of samples and procedures of training involved in the method are complicated and time-consuming, the selection of samples has a great impact on the effect of classification and its universality in different outdoor environments is poor. Hence, this study proposed a kind of fuzzy point cloud classification method which was applicable to different kinds of outdoor environment.

Using that method, robots can fulfill trafficability related outdoor terrain classification based on scene surface characteristic extraction, fuzzy reasoning and maximum entropy principle, which makes up the insufficient expression of hypsographic map on complicated environment. Redetermining hypsographic map based on the results of fuzzy terrain classification can figure out passable routes from uneven road surface.

Surface curvature and normal vector are two local geometrical characteristics which are frequently used; however they have poor expression effects in complicated outdoor environment. Currently, the classification of natural scene terrain based on distinctive characteristics has been extensively applied. Such kind of characteristic captures local spatial distribution of data point, but it ignores the fact that point cloud usually distributes on the surface of scene terrain. This study optimized the expression of scene through environmental surface feature (ESF) according to surface conditions and characteristics of outdoor environment. Three aspects of data point, i.e., the possibility of being ground data point, roughness of local surface and the angle between local surface normal vector and vertical direction were estimated based on the characteristic.

Previous research results suggest that, natural scene can be regarded as the combination of fuzzy structures and terrain structure can be explained as the continuum of land surface changes. Considering that the structure of objects in natural scene has no clear attribute determination, the classification of natural scene based on fuzzy logic is quite suitable.

Therefore, this study put forward a kind of fuzzy inference system (FIS) which integrated ESF using semantic rule to complete the expression of uncertainty of object structure in natural scene. Fuzzy membership vector is the output expression means of feature fusion system. As a high-level feature, the vector can be used to express the internal fuzziness of object structure in natural scene. The membership distribution of mode space of data point is evaluated by fuzzy entropy; the category of data point is determined based on maximum value of fuzzy entropy of local area.

ESF extraction

During the acquisition of outdoor scene data based on three-dimensional point cloud, the probability of ground point can be obtained through calculating the density of points in certain area below every data point. Filter used in taper area distinguishes ground point through determining whether the number of points in taper area below some data point is larger than some threshold. This study improved the method. First, two-dimensional rasterization segmentation was performed on point clouds. Then data points which belonged to the same grid G_{ij} as P_i was assumed as g_{ij} . B_i was used to describe point set from g_{ij} which distributes below P_i . The calculation of the probability of P_i as ground point based on feature descriptor F_g is as follows.

$$F_g(P_i) = 1 - \left[\frac{\min(\text{card}(B_i), n_p)}{n_p} \right]^\tau \quad (1)$$

In the formula,

$$P_i = (P_{ix}, P_{iy}, P_{iz}), g_i = (g_{ijx}, g_{ijy}, g_{ijz}),$$

$$B_i = \{g_{ij} \in G_{ij} | g_{ijz} < P_{iz} - \varepsilon\}, \text{ and } \tau = 1(P_{iz} < 0) \text{ or}$$

$$\tau = 0.5(P_{iz} \geq 0).$$

The function of margin constant ε is to prevent the interference of adjacent data points (e.g. $\varepsilon = 0.01\text{m}$); n_p stands for normalizing factor (e.g.

$n_p = 6$). $P_{iz} \geq 0$ suggests the elevation of P_i in vertical direction is larger than the origin of laser scanning, and at that moment, the probability of P_i being ground point

is smaller than the probability when $P_{iz} < 0$. Index τ is used to realize non-linear compensation.

In laser scanning plane, neighborhood points in a fixed number were selected as support points of P_i . Three maximum feature values of covariance matrix of support points were λ_1, λ_2 and λ_3 ($\lambda_1 > \lambda_2 > \lambda_3$) and

the corresponding feature vectors were \vec{n}_1, \vec{n}_2 and \vec{n}_3 .

Feature descriptor F_r can estimate the roughness of local surface and feature descriptor F_a can estimate the angle between normal vector and vertical direction, and the calculation of the two is as follows:

$$F_r = \sqrt{2\lambda_3 / (\lambda_1 + \lambda_2)} \quad (2)$$

$$F_a = \arccos\left(\frac{\vec{n}_3 \cdot [001]}{|\vec{n}_3|}\right) \quad (3)$$

3. The separation of point cloud

Inference and analysis of point cloud separation algorithm.

The basic principles of pseudo scanning line filtering algorithm based on slope [14 ~16] are as follows. For each scanning line, for any two adjacent points P_{i-1} and P_i , d_{zi} and S_i stand for the differences of slope and elevation between P_{i-1} and P_i . If d_{zi} and S_i were smaller than threshold Limit_dz and Limit_S , then P_i was regarded as the ground point; otherwise, P_i was regarded as the non-ground feature point [13]. Classification function is shown below.

$$\text{Points}(P_i) = \begin{cases} 0 & d_{zi} < \text{Limit_dz}, S_i < \text{Limit_S} \\ 1 & \text{else} \end{cases} \quad (4)$$

Where 0 indicates the point is a ground point and 1 indicates the point is a non-ground point.

When acquiring surrounding environmental information, three-dimensional laser scanner scans line by line and stores information according to scanning order.

Therefore, adjacent points stored in data space stand for adjacent points in actual ground surface. The selection of adjacent point in cloud point separation algorithm is shown in figure 1.

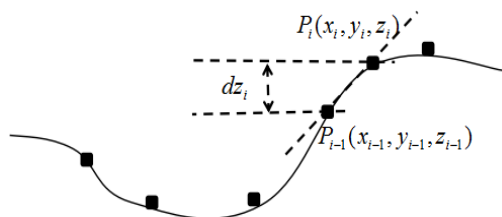


Fig.1. The selection of adjacent point

As to points on scanning lines, $a_{i,LtoR}$ and $a_{i,RtoL}$ were used to label ground point and non-ground point from left to right and from right to left respectively. At the beginning, laser points were processed from left to right along scanning lines. Besides, the first point on scanning lines was assumed as ground point, labeled as $a_{1,LtoR}$. The differences of elevation and slope between P1 and P2 were calculated. If the differences of elevation and slope both satisfied the given threshold, then P2 was considered as the ground point and moreover $a_{2,LtoR} = 0$. If it did not conform to the threshold, then it was considered as non-ground point and $a_{2,LtoR} = 1$. Then P2 and P3 were compared. The method was performed until all points on scanning lines were traversed. To ensure the completeness and accuracy of traversal, all points needed to be traversed again along scanning lines, and the result was labeled as $a_{i,RtoL}$. The results were processed after two times of traversal. Only when the two results $a_{i,LtoR}$ and $a_{i,RtoL}$ are ground points can P_i finally be confirmed as ground point. If any of the results was non-ground point, then P_i was confirmed as the non-ground point. Classification function is shown as follows.

$$\text{Points}(P_i) = \begin{cases} 0 & a_{i,LtoR} + a_{i,RtoL} = 0 \\ 1 & \text{else} \end{cases} \quad (5)$$

Different scanning systems have different scanning and storage means. To make the filtering algorithm which is similar to one-dimensional bi-directional labeling method more universal, the whole scanning point cloud was considered as being composed by many rows of data, every row of data was regarded as one group of pseudo scanning lines, and they were processed by the above filtering separation algorithm. But the initial points were all regarded as ground points.

Though the result was determined using two times of filtering, the accuracy of determination of initial points still could not be ensured because the

determination might be biased. To effectively solve the problem, the algorithm needed improvement. First, all points on every pseudo scanning line could be traversed to find out the lowest point and determine whether it was the super-low point. If it was, then it was abandoned; otherwise, it was considered as the ground point. Usually, super-low points distribute independently and are discontinuous with elevation values of ordinary values; therefore they could be filtered. Whether one point is the super-low point could be determined based on the difference of elevation of the point and the other two points on the left and right side respectively. If the difference exceeded the given threshold, then the point was determined as the super-low point; otherwise, it was determined as a normal point on scanning lines. Then filtering was performed on differences of slope and elevation on left and right sides according to the determined initial ground points. The procedures of point cloud separation algorithm are as follows.

(1) Point cloud data were divided into many pseudo scanning lines along some axis. Then the lowest point was found out from each line and whether it was the super-low point was determined. If it was, then it was removed; otherwise, it was determined as the ground point. Taking that point as the initial point, filtering algorithm was performed on differences of slope and elevation on left and right sides. The calculation formula of the slope of two adjacent points is:

$$S_i = \frac{z_i - z_{i-1}}{\sqrt{(x_i - x_{i-1})^2 + (y_i - y_{i-1})^2}} \quad (6)$$

Where (x_i, y_i, z_i) stands for the coordinate of P_i in the world coordinate system and $(x_{i-1}, y_{i-1}, z_{i-1})$ stands for the coordinate of P_{i-1} in the world coordinate system.

(2) If absolute value of the slope S_i of P_i satisfied the given threshold Limit_S , then P_i needed to be determined according to attributes of P_{i-1} , if P_{i-1} was a non-ground point, then P_i was also a non-ground point; otherwise, whether the difference of elevation of P_i and P_{i-1} , i.e., dz , satisfied the given threshold was determined. If satisfied, then the point was determined as a ground point; if not, then the point was determined as a non-ground point. The calculation equation for the difference of elevation, i.e., dz_i , is as follows.

$$dz_i = |z_i - z_{i-1}| \quad (7)$$

(3) If absolute value of the slope S_i of P_i did not satisfy the given threshold Limit_S :

(a) If $S_i < 0$, then classification function is:

$$\text{Points}(P_i) = \begin{cases} 0 & (P_{i-1} = 0, z_i - z_t < \text{Limit}_d z) \text{ or } (P_{i-1} = 1, z_i - z_t > \text{Limit}_d z) \\ 1 & (P_{i-1} = 0, z_i - z_t \geq \text{Limit}_d z) \text{ or } (P_{i-1} = 1, z_i - z_t \leq \text{Limit}_d z) \end{cases} \quad (8)$$

(b) If $S_i > 0$, then classification function

$$\text{Points}(P_i) = \begin{cases} 0 & (P_{i-1} = 0, z_i - z_t < \text{Limit_dz}) \\ 1 & (P_{i-1} = 0, z_i - z_t \geq \text{Limit_dz}) \text{ or } (P_{i-1} = 1) \end{cases} \quad (9)$$

For the participation in calculation afterwards, the above filter separates ground points and non-ground points. The detailed point cloud separation algorithm is shown in table 1. In the table, P_i stands for scanning point to be determined, TP stands for labeled ground point, NTP stands for labeled non-ground point, and Z_t stands for ground point which is closest to P_i .

Table 1. Data separation of laser scanning points

Point cloud separation algorithm	
1	if $ S_i < \text{Limit_S}$ and
2	if P_{i-1} is NTP, then P_i is NTP ;
3	else if $dz_i < \text{Limit_dz}$, then P_i is TP;
4	else P_i is NTP;
5	endif
6	endif
7	else if $S_i < 0$ and
8	if P_{i-1} is TP and $z_i - z_t < \text{Limit_dz}$, then P_i is TP;
9	if P_{i-1} is NTP and $z_i - z_t < \text{Limit_dz}$, then P_i is TP;
10	if P_{i-1} is TP and $z_i - z_t \geq \text{Limit_dz}$, then P_i is NTP;
11	if P_{i-1} is TP and $z_i - z_t \leq \text{Limit_dz}$, then P_i is NTP;
12	endif
13	else if $S_i > 0$ and
14	if P_{i-1} is TP and $z_i - z_t < \text{Limit_dz}$, then P_i is TP;
15	if P_{i-1} is TP and $z_i - z_t \geq \text{Limit_dz}$, then P_i is NTP;
16	if P_{i-1} is NTP, then P_i is NTP;
17	endif
18	endif
19	endif
20	endif

Programming according to the above procedures can achieve the separation of environmental point cloud. Non-ground point as characteristic matching point participates in the calculation of ICP matching algorithm after being uploaded to cloud end through network. Finally the updated location and environmental information can be obtained.

Matching of point cloud based on ICP

Three-dimensional images are usually matched using ICP algorithm which plays a vital role.

Model set $\mathbf{M} = \{\mathbf{m}_i\}_{i=1}^{\Delta}$ has N_m points and data

set $\mathbf{P} = \{\mathbf{p}_i\}_{i=1}^{\Delta}$ has N_p points. The conversion from data set to model set is linear conversion, taking R as rotation matrix and t as translation vector.

The main purpose of ICP algorithm is to acquire conversion parameter which can make the nearest point of points in data set and model set have minimum errors. The process can be described using formula (10).

$$\min_{R,t,j \in (1,2,\dots,N_m)} \left(\sum_{i=1}^{N_p} \|Rp_i + t - m_j\| \right) \quad (10)$$

The calculation method of ICP algorithm is as follows.

(1) Screen point pair: the closest points to points in P1 set were found out from P2 set. Then those points composed a new point pair. All point pairs of P1 and P2 could be obtained through the above method. The obtained two point pair sets were equivalent to two new point sets for effective calculation.

(2) Two point sets were obtained using the above methods; and two key points were obtained through calculation.

(3) Rotation matrix R and translation matrix t could be obtained through calculation according to the two key points obtained above.

(4) New point set P2 after rigid transformation of P2 could be obtained after calculation based on the obtained rotation matrix R and translation matrix t. Quadratic sum of distance from P2 to P2' was compared between the new and old point sets; based on that, the difference of quadratic sum of distance for successive two times was evaluated. Then the absolute values were calculated, and whether there was convergence was assessed. If the threshold value was larger than absolute value, then it can be determined as convergence and iteration stopped.

(5) Procedure (1) to (4) repeated till there was convergence or the set iteration times were achieved.

Rusinkiewicz S gave factors influencing ICP algorithm and moreover improved and expanded ICP. He divided ICP algorithm into six procedures, i.e., screening, matching, weight, removal, error measurement and minimum. There is a kind of bionic vision model screening method in ICP algorithm which is usually used to initialize three-dimensional point cloud set.

4. Human kinematics information assisted localization and mapping

Human kinematics information assisted localization

In unknown environment, local point cloud image of environment is acquired using laser scanner, and ground points and non-ground points are separated by using point cloud separation algorithm. Topographic map of the local environment can be obtained using the separated ground points. According to terrain inclination based localization algorithm, inclination model of robots can be extracted based on the planned route polarity. The localization of robots can be achieved through particle filter.

Mapping based on ICP matching algorithm

ICP is the most extensively applied three-dimensional point cloud matching method [17 ~ 19].

The purpose of ICP algorithm is to find out rotation matrix array R and translation matrix array T in laser point sets scanned by laser scanner in two times.

Assume $P = \{p_1, \dots, p_m\}$ as the reference point set and $Q = \{q_1, \dots, q_n\}$ as model set. Model set in the kth iteration could be expressed as $Q^k = \{q_1^k, \dots, q_n^k\}$.

Matrix for the transformation between P and Q^k was calculated and original transformation was updated till the average distance of data satisfied the given threshold. Detailed procedures are as follows.

(1) Point q_i^k was picked up from the model point set; the corresponding closest point q_i^k was searched in the reference point set; then point pair (q_i^k, p_i^k) was obtained;

(2) Rotation matrix R^k and translation matrix T^k were calculated; besides, $\|R^k q_i^k + T^k - p_i^k\| \rightarrow \min$.

(3) Q^{k+1} was calculated according to the formula $Q^{k+1} = R^k q_i^k + T^k$ and new number set Q^{k+1} generated;

(4) Least square error of Q^{k+1} and P were calculated; $d^{k+1} = \frac{1}{N} \sum_{i=1}^N \|q_i^{k+1} - p_i^k\|^2$. Iteration

stopped if the error d^{k+1} was smaller than the given threshold or iteration times were larger than the pre-set maximum iteration times; otherwise, new iteration started.

In this study, the matching of data in two point cloud images and the establishment of global map used for navigation was achieved based on point-to-point ICP matching algorithm. In point-to-point ICP matching, first the distance from point to set can be obtained from minimum euclidean distance from point to point, then the corresponding point is searched, and finally objective function which can solve spatial alternation can be obtained by adding the distance from the corresponding points to set together.

The advantage of ICP matching algorithm is that, precise matching based on the extraction of point set features is not needed. But the large calculated amount is one of the defects of the algorithm; besides, a relatively accurate initial estimation needs to be given, in order to avoid local optimum and failure of convergence. The traditional ICP matching algorithm based initial estimation comes from track estimation of speedometer. But in uneven outdoor terrain, the accumulated error of speedometer based track estimation will increase rapidly with the increase of distance, which restrains the travelled distance between two times of matching and increases the times of scanning and matching. In this study, we put forward terrain inclination based localization algorithm to replace track estimation, which can obtain accurate estimation of initial location without increasing extra sensor.

5. Experiment of human kinematics information based localization and mapping and result analysis

The design of experiment of human kinematics information based localization and mapping

The platform used in this study was pioneer 3-DX equipped with 3D laser scanner and inertial measurement unit (IMU). The information of surrounding environment could be acquired through laser scanner and IMU could be used for measuring the changes of posture of robots. The speed of robots was kept at v_{x_b} by the encoder on the wheel spindle of robot. Speed appeared in the direction of y_b and z_b which was caused by robot planning was ignored.

A piece of grassland with obvious terrain inclination feature outdoor was selected as the experimental environment. The place, 15 m long and 10 m wide, with uneven ground surface, was surrounded by many trees and has poor GPS signal. The scanning scope of three-dimensional scanner should be 80 degrees both in vertical direction and horizontal direction.

Experimental mode is as follows: first the mobile robot scanned the surrounding environment to obtain cloud point images; then local RTI model of the terrain was obtained according to the cloud point images; after scanning, the mobile robot moved forward; during movement, the robot was localized in real time based on terrain inclination. According to the experimental condition, the second time of scanning started after 6-m movement. The cloud point image scanned in the second time could be transformed into world coordinate system based on the estimated location of the mobile robot given by the terrain inclination based localization algorithm.

Finally, local cloud point images obtained after transformation were matched with the points obtained in the first time of scanning, thus achieving the updating of robot location and map. Lowering the number of point cloud and using kd-tree search algorithm are the main methods for accelerating ICP based matching speed of point cloud. Improving the efficacy of localization and mapping using the above methods is called fast ICP-based SLAM. This study compared the method with the method proposed by this study and carried out fast ICP-based SLAM experiment. The movement distance of robot was set as 3 m. After 3-m movement, the robot stopped and scanned the surrounding environment.

The cloud point image obtained in the first time of scanning was matched with the local cloud point image obtained in the second time; then the location of robot and map were updated. The robot moved at a speed of 0.1 m/s and the sampling cycle of sensor was 0.1 s.

Results of experiment of human kinematics information based localization and mapping and the analysis

A classification of ground point and non-ground point was performed in local cloud point image obtained in the first time of scanning. Terrain inclination model was extracted from the obtained ground points using the terrain inclination based algorithm proposed in section 2. Based on the RTI model, the mobile robot was localized using terrain inclination based localization algorithm when the mobile robot moved from the first scanning point ($T = 0$) to the second scanning point ($T = 1$ min). The movement time of mobile robot was set. The mobile robot stopped to scan and obtain the second local cloud point image after one minute passed since the mobile robot left the initial scanning point. Non-ground points were separated from the second local cloud point using cloud point separation algorithm. Combining the location information of robot obtained by terrain inclination based localization algorithm, the initial spatial coordinate of the non-ground point in world coordinate system could be obtained. Finally, ICP matching was carried out on the two scanned cloud point images; then the location of robot was updated based on translation and rotation matrix and the map was also updated. Using the updated ground point data, RTI model of the next road section could be obtained.

The localization of mobile robot moving from the second scanning point ($T = 1$ min) to the third scanning point ($T = 2$ min) was achieved through terrain inclination based localization algorithm. After matching of the third local point cloud image, global cloud point map of the experimental area could be obtained and the location map could be established. The experiment repeated for five times. Moreover, the average value and variance of errors of location estimated by different algorithms were calculated, followed by the calculation of localization error of two algorithms (Table 2). Euclidean space distance from the location estimated by algorithm to the reference point was expressed as d . Through analyzing table 2, we found that, the average value of localization error of TILAM was 79% lower than that of the traditional ICP-based SLAM; the uncertainty of localization of TILAM was 44% lower than that of traditional ICP-based SLAM.

Table 2 Comparison of localization error

Method	Average error-x axis (m)	Variance-x axis (m)	Average error -y axis (m)	Variance - y axis (m)	Average error - z axis (m)	Variance - z axis (m)	Average error of distance d (m)	Variance of distance d (m)
TILAM	-0.0125	0.0901	0.0328	0.0104	-0.0164	0.0017	0.0388	0.0903
ICP-based SLAM	-0.0124	0.1326	-0.2014	0.0851	-0.0779	0.0286	0.2168	0.1594

Through further analysis on the obtained data, we found a remarkable difference between TILAM and ICP-based SLAM in aspects of data acquisition and processing time, as shown in table 3. It can be known from table 3 that, TILAM divided the time needed for the localization of robot and mapping into two stages: the first stage was time needed for ICP matching of two cloud point images and the second stage was time needed for the localization of robot from the first scanning point based on terrain inclination feature.

Time needed by traditional ICP-based SLAM could also be divided into two stages: the first stage was time needed for ICP matching of two cloud point images and the second stage was time needed for the localization of robot from the first scanning point to the second scanning point based on track estimation. Though TILAM consumed more time than track estimation based localization in localization, the total time consumption of TILAM was 54% less than that of ICP-based SLAM due to the reduction of times of scanning and matching.

Table 3 Comparison of time consumption

Method	Time needed by localization algorithm	Matching time	Total time	Experimental distance
TILAM	$0.088s \times 3 \text{ times} = 0.264s$	$1.25s \times 2 \text{ times} = 2.5s$	2.764s	15m
ICP-based SLAM	$0.021s \times 5 \text{ times} = 0.105s$	$1.25s \times 5 \text{ times} = 6.25s$	6.355s	15m

To verify the robustness of algorithm, convergence time of algorithm was measured based on the given initial error (table 4). It can be known from the analysis result of data that, when the given initial error was smaller

than or equal to 0.2 m, the convergence time of algorithm was shorter than or equal to 4 s; when the given initial error became larger, the convergence time would become longer till diverged.

Table 4 Convergence time under different initial errors

No.	1	2	3	4
Robot speed (m/s)	0.1	0.1	0.1	0.1
Initial location error (m)	(0.1, 0.1, 0.1)	(0.2, 0.2, 0.2)	(0.3, 0.3, 0.3)	(0.4, 0.4, 0.4)
Convergence time (s)	3.8	5	25	33

6. Conclusion

When mobile robot moves in an unknown outdoor environment, laser scanner is used to acquire local cloud point image of working environment and terrain inclination based localization algorithm is used to achieve the localization of robot. When mobile robot moves to next location along the path, another local cloud point image can be obtained using laser scanner; the obtained cloud point images are matched based on ICP-based algorithm, and then the location of robot and map can be updated. It can be known from the experimental results that, the localization error and time consumption of TILAM is half that of traditional ICP-based SLAM. Besides, the experimental results suggest that, in an unknown outdoor environment, the localization and mapping method proposed by this study has good robustness and can achieve ideal results of localization and mapping within less time consumed.

7. References

[1] Neto A A, Macharet D G, Campos V C D S, et al. Adaptive complementary filtering algorithm for mobile robot localization [J]. Journal of the Brazilian Computer Society, 2009, 15(3):19-31.
 [2] Parker L E. Multiple Mobile Robot Teams, Path Planning and Motion Coordination in [J]. Encyclopedia of Complexity & Systems Science, 2009:5783-5800.

[3] Siemiątkowska B, Zychewicz A. The Application of ICP and SIFT Algorithms for Mobile Robot Localization [J]. Cism International Centre for Mechanical Sciences, 2009, 524:391-398.
 [4] Zhu X, Qiu C, Minor MA. Terrain Inclination based Three-dimensional Localization for Mobile Robots in Outdoor Environments [J]. Journal of Field Robotics, 2014, 31(3):477-492.
 [5] Zhu X, Qiu C, Minor M A. Terrain-inclination-based Three-dimensional Localization for Mobile Robots in Outdoor Environments [J]. Journal of Field Robotics, 2014, 31(3):477-492.
 [6] Tsubouchi T, Asano A, Mochizuki T, et al. Forest 3D Mapping and Tree Sizes Measurement for Forest Management Based on Sensing Technology for Mobile Robots [J]. Springer Tracts in Advanced Robotics, 2014, 92:357-368.
 [7] Wawrzyński P, Możaryn J, Klimaszewski J. Robust estimation of walking robots velocity and tilt using proprioceptive sensors data fusion [J]. Robotics & Autonomous Systems, 2014, 66(C):44-54.
 [8] Chakraborty N, Ghosal A. Dynamic Modeling and Simulation of a Wheeled Mobile Robot for Traversing Uneven Terrain Without Slip [J]. Journal of Mechanical Design, 2005, 127(5):901-909.
 [9] Ghosal A T A. A Three-Wheeled Mobile Robot for Traversing Uneven Terrain Without Slip: Simulation and Experiments [J]. Mechanics Based Design of Structures & Machines, 2013, 41(1): 60-78.

- [10]Murata N, Katsura S. Development and Control of Multi-Degree-of-Freedom Mobile Robot for Acquisition of Road Environmental Modes [J]. Transactions on Industry Applications, 2012, 132(3):301-307.
- [11]Guo N L, Zhang N M, Wang N Y, et al. Environmental Perception of Mobile Robot [J]. IEEE, 2006:348-352.
- [12]Martínez J L, González J, Morales J, et al. Mobile robot motion estimation by 2D scan matching with genetic and iterative closest point algorithms [J]. Journal of Field Robotics, 2006, 23(1):21–34.
- [13]Zhu X, Qiu C, Minor M A. Terrain Inclination Aided Three-Dimensional Localization and Mapping for an Outdoor Mobile Robot [J]. International Journal of Advanced Robotic Systems, 2013, 10(1):257-271.
- [14]Jicun H, Kwok T, Johnson R H. A simple derivation and analysis of a helical cone beam tomographic algorithm for long object imaging via a novel definition of region of interest [J]. Physics in Medicine & Biology, 2004, 49(2):205-25.
- [15]Valoroso N, Rosati L. Consistent derivation of the constitutive algorithm for plane stress isotropic plasticity. Part I: Theoretical formulation [J]. International Journal of Solids & Structures, 2009, 46(1):74-91.
- [16]Habib A F, Al-Durgham M, Kersting A P, et al. Error Budget of LiDAR Systems and Quality Control of the Derived Point Cloud [J]. Durgham, 2008, 75(9):1093-1108.
- [17]Armbruster W, Richmond R. The application of iterative closest point (ICP) registration to improve 3D terrain mapping estimates using the flash 3D ladar system [J]. Proceedings of SPIE - The International Society for Optical Engineering, 2010, 7684(1):143-153.
- [18]Chen J, Belaton B. An Improved Iterative Closest Point Algorithm for Rigid Point Registration [J]. Communications in Computer & Information Science, 2014, 481:255-263.
- [19]Wang F. Simulation of Registration Accuracy of Iterative Closest Point (ICP) Method for Pose Estimation [J]. Applied Mechanics & Materials, 2013, 475-476:401-404.

BRAND:
«SMART MECHATRON - Competitiveness,
performance and high quality through
HIGH-TECH MECHATRONIC PRODUCTS »

DEVELOPMENT AND DESIGN OF MANIPULATORS' POSITION MEASUREMENT SYSTEM BASED ON FIELD PROGRAMMABLE GATE ARRAY

Guoyang Liu

Electrical and Mechanical college, Shandong University of Science and Technology, Qianwangang Road 579th, Huangdao District, Qingdao, Shandong, 266510, China

E-mail: liuguoyang03@126.com

Abstract: A robot is the machine which can realize various functions by its own power and control ability. Recent years, robotics was widely used in the popular fields, which reflects a country's scientific and technological development level. Since the manipulator is the key tool for the robot while operating, it is vital important to develop and design manipulators. This paper studied the development and design of manipulator's position measurement system based on field programmable gate array (FPGA). Firstly, the overall design scheme of the manipulator system is given, which used FPGA as the controller to complete the data processing and control of the system. Then, according to the actual structure parameters of the manipulator, it calculated and analyzed the forward kinematics and inverse kinematics. Moreover, in order to complete the development and design of manipulators position measurement system, it analyzed trajectory planning method for manipulators in the joint space by using the method of cubic polynomial. The trajectory planning is carried out by using the spatial straight line and the spatial arc interpolation algorithm. Finally, not only this does make great contribution to the development of science and technology, but also provides strong technical support for promotion of national scientific strength and comprehensive national strength.

Keywords: Field programmable gate array (FPGA); Robot manipulator; Measurement system; Trajectory planning.

1. Introduction

Robots, as the production of mechanical electrics, advanced integrated control theory, computer and bionics, play an important role in the fields of medicine, constructions, industry and so on. It is able to run the program within the system, but also it can be carried out according to the principle of artificial intelligence technology [1-2]. Moreover, as a kind of high-technology, robot technology has more and more influence on people's life, which represents the highest achievements among mechanical and electrical integration technology.

Manipulator has been a great concern all the time because it is the most important actuator in the whole framework of robot [3-4]. The main study of the manipulator system is about hardware platform, software platform, corresponding algorithm and so on. What's more, it is also involved some other knowledge including kinematic theory, trajectory planning and computer simulation technology [5]. It is not hard to see that manipulator is complex- and-huge system engineering. In this paper, the design of the manipulator model is used as the object of study. It firstly established the hardware platform for the system by using appropriate profile and used field programmable gate array (FPGA) as the core controller to realize data

processing and motion control of the manipulator position measurement system, which analyzed and studied three different aspects including control system, trajectory planning and simulation technology. The kinematics of the manipulator is analyzed through the establishment of link coordinate system of the manipulator. Finally, it solved the kinematic equation of the manipulator system and carried out the research on trajectory planning algorithm [6-7].

Recently, many experts and scholars at home and abroad have made a certain analysis of the manipulator. The research from Poveda Rodríguez D K, Rodolfo V M and Carreño Zagarra J J in 2014 indicated that with the development of technology, the manipulator has gradually been used in our life. Meanwhile, with the application of manipulator in some complex fields, for example medical treatment, the development of the service type portable manipulator is more and more extensive [8]. In 2014, Chen Y X mentioned that the movement of the manipulator is realized by the power source and controller, and the function and related performance of the manipulator are directed effected by its hardware [9].

In order to design the better manipulator position measurement system, this paper used the PFGA as the core processor to build the control platform of the manipulator. That is the focus of present world's robot

research and major direction of the development of robot technology in the future.

2. Design scheme of Manipulator System

2.1 Realization of position measurement system

The model for FPGA of Cyclone II EP2C5T144C8 was used as the control chip for measuring system of manipulator, and the import chip with type of MAX1312 was used as the A/D conversion chip, both can provide independent multiple channels [10].

That's to say that independent sample makes circuits provide sampling simultaneously for each channel. Although the inputting sampling circuit signal bandwidth for A/D conversion circuit is only 20MHz, it is still able to digitalize the input signal quickly. Moreover, it will reduce the power consumption of the device by measuring periodic signal of bandwidth which is beyond ADC sampling rate. Overall functional framework of measurement system is seen as figure 1.

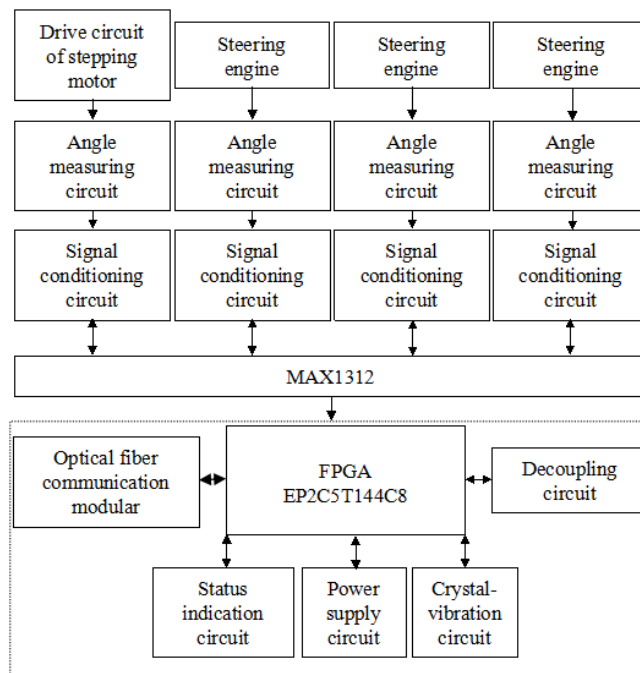


Figure 1: Block diagram of system function

According to different functions of chip MAX1312 with different pins, FPGA achieved the control of the pulse signal for three pins including of reading-writing signal (RD), chip select (CS) and starting conversion signal (CONVST), and collected the input voltage signal. EOLC is considered as a symbol pin of the end of the overall conversion for MAX1312, which means that all channels of MAX1312 stop data transitions once that pin has a low level output. What first should be done is to input low level signal for both pins of RD and CS during the process of reading data conversion results for MAX1312. Next is to release data that is locked by inputting high level for pin of RD.

2.2 Simulation of position measurement system

Compiling the data conversion program with Quartus II and simulating to the position measurement system by using Modelism, it is found that at the beginning of data conversion, the high level signal is input to the pins of CONVST, RD and CS simultaneously. In this process, once the output signal for EOLC drops, all the channels of MAX1312 will stop data transitions, which refers to that the whole data transition end now. On the other hand, inputting low level signal to both pins of EOLC and CS when reading

data, whenever the RD appears a falling edge signal, it means that the channel conversion data has been all output. Therefore, it can be seen from above simulation result that the operation sequence and way of each pin, which verifies the correctness of the simulations results.

3. Calculation and analysis of the kinematics of the manipulator

3.1 Position and pose description of the kinematics of the manipulator

(1) Description of Joint coordinate system for manipulator system (see as figure 2)

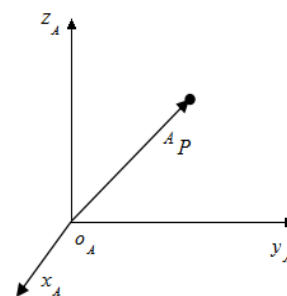


Figure 2: Schematic diagram of position vector

Figure 2 is the rectangular coordinate system. Basing on this, any point O in this coordinate system, its position can be shown with the vector ${}^A O$ as following column 3×1 :

$${}^A O = \begin{bmatrix} O_x \\ O_y \\ O_z \end{bmatrix} \quad (1)$$

Among which, ${}^A O$ is the position vector for the point O in the coordinate system, corresponded O_x , O_y and O_z separately represents the three coordinate vector for the point O in this rectangular coordinate system.

(2) Pose description of manipulator system

In this paper, for the space pose of any joint U in the manipulator, coordinate system {U} which uses U as the reference is built. Its coordinate origin is appointed as the feature point of joint. And the origin of the coordinate system can be described by the position vector ${}^A O_{U_0}$. Meanwhile, {A} is used as the reference coordinate system and rotation matrix is used to describe the direction and position of coordinate axes. That's to say that pose of U can be described as below by using coordinate system {U}:

$$\{U\} = \{R^A O_{U_0}\} \quad (2)$$

3.2 Analysis of forward kinematic

(1) Establishment of link coordinate system and kinematics equation

Step one: building D-H coordinate system and determine its origin; then selecting the appropriate axis of X and Z according to joint pose of manipulator and finally determine Y axis. What should be note is that the axis direction is determined by the right hand rule.

Step two: Establishing the linkage coordinate system of each joint of the mechanical arm once connecting rod parameters of D-H coordinate was determined.

Next is to make sure the D-H parameters of the each joint connecting rod of the manipulator.

Seen from figure 3:

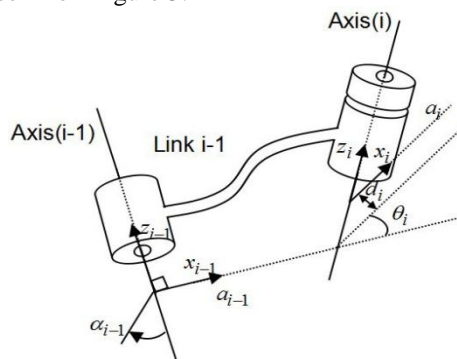


Figure 3 Description of connecting rod

Step three: solution of transformation matrix T_i ($i=1,2,3,\dots,n-1,n$).

Step four: solving the integral coordinate transformation matrix of manipulator, which is shown as below:

$$\begin{cases} T=T_1T_2T_3\dots T_n \\ T=T_n\dots T_3T_2T_1 \end{cases} \quad (3)$$

Step five: solution of manipulator kinematics equation

(2) Solution of forward kinematic equations

It is not hard to get the parameters of kinematic analysis by above establishment of manipulator linkage coordinate system. Following are the explanations for the solving step of forward kinematic equations.

Step one: once the D-H coordinate system of manipulator was completed, base of mechanical arm is set as basic coordinate system. After that, establishing corresponding coordinate system for all joints. Only follow certain principles for establishment of coordinate will it make sure the correctness of coordinate axes' direction.

Step two : D-H parameters of the connecting rod of manipulator is shown as table 1, which is obtained by determining the D-H parameters of each linkage joint according to the actual measurement data and related design parameters.

Table 1 D-H parameters of manipulator

Joint serial number	1(base)	2	3	4
θ_i	θ_1	θ_2	θ_3	θ_4
α_{i-1}	0	$\pi/2$	0	0
a_{i-1}	a_1	a_2	a_3	a_4
d_i	0	0	0	0
Connecting rod parameters (cm)	$a_1=30.03$	$a_2=41.78$	$a_3=32.23$	$a_4=20.08$

Step three: dealing with the coordinate transformation matrix T_i ($i=1,2,3,4$) according to the parameters of each connecting rod of manipulator in table 1.

Step four: basing on the previous equation 3, integral coordinate transformation matrix is shows as below.

$$T=T_1T_2T_3T_4 = \begin{bmatrix} n_x & o_x & a_x & p_x \\ n_y & o_y & a_y & p_y \\ n_z & o_z & a_z & p_z \\ 0 & 0 & 0 & 0 \end{bmatrix} \quad (4)$$

The position of manipulator terminal in the basic coordinate system can be expressed with

$$\begin{cases} \alpha = a \tan 2(n_y, n_x) \\ \beta = a \tan 2(-n_z, n_x \cdot \cos \alpha + n_y \cdot \sin \alpha) \\ \gamma = a \tan 2(a_x \cdot \sin \alpha - a_y \cdot \cos \alpha, -o_x \cdot \sin \alpha + o_y \cdot \cos \alpha) \end{cases} \quad (5)$$

It is known from analysis that data can clearly indicate terminal controller of manipulator is corresponded to the pose of basic coordinate system.

3.3 analysis of inverse kinematics

Inverse kinematics refers to the process to solve joint variable if the terminal pose of manipulator is determined. The mapping relation between joint space and cartesian space is shown as figure 4.

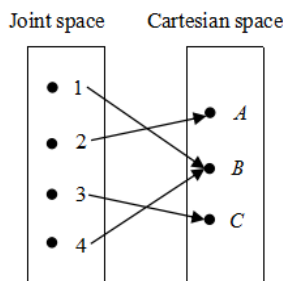


Figure 4: the relation between joint space and Cartesian space

In figure 4, there are separately 4 four groups and three kinds of terminal poses of manipulator in joint space and Cartesian space. Moreover, it is not hard to see that the relation from joint space to Cartesian space is single mapping relationship, on the contrary, the relation from Cartesian to joint space is one-to-multiple mapping relations [12-13].

In the process of controlling manipulator, the inverse kinematics was applied into the pose control for Cartesian space of manipulator. But inverse kinematics solution is not unique or it is possible not exist. Meanwhile, solutions for inverse kinematics are not single, so many kinds of way can be used as to get the results in this process.

4. Trajectory planning analysis of Manipulator

4.1 Point-to-point trajectory of Manipulator (See Figure 5)

$O=[O_x, O_y, O_z]$, and its Euler parameters of pose can be described using (α, β, γ) , that is:

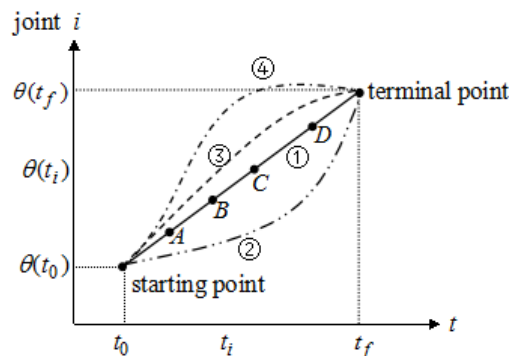


Figure 5: Schematic diagram of point-to-point trajectory

4.2 Joint space trajectory planning of Manipulator

(1) Three order polynomial trajectory planning

In order to insure the stability of the manipulator in joint space trajectory planning we need to bind respectively for the joint trajectory function $\theta(t)$ in the starting position, the end position, the starting speed and the terminal speed. When $t_0 = 0$, the value of $\theta(t)$ equals the joint angle of starting point q_0 . When the termination is t_f , the value of $\theta(t)$ equals the joint angle at the point of termination q_f . As shown in the

formula 6:
$$\begin{cases} \theta(0)=q_0 \\ \theta(t_f)=q_f \end{cases} \quad (6)$$

In the actual motion trajectory planning of manipulator the speed of above two angles is both set as zero in order to facilitate the calculation of the joint angular speed of the starting point and the end point of the

manipulator movement. That is
$$\begin{cases} \theta'(0)=0 \\ \theta'(t_f)=0 \end{cases} \quad (7).$$

According to formula 6 and formula 7 we can determine the only one of the three polynomials. That is

$$\theta(t) = a_0 + a_1t + a_2t^2 + a_3t^3 \quad (8).$$

(2) Three degree polynomial interpolation function (see Figure 6)

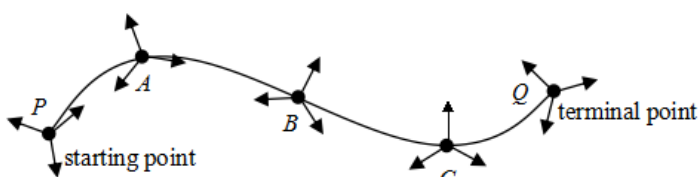


Figure 6: Trajectory planning of Manipulator over path point

In many cases, when there is a path point we need to consider whether the manipulator will stay at the point of the path. If there is, then we can take the three polynomial interpolation method. On the contrary, we can consider promote the above methods. Or we can point each path as a starting point or end point, using the inverse kinematics method to solve the corresponding values of the joint. The problem that needs to be noticed at this time is that the speed of the manipulator is not zero at the point of the path and it requires the use of the path points of the three polynomial interpolation.

We can find from Figure 6 that the 4 constraint conditions are starting position constraint, starting speed constraint, end point position constraint and terminal

speed constraint. If $\theta(t) = a_0 + a_1 + a_2 t^2 + a_3 t^3$ and the 4 constraint conditions are put into the formula it can be obtained as

$$\begin{cases} a_0 = q_0 \\ a_1 = q_0' \\ a_2 = \frac{3}{t_f^2}(q_f - q_0) - \frac{2}{t_f} q_0' - \frac{1}{t_f} q_f' \\ a_3 = -\frac{2}{t_f^3}(q_f - q_0) + \frac{1}{t_f}(q_0' + q_f') \end{cases} \quad (9).$$

Put above four relational formula into $\theta(t)$ and $\theta(t)'$, three polynomial interpolation functions of the path points will

$$\theta(t) = q_0 + q_0' t + \left[\frac{3}{t_f^2}(q_f - q_0) - \frac{2}{t_f} q_0' - \frac{1}{t_f} q_f' \right] t^2 + \left[-\frac{2}{t_f^3}(q_f - q_0) + \frac{1}{t_f}(q_0' + q_f') \right] t^3 \quad (10)$$

and

$$\theta(t)' = q_0' + 2 \left[\frac{3}{t_f^2}(q_f - q_0) - \frac{2}{t_f} q_0' - \frac{1}{t_f} q_f' \right] t + 3 \left[-\frac{2}{t_f^3}(q_f - q_0) + \frac{1}{t_f}(q_0' + q_f') \right] t^2 \quad (11).$$

4.3 Space trajectory planning

(1) Spatial linear interpolation algorithm

When the manipulator is under linear interpolation the starting point and the end point of the manipulator movement are given in advance (As shown in Figure 7) in order to solve the position and attitude of the middle point in the motion.

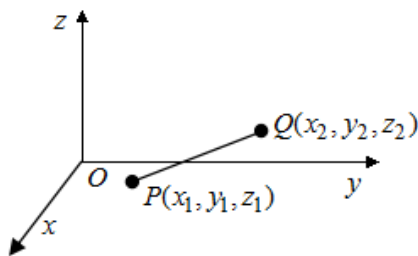


Figure 7: Schematic diagram of Spatial linear interpolation

According to Figure 7 the distance L from the starting point to the end point of the manipulator from the straight path can be calculated:

$$L = \sqrt{(x_2 - x_1)^2 + (y_2 - y_1)^2 + (z_2 - z_1)^2} \quad (12)$$

When the manipulator is under linear interpolation the interpolation precision is easily affected by the number of linear interpolation in space. What's more, with the increase of the number of interpolation, the manipulator will gradually approach the line. In this way, it is possible to make the interpolation precision increase, and then directly affect the computer's response level.

Spatial arc interpolation algorithm

Space arc refers to the manipulator in the process of exercise, the three-dimensional coordinates of any plane in the arc [14-17]. The calculation of the spatial arc interpolation algorithm is based on the plane circular interpolation. Firstly, the space arc in the coordinate space of the manipulator is transformed into the plane arc of the relative coordinate system. Secondly, the coordinates of interpolation points in the plane arc are calculated according to the interpolation algorithm of plane circular arc. Finally, the coordinates of the points calculated by the plane circular arc interpolation are obtained by transforming the value of the manipulator in space relative to the coordinate system [18-20].

The hypothesis space of circular arc coordinates with respect to the basis of the coordinate system is $o = (x_0, y_0, z_0)$. Regarding P, Q and the original coordinate point O as three points as shown in Figure 8:

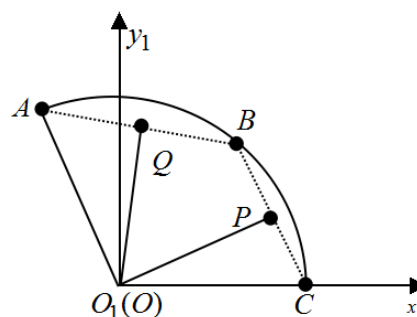


Figure 8: Schematic diagram of plane arc interpolation

BP perpendicular to OP and AB perpendicular to OQ, the equations can be obtained as follows:

$$\begin{cases} \overline{OQ} \cdot \overline{AB} = 0 \\ \overline{OP} \cdot \overline{BC} = 0 \\ \overline{OA} \cdot (\overline{AB} \times \overline{BC}) = 0 \end{cases} \quad (13)$$

Among them O_o stands for the base coordinates of the center and the relational formula is as follows:

$$\begin{cases} \overline{OQ} = (\overline{OA} + \overline{OB}) / 2 \\ \overline{OP} = (\overline{OB} + \overline{OC}) / 2 \end{cases} \quad (14)$$

If the interpolation step of circular interpolation is determined by N , the angular displacement of the interpolation process can be obtained. Further solve the coordinates of the center point of the circular interpolation, and then solve the transformation matrix.

M stands for transformation matrix of $O_0x_0y_0z_0$ to

basic coordinate system $O_1x_1y_1z_1$ and the corresponding coordinate values are as follows:

$$\begin{cases} X_1 = \overline{OC} = \{x_3 - x_0, y_3 - y_0, z_3 - z_0\} \\ \overline{OA} = \{x_1 - x_0, y_0 - x_1, z_1 - z_0\} \\ Z_1 = \overline{OC} \times \overline{OA} \\ Y_1 = Z_1 \times X_1 \end{cases} \quad (15)$$

In summary, the interpolation algorithm of plane circular arc interpolation is used to calculate the spatial arc interpolation, which can be used to solve the coordinate value of the interpolation point in the coordinate system $O_1x_1y_1z_1$.

5. Conclusion

In order to better reflect the national science and technology level and strengthen the robot technology the development and design of the manipulator position measurement system is developed based on field programmable gate array in this paper and the overall design scheme of the manipulator system is given. According to the actual structure parameters of the manipulator, the forward kinematics and inverse kinematics of the manipulator are calculated and analyzed in the paper. Finally, the trajectory planning method of the manipulator is analyzed by using the three degree polynomial in the joint space. And the trajectory planning is carried out by using the spatial straight line and the spatial arc interpolation algorithm. The development and design of the manipulator position measurement system based on field programmable gate array is completed. In the design, we make full use of the advantages of the field programmable gate array (FPGA) clock, high clock frequency, fast acquisition speed, high work efficiency, etc. and consider this as the core of the manipulator position measurement system to control the timing of the system. Based on the theory of robot kinematics, a D-H method is used to establish the kinematic equations of the manipulator and a variety of interpolation algorithm is used to carry out the trajectory planning of the manipulator to design a high efficiency, good performance, high technology of the manipulator

measurement system. It provides strong technical support for the advancement of science and technology.

6. References

- [1] Volpe A, Garrou D, Amparore D, et al. Perioperative and renal functional outcomes of elective robot-assisted partial nephrectomy (RAPN) for renal tumours with high surgical complexity[J]. *Bju International*, 2014, 114(6):903-909.
- [2] Fox D, Burgard W, Kruppa H, et al. A Probabilistic Approach to Collaborative Multi-Robot Localization[J]. *Autonomous Robots*, 2015, 8(3):325-344.
- [3] Chen Y X. A novel design of manipulator arm control system based on STM32[J]. *Applied Mechanics & Materials*, 2014, 670-671:1385-1388.
- [4] Poveda Rodríguez D K, Rodolfo V M, Carreño Zagarra J J. Nonlinear Identification of a PUMA Manipulator Arm MA2000[J]. *Applied Mechanics & Materials*, 2014, 704:288-292.
- [5] Arponen T, Piiipponen S, Tuomela J. Kinematical analysis of Wunderlich mechanism[J]. *Mechanism & Machine Theory*, 2013, 70(70):16-31.
- [6] Myaing A, Dinavahi V. FPGA-Based Real-Time Emulation of Power Electronic Systems With Detailed Representation of Device Characteristics[J]. *IEEE Transactions on Industrial Electronics*, 2011, 58(1):358-368.
- [7] Canis A, Choi J, Aldham M, et al. LegUp: An open-source high-level synthesis tool for FPGA-based processor/accelerator systems[J]. *Acm Transactions on Embedded Computing Systems*, 2013, 13(2):27-28.
- [8] Poveda Rodríguez D K, Rodolfo V M, Carreño Zagarra J J. Nonlinear Identification of a PUMA Manipulator Arm MA2000[J]. *Applied Mechanics & Materials*, 2014, 704:288-292.
- [9] Chen Y X. A novel design of manipulator arm control system based on STM32[J]. *Applied Mechanics & Materials*, 2014, 670-671:1385-1388.
- [10] Wang R Y, Yin Y H. Design of High-speed Data Acquisition and Processing Technique System for Multi-channel Ultrasonic Distance Measurement[J]. *Instrument Technique & Sensor*, 2013, 42(8):74-71.
- [11] Kung Y S, Quynh N V, Hieu N T, et al. Simulink/Modelsim Co-Simulation and FPGA Realization of Speed Control IC for PMSM Drive[J]. *Procedia Engineering*, 2011, 23(5):718-727.
- [12] Dakin G, Jourden H. High-order accurate Lagrange-remap hydrodynamic schemes on staggered Cartesian grids[J]. *Comptes Rendus Mathematique*, 2016, 354(2):211-217.
- [13] Felhi A, Sahmim S, Aydi H. Ulam-Hyers stability and well-posedness of fixed point problems for $\alpha - \lambda$ -contractions on quasi b -metric spaces[J]. *Fixed Point Theory & Applications*, 2016, 2016(1):1-20.
- [14] Qiu S S, Ma G J, Wu Z X, et al. A New Line and Arc Interpolation Algorithm Based on the Speed Control[J]. *Applied Mechanics & Materials*, 2013, 411-414:1697-1702.
- [15] Liu H, Liu Q, Zhou S, et al. Spatial circular arc and elliptic arc interpolation based on differential

model[J]. Nongye Jixie Xuebao/transactions of the Chinese Society of Agricultural Machinery, 2015, 46(8):338-343.

[16] Xiang X Y, Jangjaimon I, Madani M, et al. A Reliable and Cost-Effective Sand Monitoring System on the Field Programmable Gate Array (FPGA)[J]. IEEE Transactions on Instrumentation & Measurement, 2013, 62(7):1870 - 1881.

[17] Xiong S, Bogy D. Position error signal generation in hard disk drives based on a field programmable gate array (FPGA)[J]. Microsystem Technologies, 2013, 19(9-10):1307-1311.

[18] Rana K P S, Mitra N, Pramanik N, et al. A Virtual Instrumentation Approach to Neural Network-Based Thermistor Linearization on Field Programmable Gate Array[J]. Experimental Techniques, 2015, 39(2):23–30.

[19] Rahim N A, Islam Z. Field programmable gate array-based pulse-width modulation for single phase active power filter.[J]. American Journal of Applied Sciences, 2009, 6(9):1742-1747.

[20] Hervé C, Cerrai J, Caër T L. High resolution time-to-digital converter (TDC) implemented in field programmable gate array (FPGA) with compensated process voltage and temperature (PVT) variations[J]. Nuclear Instruments & Methods in Physics Research, 2012, 682(7):16-25.

BRAND:
«SMART MECHATRON - Competitiveness,
performance and high quality through
HIGH-TECH MECHATRONIC PRODUCTS »

THE IMPROVEMENT OF MATERIAL'S SURFACES WITH MICRO AND NANOMETRICS COATED THROUGHT INTELLIGENT MECHATRONIC TECHNOLOGIES FOR BIOMEDICAL APLICATIONS

Gornoava Valentin^{1,2, a}, Gheorghe I. Gheorghe^{1,2, b}

¹National Institute of Research and Development in Mechatronics and Measurement Technique, Bucharest, Romania

²Scientific Doctorates Coordinator – Doctoral School of Mechanical Engineering, U.V. Targoviste;

Associate Prof. with U.T.M. Bucharest, U.P. Bucharest and U.V. Targoviste;

Corresponding Member of the Academy of Technical Sciences of Romania

^a valentine_gornoava@yahoo.com, ^b geo@incdmtm.ro; geocefin@yahoo.com

Abstract - The materials with micro- and Nano metrics structures coated through intelligent mechatronics methods have their destination also in biomedical applications such as implants (dental and orthopedic prostheses, etc.) and in micro sensors. The equipment's and the methods used in the description of the surfaces with micro- and Nano metrics structures intended for biomedical application offer the possibility of an topographic characterization of the thin layers, in order to verify the physic – mechanical characteristics of the layers (micro hardness, electrical characteristics, thermal, magnetic, adhesion, etc.) and to characterize in a structural manner the thin layers deposited.

The issue of development of materials with superior characteristics of biocompatibility, high strength and low wear is a constant in the current research in the field of biomedical applications.

Keywords: nanotechnology, technological flow, High Tech.

1. Introduction

The issue of development of the materials with biocompatibility superior characteristics, high strength and low wear is a constant current research in the field of biomedical applications. Complementary of the listed analyses is added the bioactivity which are determining the osteointegrity of the implants. A solution to optimize the structural characteristics and increased operational life to implant components is the deposition of thin films - micro and nanoscale materials with properties targeted by Intelligent Mechatronic processes and technologies.[1]

Taking into account the scope considered for micro and nano structures covered - biomedical field - knowledge of functional parameters, structures, coating materials and coatings, the degree of finishing superficial deposit applicate are very important to achieve the medical objective watched as final solution : the biocompatibility.

An adequate mechanical strength of the substrate, an ultra fine structure of deposits and high adhesion thereof, will be used to ensure a proper functioning of friction couplings which are used (ferquent case of the prosthesis) by compatibility and optimal tribological system.

It is necessary that the metallic materials, ceramics and other composite used as substrates to achieve maximum hardness themes associated with a

corresponding set of features that are requesting very fine metallographic structure, up to the nanometer level in ceramics case.

The maximum mechanical strength in terms of optimal features necessary fort tribological coatings and to ensure a superior adhesive is also achieved by means of nanostructured deposits.

Depending on the particular operating follow, procedures / processes / methods of characterization are diversified. Accordingly, equipment for testing are also varied: for a single feature or multiple features, with increasing degrees high precision and high confidence levels, with or without computer equipment, etc.

The biocompatible materials are artificial products that have been imposed by the needs for improving the health of people affected by illness or injury, and this possibility of use of biocompatible materials has led to the increase of life.

It can be created an interfaces for medical devices biological environment through biochips ID that can tele-interaction, or improve a function of the affected organ. The premise is that biomaterial-body interaction is beneficial.

During use, the artificial products can be:

➤ positioned outside the body, but may have access to some fluids or tissues (devices connected to the nervous system or cardiovascular system);

➤ partially inserted into the body, which process is done by piercing the surface of an organ, so one side is

placed outside the unit on which it will act, and the second inside a cavity, without bisecting surface organ (contact lenses or dentures);

➤ products which are fully inserted inside the body.

The major disadvantages of the implants are determined by the nature of the mode of synthesis and physical and chemical properties of various materials used in relation to living tissues, such as:

➤ the ability to modify the structure and properties depending on the applications it supports (mechanical load to the bone or blood flow to the blood vessels);

➤ ability of reconstruction.

A biomaterial must meet a series of requirements in order to correspond at the using function:

➤ to be biocompatible - bioactive, bioinert or biotolerant, so to fulfill a certain function in a physiological environment, without producing any harmful effect (non-toxic, allergic, carcinogenic) on living tissues, thus provoke in the same time, an adequate response from the organism. It is known that no foreign material implanted in a living organism is not fully supported, the only substances that fully respond to this demand being the ones produced by the body himself, so the nature of welders. Any other substance is recognized as foreign and will initiate a series of reactions that allows his integration.

➤ to be biochemically stable, so do not suffer any degradation processes with the time, while in contact with the physiological environment;

➤ to have mechanical properties (tensile strength, wear, fatigue, shearing etc.), similar to the tissue substituted for taking in optimal conditions the mechanical function of this

The dental Biomaterials are also known as simple dental materials. The function of using a biomaterial, in particular, those used in dentistry and orthopedics, is provided by a set of properties, consisting of physical and mechanical characteristics, aesthetic, chemical reactivity and biological integrity demonstrated over time. The information provided in this by the manufacturing company, as a result of numerous laboratory tests performed, are designed to help the doctor in selecting a material for a specific application.

Previously their manufacturing at a large scale for sales, the materials designed and produced are subjected to tests performed in vitro (environment which simulates the conditions to be placed in work and function) and in vivo (in real environment – tested usually on animals). For most materials can not be measured in vivo the reliability and the ideal would be to use a spectroscopic technique for measuring the properties of a new material and to anticipate the using of the material for a particular area. These tests are mandatory because, besides physicochemical characteristics is established the biocompatibility compared to body tissues.[2].

On dental materials from the mouth acts a number of factors - mechanical, chemical and microbial which are leading to the deterioration of their properties and, in

time, to the deterioration of the material as such. The intensity with which these factors act depends on both the material and the body - variations in the conditions of the mouth environment. Mechanical factors are represented by occlusal pressures caused by high muscle contractions that can deform the mandible (elastic, plastic) or a fracture which can lead to dental material. The chemical factors are represented by the liquid in the mouth, with a variable pH, influenced the important nature of the food consumed. Microbial factors lie in microbial flora in the mouth; its action results, besides discolouration and reduced dental work physicochemical resistance.

Not being written an complete history of materials, can be follow their milenar development through the progress achieved in science.

The achievements in the field of biomaterials are based on three scientific fields: chemistry, biology and physics, and technical applications or "application" culminating with clinical achievements.

People always were concerned about restoration of body parts, damaged or lost due to accidents or diseases. Among the top concerns of the people was restoring teeth that usually deteriorate first due to lifestyle and food. Thus, the earliest examples of dentures seems to have been the gold works of Phoenicians, Etruscans and later of the Greeks and Romans.[3].

To exemplify this situation can be presented the situation of the inspections for imagistic characterizing: from optical microscopy to electronic microscopy and, more recently, atomic force microscopy or different combinations beetwen these.

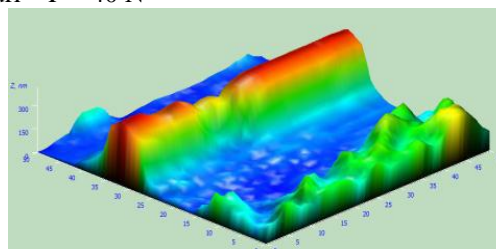
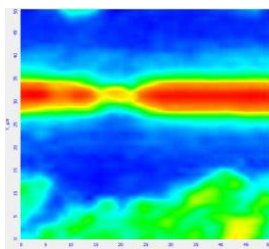
Also, experimental test results are harvestable with mechatronic equipment, stored and / or performed with dedicated software programs, complex, containing also an processing statistics, by interpolate the parameters for comparison with the ones stored in databases.

2. Application

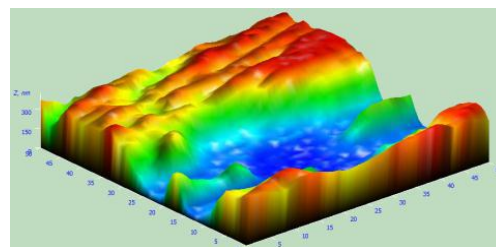
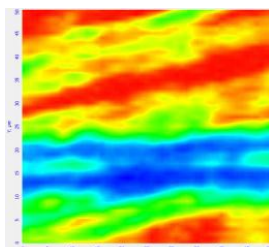
The comparative researches realised throught the SEM and AFM microscopy, on representative surfaces were conducted in the Laboratory of MEMS and NEMS Mechatronic from INCDMTM

To determine the thickness of thin sections of the samples were taken which were deposited layers. These cross sections were analyzed using optical microscopy, AFM and SEM. In this paper, from the layers deposited are presented the transversal sections achieved for the samples with TiN coating by depositing with laser spiking. The thickness of the TiN layer deposited was been generated through the surfaces scanning of with AFM. Following the characterization of these surfaces with the microscope with atomic force were been determined the thickness of TiN thin layers deposited at 5000, 10000 and 20000 pulses. Can be observed similar values in terms of size, but bigger in terms of value to those obtained by optical microscopy.

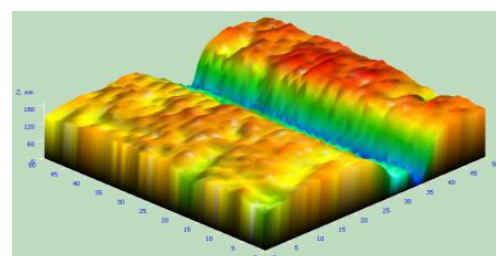
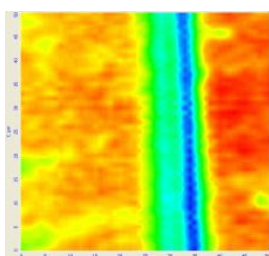
5000 pulsuri – F = 40 N



10000 pulsuri – F = 10 N



20000 pulsuri – F = 5 N



After tests of scratching on each sample and examining traces of scratching with the optical microscope have been detected several types of damage (main critical events) of the surface occurred through the actions of critical tasks: deformation and detachment of material (EC1), fragments of deposit detached (EC2), semicircular cracks in the coating (EC3), lifting the edges of the material (EC4), cutting the base material (EC5) and oxidation (EC6).

It was observed that all three layers deposited at 5000, 10000 and 20000 pulses, since the forces with low critical events occur like the EC1, EC2, EC3, EC6 are depending on thickness. A critical event EC4 and EC 5 occurs at higher values of force if the layers are deposited at 10000 and 20000 pulses. This demonstrates greater hardness compared to those layers deposited at 5000 pulses.

It has been observed that at a certain value, the layer is removed during the scratch test. The force from which the layer is deposited on the substrate is removed defines critical force (F_c). This is influenced by many factors such as substrate hardness, film thickness and contact interface.

The value of the critical force is affected by different test parameters (speed scratch tip properties, etc.) and coating-substrate composite properties (hardness and roughness, etc.).

When the layer is removed along the main scratch was observed the destruction of the substrate when the applied force is greater.

From the experimental data obtained could be achieve n comparative chart between the three layers deposited, shown in Figure 10. It can be seen that the films deposited with 5000 pulses and 10,000 pulses can't support a force greater than 80 N. The layer deposited at 20,000 pulses can resist even when on the surface is applied a force of 125 N during the scratching test.

3. Conclusions

The laboratory experimental procedures performed in this work have important results in terms of physical and mechanical characterization providing important information about the materials submitted in the previous stage.

4. Bibliography

- [1] G. Gheorghe, L. Badita, A. Cirstoiu, S. Istrateanu, V. Despa and S. Ganatsios, "Mechatronics Galaxy", a New Concept for Developing Education in Engineering," Applied Mechanics and Materials, vol. 371, pp. 754-758, 2013.
- [2] Micro si nanotehnologii avansate in mecatronica, 2009, autor: Prof. Univ. Euring. Dr. Ing. Gheorghe Ion Gheorghe, Drd. Fiz. Liliana Badita, 2009;
- [3] F. Laermer and A. Schilp, "Method for anisotropic plasma etching of substrates," U.S. Patent 5,498,312, Nov. 15, 1996;

STUDY ON THE FLIGHT PATH OF PING-PANG BASED ON THE TECHNOLOGY OF ROBOT PITCHING MACHINE

Xiaole Wang

Northwestern Polytechnical University, Shaanxi, China

E-mail: wangxiaolew@sina.com

Abstract - With the rapid development of science and technology, the robot developing can be said to flourishing. In China, the research for robot just started, so more human resources and material should be invested into to this field. The trajectory tracking algorithm of table tennis robot is one of the key researches. Also, introducing the video tracking technique into the sports training, which was use to improve the science and efficiency of physical training, has being coming an emerging research. This technology can capture and track the moving objects and analyze its moving status and characteristics by recorded data; and finally help the athletes to train. This paper chose the pitching machine of table tennis as the research object. And this pitching machine can launch a ping-pang ball in different speed, angles and rotations. Meanwhile, in order to carry out motion detection and tracking to the ball in video, this paper used SONY camera for video capture.

Keywords: robot technology, flight path of Ping-pang, objects detection, Calman tracking.

1. Introduction

As a mechanical device, the robot can automatically perform the task and complete the assigned task. At the beginning, the robot was designed to assist or replace the worker, reduce the burden of human work and improve the production efficiency [1-2]. Recent years, with the development of computer technology and artificial intelligent technology, the robot was improved on the aspects of functions and technology, which therefore plays a more and more important roles in our life and makes a positive change to our life. In fact, Ping-pang robot has only 30 years of development history, which means that it still belongs to the emerging robot research field [3]. Table tennis robot is a typical real-time intelligent robot, which can play table tennis with human beings, perceive the service route and the tracking of competitive objects, make a reasonable judgment and return strategy, and finally achieve flexible impact. At present, due to the lack of research on trajectory prediction and study of the identification of rotary ball trajectory, the study on Ping-pang robot is worthy of further exploration. Actually, recent years, many scholars at home and abroad have made some researches on this field, such as:

In 2014, Pan M, Mizuuchi I indicated that trajectory prediction plays a very important role in the process of a table tennis robot shot; he also mentioned that the accuracy of trajectory prediction has an effect on the success of hitting the ball. This is because that when it hits the ball, the non-smooth of interface generates friction to the table tennis, which makes the ball rotate and has a certain impact on its flight path, and finally leads to the inaccuracy of the trajectory prediction. On

the basis of the analysis of the rotating ball, he also discusses the effects of Magnus force on the flight path of table tennis under different rotation [4]. Kim H H, Park J S and Jung J W etc in 2013 designed omnidirectional mobile robot table tennis for the problem that the ordinary tennis serving machine can only serve but not hit ball back to complete the simulation of training. The chassis of robot applied three wheeled omnidirectional wheel structure, which can move to any direction on the site and zero turning radius; they also designed three structures including ball hitting mechanism, ball receiving mechanism and service mechanism, among which, the ball hitting mechanism consists of a three degree of freedom manipulator; and each degree of freedom is driven by a single servo motor to achieve the serving and hitting under different angles and different efforts [5]. Kundu S and Parhi D R in 2016 established a virtual prototyping model of Ping-pang serving machine with Prof/E and ADAMS, and set related constraints and motion functions to simulate dynamic to the virtual prototype. Meanwhile, they selected displacement trajectory of various types of ball and the movement speed and autorotation speed of any ball as the evaluating indicator; and compared and analyzed dynamic simulation results to verify the feasibility of the serving machine [6]. This paper carried out some experiments for the trajectory of table tennis based on the technology of robot serving machine and analyzed to its results.

2. Problem of rotating ball trajectory

Establishing the three-dimensional system of coordinate 0-xyz that the vertical direction is z axis, the long side of table of Ping-pang is x axis, the shorter side

of table is y axis, and the center of short side of the ball table is original point O, show as figure1:

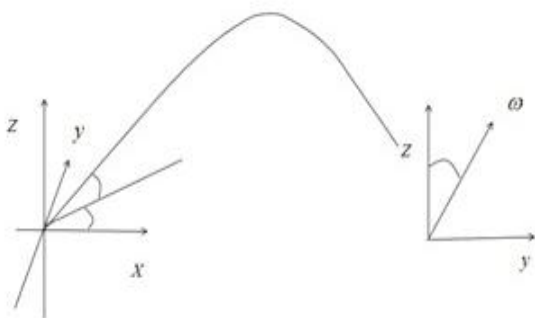


Figure 1: Three dimensional coordinate system

In the process of playing table tennis between the robot and human, the success rate of return ball of the robot depends on the following two points[7-9]:

(1) The accuracy rate of return ball of the robot which is based on the correct classification of the ball and the precise trajectory prediction. So the classification of ball trajectory determines what kind of strategy that robot should take.

(2) The robot needs time to make preparation, this requires that robot has a good real-time performance; otherwise, even if it can identify the type of ball, it still can't fight back the table tennis timely.

Considering above two factors described, we decide to classify the trajectory of the rotating ball by applying ELM algorithm, and we do the following experiments in the offline environment: firstly, to learn the flight trajectory of rotating ball by original ELM algorithm and use the flight trajectory as the inputting, its striking type as the outputting. Finally, learning the training network by a large number of historical data collected by the actual experiment is to evaluate the practical performance of the algorithm [10-12].

3. ELM Neural Network

In the traditional artificial neural network, the hidden node parameters can be optimized by some iterative algorithms and finally determined. However, the steps of those algorithms will make the training process need lots of time, which finally leads to the low efficiency of the training process. In order to enhance the overall performance of the neural network, Huang Gb et al proposed the ELM algorithm. Extreme Learning Machine (ELM) is a fast single-hidden layer neural network training algorithm.

It has the characteristic that in the training process of network parameters, the inner weight and the bias value of the hidden layer nodes are randomly selected not need to be adjusted. While its outer weight is obtained by the least square solution, the whole process does not need any iterative process, which greatly reduces the adjustment time of the network parameters.

4. Input data preprocessing

After inputting the data of the rotating ball, we need to do a series of preprocess to the original data, the most important is the normalization processing.

Normalized processing is to convert the input data that used for training into the value in the same range, which is widely used as a method to speed up the neural network training [17-20]. the advantage of this method is that it can reduce the order of magnitude difference between different data and make the training network converge quickly to complete data processing. For example, if the range of data 1 and data 2 is separately from 10 to 10 and 0.5 to 0.7, then the whole training network will be sensitive after using data 1 and 2 for training. The normalization refers to make data correspond to a value in a certain range and it is able to avoid the formation of this kind of "allergy" network.

Generally speaking, there are three kinds of normalization for neural network: the first one is to invoke the normalized function of MATLAB including `premnmx`, `postmnmx`, `mapminmax`, which can normalize the data into the range [-1,1]. The second is to invoke the the normalized processing function of MATLAB-`prestd` and `poststd`, this function is able to normalize the data to be the mean value 0 and its variance to be 1. The third is to achieve normalization by manual programming.

In this paper, coming with function `mapminmax` of MATLAB was used to map the acquisition data to the range [-1,1].

5. Experimental results and analysis

A verification experiment was done in this paper to verify the availability of the ELM classifier for the classification of the rotating ball trajectory. The hardware environment of the system used in the experiment was CPU Intel Core i7-4700MQ 2.7 GHZ with 32GB memory and development platform was the Windows 7 operating system.

250 effective data were selected in the experiment which was divided into topspin, backspin, side topspin, side backspin and side right spin. There were 50 sets of data for each class. 3 groups were selected as experimental data at each time. Among them 75% of the total data, that was 113 sets of data, were considered as training data. 37 sets of data were considered as test data. That was the rest of the 25%. ELM algorithm selected the original ELM classifier.

The experimental was divided into three categories according to the different production methods of the rotary ball. 1. Set the topspin ball 2. Set the backspin ball 3. Set the side spin (21-24).

The trajectory of the ball can be set. Each type of service can be repeated several times and the trajectory of each type of service is basically the same. So this is beneficial to classification (25-27). By setting the wheel gear on the service machine and angle, this experiment collected four kinds of table tennis movement.

They are side topspin (It was 45 degrees between the round and the horizontal line, the up round was greater than the back round.), side backspin (It was 45 degrees between the round and the horizontal line, the up round was smaller than the back round.), topspin (It was 90 degrees between the round and the horizontal line, the up round was greater than the back round.), left side spin (It was 0 degree between the round and the horizontal line, the up round was greater than the back

round.) and right side spin (It was 0 degree between the round and the horizontal line, the up round was smaller than the back round.).

In this experiment, we selected the position of each 10 frame image as the characteristic data before and after the rebound of the table tennis ball.

The results were shown in Figure 2.

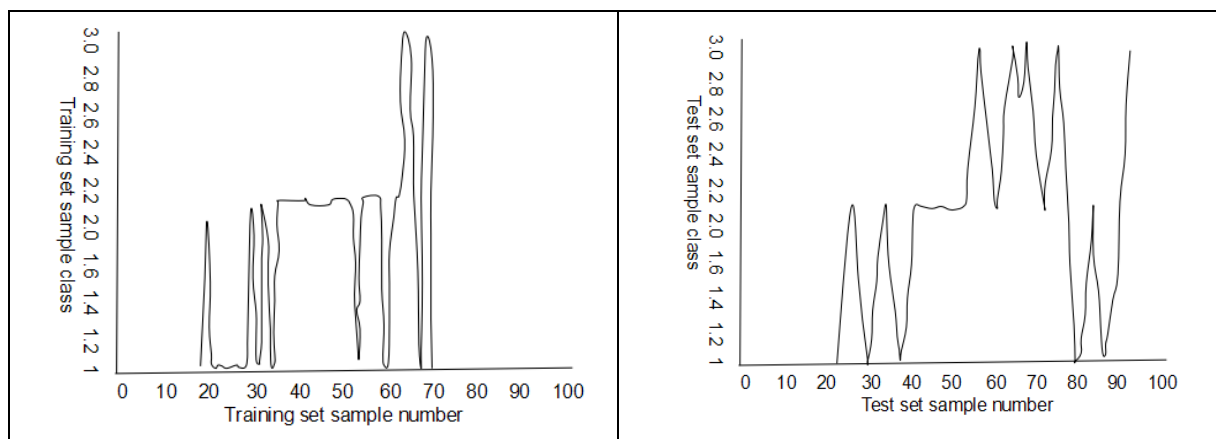


Figure 2 Table tennis ball rebound before and after the location of the 10 frames of the image

We can see from Figure 2, through the training of ELM algorithm, the training set of this experiment was the correct rate of 86.16% and the test set was the correct rate of 72.16%.

The return ball success rate of the table tennis robot depends on the accuracy of classification and prediction of the table tennis robot.

Thus, the correct rate of the test set here was not consistent with the requirements of table tennis robot system.

So we added the velocity characteristics of each trace point in the data feature inputting. Through the experimental verification, the results were shown in Figure 3.

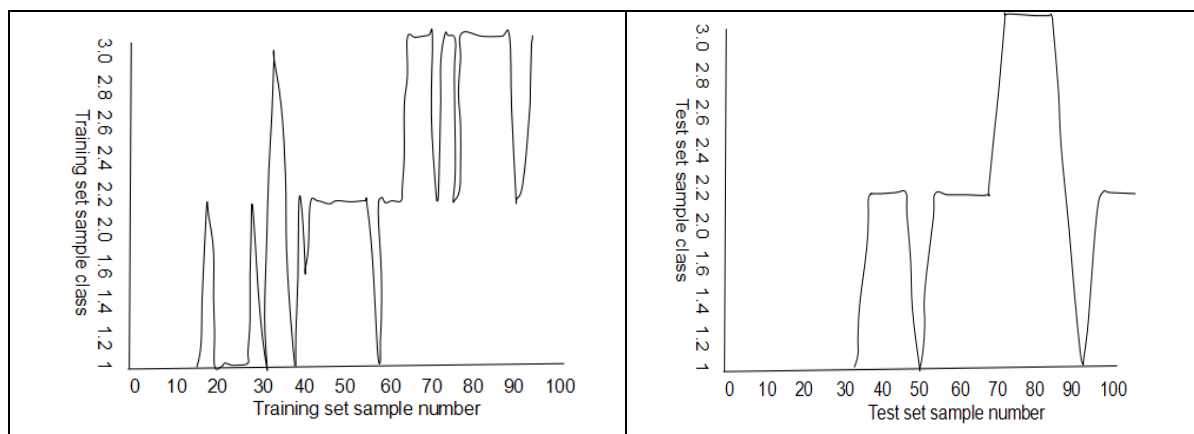


Figure 3 Velocity characteristics of each locus

The correct rate of the training set was not much different from that of the training set before the speed characteristic was added. But the test set accuracy has increased to 79.1%. It can be seen that the speed characteristics can be adjusted to improve the classification accuracy of ELM classifier.

At last, we selected different types of rotating ball trajectory to make several sets of experiments and the results of the experiment were shown in Table 1.

Table 1 Feature selection test results

Index	Pre classified trajectory	Total running time(s)	Recognition rate(%)
1	Side Topspin、 Side Backspin、 Topspin	0.013395	78.6
2	Side Topspin、 Side Backspin、 left side spin	0.021523	81.1
3	Side Topspin、 Side Backspin、 Right side spin	0.192159	80.1
4	Side Topspin、 Topspin、 left side spin	0.165913	71.2
5	Side Topspin、 Topspin、 Right side spin	0.174129	68.3
6	Side Topspin、 left side spin、 Right side spin	0.235423	80.1
7	Side Backspin、 Topspin、 left side spin	0.014926	63.1
8	Side Backspin、 Topspin、 Right side spin	0.025129	83.9
9	Side Backspin、 left side spin、 Right side spin	0.163129	71.2
10	Topspin、 left side spin、 Right side spin	0.181220	82.9

From the last column of Table 1 we could figure out the correct rate of the average classification was only 75.4%. The return ball success rate of the table tennis robot depends on the accuracy of classification and prediction of the table tennis robot. Thus, the correct rate of the test set here was not consistent with the requirements of table tennis robot system. But from another aspect, we could see that the average running time of the ELM classifier was only 0.104s. It can fully satisfy the real-time requirements for a table tennis robot.

6. Conclusion

The track of table tennis ball was classified based on ELM algorithm in this paper. After getting the results and analysis, we could improve the classification accuracy by adding the velocity features to the training data. In addition, we also introduced the ELM algorithm. However, due to the limitations of resources and conditions, there are still some deficiencies in the experimental process and the results and analysis which we will complement and improve the relevant research experiments in the future.

7. References

- [1] Taylor G, Frederiksen R, Crossman J, et al. A multi-modal intelligent user interface for supervisory control of unmanned platforms[C]// International Conference on Collaboration Technologies and Systems. 2012:117-124.
- [2] Wang C, Wiggers P, Hindriks K, et al. Learning Classifier System on a humanoid NAO robot in dynamic environments[C]// International Conference on Control Automation Robotics & Vision. 2012:94-99.

- [3] Mülling K, Kober J, Peters J. Simulating Human Table Tennis with a Biomimetic Robot Setup[C]// International Conference on Simulation of Adaptive Behavior: From Animals To Animats. Springer-Verlag, 2010:273-282.

- [4] Pan M, Mizuuchi I. 1A1-003 Development of Tabletop-type Omni-Directional Table-Tennis Robot based on Orbit Prediction of Rotating Ball(Robots for Home/Office Application)[J]. ロボティクス・メカトロニクス講演会講演概要集, 2014, 2014:90-95.

- [5] Kim H H, Park J S, Jung J W, et al. Immersive teleconference system based on human-robot-avatar interaction using head-tracking devices[J]. International Journal of Control Automation & Systems, 2013, 11(5):1028-1037.

- [6] Kundu S, Parhi D R. Navigation of underwater robot based on dynamically adaptive harmony search algorithm[J]. Memetic Computing, 2016:1-22.

- [7] Liu H, Li Z, Wang B, et al. Table tennis robot with stereo vision and humanoid manipulator II: Visual measurement of motion-blurred ball[C]// IEEE International Conference on Robotics and Biomimetics. 2013:2430-2435.

- [8] Wang Q, Zhang K J, Wang D. The trajectory prediction and analysis of spinning ball for a table tennis robot application[C]// IEEE, International Conference on Cyber Technology in Automation, Control, and Intelligent Systems. IEEE, 2014:496-501.

- [9] Wang Y, Sun L, Liu J, et al. A novel trajectory prediction approach for table-tennis robot based on nonlinear output feedback observer[C]// IEEE International Conference on Robotics and Biomimetics. IEEE, 2010:1136-1141.

- [10] Altaher M, Nomir O. Euler-Lagrange as Pseudo-metric of the RRT algorithm for optimal-time trajectory

of flight simulation model in high-density obstacle environment[J]. *Robotica*, 2015, FirstView:1-19.

[11] Azad N L, Mozaffari A, Hedrick J K. A hybrid switching predictive controller based on bi-level kernel-based ELM and online trajectory builder for automotive coldstart emissions reduction[J]. *Neurocomputing*, 2016, 173:1124-1141.

[12] Roskam I, Stievenart M, Tessier R, et al. Another way of thinking about ADHD: the predictive role of early attachment deprivation in adolescents' level of symptoms.[J]. *Social Psychiatry & Psychiatric Epidemiology*, 2014, 49(1):133-144.

[13] HARRIS DRUCKER, ROBERT SCHAPIRE, PATRICE SIMARD. BOOSTING PERFORMANCE IN NEURAL NETWORKS[J]. *International Journal of Pattern Recognition & Artificial Intelligence*, 2010, 7(04):705-719.

[14] Lakshmanan S, Ju H P, Ji D H, et al. State estimation of neural networks with time-varying delays and Markovian jumping parameter based on passivity theory[J]. *Nonlinear Dynamics*, 2012, 70(2):1421-1434.

[15] Chan Z S H, NIKOLAKASABOV. EVOLUTIONARY COMPUTATION FOR ON-LINE AND OFF-LINE PARAMETER TUNING OF EVOLVING FUZZY NEURAL NETWORKS[J]. *International Journal of Computational Intelligence & Applications*, 2011, 4(4):309--319.

[16] XIAOFAN YANG, XIAOFENG LIAO, YUANYAN TANG, et al. GUARANTEED ATTRACTIVITY OF EQUILIBRIUM POINTS IN A CLASS OF DELAYED NEURAL NETWORKS[J]. *International Journal of Bifurcation & Chaos*, 2011, 16(9):2737-2743.

[17] Sun J W, Zhang Y. The algorithm research of penetration distance based on normalization processing[C]// *International Conference on Electronic and Mechanical Engineering and Information Technology*, Emeit 2011, Harbin, Heilongjiang, China, 12-14 August. 2011:4603-4606.

[18] Strand E A, Johnson K. Gradient and Visual Speaker Normalization in the Perception of Fricatives[C]// *Natural Language Processing and Speech Technology*, Results of the, Konvens Conference, Bielefeld, October. 2010:14-26.

[19] Li Q, Zheng J, Zhou Q, et al. Robust, real-time endpoint detector with energy normalization for ASR in adverse environments[C]// *IEEE International Conference on Acoustics*. 2010:233-236 vol.1.

[20] Wu T Y, Chen J C, Wang C C. Characterization of gear faults in variable rotating speed using Hilbert-Huang Transform and instantaneous dimensionless frequency normalization[J]. *Mechanical Systems & Signal Processing*, 2012, 30(7):103-122.

[21] Allen T, Ibbitson J, Haake S. Spin generation during an oblique impact of a compliant ball on a non-compliant surface[J]. *Proceedings of the Institution of Mechanical Engineers Part P Journal of Sports Engineering & Technology*, 2012, 226(226):86-95.

[22] Tanaka K, Fujita S, Teranishi Y, et al. B35 Relationship between Golf Club Conditions and 3D Rebound Behaviours of a Ball using a Finite Element Analysis[C]// *Symposium on sports and human dynamics*. The Japan Society of Mechanical Engineers, 2011:424-429.

[23] Ball T, Rajamani S K. Automatically validating temporal safety properties of interfaces[C]// *Proceedings of the 8th international SPIN workshop on Model checking of software*. Springer-Verlag New York, Inc. 2010:103--122.

[24] Avakian H, Bosted P, Burkert V D, et al. Measurement of single- and double-spin asymmetries in deep inelastic pion electroproduction with a longitudinally polarized target.[J]. *Physical Review Letters*, 2010, 105(26):172-181.

[25] Stark L, Tofthagen C, Visovsky C, et al. The Symptom Experience of Patients with Cancer.[J]. *Journal of Hospice & Palliative Nursing Jhpn the Official Journal of the Hospice & Palliative Nurses Association*, 2012, 14(1):61-70.

[26] Reddy A S, Wozniak D F, Farber N B, et al. Bone Marrow Transplantation Alters the Tremor Phenotype in the Murine Model of Globoid-Cell Leukodystrophy.[J]. *Journal of Clinical Medicine*, 2012, 1(1):1-14.

[27] Jung H, Chun K J, Hong J, et al. Optimized balance rehabilitation training strategy for the elderly through an evaluation of balance characteristics in response to dynamic motions.[J]. *Clinical Interventions in Aging*, 2014, 116:130-138.

[28] Wang Q, Zhang K J, Wang D. The trajectory prediction and analysis of spinning ball for a table tennis robot application[C]// *IEEE, International Conference on Cyber Technology in Automation, Control, and Intelligent Systems*. IEEE, 2014:496-501.

[29] Nakashima A, Ito D, Hayakawa Y. An online trajectory planning of struck ball with spin by table tennis robot[C]// *Ieee/asme International Conference on Advanced Intelligent Mechatronics*. 2014:865-870.

[30] Chen G, Xu D, Fang Z, et al. Visual Measurement of the Racket Trajectory in Spinning Ball Striking for Table Tennis Player[J]. *IEEE Transactions on Instrumentation & Measurement*, 2013, 62(11):2901-2911.

DESIGN AND DEVELOPMENT OF MEASUREMENT SYSTEM OF SPORTS SHOT PERFORMANCE UNDER THE GUIDANCE OF VISION MEASUREMENT TECHNOLOGY

Yanlong Hao

Sanya University, 572000, Hainan, China

E-mail: haoyanll@163.com

Abstract - In recent years, computer vision detection technology based on video image processing has become a hot research topic and it has been widely used in many fields. In this paper, we proposed the development of sports shot performance measurement system under the guidance of the vision measuring technology based on the current domestic and foreign on monocular vision measurement technology related research. This paper described the design and implementation of key technologies of shot measurement system based on monocular vision and briefly analyzed the test and error of the system. The accuracy, stability and efficiency of the method were proved by the examples. Combined with the characteristics of shot field, this paper proposed rules based on the same field geometry calibration method and mathematical model of matching based on the same field of view object coordinate transformation of grid, using the monocular CCD camera image plane coordinates to measure the shot placement of the ground plane coordinates. The shot result measurement system designed and developed in this paper has been used in sports activities. The application has the advantages of simple structure, convenient operation, high efficiency, high speed, wide application range, etc. and has wide application prospect.

Keywords: Vision measurement technology, Shot range, measurement model, Geometric calibration method, Performance measurement system.

1. Introduction

With the improvement of computer processing ability and the development of sensor technology computer vision technology based on video image processing has become a hot research topic in the field of image processing in recent years. This technology has been widely used in many fields. As a result of computer vision detection technology has become a hot research the computer vision measurement technology used in sports shot performance measurement is a major breakthrough [1-3].

At present, the application of computer vision technology in sports is very extensive. Using this technique, we can not only observe the action of athletes from different angles, but also can quantify the speed, acceleration and position of the athletes. It makes the sports training and competition get rid of the state of traditional experience analysis and judgment so as to be at the state of scientific and digital. What's more, it helps to complete the test of the performance of competitive sports as well [4]. In this paper monocular vision measurement technology was applied to the measurement of the shot result for the first time. Combined with the characteristics of shot field this paper proposed mathematical model of matching based on the same field of view object coordinate

transformation of grid and at the same time the background subtraction algorithm based on target detection algorithm was improved. It reduced the time of target extraction and improved the measurement efficiency of the system [5].

We regarded the performance measurement based on video image processing as a starting point in the paper. It focused on the research of image processing technology in vision measurement, camera calibration, monocular vision measuring methods and the implementation steps and design method of measurement system of monocular video shot based on the competition results. It put forward the key technologies and solutions and verified the measurement method. At last, the paper described the problems and improvement methods of monocular vision technology [6-8]. Research of Vijayakumar V and Nedunchezian R considered that only a single camera should be used to measure the work of monocular vision measurement. It was widely used since the method had the advantages of simple structure, simple camera calibration and so on [9]. The method of plane measurement based on linear correspondence was proposed by Liu Y, Zeng L, Huang Y. The results showed that the estimation method based on linear correspondence had higher accuracy compared with method based on point correspondence [10]. In a word,

the project performance measurement system in the vision measurement technology under the guidance has been widely applied in the field of sports as it has the advantages of simple operation, high efficiency and fast speed. It is not only suitable for large competitions but also suitable for all kinds of track and field sports meetings. Thus it has the application prospect and the promotion value.

2. Monocular vision measurement technology and the establishment of the system model

2.1 Monocular vision measurement method

(1) Geometry constraint method: It aims at the specific shape of the target. Making full use of the constraint conditions on the geometry of the object and using a single camera single photo to determine the spatial 3D pose of the object.

(2) Geometric similarity method: According to the perspective projection model, the object and its image meet the resemblance relation. As long as the desired parameters are extracted from the image and the actual amplification factor is multiplied the actual geometric parameters of the object can be obtained.

(3) Geometrical optics method: The measurement of geometrical optics method can be divided into focusing method and out of focus method. Focusing method requires the focal length be changed continuously. Therefore, the hardware is complex and expensive, the processing speed is slow and measurement is not accurate. The rule of out of focus is to calculate the distance between the measured point and the camera according to the calibrated model. It avoids the problem of finding the exact location of the focus and reducing the efficiency of the measurement.

(4) Structured light method: Using laser as light source to generate points, lines, surfaces of various structural light. It uses CCD camera to receive and a certain algorithm is used to obtain the 3D information of the measured object carried by the structured light [11-12]. Because the shot field is a geometrical figure of a rule and the shot placement is identified with a fixed shape of the target under the system implementation, here we mainly combine the geometric similarity method and geometry constraint method to carry out the planning of the system.

2.2 Modeling of the shot result measurement system (As shown in figure 1)

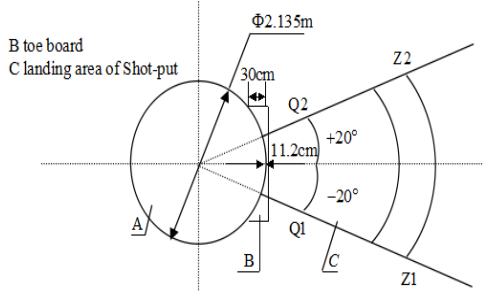


Figure 1: plan view of shot field

We can see from Figure 1 that the shot of sports venues consists of a standard concentric circle which is divided into the throwing circle, toe board and shot landing area. Diameter of throwing circle is 2.135m. The inner edge of toe board and the inner edge of throwing circle are overlapped. The plate width is 11.2-30cm. The landing area is the sector area of 40 degrees which considers the center of the throwing circle as a starting point. Assuming that O is a starting point for the throwing distance of circular arc (Origin of coordinate system), r is the radius of the circle and C is a throw point. The coordinates of C points are $C(X_c, Y_c)$ and the score of throwing shot is $S = \sqrt{X_c^2 + Y_c^2} - r$ (1)

2.3 Longitudinal calibration geometric model (As shown in figure 2)

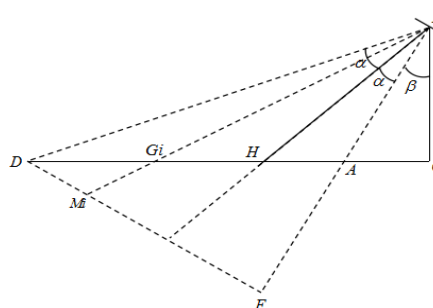


Figure 2 Longitudinal calibration geometric model

It is shown as figure 2 that point A and D separately refers to the nearest distance and the longest distance in front of the camera, point B and C are separately the camera view and camera base. It is also easy to see that DF is parallel to camera imaging plane, but BH is perpendicular to the imaging plane. Supposing the longitudinal resolution of the image plane is Dy and M_i is the i th point in Dy equal diversions points of DF. Then we can find the crossover point G_i of both $B M_i$ and AD by parallel line theorem and sine theorem of triangle, and get the Dy th points in AD. Specific calculation method is given below:

$$\begin{cases} \beta = \arctan\left(\frac{AC}{BC}\right) \\ \alpha = \frac{1}{2} \left[\arctan\left(\frac{DC}{BC}\right) - \arctan\left(\frac{AC}{BC}\right) \right] \\ \angle BAC = \arctan\left(\frac{BC}{AC}\right) \end{cases} \quad (2).$$

Through formula (2) and triangle relation, we can get that $\angle F = 90^\circ - \alpha$, meanwhile,

$$\begin{cases} DB = \sqrt{BC^2 + (AC + AD)^2} \\ AB = \sqrt{BC^2 + AC^2} \\ DF = \frac{\sin(\angle BAC)}{\sin(\angle F)} \times AD \\ AF = \frac{\sin(\alpha + \beta)}{\sin(\angle F)} \times AD \\ BF = AF + AB \end{cases} \quad (3)$$

From both formula (2) and (3), it is given below:

$$\begin{cases} FM_i = \sum_{j=1}^i \frac{DF}{D_y} \\ FM'_i = \frac{\sin(\alpha + \beta)}{\sin(\angle BAC)} \times FM_i \\ M_i M'_i = \frac{\sin(\angle F)}{\sin(\angle BAC)} \times FM_i \\ BM'_i = BF - FM'_i \end{cases} \quad (4)$$

For above formula, $i=1, 2, \dots, D_y$. So, we can get

from formula (4) that $AG_i = AB \times \frac{MM'_i}{BM'_i}$ (5)

At the same time, in formula (5), AG_i refers to the prospective field of vision of image plane in i th line that correspondence to ground level. Supposing H_y is a collection of all prospective horizons, then

$$H_y = \{AG_0, AG_1, \dots, AG_n \mid 0 \leq n \leq D_y\} \quad (6)$$

We can get the mapping function from plane vertical coordinates to vertical coordinate of ground plane through the collection H_y and the drawing rules of shot field (see as figure 1).

$$Y_p = F_y(v) = (l_{\min} - \Delta l + r) \times \cos(20^\circ) + h_v \quad (7)$$

In above formula (7), Y_p is the vertical coordinate of ground plane P, V is the imaging plane vertical coordinate corresponding to the point P, l_{\min} is lower limit of shot effective performance. Moreover, Δl is the whole effective measurement range under the shoot and the reserved width for both up and down sides, h_v is the corresponding prospective field of vision for the v th line of imaging plane.

2.4 Construction of shot performance measurement data model with guidance of the visual measurement technique

From figure 1, we get the ground plane coordinates of four points Q1, Q2, Z1 and Z2. If the arc Z1Z2 is

divided into n numbers of segments, then $n = \frac{L_{Z1Z2}}{D_c}$,

among which, the L_{Z1Z2} refers to the length of line Z1Z2. Now, we know the Z1(x_0, y_0), then we can get the coordinates of other $n-1$ points in line Z1Z2. The calculation formula is as follows:

$$x_{1i} = \sqrt{x_0^2 + y_0^2} \cdot \cos(70^\circ + 40^\circ/n) \quad (8)$$

$$y_{1i} = \sqrt{x_0^2 + y_0^2} \cdot \sin(70^\circ + 40^\circ/n) \quad (9)$$

Next, we need to divide the line Q1Z1 into m number of segments, $m = \frac{L_{Q1Z1}}{D_c}$, among which,

L_{Q1Z1} is the length of line Q1Z1. According to above two formulas (8) and (9), it is not hard to obtain the plane coordinates of $n-1$ points in m numbers of arc.

3. Shot performance measurement system under the guidance of the visual measurement technique

3.1 System composition

3.1.1 Foreground acquisition system

The foreground system consists of CCD digital video, camera stand and its mounting box, computer, image acquisition software and placement target of shot, its main workflow is shown as figure 3.

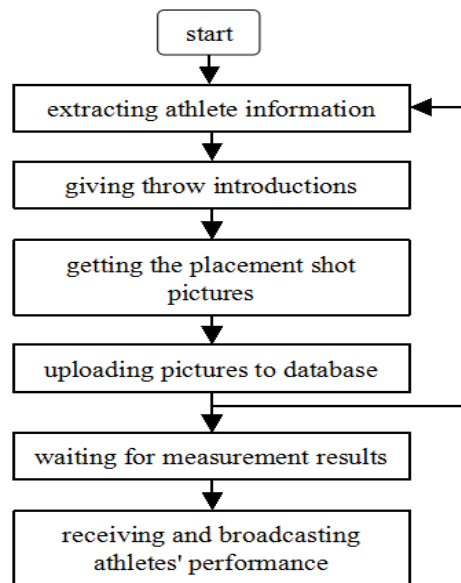


Figure 3 Main system working flow

3.1.2 Background measurement system

The background measurement system is the core of the whole system, whose function includes creating matching network, getting information about the athletes and measurement images and measuring the shot performance [13-14].

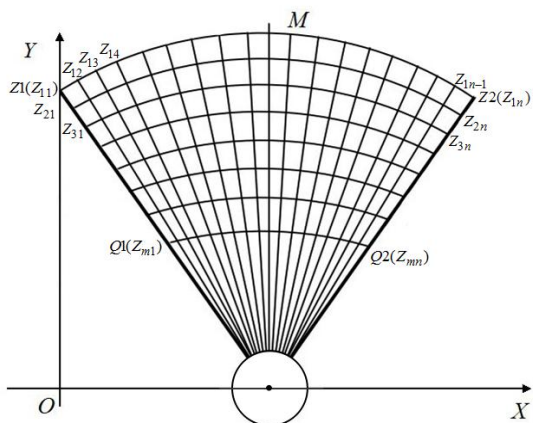


Figure 4 Network schematic diagram of shot field

3.2 Image acquisition platform

In this system, Windows XP was used as the operating system and Delphi 7.0 was used as software development language. In the processing of image acquisition, this system firstly decoded frame for video gotten from CCD video camera, then saved the frame of placement of shot as the BMP format. Finally, all these information were analyzed, which means that the image acquisition is finished.

3.3 Network transport

3.3.1 Design of network transportation structure (As shown in figure 5)

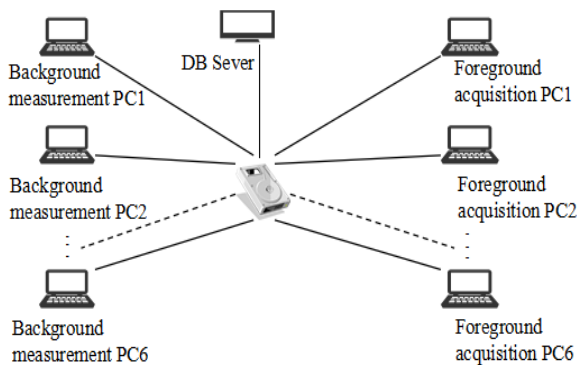


Figure 5: Network transport structure

It is seen from figure 5 that the network transport structure contains many acquisition PC, one more measurement PC, database server and network physical transmission equipment. If this system was used in basic sports, then it is better to use one background measurement PC and one foreground acquisition PC. Meanwhile, the data base is included in the background measurement PC.

3.3.2 Realization of single transmission method with one single socket

In this system, Delphi7 was used for network transmission because it is able to carry out a good package for all kinds of functions of WinSock data,

which leads the programming easier to be understood [15].

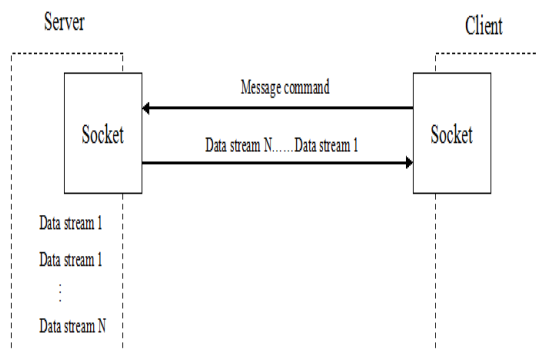


Figure 6 working schematic diagram of single socket and single transmission

The network components which used for encapsulation in Delphi7 are divided into ServerSocket and ClientSocket. For ClientSocket, it sends a request to the server and automatically establishes a connection, and Serversocket mainly receives the client request, listen and passively accept the connections from the clients. Moreover, the ServerSocket is able to establish connection with multiple ClientSocket simultaneously and keep its communication.

3.4 Implementation of Shot performance measurement system

3.4.1 Implementation technology of Delphi

The Delphi, as the rapid application development tool of Windows platform, offers the ScanLine function, meanwhile, in the process of dealing with bitmap in Delphi, it can be used as the processing unit to improve the processing speed and finally simplify the processing operation.

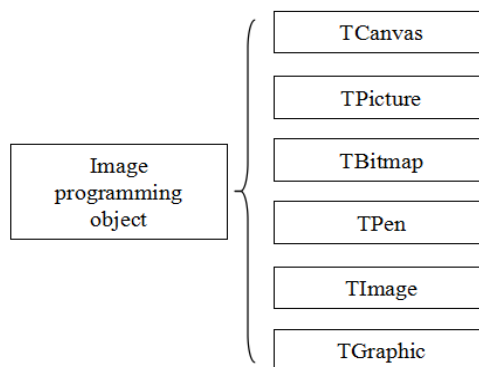


Figure 7: Delphi image programming object diagram

3.4.2 Identification of Shot placement coordinates

In this paper, the background subtraction method was used to identify the shot point coordinates, which have two main characteristics that using a static background in the current measurement environment and recognizing the target by the difference between background images and measurement placement images.

3.5 Principle of cross ratio invariance

This paper applied with camera imaging model with first order radial distortion and completed the calibration to image point by principle of cross ratio invariance, which can be seen from figure 8.

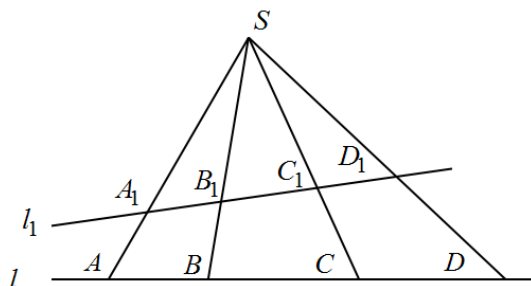


Figure 8 Orthogonal invariant graph

It can be seen from figure 8 that there are three points A, B and C on the straight line L, supposing that point A and B are the basic point, and C is the point of division. Meanwhile, the ratio of two directed line segment determined by division point and basic point is called simple ratio, shown as below:

$$SR(A, B, C) = \frac{AC}{BC} \quad (10),$$

Then for four points on the same straight line, specific value of two simple ratios is named crossratio, it can be gotten from figure 8 that

$$CR(A, B, C, D) = \frac{SR(A, B, C)}{SR(A, B, D)} \quad (11).$$

This can be proved by the geometric relations of the triangle that

$$CR(A, B, C, D) = CR(A_1, B_1, C_1, D_1) \quad (12).$$

The formula (12) is the cross ratio invariance, whose principle can be used to solve distortion coefficient.

3.6 Actual application of shot performance measurement system

In order to detect the shot performance measurement system, we obtained 800 test samples of physical education examination of Zhejiang province from 2013 to 2015. There are 800 images of shot put placement and 800 dynamic background images. We carried out the actual data measurement for those 800 samples by matching network. Table 1 is the measurement results of 8 simple in one group among those 800 samples, which conforms to requirements of measurement error.

Table 1 A group of measurement data among 800 samples

serial number	name	gender	Artificial measurement			System measurement		
			1	2	3	1	2	3
092	Le xx	male	8.3	8.6	8.8	8.3	8.6	8.8
093	Zhang xx	male	5.3	6.6	5.6	5.3	6.6	5.6
094	Yang xx	male	8.7	8.5	8.8	8.7	8.7	8.8
095	Chen xx	male	5.2	6.2	6.9	5.2	6.2	6.8
096	Jiang xx	female	5.0	5.7	5.5	5.0	5.7	5.5
097	Li xx	female	5.7	6.0	5.6	5.7	6.0	5.7
098	Zhu xx	female	5.1	4.9	5.0	5.1	4.9	5.0
099	Wang xx	female	5.7	6.1	5.9	5.7	6.1	5.9

4. Discussion and conclusion

In this paper monocular vision measurement technology was applied to the measurement of the shot result for the first time. Combined with the characteristics of shot field, this paper proposed rules based on the same field geometry calibration method and mathematical model of matching based on the same field of view object coordinate transformation of grid. The accuracy and stability of the method were proved by the practical application [16-17]. Firstly, the paper analyzed and explained the method of monocular vision measurement. On the basis of combining the characteristics of shot put and site it was proposed to model the shot put performance measurement system. The geometric model of longitudinal calibration was introduced in this paper and it completed the

construction of shot performance measurement data model under the guidance of the visual measurement technique [18-19]. Secondly, it introduced in details about the realization method of the system structure, image acquisition platform, network transmission and shot put performance measurement model and put forward a more complete solution based on monocular measurement system. It also introduced the principle for constructing the system of cross ratio invariance. Lastly, the actual application of shot put performance measurement system was carried out by using grid matching method to know that the results of the measurement of the system are in line with the requirements of measurement error [20].

In conclusion, sports shot performance measurement system established under the guidance of vision measurement technology has the advantages of

convenient operation, simple structure, low cost, high efficiency, fast speed, wide application range and so on. It is applicable to all kinds of size of sports event statistics and decision and the operation is good as well. Thus it has good commercial value and application prospect.

5. References

- [1] Liu M, Wang R, Shan S, et al. Learning prototypes and similes on Grassmann manifold for spontaneous expression recognition[J]. *Computer Vision & Image Understanding*, 2016, 147:95-101.
- [2] Jackman P, Sun D W, Allen P. Recent advances in the use of computer vision technology in the quality assessment of fresh meats[J]. *Trends in Food Science & Technology*, 2011, 22(22):185-197.
- [3] Aghbashlo M, Hosseinpour S, Ghasemi-Varnamkhasti M. Computer vision technology for real-time food quality assurance during drying process[J]. *Trends in Food Science & Technology*, 2014, 39(1):76-84.
- [4] Zhang W, Cheng B, Lin Y. Driver Drowsiness Recognition Based on Computer Vision Technology[J]. *Tsinghua Science & Technology*, 2012, 17(3):354-362.
- [5] Datta B, Durand F, Laforge S, et al. Preliminary Hydrogeologic Modeling and Optimal Monitoring Network Design for a Contaminated Abandoned Mine Site Area: Application of Developed Monitoring Network Design Software[J]. *Journal of Water Resource & Protection*, 2016, 08(1):46-64.
- [6] Hohlbein J, Gryte K, Heilemann M, et al. Surfing on a new wave of single-molecule fluorescence methods.[J]. *Physical Biology*, 2010, 7(3):1174-1178.
- [7] Lu W, Wang T T, Chu J H. The Method of Real-Time Distance Measurement Based on Monocular Vision[J]. *Advanced Materials Research*, 2012, 403-408:1451-1454.
- [8] Hao G, Du X, Zhao J G, et al. Dense surface reconstruction based on the fusion of monocular vision and three-dimensional flash light detection and ranging[J]. *Optical Engineering*, 2015, 54(7):356-356.
- [9] Vijayakumar V, Nedunchezian R. A study on video data mining[J]. *International Journal of Multimedia Information Retrieval*, 2012, 1(3):153-172.
- [10] Liu Y, Zeng L, Huang Y. An efficient HOG-ALBP feature for pedestrian detection[J]. *Signal Image & Video Processing*, 2014, 8(S1):125-134.
- [11] Glinkowski W, Michoński J, Glinkowska B, et al. Telediagnostic 3D school screening of back curvatures and posture using structured light method - pilot study.[J]. *Studies in Health Technology & Informatics*, 2012, 176(1):291-4.
- [12] Zavyalov P S, Senchenko E S, Finogenov L V, et al. A structured-light method for the measurement of deformations in fuel assemblies in the cooling ponds of nuclear power plants[J]. *Russian Journal of Nondestructive Testing*, 2013, 48(12):705-711.
- [13] Ufuk Celikcan, Ilker O. Yaz, Tolga Capin †. Example-Based Retargeting of Human Motion to Arbitrary Mesh Models[J]. *Computer Graphics Forum*, 2015, 34(1):216-227.
- [14] Subber W, Matouš K. Asynchronous space-time algorithm based on a domain decomposition method for structural dynamics problems on non-matching meshes[J]. *Computational Mechanics*, 2016, 57:1-25.
- [15] Velden Y U V D, Haramis A P G. Insights from model organisms on the functions of the tumor suppressor protein LKB1: Zebrafish chips in[J]. *Aging*, 2011, 3(4):363-7.
- [16] Wang, T, Zhang, G, Jiang Y, et al. Combined Calibration Method Based on Rational Function Model for the Chinese GF-1 Wide-Field-of-View Imagery[J]. *Photogrammetric Engineering and Remote Sensing*, 2016, 82(4):291-298.
- [17] Naikwade S R, Bajaj A N, Gurav P, et al. Development of Budesonide Microparticles Using Spray-Drying Technology for Pulmonary Administration: Design, Characterization, In Vitro, Evaluation, and In Vivo, Efficacy Study[J]. *Aaps Pharmscitech*, 2009, 10(3):993-1012.
- [18] Schleich B, Anwer N, Mathieu L, et al. Status and Prospects of Skin Model Shapes for Geometric Variations Management[J]. *Procedia CIRP*, 2016, 43:154-159.
- [19] Shiue I. Cold homes are associated with poor biomarkers and less blood pressure check-up: English Longitudinal Study of Ageing, 2012-2013[J]. *Environmental Science & Pollution Research*, 2016, 23:7055-7059.
- [20] Agnus V, Nicolau S, Soler L. Illumination Independent and Accurate Marker Tracking using Cross-Ratio Invariance[J]. *IEEE Engineering in Medicine & Biology Magazine the Quarterly Magazine of the Engineering in Medicine & Biology Society*, 2015, 35(5):22-33.

STUDY OF SOCCER ROBOT PATH PLANNING BASED ON SIMULATION ENVIRONMENT

Minting Wang

Weinan Normal University, 714099, Shaanxi, China

E-mail: wangmint12@163.com

Abstract - Soccer robot is a multi-intelligence system intersected and integrated by multi-disciplinary, which involves in Robotics, control theory, pattern recognition, mechanical engineering, material engineering, Multi Sensor Fusion Technology and so on. Robot soccer game develops the past study object of single agent into distributed multi agent; static research environment evolves into dynamic research environment; and non-real-time processing problems grow to real-time processing problems. Therefore, that is to say, robot soccer is the second milestone in the development of artificial intelligence after computer chess, which expands artificial intelligent technology to a new horizon. Because the conditions that the real robot soccer game needs are difficult to fulfill, robot soccer simulation game comes out. And the decision and path planning problems of soccer robot are studied by this under a real-time oppositional environment. The path planning is an important part of decision subsystem of soccer robot. In the soccer robot game, the path planning of soccer and robots belongs to a planning and control problem in an unknown dynamic environment, and its pros and cons will directly affect the result of the game. Based on the background of soccer robot, this thesis focuses on the path planning problems for further study, and proves the accuracy and validity of the theory and methods put forward in the study with emulation proof.

Keywords: Robot soccer; path planning recognition; simulation system; particle swarm optimization.

1. Introduction

Since the birth of the robot, it has been widely used in many fields including agriculture, building and medicine, and also played a more and more important role in people's life [1-2]. There are three developmental stages in robot: from the first-generation playback robot repeating single actions to the second-generation robot having feelings, and to the third-generation intelligent robot with high scientific and technological content and wide usage. The study of soccer of robot is based on the third-generation intelligence robot [3]. The soccer robot attracts more and more people's attention and welcome since it was put forward. It is not only a competition event with charming sports competition, but also a scientific research subject with high scientific and technological content, large development space and strong innovation [4]. Soccer robot can simulate football players to make a series of movements, such as judgment, recognition, analysis, control and so on. The soccer robot is also involved in a variety of technologies and multi-field disciplinary knowledge, which can promote the development of engineering research field in colleges and universities. And now, the more competition events soccer robot has, the higher technical content it has. And its development injects new vitality to artificial intelligence [5-6].

Path planning is the robot can plan a shortest path that can avoid obstacles from the starting point to object point in environmental space, and its performance also

can serve as a standard to measure the intelligence of soccer robot [7-8]. With the development and innovation of Computer Control Technology, the methods of path planning for soccer robot are more and more mature, which is more and more suitable to reflect intelligent robot and accurate path planning [9].

Although many algorithms of path planning have their own advantages, the algorithms of path planning are under constant improvement for the optimal path when the robot can efficiently and safely avoid the obstacles in a complex and dynamic environment. In dynamic and uncertain environment of robot, the partial path planning can combine with overall path planning to learn from each other in order to achieve better timeliness and accuracy of soccer robot [10-11].

Many experts and scholars at home and abroad have studied for improving the soccer robot path planning. For examples, Su W [12] and other experts have studied the path planning problems based on the improvement of artificial potential field, which achieves the matched objectives of improving the path planning; And Mansury E [13] put forward artificial bee colony algorithm and cubic Ferguson Splines and has a study for path planning problems.

Based on the above situation, this thesis, on the basis of particle swarm optimization, studies the path planning problems of soccer robot in the context of simulation environment.

2. Simulation system of soccer robot

2.1 Basic movements of soccer robot in simulation system

(1) Motion

The motion of soccer robot contains translation and turning. According to these two movements, soccer robot can achieve all kinds of motion trajectory [14]. When the two wheels' velocity and steering of soccer robot are same, the motion trajectory is in rectilinear motion; when the velocity and steering of the two wheels, the motion trajectory is in turning motion. In addition, the movement of soccer robot can use functions to achieve when it directly moves to one point or turn to one angle.

(2) Kicking the ball

Because of changeable soccer position, the soccer robot needs to know soccer's coordinates when the robot hits the ball before performing the movement of kicking the ball. Under this circumstance, the dynamic environment robot soccer and neutrality line with smaller calculated amount are quite practical. Specific implementation method is as follows: the robot is in position R, and the ball is in position F, if the ball wants to be kicked in position G, the robot should follow the intersection of perpendicular bisector of ligature between R and PF and Reverse extension line of FG and ligature F1; when the robot moves to next position R1, it should adjust its direction of motion again. After several direction of adjustment, the robot can adjust the direction of kicking the ball.

(3) Interception

Interception of Soccer robot includes interception of ordinary player and goalkeeper [15]. Given that no collision with other robots was involved when dribbling, case is simplified and dichotomy can be used because movement of the robot and ball can be regarded as uniform motion. Following are sketch maps, Figure 1 and Figure 2, of interception of soccer robot and ball.

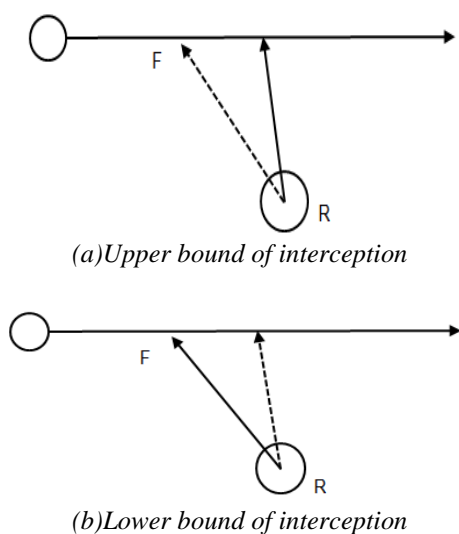


Figure 1 Dichotomy interception principle of ordinary player (R represent soccer robot, F represents position of ball when robot arrives at ball's trajectory.)

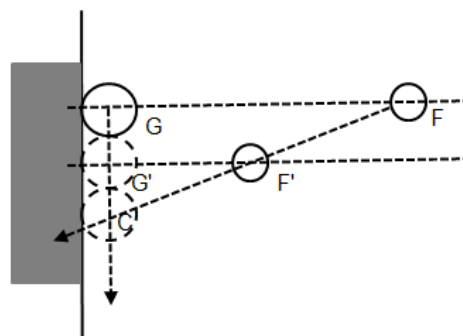


Figure 2 Process of goalkeeper's interception (F represent ball, G represents goalkeeper, and C represents cross-point of F and G)

(4) Shoot

It's vital to set a goal before shooting. When robot kicks the ball, one can easily associate it with table tennis because robot and ball is sphere on AI-RCJ soccer platform. Thus, this thesis designs a shoot method based on thoughts of playing table tennis, and it is shown as follows.

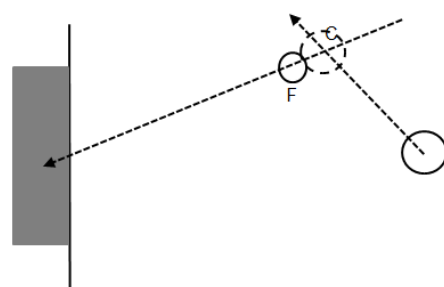


Figure 3 Table-tennis shoot (A represent soccer robot, B represents soccer, C represents destination of soccer robot.)

2.2 Construction of soccer robot's stimulation system

(1) General architecture

In terms of hardware, soccer robot system was mainly consisted by four parts [16], which is shown as following Figure 4:

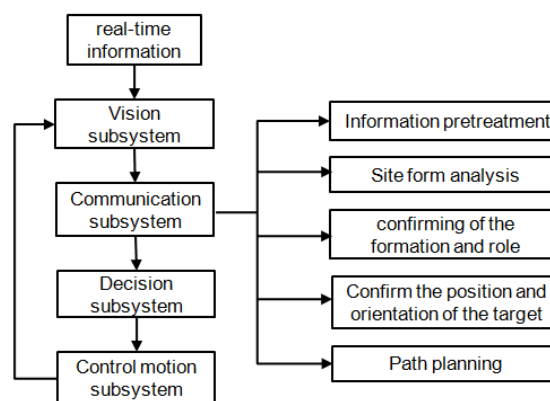


Figure 4 Architectures of soccer robot system

(2) Motion model of soccer robot

Soccer robot drives the wheels on both sides with a small car, thus motion model of the soccer robot and the small car is the same. Robot car launch radio signals to control the speed of the two wheels, which means to adjust the speed and direction of the robot, to move towards the destination. Assume that R is the radius of rotation, and S and theta are arc length and central angel of the car moved in unit interval respectively; A represents position of the car at time t and B represents position of the car at time t+Δt. Suppose no sliding between the wheels and floor, car makes circular motion from position A (X, Y, theta) to position B (X+0x, Y+Δy, theta+Δtheta) after time At, and S_t and S_r represent distance of the two wheels moving from A to B respectively. L represents distance of the two wheels. When the car goes straight, Δtheta = 0 and sin (Δtheta/2) = 0, thus formula is shown as follows,

$$\begin{cases} X = S \cdot \cos(\theta) \\ Y = S \cdot \sin(\theta) \end{cases} \quad (2-1)$$

From formula (2-1) shown above, it can be concluded that if sample time Δt is short enough, actual moving track will be quite similar to ideal model.

3. Soccer robot's path planning based on improved particle swarm optimization

3.1 Adaptability function based on global path

$$Y_{fit1} = \sum_{i=1}^n \sqrt{(x_{ji} - x_{j(i-1)})^2 + (y_{ji} - y_{j(i-1)})^2} \quad (3-1)$$

Adaptability function is the base of particle swarm optimization and the standards for particle swarm optimization to measure and judge the fitness of particle [17]. Based on the optimal path, this thesis takes the length path of the robot as adaptability function to weight balanced all parameters of waypoints. If there are no obstructions, path planning is based on the length of present position and object position. If the obstacle is within the detection range of the robot and the coordinate, particle swarm optimization can be applied to find a shortest path by the soccer robot. In this case, adaptability function of the particle swarm optimization can be divided into two parts includes ① path length between the robot's present point and the next predicted position. ② path length between the robot's next predicted position and object position. In order to optimize the global path planning, those two paths should be weighted. When the robot is moving along track j and all points i on the track form the shortest path, adaptability function should be as follows (3-1),

$$Y_{fit1} = \sum_{i=1}^n \sqrt{(x_{ji} - x_{j(i-1)})^2 + (y_{ji} - y_{j(i-1)})^2} \quad (3-1)$$

Coordinate (x_{ji}, y_{ji}) represents of point i on the track j, so the next predicted position of the robot path planning is (x_{jn}, y_{jn}). Connect (x_{jn}, y_{jn}) and object position (g₁, g₂) to calculate the path length which is show as following formula 3-2,

$$Y_{fit2} = \sqrt{(x_{jn} - g_1)^2 + (y_{jn} - g_2)^2} \quad (3-2)$$

Thus, this adaptability function represents the weight sum of above two functions which is shown as following function 3-3,

$$Y = AY_{fit1} + BY_{fit2} \quad (3-3)$$

3.2. Adaption of security constraint function

During a soccer robot competition, security should take into consideration to avoid obstacles because soccer robot has a definite volume. If Assume that soccer robots, in the motion region, are circles of radius r, critical safe distance is 2r when two robots colliding. Security constraint function can be shown as following function 3-4,

$$OB(i) = \min \left\{ 0, \left[\sqrt{(x_{ji} - x_k)^2 + (y_{ji} - y_k)^2} - 2r \right] \right\} \quad (3-4)$$

Function 3-4 can be analyzed based on Figure5.

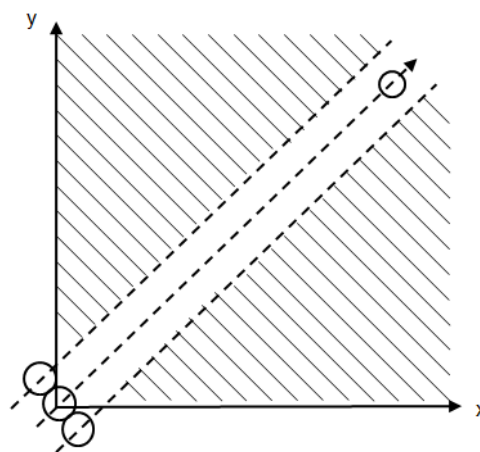


Figure 5 Constraint function sketch

As Figure 5 shows, there are no obstacle on the way of robot from the start position to the object position when robots of the other party is outside the critical security region which is the dash area shown in the Figure. Thus, path planning is the connected lines of the two positions. In order to increase safe coefficient of obstacle avoiding, width of this safe region should be 4r. Constraint function of the straight path is finite element boundary. Figure 5 shows the safe region which can be set as following function 3-5,

$$\begin{cases} y = kx \\ kx - 2r\sqrt{1+k^2} \geq y \\ kx + 2r\sqrt{1+k^2} \leq y \end{cases} \quad (3-5)$$

3.3 Particle Swarm Optimization in the dynamic environment

The race environment of the soccer robot is dynamic, complex and uncertain. Since most obstacles in the court are mobile, it is important to control the speed of the soccer robot in order that the soccer robot can successfully avoid obstacles. Particle Swarm Optimization is a algorithm to describe global path planning, but simulation analyses can be made for the algorithm in the dynamic environment as a result of the environment of polar coordination and model and its strong global and local searching ability. Blocking robot and moderate speed [18] of the objective point can be introduced to it. The moving blocking robot and pace of the objective point can be described as follows:

Obpoint (1, 1)=obpoint (1, 1)+Vo (1) ;
 Obpoint (1, 2)=obpoint(1, 2)+Vo (2) ;
 Gpoint (1) =gpoint (1)+Vg (1) ;
 Gpoint (2) =gpoint (2)+Vg (2) ;
 Via above means speed vector of obstacles and Vg means the speed vector of objective point.

3.4. Processes to improve algorithm

There are two parts for the way to make path planning in the use of particle swarm optimization: one part is path planning, and the other is particle swarm optimization. The path planning part generally contains the setting of initiation parameter for moving area of the robot, searching path of the robot and its visible drawing, which are bases of path planning simulated program. When the robot meet obstacles and can not move in straight line, the particle swarm optimization works to make path planning, including algorithm initiation program, fitness function, obstacles inspecting, changing program of polar and rectangular and so on.

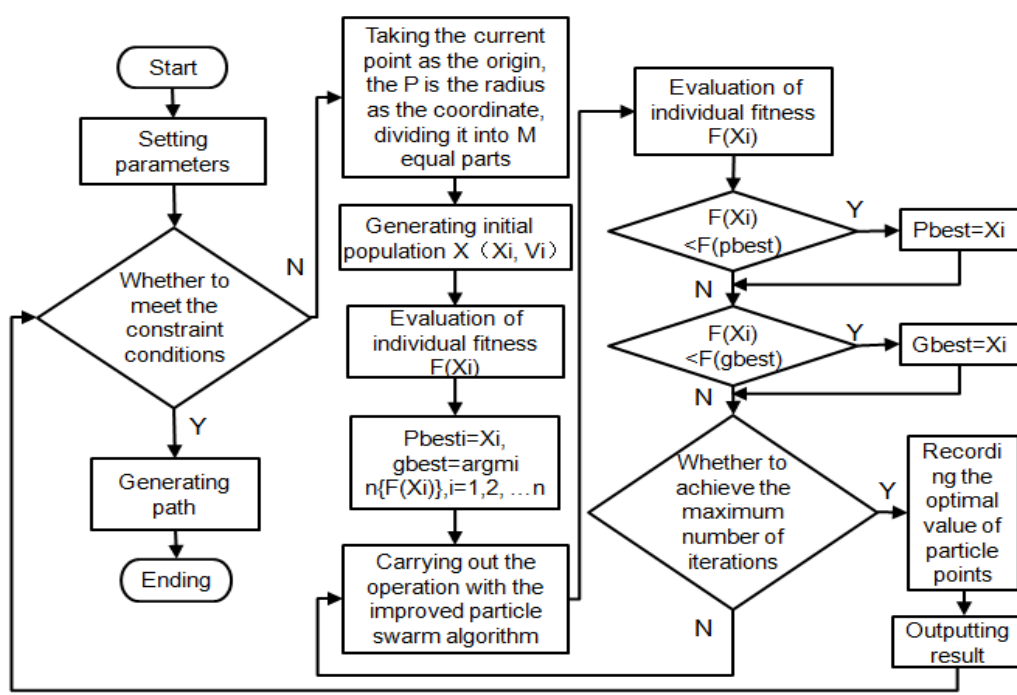


Figure 6 Path planning flow chart through particle swarm optimization

From the chart 6, it can be seen that in the algorithm of describing the path of the soccer robot, the soccer robot makes pre-judgment in every circulative iteration process. If the robot meets obstacles, it will make path planning in using of particle swarm optimization, otherwise, it will move straight ahead. Meanwhile, obstacles are moving in circulative iteration. So, the soccer robot, both moving obstacles and object point are carried out in the polar coordination environment and algorithm path planning, and path planned through this way is the most favorable one.

4. Inspection and analyses

4.1 simulation experiment

Comparative analyses are made between unimproved and improved standard particle swarm optimization algorithms, and parameters are set as follows:

Standard PSO algorithm: Group size, namely m, is set as 50. Learning factor c1 and c2 is 1.5. ω is set as

$$\omega = \omega_{\max} - \frac{\omega_{\max} - \omega_{\min}}{K} * k, \text{ in which } \omega_{\max}=0.9,$$

wmin=0.4, decreasing progressively from 0.9 to 0.4 as the increasing of iteration times. Iteration times, namely, GK is 300.

Improved PSO algorithm: Because of the newly initiated particle swarm, group size here is set as 100 so as to find the position of most optimized solution. Learning fact c1 and c2 is 1.5. ω is set as

$$\omega = \omega_{\max} - \frac{\omega_{\max} - \omega_{\min}}{K} * k, \text{ in which } \omega_{\max}=0.9,$$

wmin=0.4, decreasing progressively from 0.9 to 0.4 as the increasing of iteration times. Iteration time is 300.

Simulation results of the two algorithms are as follows:

Table 1: Simulated Data of Unimproved and Improved PSO Algorithm (*e+003)

	Max1	Min1	Max2	Min2
1	3.1896	0	3.2153	0
2	3.2507	0	3.1242	0
3	3.2659	0	3.3369	0
4	3.1756	0	3.2748	0
5	3.7489	0	3.3573	0
6	3.1524	0	3.4186	0
7	3.2109	0	3.7462	0
8	3.5968	0.6589	3.1246	0
9	4.1532	0	3.2015	0
10	3.8062	0	3.3595	0
11	3.1550	0	3.4806	0
12	3.3198	0	3.1107	0
13	3.9883	0	3.1984	0
14	3.6805	0.4295	3.5862	0
15	3.4185	0	3.1486	0

Table 1 shows the simulation data after the two algorithms have ran for 15 times. Max1 and Min2 are respectively the maximum and minimum of fitness function after standard PSO algorithm has ran for 15 times; Max2 and Min2 are respectively the maximum and minimum of fitness function after improved PSO algorithm has ran 15 times.

4.2 Results analyses

From Table 1, it is clear that standard PSO algorithm is tapped in local optimum for twice in running for 15 times. But is has reached a certain precision. Improved PSO algorithm is not tapped in local algorithm in running for 15 times, which shows the strong reliability of the improved one. Through comparing the average fitness of the two algorithms, it can be seen that standard PSO algorithm reaches the local optimal value in the 40th iteration, and the improved one in the 5th iteration, indicating that the improved algorithm works better than the standard one in the rate of convergence with stronger reliability. When the improved algorithm is applied in path planning, it can be found that particle swarm is initiated in each iteration so that the problem

standard PSO algorithm is easy to be trapped in local optimum is solved. At the same time, the improved algorithm can be used in path planning in dynamic environment and proves the conclusion. Final result show that the simulation path of the standard PSO algorithm is 10419.45mm in length, iteration times is 300, that the time simulation experiment takes is 1.5315s, and that the average iteration time is 5ms; the simulation path of the improved PSO algorithm is 6514.4mm in length, iteration times is 134, that the time simulation experiment takes is 0.44712, and that the average iteration time is 3.34ms. It proves that the improved algorithm works better than the standard one.

4. Conclusion

Soccer robot is a system with multiple intelligent agents. In the race filled with complex, dynamic and unpredictable factors, the key and difficult point to study robotics and artificial intelligence is its path planning. Analyses are made in the paper about how soccer robot makes the confrontational path planning in the dynamic environment through the improved PSO algorithm. Through improving PSO algorithm, it is put forward the fitness functions and safety degree constraint function in the certain environment so that the path planning is more reliable, and the dynamic programming period of velocity vector is introduced to meet the dynamic complex environment. Finally, both standard algorithm and the improved one is applied in simulation checking of path planning. Results show that the improved algorithm is better than the standard one in path length, simulation time, iteration times, the rate of convergence. Thus, the improved algorithm is of more feasibility and effectiveness.

5. References

[1] Beetz M, Bennewitz M, Burgard W, et al. Probabilistic Algorithms and the Interactive Museum Tour-Guide Robot Minerva[J]. International Journal of Robotics Research, 2010, 19(11):972-999.
 [2] Aramaki S, Sayama I, Nakazawa M, et al. Robot Development and the Effect of Robot-aided Bilateral Training of Hemiplegic Upper Limbs in Subacute Stroke Patients : A Randomized Controlled Trial[J]. Japanese Journal of Rehabilitation Medicine, 2011, 48(9):612-622.
 [3] Chung L Y. Remote Teleoperated and Autonomous Mobile Security Robot Development in Ship Environment[J]. Mathematical Problems in Engineering, 2013, 2013(2):133-174.
 [4] Snášel V, Svatoň V, Martinovič J, et al. Optimization of Rules Selection for Robot Soccer Strategies[J]. International Journal of Advanced Robotic Systems, 2014, 11(4):257-267.
 [5] Shi H, Lincheng X U, Zhang L, et al. Research on self-adaptive decision-making mechanism for competition strategies in robot soccer[J]. Frontiers of Computer Science, 2015, 9(3):1-10.

- [6] Haobin S, Lin Z, Wei P, et al. Robot soccer confrontation decision-making technology based on MOGM: Multi-objective game model[J]. *Journal of Intelligent & Fuzzy Systems*, 2015, 28(2):713-724.
- [7] Liu Z X, Yang L X, Wang J G. Soccer Robot Path Planning Based on Evolutionary Artificial Field[J]. *Advanced Materials Research*, 2012, 562-564:955-958.
- [8] Hidalgo-Paniagua A, Vega-Rodríguez M A, Ferruz J, et al. Solving the multi-objective path planning problem in mobile robotics with a firefly-based approach[J]. *Soft Computing*, 2015:1-16.
- [9] Elsheikh E A, El-Bardini M A, Fkirin M A. Practical Design of a Path Following for a Non-holonomic Mobile Robot Based on a Decentralized Fuzzy Logic Controller and Multiple Cameras[J]. *Arabian Journal for Science & Engineering*, 2016:1-15.
- [10] Korayem M H, Eshfedan R A, Nekoo S R. Path planning algorithm in wheeled mobile manipulators based on motion of arms[J]. *Journal of Mechanical Science & Technology*, 2015, 29(4):1753-1763.
- [11] Zheng Y, Fang L. Path Planning of Mobile Robot Based on Improved Artificial Immune Algorithm[J]. *Open Automation & Control Systems Journal*, 2015, 7(1):1768-1775.
- [12] Su W, Rui M, Yu C. A Study on Soccer Robot Path Planning with Fuzzy Artificial Potential Field[C]International Conference on Computing, Control and Industrial Engineering. IEEE Computer Society, 2010:386-390.
- [13] Mansury E, Nikookar A, Salehi M E. Artificial Bee Colony optimization of ferguson splines for soccer robot path planning[C]First Rsi/ism International Conference on Robotics and Mechatronics. IEEE, 2013:85-89.
- [14] Sudin M N, Nasrudin M F, Abdullah S N H S. Humanoid localisation in a robot soccer competition using a single camera[C] IEEE, International Colloquium on Signal Processing & ITS Applications. 2014:77 - 81.
- [15] Wang R, Veloso M, Seshan S. Multi-robot information sharing for complementing limited perception: A case study of moving ball interception[C] Proceedings - IEEE International Conference on Robotics and Automation. 2013:1884-1889.
- [16] Sadeli A M I, Prihatmanto A S, Rijanto E. Design and implementation of heuristic intelligent attack algorithm in robot soccer system small size league[C] IEEE, International Conference on System Engineering and Technology. IEEE, 2015:52-65.
- [17] Doitsidis L, Tsourveloudis N C, Piperidis S. Evolution of Fuzzy Controllers for Robotic Vehicles: The Role of Fitness Function Selection[J]. *Journal of Intelligent & Robotic Systems*, 2009, 56(4):469-484.
- [18] Campos J A F, Flores J A R, Montufar C P. Robot Trajectory Planning for Multiple 3D Moving Objects Interception: A Polynomial Interpolation Approach[C]Electronics, Robotics and Automotive Mechanics Conference. 2008:478-483.

BRAND:
«SMART MECHATRON - Competitiveness,
performance and high quality through
HIGH-TECH MECHATRONIC PRODUCTS »

NUMERICAL MODELING ANALYSIS ON AERODYNAMIC PERFORMANCE OF SAILING WINGS FROM CATIA

Ruicheng Pan

Northwest University of Political Science and Law, Shaanxi, China

E-mail: panprcheng@sina.com

Abstract - Sailing is an aquatic sport that sailor manages the force of the wind on the sails to steer and race pace within a certain competition area. With no mechanical power, sailing is wind-powered of sail wing, thus aerodynamic performance of sail wing is vital in sailing. Creating a models based on numerical modeling is a premise to study aerodynamic performance of sail wing. Different modeling method of the model will make a great different in numerical accuracy and calculating work. In conclusion, it's necessary to study the modeling method of numerical modeling of aerodynamic performance.

Keywords: CATIA, sailing, aerodynamic performance, numerical modeling, sail wing.

1. Introduction

Sailing is an aquatic sport that sailor manages the force of the wind on the sails to steer and race pace within a certain competition area. With no mechanical power, sailing is wind-powered of sail wing, thus aerodynamic performance of sail wing is vital in sailing. Sailor needs to adjust angle of the force of the wind on the sail to keep the sail craft moving forward fast and to generate the maximum of power of the wing, thus sailing is a high intellectual sports [4~6]. Study on aerodynamic performance of sail-wing is carried out by three aspects: experimental study, theoretical analysis and numerical modeling. To some extends, numerical modeling have a deeper insight into fluid mechanics than experimental study and theoretical analysis because it can detect the integral or partial small disturbance. Study on fluid dynamic performance of sailboat used to based on unsteady and steady potential flow theory of numerical modeling to calculate relevant values. However, there would be flow separation phenomenon whether it is windward, crosswind and leeward or not. In this case, effect of viscosity on calculation result should not be ignored. Generally, finite element method is one of the frequently used numerical methods, which discrete continuum body into an aggregation of finite-sized units to solve continuous mechanics problems [7~9].

Before design a model, reasonable programming model, reasonable analysis of problems to be solved and goal-set should be done in order to achieve desired outcome. When designing a model, reasonable modeling method should be choice after take time-consumed and accuracy of calculation results into consideration. Therefore, appropriate modeling method is the key to the correctness results of numerical modeling of sail wing's aerodynamic performance.

CATIA is of strong 3D design capacity, abundant product solutions, user friendly interface, strong surface modeling, and rich functions [10~12]. CATIA has a strong hybrid modeling ability and interactive operation can be implemented no matter is it surface modeling or solid modeling. Working hour is greatly reduced because CATIA uses only one database which ensures data transmission, strengthens model's generalized ability, and operation in different systems can be done individual at the same time. Besides, CATIA hierarchy system is correlative, which is like the parent-child relationship of Window's operation interface. When parent system changes, so does the child system. Take surface modeling as an example, when one of the control points of the surface changes, position of the line box and surface relative to this control point will be changed [13~15]. This thesis is to study the modeling method of numerical modeling of sailing wing's aerodynamic performance based on modern CATIA. According to the study, modeling methods, applicable for fluid dynamic performance of sailing wings, is used to provide scientific basis to fluid dynamic performance study of the sail wing.

2. Aerodynamics of sailing wing

As shown in following graph 1, sailing wing is a camber with no thickness. When airflow W past sail wing at an angle of α , the air speed of the upper surface is accelerated while of the lower surface is decelerated, thus the upper surface is suction surface while the lower surface is pressure surface. Resultant force of suction and pressure is aerodynamics N . Resultant force N is perpendicular to AB , which is upward.

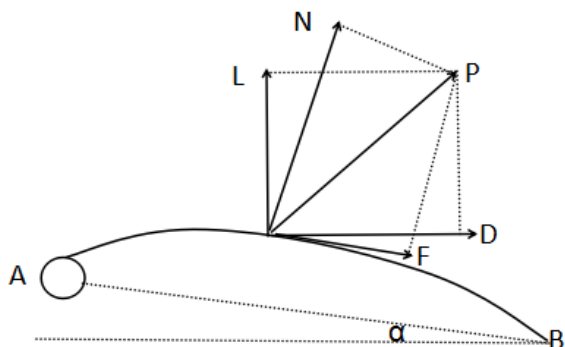


Figure 1: Graph a sailing wing's atress

When airflow passes sails, friction resistance F is produced and its direction is the same with the surface of sail's. Generally, friction resistance F is lower than resultant force N, thus friction resistance usually can be ignored. Resultant force of F and N is total aerodynamic P.

Profile lift force of sailing wing is denoted by \vec{L} . Lift coefficient is denoted by C_L . And relation between \vec{L} and C_L shown as follows.

$$C_L = \frac{L}{1/2\rho v^2 S} \quad (1)$$

Relation curve of lift coefficient and attack angle is detonating the typical characteristics of lift force, which is shown as Figure a. With the increasing of attack angle, lift coefficient is rising perpendicularly and reaches the maximum at a certain attack angle. If the attack angle keeps increasing, life coefficient will decline rapidly. The phenomenon of lift coefficient declining and resistance increasing is called stall phenomenon, which is caused by flow separation. Generally, stalling angle of rigid wing is at 10 to 20 degree while stalling angle of flexible wing is at 30 degree which is bigger than the former. Therefore, when adjusting the sailing wing in sailing or sail boarding, sailor has to avoid stall phenomenon and keep a relatively big attack angle [16~18].

Surface friction drag and pressure drag (form drag) make up profile drag. Force of the profile drag is closely related to the attack angle size and profile parameter, which is determined by experiment. Profile resistance \vec{D} is denoted by resistance coefficient C_D :

$$C_D = \frac{D}{1/2\rho v^2 S} \quad (2)$$

Typical expressive method of resistance curve is similar to that of life curve. In practical application, polar curve is frequently used to describe wing's dynamic characteristics. This means that relation curve of lift coefficient is denoted by drag coefficient, which is shown as following figure b and named pole figure.

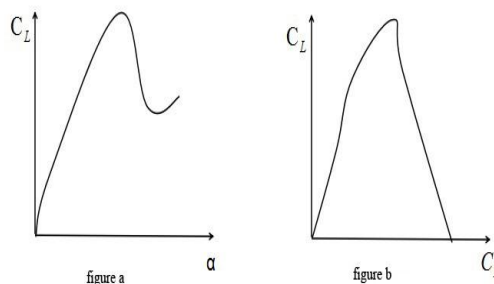


Figure 2 Graph b life coefficient and pole figure

3. Establishment of geometric model based on CATIA

The prerequisite of numerical modeling is establishing a geometric model because the established geometric model will directly influence the accuracy of numerical modeling. The more similar of geometric model to real object, the more accurate of numerical modeling results will be. However, is it very hard to establish a model which is exactly to the real object because that kind of model is demanding in modeling software and modeler's proficient level of modeling software and computer. What is more important is that the model established will affect quality of mesh generation of next step. Complicated model makes mesh generation more difficult and lowers the quality of local mesh. Therefore, model can be simplified according to focuses of those researched question and the influence level of real objects to focuses [19~21].

After take into consideration of all advantages and disadvantages of all kinds of modeling software and interface compatibility of ANSYS software, this thesis establishes entity modeling of wing with CATIA software, an advanced hybrid modeling technique, to establish a model which is more close to real wing. The shape of sailing wing changes under the wind power and is influenced by different design materials and flow field force. Besides, the changed sailing wing exerts influence to flow field around it, which, in turn, influences the shape of sailing wing, thus sailing wing's modeling is complex. In this thesis, there are following hypotheses:

- (1) According to kinetic theory, free path of gas molecules is 10^{-11} mm. Compared to characteristic length of sailboard and sail wing, this free path is higher order small, which means $l/L \ll 1$. Thus, air inflow of sailboard pumping is considered to be continuum.
- (2) Flow is steady.
- (3) If flow rate are small enough compared to sound velocity and mach number M and $M = U/a \leq 0.25$, compressibility of air is negligible. Speed of sound in air is denoted by a and $a=340\text{m/s}=1225\text{km/h}$. when sailboard pumping, the fastest speed is nowhere near speed of sound. Pressure and temperature in flow field changes slightly compared with that of in free flow, thus corresponding density

changes can be ignored, which means air is incompressible and density is invariant.

(4) Air temperature in flow field is invariant during sailboard pumping.

(5) Wing is of a rigid film sheet if the wing makes no change.

(6) Sail is pumped with uniform velocity.

(7) Hull and sail system never tilt and is perpendicular.

4. Flow field simulation of sailing wind and aerodynamic calculation

Partition of computation grid is the most timing-consuming part in numerical simulation process, because the accuracy of numerical simulation result or even the convergence of numerical simulation relies on the grid quality. Research have that computation accuracy can be further improved by improved grid quality than improved calculation formulas. Therefore, more attention should be paid to controlling the grid quality in the improvement of computational accuracy.

This thesis makes modeling with structured grid, unstructured grid and mixing network respectively. In order to compare the computation impact of three modeling approaches, it should use the same computational domain of which the bottom chord of sailing wing is 6 times in the front, 6 times on the right and left, 6 times upside and 10 times rear. Incoming flow direction is kept with 30°, and Realizable $k-\varepsilon$ model is selected for turbulence model to calculate respectively aerodynamic performance and flow field of different types of grid and quantitative models in the same operating condition. In the calculation, the inflow velocity is 6m/s, Reynolds number is $Re=0.92 \times 10^6$, and Realizable $k-\varepsilon$ model is selected for turbulence model.

Realizable $k-\varepsilon$ model v_t is not a constant that should be related to strain rate and put forward Realizable $k-\varepsilon$ model [22~23] in order to conform to the physical law of turbulence flow. This model brings

in rotation and curvature. v_t is defined as

$$v_t = C_u \frac{k^2}{\varepsilon} \tag{3}$$

C_u is expressed as follows:

$$C_u = \frac{1}{A_0 + A_s \frac{U^* k}{\varepsilon}} \tag{4}$$

Among this:

$$U^* = \sqrt{S_{ij} S_{ij} + \Omega_{ij} \Omega_{ij}} \tag{5}$$

$$S_{ij} = \frac{1}{2} \left(\frac{\partial u_i}{\partial x_j} + \frac{\partial u_j}{\partial x_i} \right) \tag{6}$$

$$\Omega_{ij} = \frac{1}{2} \left(\frac{\partial u_i}{\partial x_j} - \frac{\partial u_j}{\partial x_i} \right) \tag{7}$$

$$A_0 = 4.0, A_s = \sqrt{6} \cos \phi,$$

$$\phi = \frac{1}{3} \arccos(\sqrt{6}W)$$

$$W = \frac{S_{ij} S_{jk} S_{ki}}{\tilde{S}}, \tilde{S} = \sqrt{S_{ij} S_{ij}}$$

Turbulence energy k is calculated by the following

$$\frac{\partial k}{\partial t} + \frac{\partial(u_j k)}{\partial x_j} = \frac{\partial}{\partial x_j} \left[\left(\nu + \frac{\nu_t}{\sigma_k} \right) \frac{\partial k}{\partial x_j} \right] + G - \varepsilon \tag{8}$$

In the form, the ε represents dissipation rating of turbulence energy, G is defined as follows:

$$G = \nu_t \left(\frac{\partial u_i}{\partial x_j} + \frac{\partial u_j}{\partial x_i} \right) \frac{\partial u_i}{\partial x_j} \tag{9}$$

Dissipation rating ε of turbulence energy is defined as:

$$\frac{\partial \varepsilon}{\partial t} + \frac{\partial(u_j \varepsilon)}{\partial x_j} = \frac{\partial}{\partial x_j} \left[\left(\nu + \frac{\nu_t}{\sigma_\varepsilon} \right) \frac{\partial \varepsilon}{\partial x_j} \right] + S_\varepsilon \tag{10}$$

Realizable $k-\varepsilon$ model:

$$S_\varepsilon = C_{\varepsilon 1} S_\varepsilon - C_{\varepsilon 2} \frac{\varepsilon^2}{k + \sqrt{\nu \varepsilon}} \tag{11}$$

In the above formulas,

$$\sigma_k = 1.2, C_{\varepsilon 2} = 1.9,$$

$$C_{\varepsilon 1} = \max \left(0.43, \frac{\eta}{\eta + 5} \right), \text{ and among them,}$$

$$\eta = S k / \varepsilon$$

5. Computation result and analysis

5.1 Resistance coefficient

According to the computational formula of resistance coefficient:

$$C_D = \frac{D}{1/2 \rho S U_a^2} \tag{12}$$

Among them, D represents resistance, S represents compression area, U_a represent apparent

wind. In the computation, U_a is inflow velocity with 6m/s, compression area is about half of total surface area of object of study. The computation result of fluent is as following table 1.

Table 1 Resistance coefficient

Type of network	Resistance coefficient
Structured network	0.531
Unstructured network	0.562
Mixing network	0.582

Compared with 3 computation results and experimental values, the error is:

$$E_{C_D} = \left(\frac{C_{D(\text{computation results})} - C_{D(\text{experimental values})}}{C_{D(\text{experimental values})}} \right) 100\% ,$$

the result is as following figure 3.

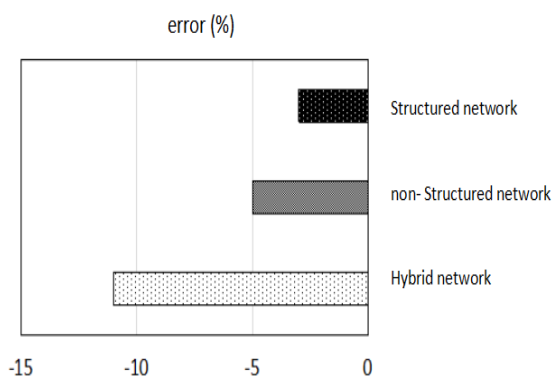


Figure 3: error analysis acquired from Resistance coefficient and experimental values by different numerical procedure

5.2 Lift coefficient

According to the computational formula of lift coefficient:

$$C_L = \frac{L}{1/2 \rho S U_a^2} \tag{13}$$

Among them, L represents lift force, ρ represents air density, S represents compression area, and U_a represents apparent wind. In the computation, U_a is inflow velocity with 6m/s, compression area is about half of total surface area of object of study. The computation result of fluent is as following table 2.

Table 2 Lift coefficient

Type of network	Lift coefficient
Structured network	1.274
Unstructured network	1.286
Mixing network	1.322

Compared with 3 computation results and experimental values, the error is:

$$E_{C_L} = \left(\frac{C_{L(\text{computation results})} - C_{L(\text{experimental values})}}{C_{L(\text{experimental values})}} \right) 100\% ,$$

the result is as following figure 4.

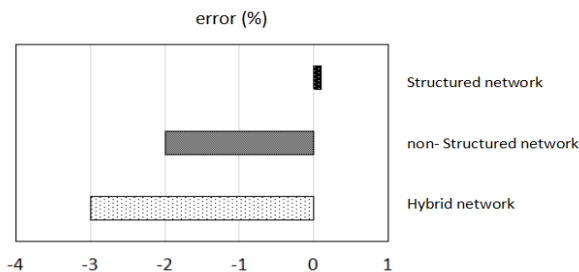


Figure 4: error analysis acquired from Lift coefficient and experimental values by different numerical procedure

From the figure 3 and figure 4, although all the three numerical procedures: structured grid, unstructured grid and mixing grid have errors in the simulated results and experimental results, their errors are small. Because all the unstructured grids of numerical procedure adopt unstructured grid whose quality of grid generation is hard to guarantee and is easy to have gridding with bigger curvature. And in the meanwhile, due to the larger number of gridding, numerical computation costs too much time. Therefore, computational accuracy, modeling time, computational time consumption and other factors are taken into consideration to adopt mixing grid to compute the sailing wing on the premise of guaranteeing accuracy.

6. Conclusion

First, this thesis discusses and ensures the model and condition of sailing wing's aerodynamic numerical computation. And then, it introduces and analyzes the result of numerical simulation, which includes the analysis of resistance and lift. The difference of numerical computation results under the three different modeling approaches is analyzed in detail. And from that, the simulation result of structured grid is not more real. Although the structured grid is easy to converge and significantly decrease time consumption and memory space, if the size of structured grid is larger, it cannot catch geometrical information of object of study, so the error of simulation result would become larger. Therefore, if computing power permitted, it should refine the grid as much as possible, especially the more concerned part. The mixing grid is more suitable for the computation of sailing wing.

7. References

[1] Pezzoli A, Bellasio R. Analysis of Wind Data for Sports Performance Design: A Case Study for Sailing Sports[J]. Sports, 2014, 2(4):99-130.

- [2] Ingrassia T, Mancuso A, Nigrelli V, et al. A multi-technique simultaneous approach for the design of a sailing yacht[J]. *International Journal for Interactive Design & Manufacturing*, 2015:1-12.
- [3] David A C D, Al. E. Visual search, movement behaviour and boat control during the windward mark rounding in sailing[J]. *Journal of Sports Sciences*, 2014, 33(4):398-410.
- [4] Chen J, Xie S, Li H, et al. Roughness effect on airfoil aerodynamic performance for land-yacht robot[J]. *Journal of Renewable & Sustainable Energy*, 2016, 8(2):336-343.
- [5] Izaguirrealza P, Flay R G J, Pelley D J L, et al. A wind tunnel investigation of the aerodynamics of sailing dhows[J]. *Proceedings of the Institute of Marine Engineering Science & Technology Part A Journal of Marine Engineering & Technology*, 2014, volume 13(1):13-22(10).
- [6] Lee T, Su Y Y. Aerodynamic performance of a wing with a deflected tip-mounted reverse half-delta wing[J]. *Experiments in Fluids*, 2012, 53(5):1221-1232.
- [7] Sfakianaki K N, Liarokapis D E, Trahanas G P, et al. The influence of a keel bulb on the hydrodynamic performance of a sailing yacht model[J]. *Journal of Maritime Research Jmr*, 2013, 10:51-58.
- [8] Wang S, Su Y, Wang Z, et al. Numerical and Experimental Analyses of Transverse Static Stability Loss of Planing Craft Sailing at High Forward Speed[J]. *Engineering Applications of Computational Fluid Mechanics*, 2014, 8(1):44-54.
- [9] Liu P, Su Y M, Liao Y L, et al. Experimental study of hydrodynamic performance of unmanned wave glide vehicle[J]. *Shanghai Jiaotong Daxue Xuebao/journal of Shanghai Jiaotong University*, 2015, 49(2):239-244.
- [10] Yang C, Yinwu L I, Wang J, et al. Visualization and Feature Extraction of the Surface Morphology of the Abdomen of Red Swamp Crayfish[J]. *Advances in Natural Science*, 2012, 5(2):45-50.
- [11] Whitty J, Haydock T, Johnson B, et al. On the Deflexion of Anisotropic Structural Composite Aerodynamic Components[J]. *Journal of Wind Energy*, 2014, 2014(2):1-13.
- [12] Potocnik D, Dolsak B, Ulbin M. Concurrent computer-aided design system for supporting technological aspect of cutting die design[J]. *Concurrent Engineering*, 2013, 21(2):155-168.
- [13] Jeong J W, Kim I S, Chand R R, et al. A study on simulation model and kinematic model of welding robot[J]. *Journal of Achievements in Materials & Manufacturing Engineering*, 2012, 55(1):66-73.
- [14] Andrade D, Alberto L, Santos C D, et al. Analysis of Radar Cross Section Reduction of Fighter Aircraft by Means of Computer Simulation[J]. *Journal of Aerospace Technology & Management*, 2014, 6(2):177-182.
- [15] Mei Z Y, Zhou J, Mei L, et al. Research on case base for composite part design[J]. *Modern Manufacturing Engineering*, 2008, 29(5):92-95.
- [16] Mylonas D, Sayer P. The hydrodynamic flow around a yacht keel based on LES and DES[J]. *Ocean Engineering*, 2012, 46(6):18-32.
- [17] Parolini N, Quarteroni A. Mathematical models and numerical simulations for the America's Cup[J]. *Computer Methods in Applied Mechanics & Engineering*, 2005, 194(9-11):1001-1026.
- [18] Nishizawa Y, Taguchi T, Onodera T, et al. An Experimental Study on Characteristic of Vertical-Axis Sail-Wing Type Variable Paddle Windmill(The 14th National Symposium on Power and Energy System)[J]. *Transactions of the Japan Society of Mechanical Engineers B*, 2010, 76:369-370.
- [19] Nakata S, Doi Y, Kitahata H. Synchronized sailing of two camphor boats in polygonal chambers.[J]. *Journal of Physical Chemistry B*, 2005, 109(5):1798-802.
- [20] Zhang Y, Jia Y, Wang S S Y, et al. Composite Structured Mesh Generation With Automatic Domain Decomposition In Complex Geometries[J]. *Engineering Applications of Computational Fluid Mechanics*, 2013, 7(7):99-102.
- [21] Li Y, Jing Y T, Li L. Calculation and Analysis of Winding Temperature Rise for ODAF Power Transformer[J]. *Advanced Materials Research*, 2012, 516-517:1580-1583.
- [22] El-Amin M F, Sun S, Heidemann W, et al. Analysis of a turbulent buoyant confined jet modeled using realizable $k - \epsilon$ model[J]. *Heat & Mass Transfer*, 2010, 46(8-9):943-960.
- [23] Lateb M, Masson C. Comparison of various types of $k - \epsilon$ models for pollutant emissions around a two-building configuration[J]. *Journal of Wind Engineering & Industrial Aerodynamics*, 2013, 115(115):9-21.
-

RESEARCH ON THE APPLICATION OF PID CONTROL TECHNOLOGY COMBINED WITH FNN ALGORITHM IN INTELLIGENT WHEELCHAIR OBSTACLE AVOIDANCE FOR DISABLED ATHLETES

Yarong Zheng

Xi'an University of Posts & Telecommunications, Shaanxi, China

E-mail: zhengyarr@sina.com

Abstract - With the development of competitive sports, some people with disabilities are also involved in the sports. In order to provide superior transport for the disabled, experts and scholars in many countries has conducted the research on the intelligent wheelchair. In this study, an obstacle avoidance strategy based on the strategy conversion mechanism was established according to the specific circumstances of the disabled athletes in the process of movement. In combination with the improved fuzzy neural network (Fuzzy Neural Networks, FNN) and the condition control variables, the obstacle avoidance processing method for intelligent wheelchair was also studied. In addition, this research mainly regarded the disabled athlete to use the intelligent wheelchair to carry on the sports as the research object and it studied the strategy conversion mechanism of intelligent wheelchair obstacle avoidance strategy based on sports. In order to avoid the collision between the teammates in wheelchair sports, the state control was given variables of different weights in the study to solve the obstacle avoidance problem in the wheelchair sports. When the obstacles encountered in the process of movement of disabled athletes in the inner angle of view, the algorithm based on improved fuzzy neural network was considered as the main algorithm of obstacle avoidance. In contrast the control algorithm based on state variable should be considered as the main algorithm of obstacle avoidance. The obstacle avoidance strategy based on conversion mechanism effectively improves the result of obstacle avoidance for intelligent wheelchair in sports.

Keywords: PID control technology, obstacle avoidance, FNN algorithm, intelligent wheelchair.

1. Introduction

Population aging and disability has become a major problem facing the Chinese. In order to provide superior performance means of transport for people with disabilities, intelligent robot technology was applied to intelligent wheelchair motorized wheelchair by the researchers (1). Intelligent wheelchair has made great progress both at home and abroad. As a kind of service robot for people with disabilities it should be human-oriented designed (2). Intelligent wheelchair will inevitably encounter some obstacles in the course of the road and it should be fast and safe to protect the user's security.

Project MAID of University of Ulm in Germany (3): Intelligent wheelchair was able to move forward in crowded places and judge whether there were people or obstacles around to make a decision to pass or not. If you could not pass, the intelligent wheelchair would begin to take measures to avoid obstacles or to remind pedestrians to give way. Project SIAMO of (4):

Constructing a multi function system to meet the needs of different degree of disability and users with special needs and the system consisted of three parts. They were advanced decision scheme and its control

subsystem, integrated environment perception and its integrated subsystem, human computer interaction system. Advanced decision making and its control subsystem included human computer interaction system and sensing system (Ultrasonic and infrared sensors). Human computer interaction system had different control methods such as speech recognition and intelligent operating lever and the human nature and intelligence of the intelligent wheelchair had been greatly improved.

There are a number of projects that are involved in many people at the same time in the Paralympic Games. The collision between teammates easily happens when there are many players in the wheelchair sports. At this time, the obstacle avoidance process needs to be carried out with the help of the intelligent wheelchair. Common obstacle avoidance methods are as follows: Artificial potential field method proposed in 2015 by Khatib (5), a method of obstacle avoidance based on raster map VFH (vector field histogram) proposed by Borenstein et al. (6). The artificial potential field method proposed by SP Parikh et al. (7) was applied to the intelligent wheelchair's obstacle avoidance problem and achieved a good result.

Thus, the problem of Safe Obstacle Avoidance of the disabled athletes in the use of intelligent wheelchair was studied in this paper based on the previous research results and combined with PID control technology and PNN algorithm.

2. Research on Application of fuzzy neural network in obstacle avoidance algorithm

Fuzzy Neural Networks (FNN) means neural network for fuzzy information processing (8). Fuzzy neural network is a combination of neural network and fuzzy logic. It brings together the advantages of fuzzy logic and neural network and the two are complementary (9). Compared with such a complex system like wheelchair obstacle avoidance, Fuzzy neural network has a great advantage.

The flexibility of obstacle avoidance function is an embodiment of intelligent wheelchair, on which many research scholars in this field at home and abroad have done many researches. A number of research scholars have given a variety of intelligent wheelchair planning and navigation obstacle avoidance method (10-12). But because the wheelchair's movement direction is always in the inner angle of view of the disabled athletes, human subjective consciousness plays a decisive role in the process of obstacle avoidance. When the direction of motion was outside the user's field of view this study used ultrasonic sensors to obtain environmental information to achieve security. The schematic diagram of the system structure was shown in Figure 1.

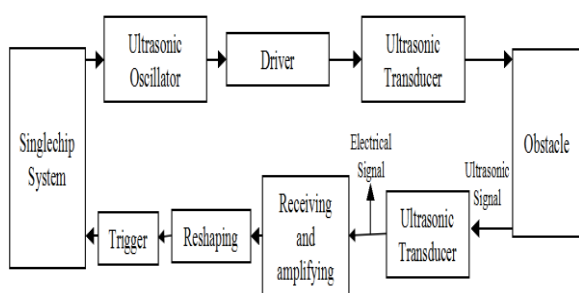


Figure 1 : Obstacle detection principle diagram of ultrasonic sensor

An improved fuzzy neural network control method was proposed in this paper. The learning function of neural network was used to adjust the parameters of membership function to improve the adaptive ability of the controller and it solved the problem of obstacle avoidance in dynamic environment to a certain extent.

Figure 2 is flow chart of fuzzy neural network algorithm.

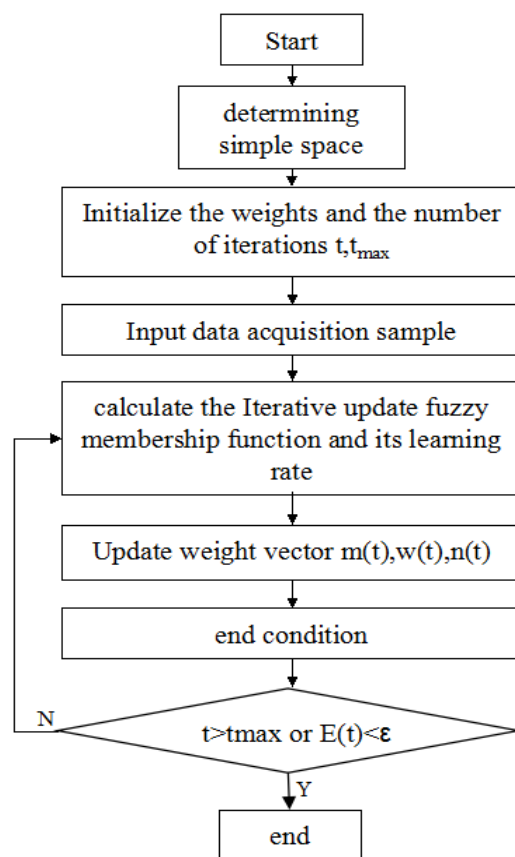


Figure 2: Flow diagram of fuzzy neural network algorithm

The fuzzy logic control mainly included three processes such as fuzzy logic, fuzzy reasoning, and the solution of the model [13,14]. In order to make the intelligent wheelchair reach the effect of the non collision this study collected the obstacle distance information of the intelligent wheelchair by the ultrasonic sensor and classified the distance information of the obstacle. A fuzzy neural network was designed and the 5 input variables were defined as L_l, L_m, L_r, θ, v . They respectively represented the distance information between the left, middle and right obstacles, the driving direction and speed of the wheelchair. ω and Δv were output variables and They respectively represented the rate of change in the direction of the wheel and the driving acceleration.

The intelligent wheelchair mainly moves in the ground plane under normal circumstances. So here we would use the two-dimensional coordinates of the plane and the direction of the wheelchair to describe the movement of the wheelchair. Two rear wheels of the wheelchair are driving wheels and they are used to drive by two motors. The running speed and operating angular velocity of the wheelchair will be realized by controlling the speed of the driving wheel.

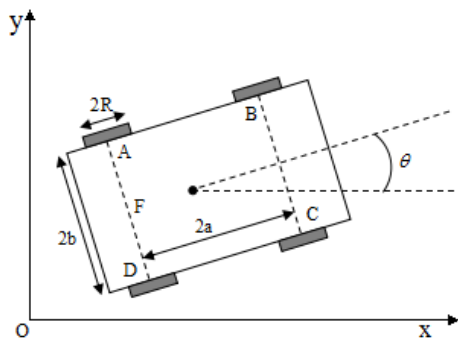


Figure 3: Motion model diagram

Among them, A, B, C, D are the centers of the four wheels and R is the rear wheel radius of intelligent wheelchair. The kinematic equation of intelligent wheelchair is

$$\dot{q} = \begin{bmatrix} \dot{x} \\ \dot{y} \\ \dot{\theta} \end{bmatrix} = \begin{bmatrix} \cos \theta & 0 \\ \sin \theta & 0 \\ 0 & 1 \end{bmatrix} \begin{bmatrix} v \\ \omega \end{bmatrix} \quad (1).$$

The rear wheels of the intelligent wheelchair are controlled by two independent motors. Figure 4 shows the wheelchair in the turning process of the movement model.

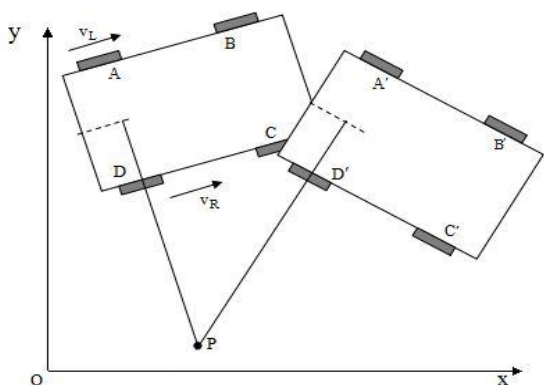


Figure 4: Diagram of speed control transmission

In Figure 4, r stands for wheelchair turning radius and P stands for speed instantaneous center of intelligent wheelchair. Line speed and angular velocity of intelligent wheelchair can be figured by $v = \frac{v_L + v_R}{2}$

(2) and $\Delta\theta = \frac{v}{r} = \frac{v_L}{r+b} = \frac{v_R}{r-b}$ (3). The structure of the

fuzzy neural network with membership function parameters of neural network is shown in Figure 5.

In Figure 5, $X=(x_1, x_2, \dots, x_n)$ is the Network input ($n=5$ in this study) and $Y=(y_1, y_2)=(\Delta v, \omega)$ is the output variable.

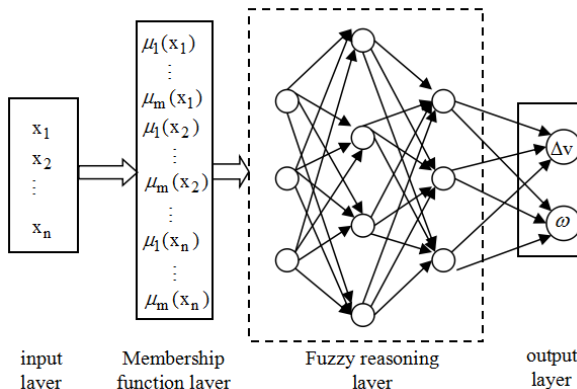


Figure 5: Structure of improved fuzzy neural network

The first layer is the input layer. There are five inputs totally and they are L_l, L_m, L_r, θ, v . The number of nodes is 5.

The second layer is the membership function layer. $w_{ij} (i=1, 2, \dots, 5, j=1, 2, \dots, 36)$ and $n_{ij} (i=1, 2, \dots, 5, j=1, 2, 3)$ are the network weights. The number of nodes is 11.

The third layer is the fuzzy reasoning layer. The number of total knot points is 36. Each node represents a fuzzy rule which is used to match the fuzzy rules relocation to calculate the applicability of each rule, $S_k = \min(q_{1k}, q_{2k}, q_{3k}, q_{4k}, q_{5k})$ (4)

Among them, q_{ik} represents degree of applicability about input i to rule $k (k=1, 2, \dots, 36)$. Take one of the rules as an example. $L_l, L_m, L_r, \theta, v, \omega, \Delta v$ are respectively considered as F, N, F, R, FS, PS, Z. F means that the obstacles are far away. N means that the obstacle is near. R means that the aim is in the direction of movement of the right wheelchair. FS means that the wheelchair is fast. PS indicates a slow increase or decrease of the direction angle. Z means to keep the wheel chair speed unchanged. Thus, this rule shows that if the left side of the obstacle is far, the middle the closer, the right the farther, the goal in the right side of the obstacle and the wheelchair is running faster it should be a slow increase in the direction of the angle and keep the wheel speed unchanged at this time.

The fourth layer is the output layer. It is the realization of the calculation of the solution. we used the center of gravity method to solve the fuzzy set in this research. The output of the system at this time would be

$$\Delta v = \frac{\sum_{k=1}^{36} v_{k2} S_k}{\sum_{k=1}^{36} S_k}, \omega = \frac{\sum_{k=1}^{36} v_{k1} S_k}{\sum_{k=1}^{36} S_k} \quad (5),$$

v_{k1}, v_{k2} represents a weight of the output j of the rule K . Matching the relationship between v_{k1}, v_{k2} and n_{ls} according to fuzzy rules such as $v_{1,1}=n_{15}, v_{1,2}=n_{23}, v_{2,4,2}=n_{21}$ and so on.

3. Obstacle Avoidance Strategy of Competitive Sports

For intelligent wheelchair sports, the cooperation and tacit understanding between the teammates is crucial to the whole competition. In this study, motion direction will be out of the angle of viewing field if the wheelchair user moves backward, which leads to collision easily. So, state control variables are added to solve the obstacle avoidance out of angle view field. Generally speaking, state controlling variables are used to record the state of the disabled athletes in the process of movement or hitting, which can help athletes to avoid hitting obstacles or teammates and move to the original direction as close as possible.

Supposing the state variable is $s_t = [\omega_t \ v_t]^T, t = \tau - 1, \tau, \tau + 1$, and recording the changes of wheelchair movement status in three time periods, then we can get the following state variable formulas:

The average value of state control variable s_a :

$$s_a = [\theta \ v]^T = \frac{1}{3}(s_{\tau+1} + s_{\tau} + s_{\tau-1}) = \frac{1}{3}[\omega_{\tau+1} + \omega_{\tau} + \omega_{\tau-1} \ v_{\tau+1} + v_{\tau} + v_{\tau-1}]^T \quad (6),$$

the change value $\Delta s_{\tau+1}$ at two different time $\tau + 1$ and τ :

$$\Delta s_{\tau+1} = [\Delta \theta_{\tau+1} \ \Delta v_{\tau+1}]^T = s_{\tau+1} - s_{\tau} = [\omega_{\tau+1} - \omega_{\tau} \ v_{\tau+1} - v_{\tau}]^T \quad (7),$$

the change value Δs_{τ} at two different time $\tau + 1$ and τ :

$$\Delta s_{\tau} = [\Delta \theta_{\tau} \ \Delta v_{\tau}]^T = s_{\tau} - s_{\tau-1} = [\omega_{\tau} - \omega_{\tau-1} \ v_{\tau} - v_{\tau-1}]^T \quad (8).$$

if we assume that the moving direction of player has the following eight: the front, the back, the left, the right, the left anterior, the left rear, the right front and the right rear; meanwhile, the intersection angle between two directions is 45° . Once the moving is out of the angle of viewing field, if the athlete moves backward, then target direction can be determined by the three values $s_a, \Delta s_{\tau+1}, \Delta s_{\tau}$,

$$\text{that is } M_s = \begin{cases} 0 & \Delta \omega_{\tau+1}, \Delta \omega_{\tau} < 0 \\ -N\theta & \Delta \omega_{\tau+1}, \Delta \omega_{\tau} > 0 \\ 1 & \text{others} \end{cases} \quad (9),$$

among which $0 < N < 1, -N\theta$ is the direction angle of wheelchair obstacle avoidance control. Both 0 and 1 refers to the weight that wheelchair avoid obstacles in accordance with the direction of human goals.

It is known that the cooperation of teammates is crucial for intelligent wheelchair sports.

Does this only not means the sense of cooperation, but also refers to the technology and skills [15-16].

For this paper, strategy conversion mechanism was applied into intelligent wheelchair competitive sports. Meanwhile, M was used to represent the wheelchair avoidance direction for the output of conversion mechanism of obstacle avoidance strategy (see as the below formula).

$M = aM_f + bM_s$ (10), in this equation, M_f is the avoidance direction of improved fuzzy neural network strategy, M_s is the avoidance direction of state control variable strategy in formula (9). Also, 'a' and 'b' represents the weight coefficient. Moreover, avoidance strategy was chosen by changing the weight coefficient.

4. The experiment and result analysis of the intelligent wheelchair sports

4.1 Man-machine interactive system with PID technology

Firstly, the system architecture of intelligent wheelchair was made by sing PID control technology (shown as figure 6).

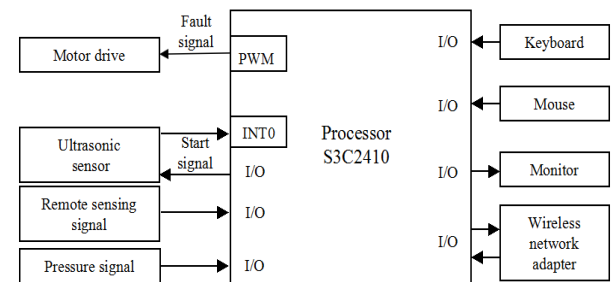


Figure 6: Frame of intelligent wheelchair system

On the other hand, in order to facilitate the human-computer interaction, this study also set up an interactive interface to facilitate the control of intelligent wheelchair.

4.2 Experimental result analysis

In this study, many obstacles were set up at the initial position and the terminal position. Meanwhile, we assumed that the user's expected direction is inherent. Finally, improved fuzzy neural network controller was applied in this study, then we found that the intelligent wheelchair safely went through the barrier area and reached to the terminal.

It can be seen from figure 7 that all circular and rectangular objects are obstacles, and the orientation angle $\theta = 180^\circ$. For points from ①-⑧ represent the track changes of wheelchair when obstacles are encountered. When the wheelchair arrived at the point ③ the target direction experienced a series of changes to the right and finally faced with obstacle. Then, it applied state control variable to make the wheelchair move to the left to avoid the obstacle according to the avoidance principles.

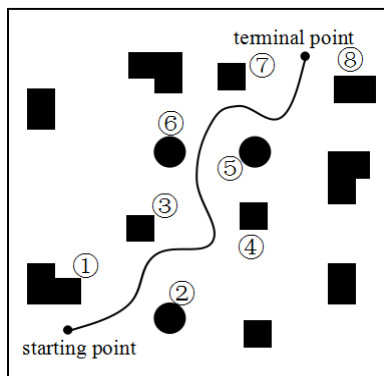


Figure 7: Obstacle avoidance trajectory (fuzzy control)

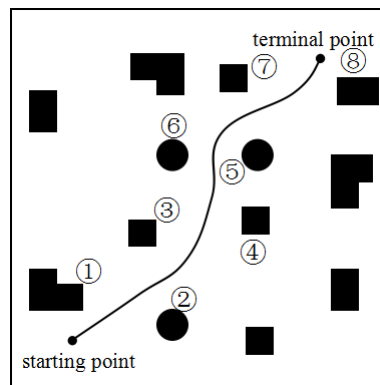


Figure 8: Obstacle avoidance trajectory (Improved fuzzy neural network control)

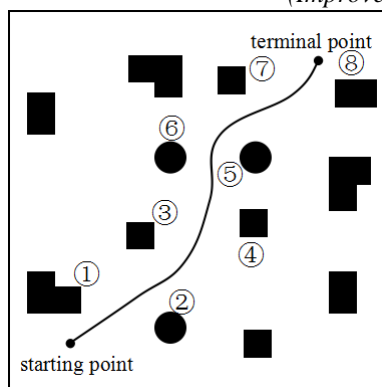


Figure 8: Obstacle avoidance trajectory (Improved fuzzy neural network control)

Seeing from figure 8 above, compared with fuzzy control in figure 7, the motion trajectories become relatively smooth under the system of improved fuzzy neural network control, which makes the whole process to be more comfortable. When the wheelchair is at the point ③ the state control variable recorded a series of changes to the right of the target direction for users, so when the motion direction is on the cone, it did not avoid the obstacle according to the principle but moved to the right avoiding the obstacle according to the sense of user. This finally reduced the difference between user target direction and obstacle avoidance direction.

5. Conclusion

In summary, on the one hand, this paper described the problem of intelligent wheelchair in the obstacle avoidance of competitive sports and compared and studied on the fuzzy logic, neural network and fuzzy neural network theory for sports strategy. Meanwhile, it proposed the improved fuzzy neural network algorithm and obstacle avoidance algorithm of state control variables, and finally implemented the study of obstacle avoidance for intelligent wheelchair in the sports. On the other hand, this paper realized the real-time monitoring to the running state of the intelligent wheelchair and data of display sensor through the PID control technology and intelligent wheelchair monitoring software of human-computer interaction, which not only ensured the normal operation of the intelligent wheelchair but also proved the validity of the

algorithm by experiments. Moreover, this paper also has some deficiencies, which should be improved.

6. References

- [1] Montesano L, Diaz M, Bhaskar S, et al. Towards an intelligent wheelchair system for users with cerebral palsy.[J]. IEEE Transactions on Neural Systems & Rehabilitation Engineering, 2010, 18(2):193-202.
- [2] Lei L, Guan T M, Tao Y. Design and Analysis of the Table Tennis Wheelchair Based on the Human Engineering[J]. Advanced Materials Research, 2011, 308-310:2388-2392.
- [3] Prassler E, Scholz J, Fiorini P. A Robotic Wheelchair for crowded public environments[J]. IEEE Robotics & Automation Magazine, 2001, 8(1):38-45.
- [4] Mazo M, García J C, Rodríguez F J, et al. Integral system for assisted mobility[J]. Information Sciences—informatics & Computer Science An International Journal, 2000, 129(1-4):1-15.
- [5] Khatib O. Real-Time Obstacle Avoidance for Manipulators and Mobile Robots[C]// IEEE International Conference on Robotics and Automation. Proceedings. IEEE, 2015:396-404.
- [6] Borenstein J, Koren Y. The vector field histogram-fast obstacle avoidance for mobile robots[J]. IEEE Transactions on Robotics & Automation, 2010, 7(3):278-288.
- [7] Parikh S P, Grassi V, Kumar V, et al. Integrating Human Inputs with Autonomous Behaviors on an

Intelligent Wheelchair Platform[J]. Intelligent Systems IEEE, 2007, 22(2):33-41.

[8] Rao D H. Fuzzy Neural Networks[J]. Iete Journal of Research, 2015, 44(4-5):227-236.

[9] Han M K, Han S I, Kim J S. Precision position control of servo systems using adaptive back-stepping and recurrent fuzzy neural networks[J]. Journal of Mechanical Science & Technology, 2012, 23(11):3059-3070.

[10] Jia S, Gao L, Fan J, et al. Intelligent tennis wheelchair control method based on Webots platform[C]// Mechatronics and Automation (ICMA), 2011 International Conference on. IEEE, 2011:1207 - 1212.

[11] Jia S, Yan J, Fan J, et al. Multimodal intelligent wheelchair control based on fuzzy algorithm[C]// International Conference on Information and Automation. 2012:582 - 587.

[12] Sindall P, Lenton J P, Malone L, et al. Effect of low-compression balls on wheelchair tennis match-play[J]. International Journal of Sports Medicine, 2014, 35(5):424-431.

[13] Pizzileo B, Li K, Irwin G W, et al. Improved Structure Optimization for Fuzzy-Neural Networks[J]. IEEE Transactions on Fuzzy Systems, 2012, 20(6):1076-1089.

[14] Hsu C F. Intelligent tracking control of a DC motor driver using self-organizing TSK-type fuzzy neural networks[J]. Nonlinear Dynamics, 2012, 67(1):587-600.

[15] Elizabeth L. Blickensderfer, Rosemarie Reynolds, Eduardo Salas, et al. Shared Expectations and Implicit Coordination in Tennis Doubles Teams[J]. Journal of Applied Sport Psychology, 2010, 22(4):486-499.

[16] Nishita Y, Tanaka S, Izumi K, et al. Research for Improving Tactics in Tennis Doubles[J]. Journal of the Institute of Image Information & Television Engineers, 2011, 65(7):983-993.

BRAND:
«SMART MECHATRON - Competitiveness,
performance and high quality through
HIGH-TECH MECHATRONIC PRODUCTS »

STUDY AND ANALYSIS ON STRATEGY OF AI SOCCER MATCH BASED ON IMPROVED MOBILE ROBOT TECHNOLOGY

Xuelin Pang, Zhengze Zhang
Harbin Engineering University, Heilongjiang, China
E-mail: zhenzezh@163.com

Abstract - Machine intelligence-human game was a classic research topic during the study of artificial intelligence (AI), which greatly advanced the development of AI. Picture processing, automatic control, communications, sensor and AI are involved in soccer robot system. First, this thesis introduced the four-layer decision structure used in the study of which elaboration on hierarchical structure was made. Second, based on influence done by soccer robot's control lag of closed-loop control system to real-time competition, improved extended Kalman filter (elf algorithm) was used to predict the position of soccer in soccer robot system and motion model of predicted soccer position was established. Finally, the efficiency of this algorithm was confirmed by simulation environment.

Keywords: Soccer robot, artificial intelligence, competition strategy, kalman filtering algorithm

1. Introduction

Robot combines different technologies includes kinematics, dynamics, machinery, material, control theory, sensor technology and artificial intelligence [1-3], which is a typical products of multidisciplinary research fields. Many studies were done by researchers with good results in information processing, decision making planning, pattern recognition, physical design, kinematic and dynamics [4], which promotes the implementation of robot in industry, agriculture and military affair. Soccer robot system is a technology concentrated artificial intelligence, which combines machine design, mechatronics, data fusion, decision-making mechanism, trajectory planning [5], as well as multi-robots' collaboration and coordination of robot intelligence technology.

AI soccer robot system should adapt to the real soccer match with soccer robots' accurate movement, agile and flexible strategy. The decision-making subsystem is the core of the artificial intelligence of soccer robot system [6], as well as an important way to verify the latest research results in the system [7]. According to those theories, this research studies general design method of decision-making system based on soccer robot system and analyzed functional and design-related difficulties in different decision layers based on the four-layer decision making structure of six-steps reasoning model which mainly focuses on the design of strategy pattern in decision-making awareness. Stimulation study on competition strategy of soccer robot was made based on improved kalman filtering algorithm.

2 Analysis and design of AI soccer robot based on mobile robot

2.1 Work mode of robot soccer system

Soccer robot match was designed based on simulation of human being's soccer match. There are many ways to establish robot system and RoBoCup small size soccer robot system was used in the study, following figure 1 shows its individual architecture:

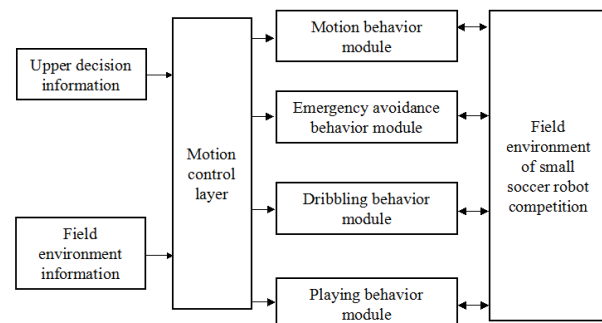


Figure 1 Individual architecture of RoBoCup small size robot system

Mobile robot is usually made of control system, communication system and sensor system [8], among them control system act as a core in the system, sensor system act as eyes of the robot to catch information. Decision-making subsystem is the brain of soccer robot system which needs to be designed with flexible competition strategy to make the robot moves agile and accurately during the match [9]. The design of decision-making system involves many different theories relative to AI and intelligent control such as path planning and intelligence algorithm, intelligent decision, multi-robot cooperation and self organization and self training. RoboCup small size soccer robot is a typical intelligent

control system, in which intelligent decision-making system in upper level involves mode selection strategy, formation, roles assigning and tactics design. This study focuses on intelligent decision-making system in upper level.

2.2 Architecture model of system decision

Relevant studies have shown that six-steps reasoning model was put forward to describe competition decision-making of RoBoCup small size soccer robot [10], thus decision-making process and knowledge base was formed.

The main design ideas of six-steps reasoning model was: first, analyze visual information based on information pre-processing; second, predicting the competition status based on analysis of vision sub-system. Third, path planning and obstacle escaping was made based on position of soccer robot on the field. Finally, commands were generated and send to robots through wireless communication system.

This study simplified six-steps reasoning model to four-layer decision making structure includes information pre-processing layer, team cooperation and coordination layer, robot path planning layer and basement moves layer. Following figure 2 shows its specific model structure:

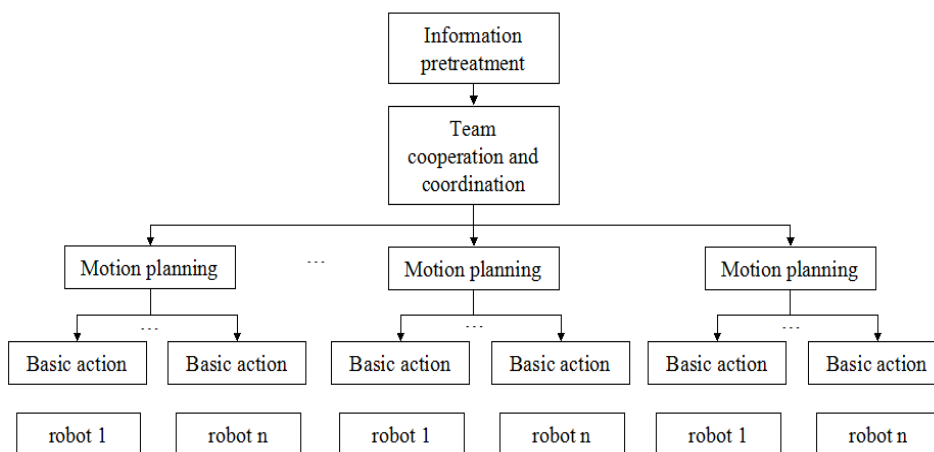


Figure 2 Specific model structure diagram of four-layer decision making

In competition system of soccer robot, decision-making system obtains actual game information only in figures, thus digital processing should be done to convert the figure into useful information. This is called information pre-processing [11, 12].

Team coordination layer judges groups' intention and transfers its intention of strategic decision to the next layer based on game situation in the field obtained by cameras. Selection of strategy pattern is needed in design of this layer, thus high performance and good strategy is premise of all decision.

The robot's path planning layer split the decision information received from the upper layer into moving target which after further improved, specific movement mode of RoBoCup small size soccer robot was formed.

The key in this layer is design of robot's action design. Input of this layer is intention of team coordination, but it can't be seen as a black box structure as there is no actual output. Action output in this layer to control robot was done by calling function in basic movement layer.

Information that path planning layer delivered to the next layer is the next moving object that should be carry out by all robots, thus target action in basic movement layer was completed. The forward, step back and turn was completed by robot's wheel speed control commands generated by path planning layer. Actually, all relevant information processed in basic movement layer is directly linked to robot's motion control and its

function, to some extends, overlapped with that of robot's vehicle-mounted controller. Therefore, pressure on onboard controller system's chip should be shared as much as possible to compensate its disadvantages when designing the basic movement layer.

2.3 Strategy mode for competition

Among the soccer robot system, it can be divided into offensive mode and defensive mode which is the simplest way of divide. Besides, there are also tackling mode and defend the area to the last mode. Mainly, following will introduce offensive mode and defensive mode.

(1) **Offense mode**

When the distance between the soccer ball and our goal line is greater than the defense line made in decision, our robot player should use the following mode shown as figure3 when they holding the ball. Position of playmaker substitute is behind the playmaker in a distance. Playmaker and playmaker substitute should exchange roles with each other immediately if the playmaker loses control of the ball and the ball is behind the playmaker. If there have no playmaker substitute, efficient will be greatly lowered because the playmaker have be follow the ball himself/herself which is a complicated process of turn-back, positioning and turn-back again.

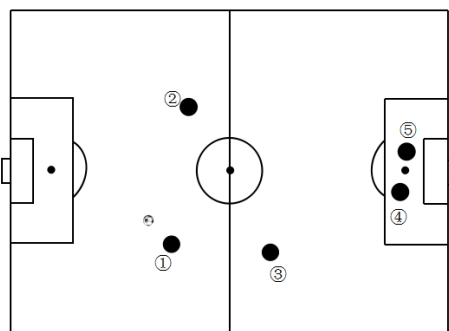


Figure 3 Offensive mode diagram (number ① is playmaker, number ② is assist playmaker, number ③ is playmaker substitute, number ④ is defensive player and number ⑤ is goalkeeper)

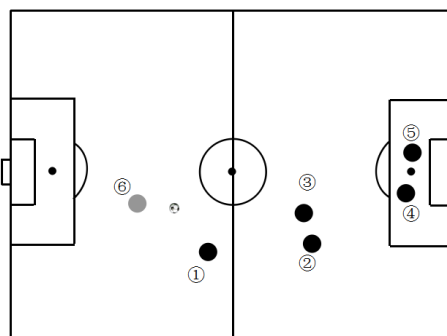


Figure 4 Defensive mode diagram (number ① is playmaker, number ② is playmaker substitute 1, number ③ is playmaker substitute 2, number ④ is defensive player, number ⑤ is goalkeeper and number ⑥ is opposing ball-holding player)

(2) Defensive mode

When the distance between the soccer ball and our goal line is greater than the defense line made in decision and the opposing robot is holding the ball which is a threaten to our goal, defensive mode need to be considered firstly. Following figure 4 shows the defensive mode.

Tactic cooperation in field should be taken into consideration after determined the overall decision mode and basic intelligent movement. However, some relatively completed tactic is hard to design, simple and classic tactic should be reached.

“Two to one” tactic. This tactic cooperation mode is frequently used in soccer match, which is used when three players (only one of them is of the opposite side) is facing each other. In this strategic mode of match, two our offensive players should reach a tacit agreement to shoot and score a goal within twice ball-passing [13]. “Two to one” tactic in robot match in shown as figure 5.

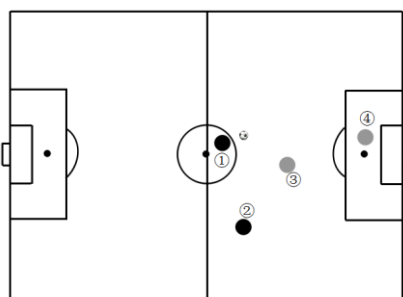


Figure 5 “Two to one” tactic (number ① and ② is our offensive player, number ③ is opposing defensive player, and number ④ is opposing goalkeeper.)

“Diversion” tactic is used when opposing player is defense loosely and no offence opportunity was found by our our player, or the soccer ball is passed but with no appropriate scoring angle [14,15]. In this case, fake attack is used to change the opposing players’ defensive, which is shown as figure 6.

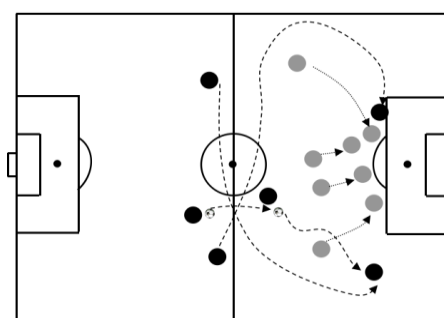


Figure 6 “Diversion” tactic

3. Technological improvement algorithm

During a soccer robot match, camera was used to get the picture of field based on which recognition and location of robot and soccer ball were done through image manipulation program. The information is then passed to strategy program to plan motion and allocate task and the generated commands would be send by wireless communication to robots to complete the assigned actions.

There are a great delay between the picture capture the complete of the commands, thus information offered by visual system cannot accurately reflect the position of soccer ball and robot at present [16-18]. In the actual match, soccer robot system is real-time which testifies that control the delay is necessary. During the match, noise jamming can be seen as a random process. Kalman filter theory is applied in a system with noise as a random process to predict information [19].

State-space mode and system observation model should be established before using the kalman filter theory. In the following discussion, denotes state estimation and denote state variance. These two random difference equations were used to modeling kalman filtering algorithm and modeling extended kalman filtering algorithm. The results were shown in following table 1.

Table 1 Modeling of kalman and extended kalman filtering algorithm

	Time update equation	Measurement update equation
Kalman filtering algorithm	$\hat{x}_k^- = A\hat{x}_{k-1} + B\hat{U}_{k-1}$ $P_k^- = AP_{k-1}A^T + Q$	$K_k = P_k^- H^T (HP_k^- H^T + R)^{-1}$ $\hat{x}_k = \hat{x}_k^- + K_k(Z_k - H\hat{x}_k^-)$ $P_k = (1 - K_k H)P_k^-$
Extended filtering algorithm	$\hat{x}_k^- = f(\hat{x}_{k-1}, u_{k-1}, 0)$ $P_k^- = A_k P_{k-1} A_k^T + W_k Q_{k-1} W_k^T$	$K_k = P_k^- H_k^T (H_k P_k^- H_k^T + V_k R_k V_k^T)^{-1}$ $\hat{x}_k = \hat{x}_k^- + K_k (Z_k - h(\hat{x}_k^-, 0))$ $P_k = (1 - K_k H_k) P_k^-$

Among them, A_k , W_k , H_k and V_k denotes Jacobian matrix of partial derivation function $f()$ to x and w and partial derivation function h to x and v . Q_k and R_k denote noise variance. A , W , H and V were update at every hour K .

For moving soccer ball on the field, there are no input commands because the soccer itself has no power. When soccer ball move freely on the field, it makes decelerated rectilinear motion because there are force of friction on the field. If the friction that impedes the motion of the soccer ball is a constant, following system model can be concluded.

$$\hat{x}_k = M\hat{x}_{k-1} + acc_k = \begin{bmatrix} 1 & 0 & \Delta t & 0 \\ 0 & 1 & 0 & \Delta t \\ 0 & 0 & 1 & 0 \\ 0 & 0 & 0 & 1 \end{bmatrix} \hat{x}_{k-1} + \begin{bmatrix} 1/2a_x \Delta t^2 \\ 1/2a_y \Delta t^2 \\ a_x \Delta t \\ a_y \Delta t \end{bmatrix}$$

$$a_x = \begin{cases} -a_{fr} \cos \psi & |v| > a_{fr} \\ -v_x / \Delta t & others \end{cases}$$

Among this model, ψ denote the direction of the soccer ball, v denote the speed of the soccer ball and a_{fr} denote the accelerated speed constant of soccer ball in horizontal direction by friction, which is acquired in the experiments. For the y -direction, there is the same control relationship.

When extended kalman filtering algorithm applies in cases that demanding high real-time, the real-time data forecasting may be influenced because of a great deal of calculations [20, 21]. Extended kalman filtering algorithm will be improved based on these disadvantages. Linear combination of nonlinear function $f()$ was used to substitute the derivative and taylor formula was used to determine the coefficient to improve the computational accuracy and speed. Following shows the improved algorithm.

$$X_{k+l} = X_k + h \sum_{m=1}^v a_m K_m$$

In this function, a_m denote undetermined factor, v denote numbers of the used function $f()$, thus as for K_m , following function can be concluded.

$$K_m = f(t_k + c_m l, X_k + l \sum_{m=1}^v b_{mj} K_j)$$

In this function, l denote account step.

Parameter was further simplified based on the improved algorithm and the characteristics of soccer robot system, which generates the following data.

$$A_k = M, P = \begin{bmatrix} \tau_{xy}^2 & 0 & 0 & 0 \\ 0 & \tau_{xy}^2 & 0 & 0 \\ 0 & 0 & \tau_{xy}^2 & 0 \\ 0 & 0 & 0 & \tau_{xy}^2 \end{bmatrix}, H = \begin{bmatrix} 1 & 0 & 0 & 0 \\ 0 & 1 & 0 & 0 \end{bmatrix}, Q_k = \begin{bmatrix} \delta_v^2 & 0 \\ 0 & \delta_v^2 \end{bmatrix}$$

$$W = \begin{bmatrix} 0 & 0 & 1 & 0 \\ 0 & 0 & 0 & 1 \end{bmatrix}, z_k = [x_{obs} \quad y_{obs}]^T, R = \begin{bmatrix} \delta_v^2 & 0 \\ 0 & \delta_v^2 \end{bmatrix}, V = \begin{bmatrix} 1 & 0 \\ 0 & 1 \end{bmatrix}$$

There are no modeling of collide between soccer robot and soccer ball. In order to fasten the response of system, state variable should show a rising trend with decreasing distance between soccer ball and robot. When the distance between one of the soccer ball and the robot is close enough (d denote distance), variate of kinestate of the ball is increasing, based on which comparison expression can be concluded as following.

$$\delta_v = \max\left(\frac{K \cdot (R + r)}{d} \delta_R, \delta_R\right)$$

In this expression, R denote radius of the robot ($R = 75mm$ in this research) and r denote radius of the ball ($r = 20mm$). Under normal conditions, $d \geq R + r$, K denote gain ($K = 10$) and $\delta_R = 100mm/s$.

4 Study on match strategy of soccer robot based on improved technological algorithm

4.1 study on match strategy

Based on above algorithm analysis and match strategy study, effectiveness of the strategy will be testified through simulation experiment of soccer robot match in simulation platform.

(1) Simulation of “two to one” match strategy

“Two to one” match strategy used in simulation experiment was shown as the following dynamic graph 7. In the graph, black dot denote our players and grey dot denote opposing players. At the first time, two our players and one opposing defensive player were facing each other, and the three of them forms a triangle.

The shooting angle of one of the offensive player was blocked. At the first ball-passing positioning, our offensive player passes the ball to the opposing offensive player.

Meanwhile, the two offensive player turn round to defense and goalkeeper makes sideways movement. In the second ball-passing positioning, the ball is passed back to our offensive player. At this moment, the two defensive players and soccer robot will have no time to adjust its position, thus our offensive player will face a free shot to unhurriedly making this shooting. According to above simulation research results, the designed match strategy is practicable.

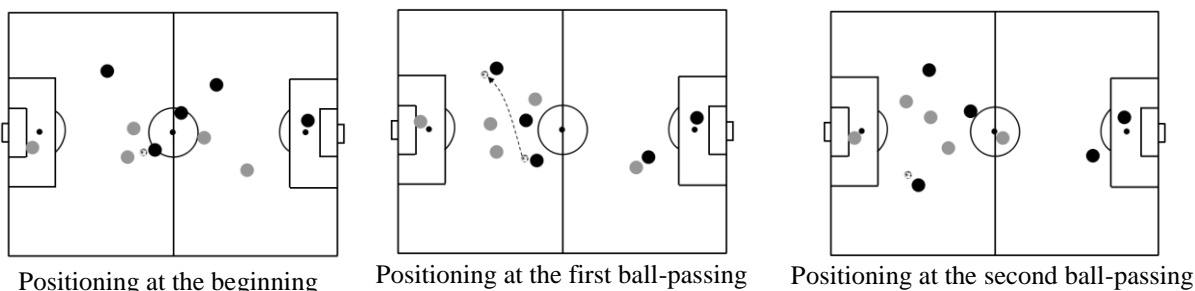


Fig. 7 Simulation result of “two to one” match strategy

(2) Simulation of “diversion” match strategy

Graph 8 shows three screenshot at three different time when apply this match strategy. At T1 (time 1), defensive of opposing robot player is relatively loose but almost blocked all direct shooting route of our players. At the T2 (Time 2), after slow dribbling of our player, opposing player is going to ring-fence because they thought our player is going to shoot.

At this moment, our players were already run to the left and right side of the field to wait for the right time to shooting. At the T3 moment, our player passes the ball very fast to our players at the right moment. Though the opposing players have reached the defensive position, our player is to offense immediately to shooting. According to this simulation results, “diversion” match strategy is practicable.

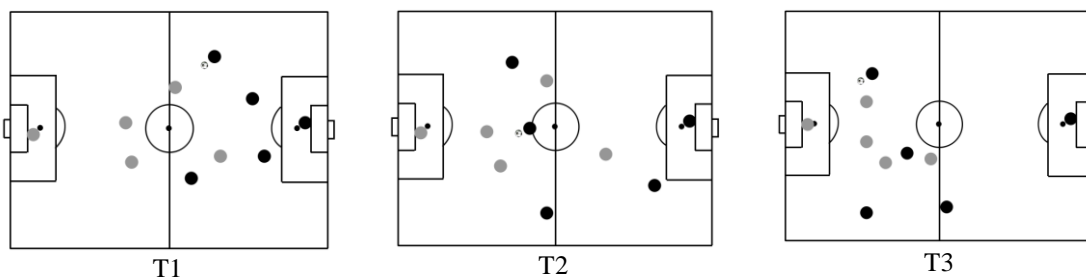


Fig. 8 Simulation results of “diversion” match strategy

4.2 Prediction of soccer robot position based on improved algorithm

Soccer robot is easy to have collides with boundaries of the court when undergo a linear motion. Collision schematic diagram was shown as following figure 9.

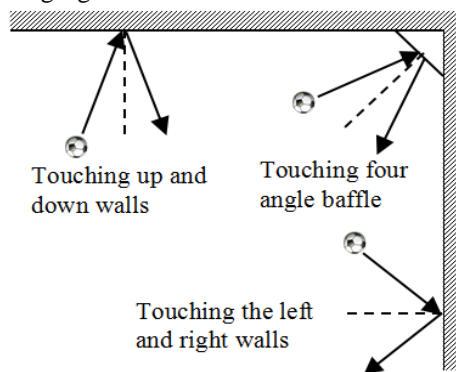


Figure 9 Collision to the wall schematic diagram of Soccer

Next, we will forecast and simulate the position of the soccer ball when it collides during the linear motion. According to actual test, accelerated speed due to the friction between robot and carpet can be set as $a_{fr} = 23cm^2$, decision-making period is $40ms$ and $\delta_{xy} = 25mm$, and velocity misalignment after collision of the robot is $\delta_R = 100mm/s$. Input above data into the established motion model and analyze the simulation modeling, the prediction curve of which is shown as following figure 10.

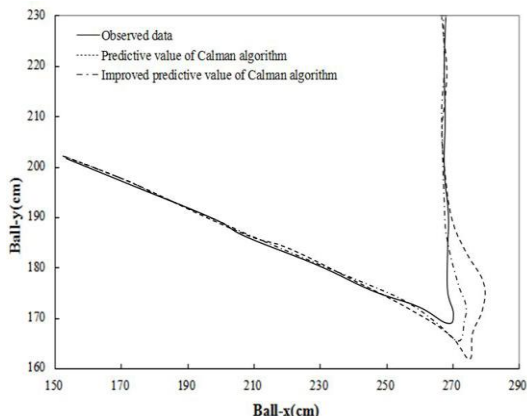


Figure 10 Comparison diagram of predicted robot's position when colliding before and after the improvement of the algorithm

The figure shows that before collision, soccer robot is undergoing the linear motion and error of the two prediction curve is relatively small because after more than 100 prediction period, those two algorithms are becoming stable. When colliding, motor direction of the soccer robot is changed and rebound at a certain angle. After a period of adjustment, forecast error decrease gradually. Though these two algorithm are convergent at the end and real-time of the system was improved, unimproved algorithm converges after another 10 period.

In the simulation environment of this study, hit rate and rate of successfully goalkeeping of soccer robot were continued to be studied based on improved algorithm, statistical result of which is shown as following table 2.

Table 2 Comparison of hit rate and rate of successfully goalkeeping of soccer robot before and after the improvement of algorithm

	Before algorithm improving	After algorithm improved
Hit rate	71.67%	88.05%
Rate of successfully goalkeeping	74.27%	91.03%

Data in the table shows that after improvement of the algorithm, accuracy of hit was improved in a certain

extent and rate of successfully goalkeeping was rising from 74.27 to 91.03, which shows a great increase.

5. Conclusion

After study of the design method of decision-making subsystem of Soccer robot, this thesis analyzes and studies the match strategy of soccer match. Improved extended kalman filtering algorithm was applied in the prediction of position of soccer ball, hit rate and rate of successfully goalkeeping. Precision of position prediction when the soccer robot colliding was greatly improved after improvement of the algorithm. Besides, prediction behavior of improved algorithm is also better than that of unimproved algorithm. Though some development in the soccer robot's decision-making subsystem was made, further improvement should be done because there are disadvantages in many aspects due to the limitation of research time.

6. Reference

[1]Nadarajah S, Sundaraj K. Vision in robot soccer: a review[J]. Artificial Intelligence Review, 2015, 44(3):1-22.
 [2]Aşık O, Akın H L. A visual compass for robot soccer[C]// Signal Processing and Communications Applications Conference. IEEE, 2014:2003-2006.
 [3]Riedmiller M, Gabel T, Hafner R, et al. Reinforcement learning for robot soccer[J]. Autonomous Robots, 2009, 27(1):55-73.
 [4]Budden D, Fenn S, Walker J, et al. A Novel Approach to Ball Detection for Humanoid Robot Soccer[C]// Advances in Artificial Intelligence. 2012:827-838.
 [5] Kitano B H. RoboCup-97: Robot Soccer World Cup 1[J]. Kybernetes, 2012, 25(5):1-4.
 [6] Playne D. Knowledge-based role allocation in robot soccer[C]// International Conference on Control, Automation, Robotics and Vision. IEEE, 2008:1616-1619.
 [7] Michel O, Bourquin Y, Baillie J C. RobotStadium: Online Humanoid Robot Soccer Simulation Competition[M]// RoboCup 2008: Robot Soccer World Cup XII. Springer Berlin Heidelberg, 2008:580-590.
 [8] Bai A, Wu F, Chen X. Towards a Principled Solution to Simulated Robot Soccer[M]// RoboCup 2012: Robot Soccer World Cup XVI. Springer Berlin Heidelberg, 2013:141-153.
 [9] Jang J, Han S, Kim H, et al. Rapid control prototyping for robot soccer[J]. Robotica, 2009, 27(7):1091-1102.
 [10] R.G Reynolds,C.-J.Chung..The use of culture algorithms to evolve multi-agent cooperation.In Proceedings of Micro-Robot World Cup Soccer Tournament,Taejon,1996,11,Page(s): 53-56.
 [11] Monajjemi V, Koochakzadeh A, Ghidary S S. grSim – RoboCup Small Size Robot Soccer Simulator[C]// Robot Soccer World Cup XV. 2012:450-460.

- [12]Jang J, Han S, Kim H, et al. Rapid control prototyping for robot soccer[J]. *Robotica*, 2009, 27(7):1091-1102.
- [13]Phillips M, Veloso M. Robust Supporting Role in Coordinated Two-Robot Soccer Attack[C]// *Robocup 2008: Robot Soccer World Cup Xii*. 2008:235-246.
- [14]Haddadin S, Laue T, Frese U, et al. Kick it with elasticity: Safety and performance in human–robot soccer[J]. *Robotics & Autonomous Systems*, 2010, 57(2009-07-31):761-775.
- [15]Chen X, Stone P, Sucar L E, et al. RoboCup 2012: Robot Soccer World Cup XVI[J]. *Robocup Robot Soccer World Cup XII*, 2013, 7500(2):637-644.
- [16] Peng S, Wen Y. Research Based on the HSV Humanoid Robot Soccer Image Processing[C]// *International Conference on Communication Systems*. 2010:52 - 55.
- [17]Guerrero P, Del Solar J R, Romero M, et al. An integrated multi-agent decision making framework for robot soccer[C]// *Robotics Symposium*. 2009:1 - 6.
- [18]Bailey D, Gupta G S. Automatic Estimation of Camera Position in Robot Soccer[C]// *Machine Vision and Image Processing Conference*, 2008. *IMVIP '08*. *International*. 2008:91-96.
- [19]Taleghani S, Aslani S, Shiry S. Robust Moving Object Detection from a Moving Video Camera Using Neural Network and Kalman Filter[C]// *Robocup 2008: Robot Soccer World Cup Xii*. 2008:638-648.
- [20]Nadarajah S, Sundaraj K. Vision in robot soccer: a review[J]. *Artificial Intelligence Review*, 2015, 44(3):1-22.
- [21]Dong P, Hui-Min L U, Yang S W, et al. Ball velocity estimation method based on RANSAC and Kalman filter for soccer robots[J]. *Journal of Computer Applications*, 2010, 30(9): 2305-2309.

BRAND:
«SMART MECHATRON - Competitiveness,
performance and high quality through
HIGH-TECH MECHATRONIC PRODUCTS »

A TOOL TOWARDS EEG SEMI-AUTONOMOUS ELECTRODE PLACEMENT

¹Pan Liu, ¹Ariston Reis, ²Paulo J.S. Gonçalves

¹Université de Montpellier, Faculté des Sciences, 2 rue ST Priest Place Eugène 34095 Montpellier, France
liupanronald@hotmail.com, alessiodosreis@hotmail.com

²Instituto Politécnico de Castelo Branco, Escola Sup. de Tecnologia, Av. Empresário, 6000-767 Cast. Branco, Portugal
 IDMEC, Instituto Superior Técnico, Universidade de Lisboa, Av. Rovisco Pais, 1049-001 Lisboa, Portugal
paulo.goncalves@ipcb.pt

Abstract - The paper proposes a novel medical device based on a 9 dof IMU to help health professionals performing more precisely the electrode placement task in EEG exams. The tool precisely tells the operator if the 10-20 electrode placement system is being correctly followed. The manual task is of major importance and time consuming, because all the electrodes must be correctly and very precisely placed in the head of the patient. The gold standard process is manual, and although several medical devices (developed to other types of medical procedures) can be applied to increase the precision of the electrode placement, they are still very expensive. The proposed medical device, based only on the sensors of a 9 dof IMU, and the processing capabilities of a microprocessor, diminish the price of the device. Moreover, the size of the apparatus is also diminished, when compared with infrared vision based systems. The developed system includes a visualization sub-system that visualises the position of the electrodes in a virtual head of the patient, using a specific tool, 3DSlicer, to receive and visualise the 3D pose of the medical device when point to the patient head. Preliminary results showed the validity of the proposed device.

Keywords: Medical Devices; Sensors; Visualization; Signal Processing

1. Introduction

Obtaining the 3D pose of an object in real environments is complex, and requires sophisticated tools if high accuracy is required, especially in medical applications [1]. The problem becomes even bigger if the object is moving in the environment, or if it can change its position a few millimetres [2]. Classic vision systems, even with the use of fiducial markers [1] have some drawbacks when tracking objects [2]. Taking this into account the paper proposes to study a 9-dof Inertial Measuring Unit (IMU) to add further sensor data, and add value to the previous work framework and enhance the previous obtained results. As such the paper proposes, a medical device to output the 3D pose an object, where the device is moving in.

As depicted in figure 1, if the medical device proposed is attached to a pointer, that points to the head it outputs the 3D pose of all the points that are present, only based in the IMU data. As depicted, the application in this paper is EEG electrode placement.

The paper presents the state-of-the-art on manual electrode placement for EEG in section 2. Section 3, presents the developed medical, both the electronics components, sensors and microprocessor, along with the mechanical drawings. The signal processing needed to obtain the pose of the medical device, to define the electrode placement, is presented in Section 4. In section 5 are presented results with the tool developed along with the visualization results in 3DSlicer. Finally, some conclusions are drawn in section 6.

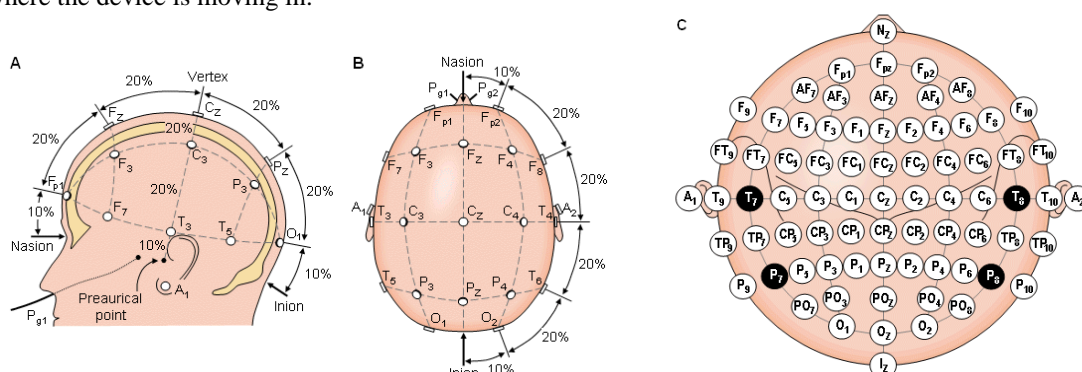


Figure 1: Electrodes Position in the Scalp [3]

2. Electrodes position in EEG exam

The 10–20 system [3] or International 10–20 system is an internationally recognized method to describe and apply the location of scalp electrodes in the context of an EEG test or experiment. This method was developed to ensure standardized reproducibility so that a subject's studies could be compared over time and subjects could be compared to each other. This system is based on the relationship between the location of an electrode and the underlying area of cerebral cortex. The "10" and "20" refer to the fact that the actual distances between adjacent electrodes are either 10% or 20% of the total front–back or right–left distance of the skull.

Each site has a letter to identify the lobe and a number to identify the hemisphere location. The letters F, T, C, P and O stand for frontal, temporal, central, parietal, and occipital lobes, respectively. (Note that there exists no central lobe; the "C" letter is used only for identification purposes.) Even numbers (2, 4, 6,8) refer to electrode positions on the right hemisphere, whereas odd numbers (1, 3, 5,7) refer to those on the left hemisphere. A "z" (zero) refers to an electrode placed on the midline. In addition to these combinations, the letter codes A, Pg and Fp identify the earlobes, nasopharyngeal and frontal polar sites respectively.

Two anatomical landmarks are used for the essential positioning of the EEG electrodes: first, the nasion which is the distinctly depressed area between the eyes, just above the bridge of the nose; second, the inion, which is the lowest point of the skull from the back of the head and is normally indicated by a prominent bump.

In the semi-autonomous procedure proposed in the paper the operator must identify the nasion and the inion, precisely. Additionally, points A1 and A2, in the ear of the patient are also fundamental to define the four lower points of the semi-sphere of the approximate skull of the patient. These four points are the first land marks from where the remain points will be obtained, using the 10-20 system.

3. Medical Device

The medical device is comprised by electronic components and mechanical components to encapsulate the prior. This section is divided in two sub-sections: first the electronic components are depicted, after the designed mechanical components are presented.

Electronic Components

The electronic components are depicted in figure 2:

- a 9DOF Razor IMU that incorporates three sensors: an ITG-3200 (MEMS triple-axis gyro), an ADXL345 (triple-axis accelerometer), and an HMC5883L (triple-axis magnetometer) (horizontal board);
- an on-board ATmega328 (horizontal board);
- a basic breakout board for the FTDI FT232RL USB to serial IC (vertical board, to interface with the signal processing unit defined in the next section);



Figure 2: Electronic components of the medical device

The on-board ATmega328 have the following capabilities that were programmed:

- to output the orientation angles of the device, according to the AHRS algorithm proposed in [4];
- the acceleration raw values from the accelerometer;
- the angular velocity raw values from gyroscope;

Design

In figures 3 and 4 are depicted the enclosures of the electronic components present in figure 2, along with the pointer to the points of the EEG landmarks in figure 1.



Figure 3: Medical Device Pointer with enclosure.



Figure 4: Medical Device Pointer without enclosure.

4. Signal Processing

In this section are presented the signal processing algorithms used to process the signal captured from the sensors. To a better understanding of the process, the output signals will be presented.

Figure 5, presents the raw data captured from the gyroscope and the accelerometer, i.e., the angular velocity of the device and its acceleration. It can be seen that the capture starts at second 4 and lasts 2 seconds. The device first moves, stops and moves again, as depicted in the acceleration and velocities graphs. All

the presented signals are captured with a sample time of 0.004[seconds] and all filtered first with a high and after with a low pass Butterworth filter, with DC gain $G_0=1$

and $n=2$, with appropriate cut-off frequencies. If the acceleration is below a given threshold the medical device is not moving, i.e., is stationary.

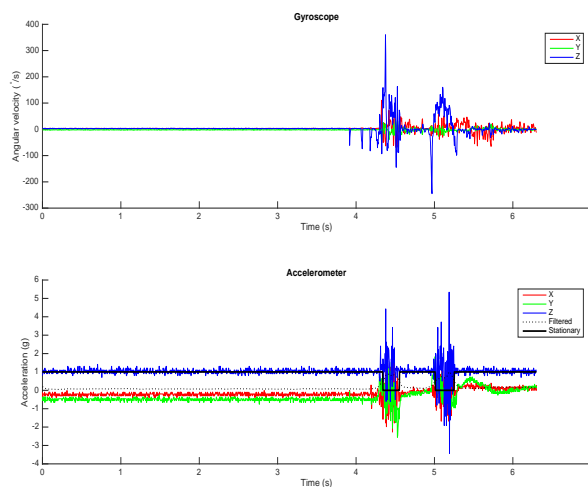


Figure 5: Raw Sensor Data from the Sensor. Angular Velocity and Acceleration.

The rotation of the medical device, is obtained according with the AHRS algorithm proposed in [4]. The outputs quaternions are used directly to obtain the Euler angles of the pose of the device.

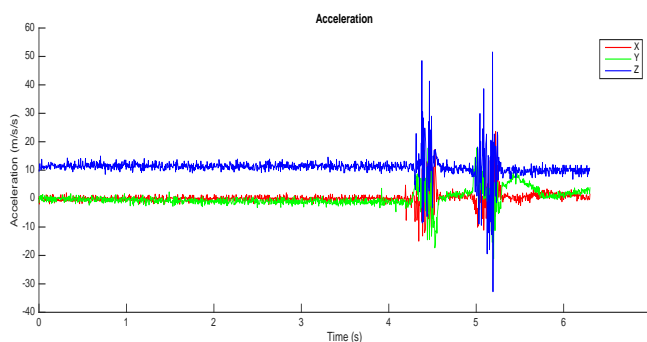


Figure 6: Linear Acceleration

The next step of the processing part is to obtain the linear velocity from the linear acceleration measured, depicted in figure 6. This is performed by first order numerical integration of the acceleration measured, starting from a stop position. The result, depicted in figure 6, is calculated taking into account a numerical

compensation for the velocity drift due to the numerical calculus. When the sensor is not stationary the velocity drift is incremented to compensate the numerical error. When the medical device is steady the velocity drift is set to zero and the process starts again.

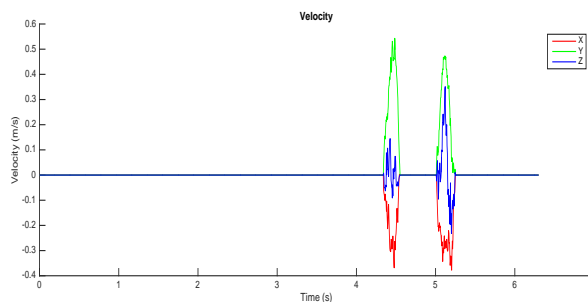


Figure 7: Linear Velocity

Finally, to obtain the pose of the device a final integration is performed, using the same technique from the prious integration, starting from a stop position.

The results is depicted in figure 8, where is presented the X, Y, Z path of the medical device coordinates.

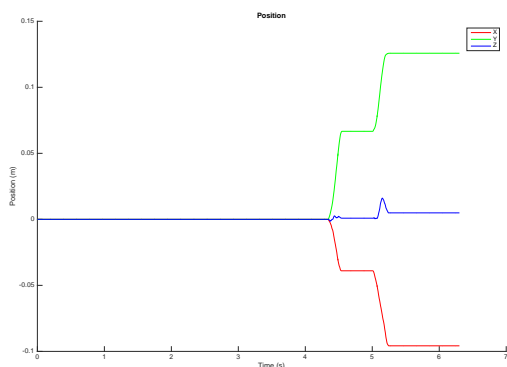


Figure 8: Position of the Medical Device.

5. Results and Discussion

In this section are presented the final results of the application of the medical device to obtain the 3D pose and to follow a path in a real world scenario.

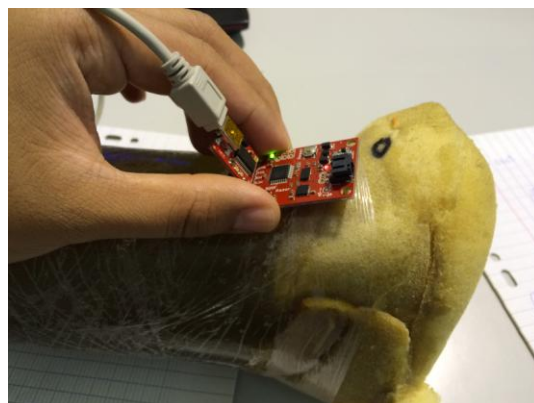


Figure 9: Real Scenario for Capture in Bone Phantom

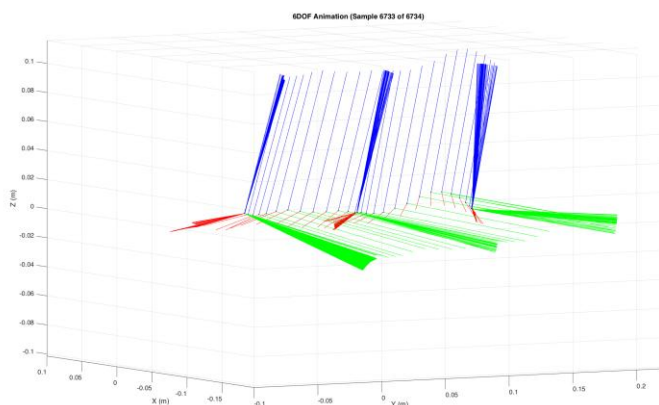


Figure 10: Captured Path along a Bone Phantom

The final result, depicted in figure 10, of the experiment shows the 3D path captured along the bone, i.e., at each capture point a reference frame is depicted, clearly showing the rotation angles differences between captures. It is also verified that the trajectory is smooth. At the initial point of the path, left side of figure 10, a large concentration of frames are observed, due to noise.

Visualization

For Visualization of the results obtained from the signal processing unit, running in Matlab, 3D Slicer [5] was used to receive data and to visualize it in the head of a human. 3D Slicer (Slicer) is a free and open source software package for image analysis and scientific visualization.

In figure 11 is depicted the visualization of the head of a human with the pointer receiving input directly from matlab from the MatlabOpenIGTLinkInterface of 3D Slicer.

6. Conclusions

The paper proposed a medical device capable to deliver the 3D pose of a pointer. The medical device helps health professionals performing more precisely the electrode placement task in EEG exams. The tool precisely tells the operator if the 10-20 electrode placement system is being correctly followed.

The proposed medical device, based only on the sensors of a 9 dof IMU, and the processing capabilities of a microprocessor, diminish the price of state-of-the-art devices. Moreover, the size of the apparatus is also diminished, when compared with infrared vision based systems.

The developed system includes a visualization subsystem that visualises the position of the electrodes in a virtual head of the patient, using a specific tool, 3DSlicer, to receive and visualise the 3D pose of the medical device when point to the patient head. Preliminary results showed the validity of the proposed device to track trajectories in 3D space.

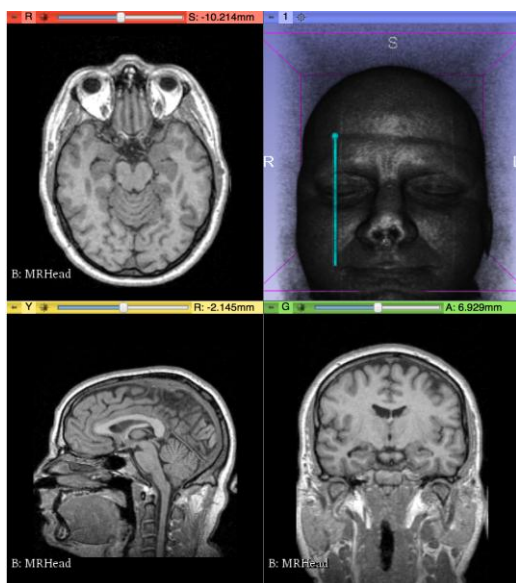


Figure 11: 3D Slicer Human Head Rendering with Pointer visualization

Acknowledgements

This work was partly supported by Instituto Politécnico de Castelo Branco and by FCT, through IDMEC, under LAETA, project UID/EMS/50022/2013.

7. References

- [1] P.J.S. Gonçalves, P.M.B. Torres, F. Santos, R. Antonio, N. Catarino, J.M.M. Martins, 2015, A Vision System for Robotic Ultrasound Guided Orthopaedic Surgery. *Journal of Intelligent & Robotic Systems* 77 (2) pp. 327-339.
- [2] P. Torres, P. J. S. Gonçalves, J.M.M. Martins, 2015, Robotic motion compensation for bone movement, using ultrasound images. *Industrial Robot: An International Journal* 42 (5) pp. 466–474.
- [3] Sharbrough F, Chatrian G-E, Lesser RP, Lüders H, Nuwer M, Picton TW, 1991, American Electroencephalographic Society Guidelines for Standard Electrode Position Nomenclature. *J. Clin. Neurophysiol* 8: 200-2.
- [4] D. Gebre-Egziabher, R. C. Hayward and J. D. Powell, 1998, A low-cost GPS/inertial attitude heading reference system (AHRS) for general aviation applications, *Position Location and Navigation Symposium, IEEE 1998, Palm Springs, CA*, pp. 518-525
- [5] <https://www.slicer.org/>, visited at 30th june 2016.

BRAND:
«SMART MECHATRON - Competitiveness,
performance and high quality through
HIGH-TECH MECHATRONIC PRODUCTS »

KNOWLEDGE BASED ROBOTIC SYSTEM, TOWARDS ONTOLOGY DRIVEN PICK AND PLACE TASKS

¹Rodolfo A. A. Farinha, ²Paulo J.S. Gonçalves

Instituto Politécnico de Castelo Branco, Escola Sup. de Tecnologia, Av. Empresário, 6000-767 Cast. Branco, Portugal
rodolfo.alves.farinha@gmail.com

Instituto Politécnico de Castelo Branco, Escola Sup. de Tecnologia, Av. Empresário, 6000-767 Cast. Branco, Portugal
IDMEC, Instituto Superior Técnico, Universidade de Lisboa, Av. Rovisco Pais, 1049-001 Lisboa, Portugal
paulo.goncalves@ipcb.pt

Abstract - The paper proposes an ontology driven framework to define a machine used for automatic pick and place robotic tasks. The developed framework was successfully simulated and validated in an automotive manufacturing environment where seals have to be placed in a cable plug terminal. The developed framework builds on the IEEE ORA standard, which defines the Core ontologies for Robotics and Automation (CORAs). Specific contributions were developed to extend the previous ontologies to the presented application case, e.g., for interaction with environment and robot movement. Moreover, a database of seal patterns is implemented in the cloud to be fetched, as needed, by the robot. Based on the tasks/processes obtained from the developed framework, the robot will seal a batch of cable terminals, automatically. The system was implemented in a simulated scenario, in V-REP, using a 3 dof, Scara Robot. Using the knowledge base, specially defined for the developed framework, based in CORAs, reasoning actions can be performed to obtain valuable data for production and maintenance at the factory level.

Keywords: Industrial Robotics; Automation; Knowledge Representation; Ontologies; Simulation.

1. Introduction

Robotic manufacturing systems are widely used in industry. However, in specific industries, e.g., automotive cable industry the robot has not been deployed with great success, as of other branches of automotive industry, e.g., car assembly. The main reason for this issue is the complexity of existing tasks and its large number. For automotive plug sealing, of the produced car cables, robot cells do exist, but its programming is not adequate to an agile manufacturing system. In fact, the work cell program must be developed by scratch for each new plug of the various cables produced in factories. As such, hundreds of sealing patterns can exist in the factory database.

The paper proposes an ontology driven framework to define the tasks needed for the robotic cell to operate for a given seal pattern. From the robot, environment, and process knowledge, the knowledge model, i.e., the ontology is obtained. Part of the knowledge model is stored in the cloud, making the system modular and more flexible. Moreover, special tools were developed to communicate from the cloud and the machine. The latter is built from the core ontologies and also from the manual process that is currently in place at the factory.

The paper presents the application scenario in section 2, where the complete process to be automated is presented. Section 3, presents a simulation scenario of the system where a 3dof scara robot is used. The Application of the Core Ontology for Robotics and

Automation is presented in Section 4, and the following section, 5, depicts the ontology application domain where the main tasks were defined. In section 6 are presented results on reasoning with the ontologies and are also discussed. Finally, some conclusions are drawn in section 7.

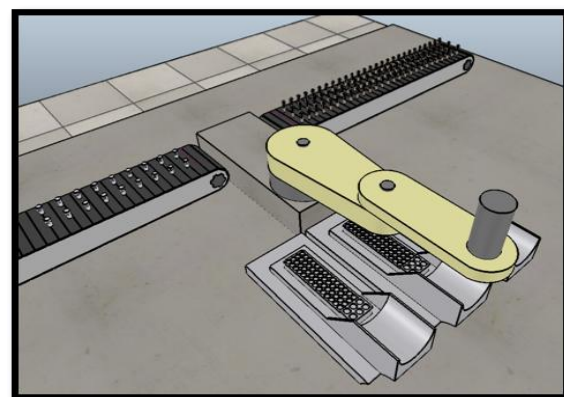


Figure 1: Simulation Scenario. Two conveyors for each type of seal. One 3 dof robot. Three cable terminals.

2. Application Scenario

The application scenario, depicted in figure 1, consist on the placement of two different types of seals in a plug terminal with 56 holes, isolating those who do not receive electric cables. One type of seal is placed

manually and the second is placed automatically by the robot.

The operator, before starting the process must verify the machine electricity and compressed air power supplies. Also, must be checked if the security doors are closed and the emergency buttons are disabled.

First, must have to be set the power of the machine. After the power being set, "Homing" must be performed, that enables the localization (X , Y) of the "Gripper" in relation to a reference point (X_0 , Y_0) in the robot workspace.

In the next step, the operator starts by creating or selecting the seal pattern to be produced. After selecting the seal pattern, press the button "Start" and triggers the three-phase motor that will rotate the base of the plug terminals in the robot workspace. The motor of the basis stops when its inductive sensor provides a signal to the robot controller.

A vibrating reservoir carries the seals, through vibratory waves, to a feeding line, which in turn, also via similar waves, forwards these to the feed zone of the "Gripper" machine, triggering a fiber optic sensor that indicates to the robot controller that the seal is in position to be picked by the robot.

This feed zone consists of two cylinders. A cylinder (X) preparing the seal for placement in the "Gripper" and a second one (Z) laying the seal within the "Gripper". This is fixed due to the frictional force caused by the double cylinder (Z) which is the "Gripper". The (Z) cylinder is the vertical motion of the gripper depicted in figure 1.

After the seal is within the gripper, the robot, will move the "Gripper" in the (XY) plane to the desired position and place the seal in the cable plug terminal.

After positioning the "Gripper", the cylinder containing the seal is activated, approaching the hole (where the seal will be placed). Subsequently, the other cylinder is actuated a first time to put the seal into the hole and a second time to ensure the correct placement of the seal in the hole. Finally, the "Gripper", return to the feed position.

When completed the seal pattern for a plug terminal, the robot controller expects a new button press "Start" by the operator, for continuing the process.

The next section presents a simulation of the above described process, where the feeding zone and the vibratory reservoir are simulated by two conveyors.

3. Simulation Scenario

To simulate the developed machine a simulation scenario was built using a physical robotic simulation environment (V-REP) and Matlab. The needed software modules were developed, that included the communication layers, between Matlab and V-REP, and also between a MySQL database, to store the knowledge to the system, related to the sealing patterns.

As such the full system comprises, as depicted in figure 2:

- a 3 dof scara robot, two conveyors, two types of seals and the plug terminals, simulated in **V-REP**;

- the robot controller, calibration and GUI interface, simulated in **Matlab**;
 - the **MySQL** database;
- that will be depicted in the next subsections.

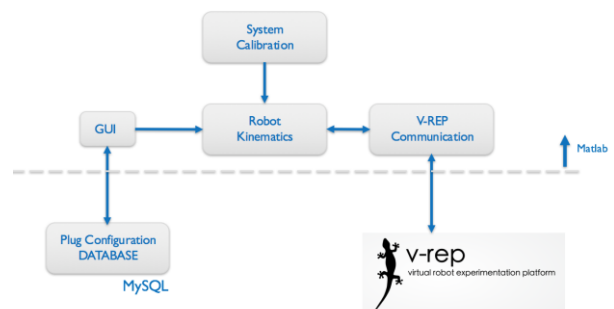


Figure 2: Simulation Components overview.

V-REP Simulation Components

The V-REP [1] simulation consists of the following parts:

- a 3 DOF robot, figure 1, with two rotational joints (with planar motion) and one prismatic joint with vertical motion, to pick and place the seals (figure 3, right);
- two conveyors, depicted in figure 1, to transport the two types of seals;
- three cable terminal plugs, as depicted in figure 3 left, where the seals are to be placed;

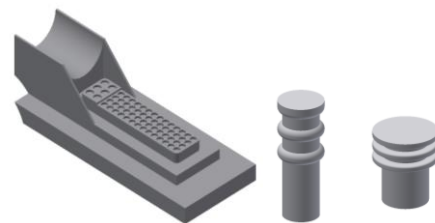


Figure 3: Cable plug terminal for seal placement (left). Seals of different size (right). (3D CAD model).

The Matlab Environment Components

The Matlab environment components consists of the following parts:

- the robot controller;
- the Matlab communication to V-REP;
- a System Calibration based on a vision module, not presented in this paper.

The MySQL Database Components

The MySQL Database components consists of the following parts, depicted in figure 4:

- a software module in Matlab to connect to the Robot controller;
- the 'id' and 'code' for each seal pattern, e.g., the 'id' is the name of the seal pattern and the '1' and '0' states if there is to be, or not, a seal a given plug terminal position;
- the GUI interface, figure 5, that comprises an interface, from the Matlab environment to the MySQL database, communicating in both directions;

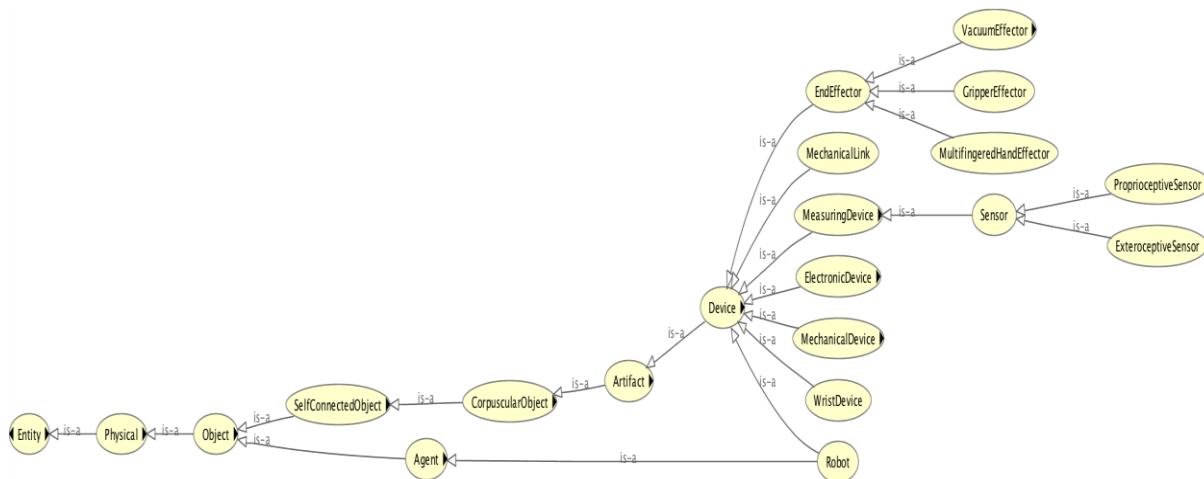


Figure 6: Sub-part of Core Ontology for Robotics and Automation.

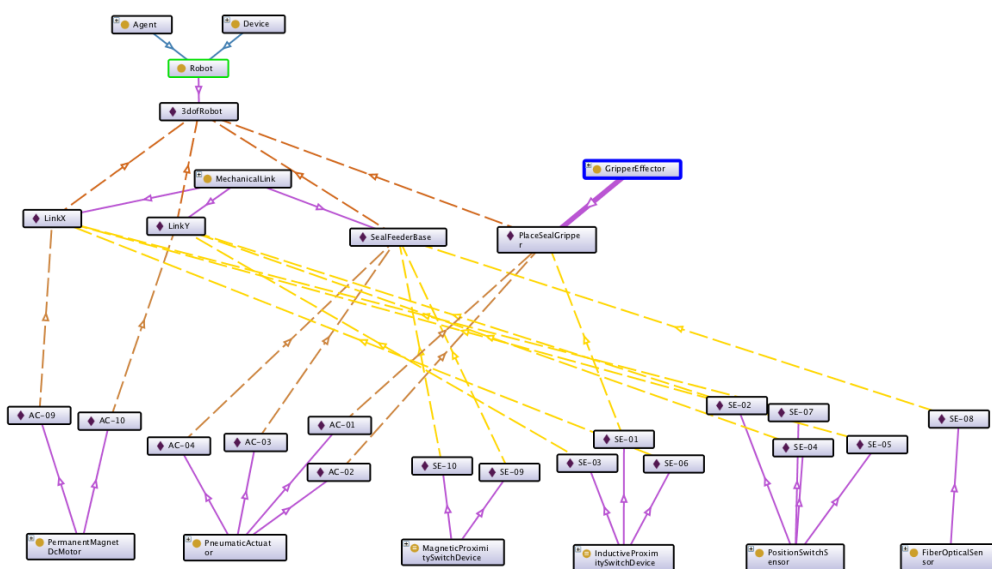


Figure 9: Components knowledge model based on the ontology

The main sensors and actuators are present in the knowledge model depicted in figure 9, where all the instances are present. Moreover, several information can be inferred from the diagram. The actuator ‘AC-09’ is attached to ‘LinkX’ that is also attached to the ‘3dofRobot’, being the latter an instance of the class ‘Robot’. Similar inferences can be drawn for the sensor, e.g., ‘SE-08’ is attached to the ‘SealFeederBase’.

5. Application Domain Ontology

In this section are presented the tasks that the robot must perform to achieve the goals defined in section 2, i.e., to place the seals in the cable plug terminal.

Figure 9, presents the main sub-processes within the main class defined in CORA ‘RobotMotion’. The tasks are high level defined in the ontology and have a low level implementation in the robot controller.

The Tasks defined are directly related to the actuators. The tasks ‘ReleaseSeal’ and ‘CaptureSeal’ use the pneumatic actuator. The task ‘RotateBase120’ use a 3 phase electric motor to rotate the base where the cable plug terminals are to be located, for seal insertion. All the other tasks use the two DC motors of the robot joints to move the robot in the XY plane.

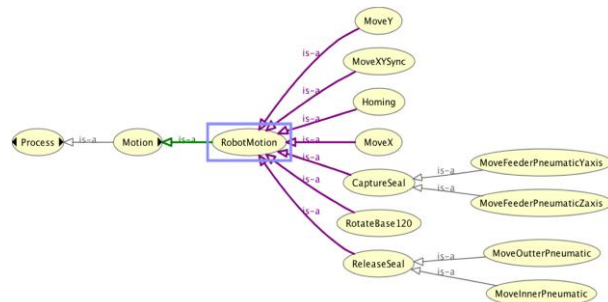


Figure 9: Snapshot of the application domain ontology, related to the High Level Robot Motion Processes.

6. Results and Discussion

In this section are presented the results of using the knowledge model defined in the ontology. The main results were obtained by reasoning with the ontology, and by using the GUI interface to program the robot controller in the simulation scenario, and also to interface with the cloud with the sealing patterns.

Reasoning

Using the ontology and description logic queries is possible to is a straight forward way to obtain, to obtain the following information:

- Sensors on the end-effector of the robot, as depicted in figure 10.
- Actuators on the end-effector of the robot, as depicted in figure 11.
- Devices that are needed in a defined task, as depicted in figure 12.
- A clear explanation for some of the information given on a query, as depicted in figure 13, for the query depicted in figure 12.

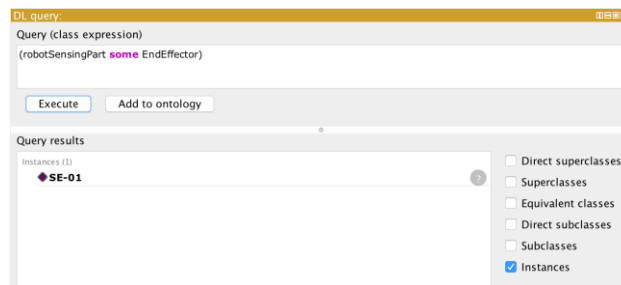


Figure 10: Query about sensors on the end effector.

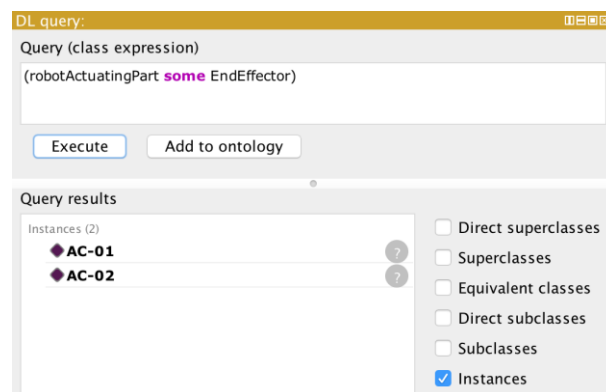


Figure 11: Query about actuators on the end effector.

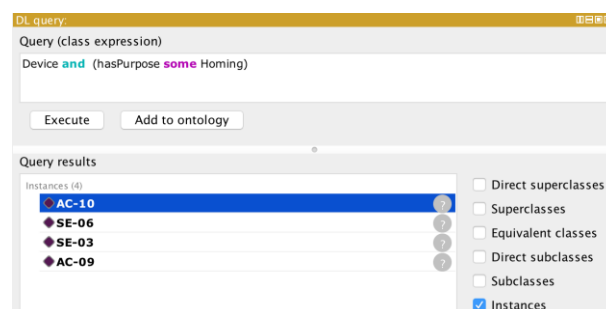


Figure 12: Query about devices involved in a task.



Figure 13: Explanation why AC-10 is involved in a task

In figure 14 is presented the robot in operation, using V-REP, where the sealing pattern defined in figure 15, was stored in the cloud.

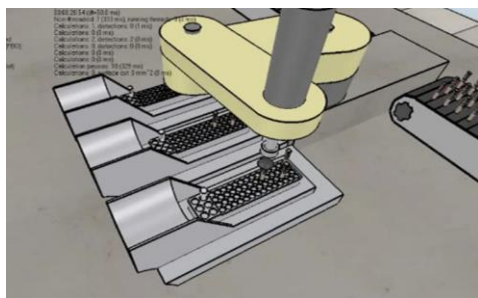


Figure 14: Sealing Machine in Operation, V-Rep Simulation.

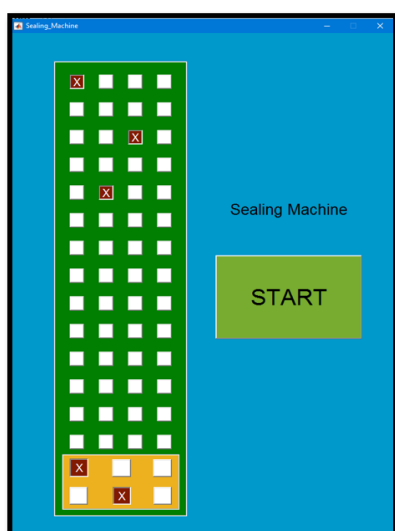


Figure 15: Sealing Machine in Operation, Matlab GUI interface.

7. Conclusions

The paper proposed an ontology driven framework to define a machine used for automatic pick and place robotic tasks. The developed framework was successfully simulated and validated in an automotive manufacturing environment where seal have to be placed in a cable plug terminal.

The developed framework was built based on the IEEE ORA standard. Specific contributions were developed to extend the previous ontologies to the presented application case, e.g., for interaction with environment and robot movement. Moreover, a database of seal patterns is implemented in the cloud to be fetched, as needed, by the robot. Based on the tasks/processes obtained from the developed framework, the robot will seal a batch of cable terminals, automatically.

The system was validated by the implementation in a simulated scenario, in V-REP, using a 3 dof, Scara Robot. The knowledge base, specially defined for the developed framework, based in CORA, was also validated by performing first order logic reasoning actions to obtain valuable data for production and maintenance at the factory level, namely information about sensors, actuators, and its purpose in the tasks defined in the ontology.

Acknowledgements

This work was partly supported by Instituto Politécnico de Castelo Branco and by FCT, through IDMEC, under LAETA, project UID/EMS/50022/2013.

8. References

- [1] V-REP, Virtual Robot Experimentation Platform, <http://www.coppeliarobotics.com/>, visited 28th june 2016.
- [2] Edson Prestes, Joel Luis Carbonera, Sandro Rama Fiorini, Vitor A. M. Jorge, Mara Abel, Raj Madhavan, Angela Locoro, Paulo Goncalves, Marcos E. Barreto, Maki Habib, Abdelghani Chibani, Sébastien Gérard, Yacine Amirat, Craig Schlenoff, 2013, "Towards a core ontology for robotics and automation", Robotics and Autonomous Systems, 61(11), pp. 1193-1204.
- [3] IEEE 1872-2015, IEEE Standard Ontologies for Robotics and Automation, STANDARD by IEEE, 04/10/2015.

EQUIPMENT FOR AUTOMATIC POSITION DETECTION OF NODAL POINT OF AN OPTICAL SYSTEM

Iulian Ilie, Gheorghe Gheorghe

The National Institute of Research and Development in Mechatronics and Measurement Technique, Bucharest, Romania, Sos. Pantelimon, Nr. 6-8 Sector 2, Bucuresti

Abstract - The paper aims to obtain automate positioning of nodal points through an equipment that basically consists of a microscope objective with 6.3 that project the image given by objective in electronic component called quadrant.

Keywords: nodal point, CO2 emissions, microscope, smart measuring.

1. Introduction

Optical increases determine dimensionless ratio of linear dimensions of the lens / objective and image. If to a linear element ds from object space corresponds to a linear element ds' in space image, then report ds' / ds is called linear magnification / zoom. In view of the projections ds and ds' elements on the coordinate axes (Figure 1) and the equation (1):

$$\begin{aligned} z' &= \bar{f} \times f' / z \\ y' &= \bar{f} \times y / z \\ x' &= \bar{f} \times x / z \end{aligned} \quad (1)$$

can be defined:

- axial increasing

$$\alpha = dz' / dz = -\bar{f} \times f' / z^2 = -z'^2 / \bar{f} \times f' \quad (2)$$

- transversal increasing

$$\beta' = dy' / dy = y' / y = \bar{f} / z = z' / f' \quad (3)$$

- angular increasing

$$\gamma = \text{tg} \sigma' / \text{tg} \sigma = -z / f' = \bar{f} / z' \quad (4)$$

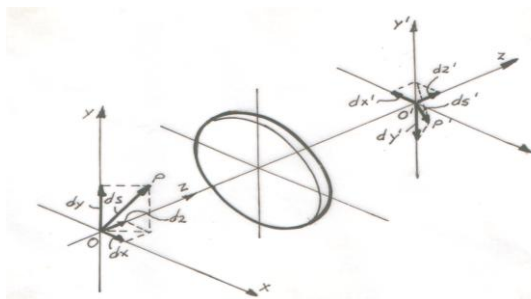


Figure 1

The cardinal points are points that optical magnification / zoom take unit values:

$$\alpha = \pm 1 \quad ; \quad \beta' = \pm 1 \quad ; \quad \gamma = \pm 1$$

Cardinal planes are planes perpendicular to the optical axis passing through the points mentioned. We have practical interest only cardinal and planes points that correspond to values β' and γ . From:

$\beta' = y' / y = +1 = \bar{f} / z = z' / f'$ result $z = \bar{f}$ and $z' = f'$ where z and z' are distances of principal object plane and image from image focal planes. At the intersection of the main optical planes with optical axis result points H (object) and H'(image) (Figure 2 and 3).

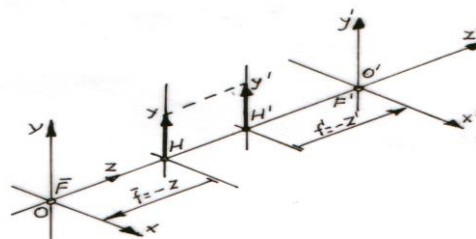


Figure 2

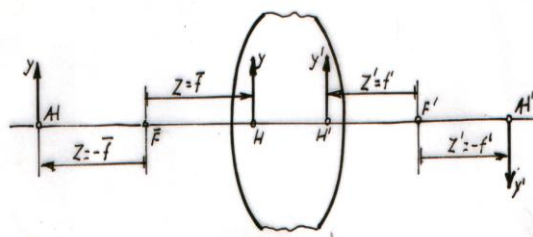


Figure 3

It is assumed that the optical system of Figure 4 turns around of the nodal point $N' \cong H'$ until the incident beam R, which make the angle σ with optical axis becomes parallel to the optical axis, that means the point O' in the image focal plane become the point O' on the optical axis.

By this rotation, the focus F' is moving in (F') , and between initial position F' and point (O') appear a position error $\Delta f'$.

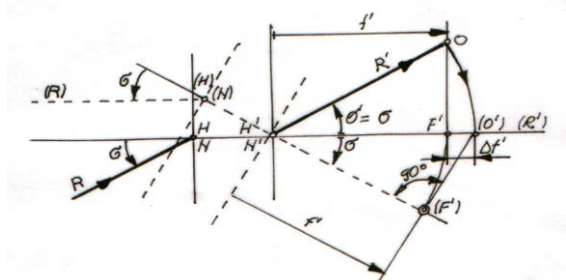


Figure 4

From the triangle $N'(F')(O')$ result:

$$\Delta f' = f' / \cos \sigma - f' = f'(1 / \cos \sigma - 1) \quad (5)$$

2. Equipment presentation and technical details

The equipment is designed for laboratory use and aims to obtain automate positioning of nodal points through an intelligent equipment. The quadrant provides a combination of signals that enter into a scheme of automation.

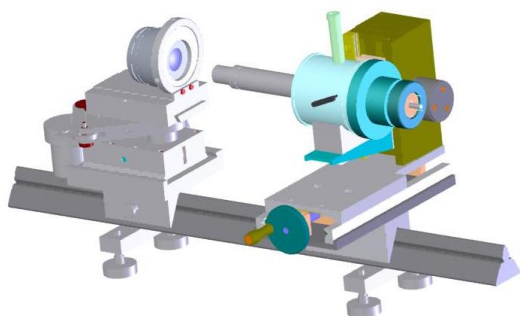


Figure 5: 3D view of the equipment

The equipment requires a 3 distinct translations axis X, Y, and Z.

Z axis is required to bring in coincidence the image plane of photographic objective with object plane of the microscope objective of the projected equipment.

Movements on X and Y axis are required to align the optical axes of the two systems. The working step is done by watching through ocular of the equipment which comes into operation by switching / reversing a mirror.

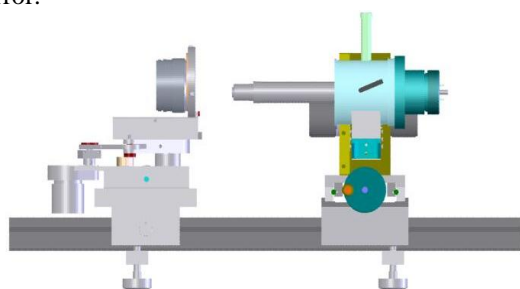


Figure 6: Lateral view of the equipment

Light spot image of a collimator lens captured by photographic objective through a microscope objective goes to the quadrant.

Due to the oscillatory movement gave to photographic objective from equipment mechanism, the image obtained is moved left and right around a vertical axis. This movement is captured by equipment microscope and placed on the quadrant.

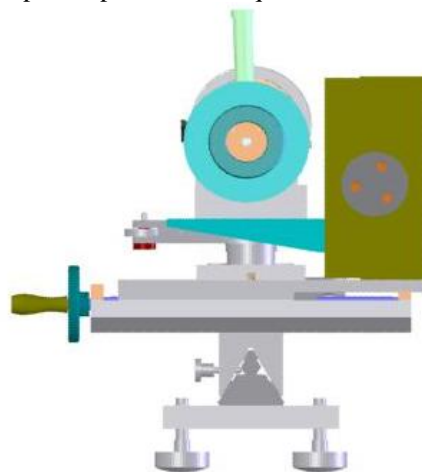


Figure 7: Frontal view of the equipment

This image excites the photovoltaic elements of quadrant at a time, the two excitations being in reverse phase.

Initially mechanism is in one extreme position, and software that control the engine begins his movement in the opposite direction. At a time when the oscillation axis of objective passing through the nodal point of the lens, the light beam is on the optical axis of the system at the same time. At that time, the two components of photovoltaic quadrant are equally excited and the motor stops.

The components used developed for equipment are mechanical types, some can be bought (objective, eyepiece, mirror dump), others where been designed and built.

Movement after X axis is done via a screw with 1mm step that moves the mechanical stage - which is placed on two cylindrical steel bars. Answering to the mechanical clearance and avoid the return stroke when changing the direction, is using an assembly of two nuts and having a spring expansion between them

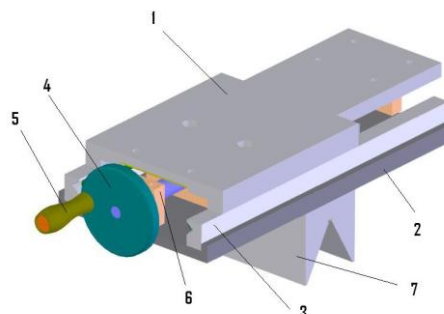


Figure 8: Mouvement after X axis: 1- Stage after X direction; 2-Support table / stage; 3- Guide element; 4- Handle; 5- Drive handle; 6- Bearing support; 7- Rider

Movement after Y axis is also performed / guided on ball bearings, with the help of a rack controlled by a worm gear whose worm is activated by the buttons of ax.

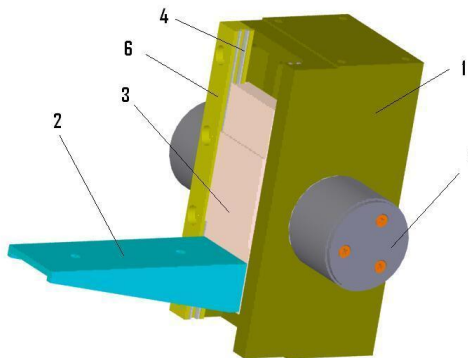


Figure 9: Mouvement after Y axis: 1- Stage body Y; 2- Support platform; 3- Guide element after Y; 4- Worm gear; 5- Drive handle; 6- Guided element after Y axis

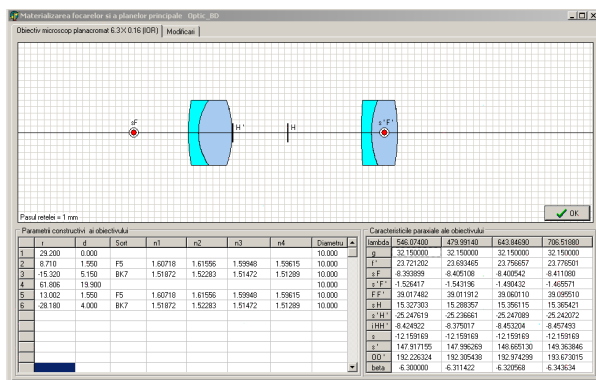


Figure 10: Constructive data and characteristics paraxially

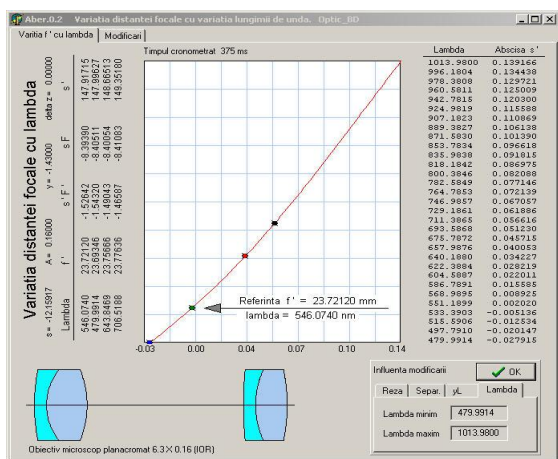


Figure 11: The variation of the focal length to the wavelength

3. Conclusions:

The equipment is designed for laboratory use and aims to obtain automate positioning of nodal points through an intelligent equipment. The equipment was improved constantly and is free to use by student and researchers.

4. References

[1] Prof.PhD Eng. Gheorghe I. GHEORGHE, PhD Student Eng. Ilie Iulian "MECHATRONICS, INTEGRONICS & ADAPTRONICS, excellence in the field of intelligent specialization" - Romanian Review Precision Mechanics, Optics & Mecatronics no. 47/ 2015;

[2] Anghel C-tin, Gheorghe Ion Gheorghe, "Research on Tactile Sensors Interface - Review of Theoretical and Practical Approach", Applied Mechanics and Materials, Vol. 772, pp. 299-304, Jul. 2015; ISI, <http://www.scientific.net/AMM/details> <http://www.scientific.net/AMM.772.299>

[3] Sorea Sorin, Dumitru Sergiu "Electronics control and interface architectures for mems sensors and actuators" - Romanian Review Precision Mechanics, Optics & Mecatronics no. 48 / 2015;

[4] G. Gheorghe, L. Badita, A. Cirstoiu, S. Istriteanu, V. Despa and S. Ganatsios, "Mechatronics Galaxy", a New Concept for Developing Education in Engineering," Applied Mechanics and Materials, vol. 371, pp. 754-758, 2013

[5] Badita Liliana Laura; Gheorghe Gheorghe, „Physical characterization of nanostructured thin films used to improve hip prostheses”, Journal of Optoelectronics and Advanced Materials, Volume: 16, Issue: 7-8, Pages: 945-950 Published: JUL-AUG 2014, ISI, http://uefiscdi.gov.ro/userfiles/file/CENAPOSS/rev_ro_m_isi_9%20oct_2015_factori.pdf <http://joam.inoe.ro/index.php?option=magazine&op=view&id=3533&catid=85file:///C:/Users/client/Desktop/29Badita.pdf>

[6] Rotar Dan, Culea George, Andrioaia Dragos; „Soft core microprocessor for mechatronics systems”, Romanian Review Precision Mechanics, Optics & Mecatronics no. 47 / 2015;

[7] Gerrard, A Burch J.M, [Introduction to matrix methods in optics] A Wiley Interscience Publications, John Wiley & Sons .London New York Sydney (1978);

[8] ISO 10110 -12 Optics and photonics — Preparation of drawings for optical elements and systems.

ISSN 1584-5982

49 / 2016



Ministry of National Education and Scientific Research
National Authority for Scientific Research and Innovation

NATIONAL INSTITUTE OF RESEARCH AND
DEVELOPMENT FOR MECHATRONICS AND
MEASUREMENT TECHNIQUE



THE PROFESSIONAL ASSOCIATION OF
THE ROMANIAN PATRONAGE OF PRECISION MECHANICS,
OPTICS AND MECHATRONICS



THE ASSOCIATION OF
PRECISION MECHANICS & OPTICS
OF ROMANIAN



Biannual publication • INCDMTM, AMFOR, APROMECA

SUPPLEMENT TO ROMANIAN REVIEW PRECISION MECHANICS, OPTICS & MECHATRONICS

Special Issue on:

„Innovation and Technology
Transfer on Mechatronics“

Guest Editors:

♦ **José Machado,**

University of Minho, Portugal

♦ **Luís Farinha,**

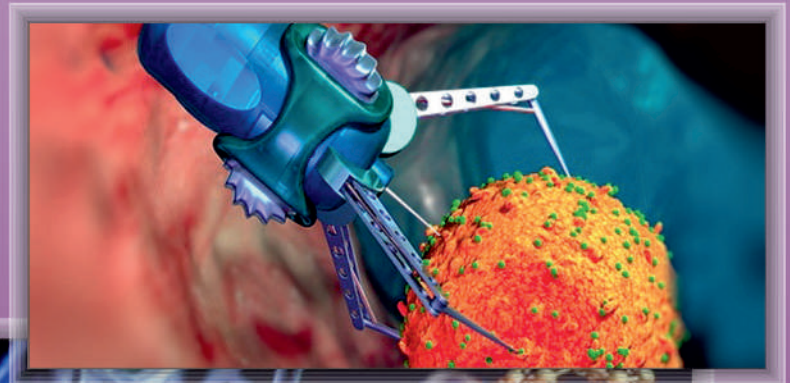
Polytechnic Institute of Castelo Branco
and University of Beira Interior/ NECE
– Research Unit, Portugal

♦ **Nuno O. Fernandes,**

Polytechnic Institute of Castelo Branco,
Portugal

♦ **Pedro Torres,**

Polytechnic Institute of Castelo Branco,
Portugal.





SUMMARY

Cláudia Barros, Cristiana Silva, Sandra Martins, Luís Dias, Guilherme Pereir, Nuno O. Fernandes, S. Carmo-Silva	ARE CARD-BASED SYSTEMS EFFECTIVE FOR MAKE-TO-ORDER PRODUCTION?	5
Tiago Manuel Matias Gonçalves, José Mendes Machado, João Sena Esteves	AERO-STABILIZER WORKBENCHES FOR THE TEACHING OF PID CONTROL	10
Paulo Torres, António Gusmão	UPLINK DETECTION PERFORMANCE REGARDING BANDWIDTH-EFFICIENT BROADBAND TRANSMISSION IN A LARGE- SCALE MU-MIMO SYSTEM	15
Mónica Martins de Andrade Régio, Marcelo Rudolfo Calvete Gaspar, Luís Manuel do Carmo Farinha, Maria Margarida Afonso de Passos Morgado	FORECASTING THE DISRUPTIVE SKILLSET ALIGNMENT INDUCED BY THE FORTHCOMING INDUSTRIAL REVOLUTION	24
Ana Carolina Kayser, Dusan Schreiber, Rafael Stoffel Dal Ri	INNOVATION IN FIRMS FROM COLLABORATIVE PROJECTS	30
Marco Feiteira, Pedro M. B. Torres, Nuno Marques	AUTOMATION OF REFRIGERATION SYSTEM WITH PLC AND LABVIEW, AN ACADEMY INDUSTRY COOPERATION CASE STUDY	39
A. Araújo, L. Kapisch, M. L. R. Varela, J. Machado	INFORMATION ORGANIZATION AND PRODUCTION PLANNING IMPROVEMENT IN A CLOTHES COMPANY IN PORTUGAL	44
L. Kapisch, A. Araújo, M. L. R. Varela, J. Machado	PURCHASE MANAGEMENT IMPROVEMENT IN A TV COMPANY FROM THE INDUSTRY DISTRICT OF MANAUS (PIM)	48
Vitor Braga, Ana Cristina Gonçalves, Alexandra Braga	THE PORTUGUESE TEXTILE INDUSTRY BUSINESS CO-OPERATION: INFORMAL RELATIONSHIPS FOR INTERNATIONAL ENTRY	52



ARE CARD-BASED SYSTEMS EFFECTIVE FOR MAKE-TO-ORDER PRODUCTION?

Cláudia Barros¹, Cristiana Silva¹, Sandra Martins¹, Luís Dias², Guilherme Pereir³, Nuno O. Fernandes⁴, S. Carmo-Silva⁵

¹Dpt. of production and systems, University of Minho, Campus de Gualtar, 4710-057, Braga, Portugal

²ALGORITMI research unit, Dpt. of production and systems, Campus de Gualtar, 4710-057, Braga, Portugal, lsd@dps.uminho.pt

³ALGORITMI research unit, Dpt. of production and systems, Campus de Gualtar, 4710-057, Braga, Portugal gui@dps.uminho.pt

⁴Instituto Politécnico de Castelo Branco, Av. Empresário, 6000-767, Castelo Branco, Portugal, &ALGORITMI research unit, Dpt. of production and systems, Campus de Gualtar, 4710-057, Braga, Portugal, nogf@ipcb.pt

⁵ALGORITMI research unit, Dpt. of production and systems, Campus de Gualtar, 4710-057, Braga, Portugal scarmo@dps.uminho.pt

Abstract - Card-based production control systems, such as CONWIP and POLCA, were developed for manufacturing companies operating under non-repetitive and high-variety production. They implement simple approaches to production control - but are they effective in the make-to-order? This paper analyses and compares the performance of these two card-based systems in the context of a make-to-order general flow shop operated under different lot splitting policies. Lot splitting allows large jobs to be split into smaller transfer sublots so they can move more quickly and independently through the production process as result of operations overlapping. Results highlight the importance of splitting jobs in order to increase the effectiveness of both production control systems.

Keywords: Production Control; CONWIP; POLCA, Lot Splitting; Simulation.

1. Introduction

The Toyota Kanban System (TKS) [1] is a card-based production control system that implements a simple and effective approach to production control under make-to-stock (MTS) manufacturing. TKS was developed for the repetitive and low-variety production, and designed to maintain a certain amount of inventory for each part number at each production stage. For the non-repetitive and high-variety production different control approaches are necessary [2]. Therefore, several alternatives to TKS have been proposed over the last decades that apparently address this need. Two paradigmatic examples are CONstant Work in Process (CONWIP) [3] and Paired-cell Overlapping Loops of Cards with Authorization (POLCA) [2]. These production control systems share the TKS simplicity - also using production authorisation cards - but are they effective in the make-to-order production? Moreover, their effectiveness under lot splitting, to the best of our knowledge, has not been thoroughly assessed. In order to assess such effectiveness, we compare the performance of these two production control systems for a make-to-order general flow shop operated under different lot splitting policies.

Lot splitting allows large jobs to be split into smaller transfer sublots so that they can move independently through the production process. This aims at shortening

throughput times of jobs and making a better use of manufacturing resources. The basic idea is not to process the whole job at one workstation and then move it to the next, but to move smaller quantities (sublots) to the next workstation as soon as they are completed. This allows job progress to be accelerated and due date performance to be improved as result of operations overlapping, as pointed out by [4, 5], among others. Further benefits of lot splitting are the reduction of the amount of storage space needed as well as the capacity of material handling equipment required.

Although, much simulation research has been done on comparing production control systems (e.g., [6], [7], [8], [9] and [10]) most studies assume that jobs are released to the shop floor without being split. Two noticeable exceptions are [11] and [12]. The former includes the impact of lot splitting in the specific context of Drum-Buffer-Rope (DBR), while the later includes the impact of lot splitting within Workload Control (WLC). Both studies found that significant improvement in shop performance can be realized if lot splitting is used.

This research work gives a contribution to fill the identified research gap, by using discrete event simulation to model and analyse the impact of lot splitting in the context of card-based production control systems. In particular, the following research questions are addressed:

1. How card-based systems perform in the context of make-to-order production?
2. How lot splitting impacts the performance of card-based systems?

The remainder of the paper is organized as follows. In Section 2, we present the simulation study carried out, including the simulation model, the experimental set-up and the performance measures considered. In Section 3, we discuss the results of the simulation study, and finally, in Section 4 of the paper, we summarize key results and managerial implications.

2. Simulation Study

Simulation will next be used to experimentation towards answering the above research questions. A discrete event simulation model was developed using Arena® software.

2.1 Simulation Model

In this study, we consider a six-stage manufacturing system with one machine per stage. Table 1 summarises the characteristics of the simulation model.

Table 1. Job and Shop Characteristics

Shop configuration	General flow shop; no re-entrant flows
No. of workstations	6
Workstation capacities	All equal and constant over time
Workstation utilization	90%
Inter-arrival times	Exponentially distributed; mean = 0.647 time units
No. of operations per job	Discrete uniformly distributed [1, 6] operations
Job size (quantity)	Discrete uniformly distributed [1, 4] units
Unit operation times	2-Erlang, mean = 0.4 and truncated at 1.6 time units
Set-up time	Sequence independent

Production flows are in accordance with the general flow shop, which is seen as a more realistic model of the flow structure of job shops in practice than pure job shops [13, 14].

As customer orders arrive to the production system, their operation times and due dates are established. It is assumed that all orders are accepted and enough raw materials inventory is always available. Orders inter-arrival times follow an exponential distribution and due dates are market driven and set by adding a uniformly distributed time allowance to the time of order arrival. In this study, the allowance varies between 35 and 55 time units. This leads to approximately 18% of orders being tardy under immediate release if orders are not split.

Arriving orders (or job lots) are split into smaller sublots of equal size, which can be processed independently in the different stages of job progress. The number of possible sublots in each job is directly related with the job size, i.e. the order quantity. To reflect the environment where customers demand unique or small quantities of products, the order quantity is randomly generated according to a discrete uniform distribution between one and four units. Thus, also the number of sublots for each job can range from one to four.

In our simulation model, unit processing times at each operation are drawn from a truncated 2-Erlang distribution with a mean of 0.4 time units and a maximum of 1.6 time units. These are then multiplied by the job size to obtain the processing time of each operation of the job. The arrival rate combined with routings and processing times ensures that utilisation is 90% at all workstations. Additionally, assumptions are:

- Workstations capacity remains constant over time and no breakdowns have been modelled.
- Set-up times are assumed to be sequence-independent and included in the operation processing times.
- Distances and transportation times between workstations and between production stages are assumed to be negligible.
- Information of production control events and production control cards are transmitted instantly.

The simulation model presented here was kept simple in order to ensure easy and correct interpretation of the effects and getting results that may contribute for the understanding of the behaviour of more complex production systems.

2.2 Production Control: order release and dispatching

Production Control addresses two main functions: order release and priority dispatching. Order release determines the time and the orders (jobs) to be released into production. Release decisions are usually based on the jobs' urgency and on their influence on the current shop floor situation [15]. Priority dispatching determines which jobs in queue should be selected next for processing once a workstation becomes idle.

In the manufacturing system considered, an arriving customer order immediately flows into a pre-shop pool, waiting its release to the shop floor for processing. This means that orders (jobs) are not immediately released to the shop as they arrive. Rather, they must wait for capacity availability at the shop floor. The use of a pre-shop pool is expected to reduce the level of work-in-process and allow better control over the flow of production orders through the shop. Jobs in the pool are sequenced according to their urgency, i.e., a planned release date (Equation 1), and released under one of the following card-based production control systems: CONWIP and POLCA.

$$\tau_j = d_j - \sum_{k \in R_j} b_k \quad (1)$$

Where:

τ_j is the planned release date of job j;

d_j is the due date of job j;

b_k is the lead time at workstation k;

R_j is the set of workstations in the routing of job j.

Lead times at each workstation were fixed at 7 time units based on the throughput times observed in preliminary simulation runs under immediate release;

In both production control systems cards are not part number specific (i.e. are job anonymous) and can be acquired by any job waiting release in the pre-shop pool. One production authorisation card per subplot is attached to the job. Under CONWIP, cards are attached to the job at release and detached when the job completes processing. Detached cards are sent back to the pre-shop pool where they can be attached to new jobs entering the system. POLCA uses overlapping loops of cards between successive workstations in the routing of the job. These ensure a workstation will only process jobs for which capacity has been reserved at the next downstream workstation in the routing of the job. Cards can be acquired by any job entering the first workstation of pair. These are attached to a job at the first workstation of the pair and detached after job completion at the second workstation of the pair. Detached cards are sent back to the first workstation of the pair, where they can be attached to new arriving jobs.

The role of priority dispatching tends to be modest when order release control is applied, because the choice among jobs is limited due to short queues [16]. Thus in this study shop floor dispatching is based on *first-come-first-served* (FCFS) priority dispatching rule that supports the natural flow of the orders through the shop, stabilizing operation throughput times.

2.3 Lot Splitting

Regarding lot splitting three alternative policies are analysed to determine whether splitting should be considered or not and when, i.e. before or after release:

- Policy P0: The job is not split, and thus released as a whole.
- Policy P1: The job is split before release and sublots are released independently to the shop floor.
- Policy P2: The job is released as a whole and then split on the shop floor into sublots.

2.4 Experimental Design and Performance Measures

The experimental factors and simulated levels of the study are summarised in Table 2. Two production control systems, CONWIP and POLCA, are applied to release jobs and control the materials flow. Both

production control systems were tested at 6 card counts and for 3 lot splitting policies. Thus, 36 simulation cases are tested (2 production control systems x 6 card counts x 3 lot splitting policies). Each test case runs 100 replicates. The time horizon for a simulation case is 13 000 time units and only data of the last 10 000 time units are collected, i.e., a warm-up period of 3 000 time units is considered.

The number of production authorisation cards is an experimental factor in our study. CONWIP uses a single-type production authorisation card. POLCA requires one card type per pair of workstations. Once we have a balanced shop we define the number of cards per pair of workstations to be equal in POLCA.

Table 2. Experimental factors and levels

Experimental factor	Levels		
Production control systems	CONWIP	POLCA	
Number of cards	6 levels of restriction		
Lot splitting policies	P0	P1	P2

We use two types of criteria to evaluate the system's performance: (1) the ability to deliver jobs on time, and (2) the ability to provide short delivery times. To measure performance with regard to the first, the percentage of tardy jobs and the standard deviation of lateness are recorded. To measure performance with regard to the second, the shop throughput time and the total (or system) throughput time are used. The shop throughput time refers to the time that elapses between job release and job completion. The total throughput time is the shop throughput time plus the pool delay of jobs. Note that job lot is not completed until all the sublots that belong to it are fully processed. The synchronization time is the time that elapses between the completion of the first and last subplot of a job.

3. Simulation Results and Discussion

Here we present and discuss the results of the simulation study described in the previous section. Section 3.1 focuses the impact of production control systems on performance when jobs are not split. A detailed analysis of their impact under two splitting policies is presented in Section 3.2.

3.1 Impact of Production Control Systems

Figure 1 (a, b and c) plot the percentage of tardy jobs, total throughput time, and the standard deviation of lateness, respectively, against the shop throughput time for production control systems. By comparing performance curves, we can determine performance differences for different values of card counts. A marker on a curve is the result of simulating a production control system at a specific card count. Six card counts have been simulated, including infinity. This means unrestricted release of jobs to shop and is used as a base line for performance comparisons in the study.

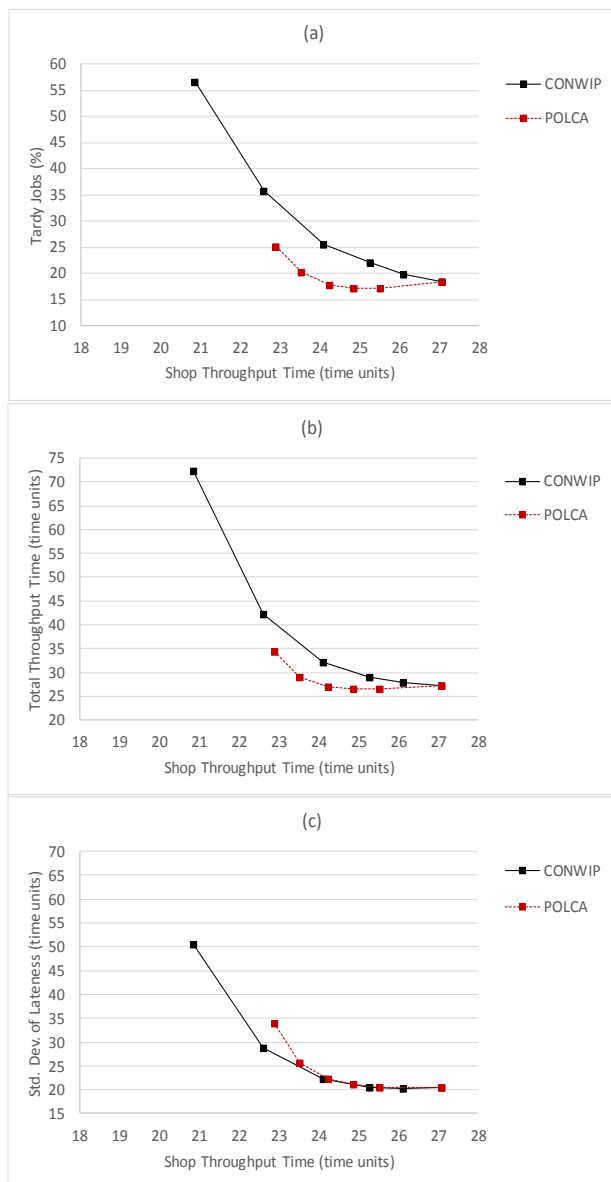


Figure 1. Performance of production control systems under Policy P0 for: (a) percentage of tardy jobs; (b) total throughput time; and (c) standard deviation of lateness.

This Figure shows that decreasing the number of production authorisation cards, i.e. from right to left, leads to lower shop throughput time. This is due to having fewer jobs, i.e., less working-in-process, on the shop floor. As expected, unrestrictive release, shown by the right hand point on each curve, results in the highest level of shop throughput time. For an initial reduction in the number of cards available, a slight reduction in the percentage of tardy jobs and on the total throughput time is observed under POLCA control. However, if CONWIP is used, such a reduction on the number of cards available lead to an increase on this two performance measures. Germs and Riezebos (2010) already concluded about the lack of balancing capability of CONWIP, expressed by the increase of total throughput time when cards are restricted.

POLCA clearly outperforms CONWIP for the

percentage of tardy jobs and total throughput time. However, this is obtained at the cost of a higher standard deviation of lateness, particularly under low card counts, i.e. low work-in-process.

3.2 Impact of the Lot Splitting Policy

Figure 2 (a, b, c and d) plots the percentage of tardy jobs, total throughput time, standard deviation of lateness and synchronisation time, respectively, against the shop throughput time for different combinations of the experimental factors. From this Figure it can be observed that splitting policies P1 and P2 perform better than the non-splitting Policy P0. Splitting jobs decrease throughput times through operations overlapping. This is independent of the production control system applied, i.e. POLCA or CONWIP.

Comparing splitting policies P1 and P2, it can be seen that policy P2 allows for a better performance in what concerns the percentage of tardy jobs and total throughput time. This is obtained at the cost of a higher standard deviation of lateness under CONWIP, when compared with POLCA. This seems to be explained by the fact that CONWIP tends to retain large jobs (particularly with long routings) in the pre shop pool when there aren't enough available production authorisation cards to release them to the shop. This behaviour of the standard deviation of lateness is not noticeable under POLCA release. Apparently, since POLCA controls the release of jobs based only on the first pair of workstations in the routing of the job, and not on the complete routing of the job, makes the release decision easier for long-routing jobs than does CONWIP. This problem with CONWIP is mitigated by policy P1 because jobs are splitted before release. This means that in case of lack of enough authorization cards for releasing the whole job, some sublots of the job may still be released with the available cards. However, this creates another problem, as we can see from figure 1d. Since sublots that are released independently have to wait, after processing, for others released later, synchronization time of jobs will increase under policy P1 in relation to Policy P2.

4. Conclusions and Managerial Implications

In this paper we compare, using discrete simulation, the performance of two card-based systems, CONWIP and POLCA in the context of a make-to-order (MTO) general flow shop. Both, restrict the workload on the shop floor based on the number of production authorisation cards available in system.

The following can be concluded from our simulation study: (1) POLCA shows to be an effective production control approach in the make-to-order production, reducing shop floor throughput time, total throughput time and percentage of tardy jobs, comparatively to immediate release. Its performance can be improved if jobs are split after its release to the shop floor.

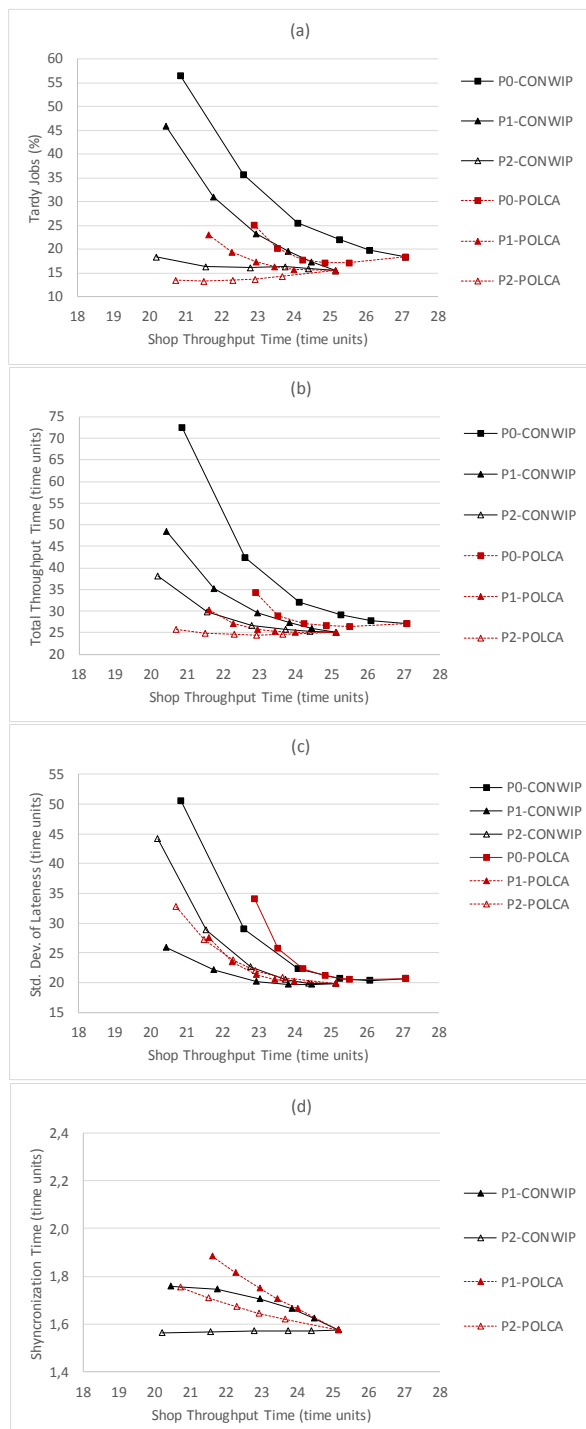


Figure 2. Global Performance results for: (a) percentage of tardy orders; (b) total throughput time; (c) standard deviation of lateness and (d) synchronization time.

(2) CONWIP on the other hand results in higher values of total throughput time and percentage of tardy jobs relatively to immediate release, even when jobs are split. A major limitation of our study is the reduced number of manufacturing environmental factors considered. Thus, future research work should extend our environmental setting, including for example other shop configurations.

Acknowledgements

This study had the financial support of COMPETE: POCI-01-0145-FEDER-007043 and FCT – Fundação para a Ciência e Tecnologia within the Project Scope: UID/CEC/00319/2013

5. References

- [1] Sugimori, Y., Kusunoki, K., Cho, F. and Uchikawa, S. (1977). Toyota production system and kanban system materialization of just-in-time and respect-for-human system. *International Journal of Production Research*, 15(6), 553-564.
- [2] Suri, R. (1998). Quick response manufacturing: a companywide approach to reducing lead times. Productivity Press.
- [3] Spearman, M. L., Woodruff, D. L. and Hopp, W. J. (1990). CONWIP: a pull alternative to kanban. *International Journal of Production Research*, 28(5), 879-894.
- [4] Jacobs, F.R. and Bragg, D.J. (1988). Repetitive lots: flow time reductions through sequencing and dynamic batch sizing. *Decision Sciences*, 19 (1), 281-294.
- [5] Wanger, B.J. and Ragatz, G.L. (1994). The impact of lot splitting on due date performance. *Journal of Operations Management*, 12 (1), 13-25.
- [6] Bonvik, A.M., Couch, C.E. and Gershwin, S.B. (1997). A comparison of production-line control mechanisms. *International Journal of Production Research*, 25(3), 789-804.
- [7] Fernandes, N.O. and Carmo-Silva, S. (2006). Generic POLCA—A production and materials flow control mechanism for quick response manufacturing. *International Journal of Production Economics*, 104(1), 74-84.
- [8] Jodlbauer, H. and Huber, A. (2008). Service-level performance of MRP, kanban, CONWIP and DBR due to parameter stability and environmental robustness. *International Journal of Production Research*, 46 (8) 2179–2195.
- [9] Germs, R., and Riezebos, J. (2010). Workload balancing capability of pull systems in MTO production. *International Journal of Production Research*, 48, 8, 2345-2360.
- [10] Thürer, M., Land, M. J. and Stevenson, M. (2014). Card-based workload control for job shops: Improving COBACABANA. *International Journal of Production Economics*, 147, 180-188.
- [11] Russell, G.R., and Fry, T.D. (1997). Order review/release and lot splitting in drum-buffer-rop. *International Journal of Production Research*, Vol. 35, No. 3, pp. 827-84.
- [12] Fernandes, N.O., Land, M.J. and Carmo-Silva, S. (2016). Aligning Workload Control Theory and Practice: Lot Splitting and Operation Overlapping Issues. *The International Journal of Production Research*, Forthcoming.
- [13] Enns, S.T. (1990). An integrated system for controlling shop loading and workflows. *International Journal of Production Research*, 33(10), 2801-2820.
- [14] Oosterman, B., Land, M. and Gaalman, G. (2000). The influence of shop characteristics on workload control. *International Journal of Production Economics*, 68(1), 107-119.
- [15] Henrich, P., Land, M. and Gaalman, G.J.C. (2004). Exploring applicability of the workload control concept. *International Journal of Production Economics*, 90 (2), 187-198.
- [16] Bechte, W. (1994). Load-oriented manufacturing control, just-in-time production for job shops. *Production planning & Control*, 5 (3), 292-307.

AERO-STABILIZER WORKBENCHES FOR THE TEACHING OF PID CONTROL

Tiago Manuel Matias Gonçalves, tiagoncalves92@gmail.com, University of Minho

José Mendes Machado, jmachado@dem.uminho.pt, University of Minho

João Sena Esteves, sena@dei.uminho.pt, Centre Algoritmi, University of Minho

Abstract: Teaching Engineering students some theoretical concepts of Control Theory is a quite a challenge. Practical and theoretical skills must be taught in parallel because those students are being prepared for working at industry, developing added value for the economy of the country where they belong. In Portugal, the domain of control and automation is quite important due to the fact that economy grows based on knowledge and development of high added value products. This ideas are being invoked by government institutions and accepted by industry and universities. So, this work has been developed on the context of Triple Helix of university-industry-government relationships. Hand-on experiments related to those concepts may be a significant help. This paper presents two aero-stabilizer workbenches that were designed in order to help the teaching of Proportional–Integral–Derivative (PID) controllers. Each workbench has a bar which is free to rotate about one of its extremities. A motor propeller assembly at the other end of the bar raises it. The desired bar orientation is obtained by controlling the rotation speed of the motor. Bar orientation is measured with an optical encoder that sends a feedback signal to a PID controller. The two workbenches differ only on the electronic system that performs the PID control. One of them uses an industrial Programmable Logic Controller (PLC) for that purpose. The other uses an *Arduino* platform. Having both workbenches will allow students to work with two widely used microcontroller technologies and to compare them. Some fundamental concepts and the main components required to build the workbenches are described.

Keywords: Proportional–Integral–Derivative (PID) control, Programmable Logic Controller (PLC), *Arduino*, Hands-on Experiments.

1. Introduction

One of the main challenges of Engineering teaching is the proper combination of theoretical knowledge with practical experience. Theoretical teaching can be easily addressed in lectures, exercise classes and books, while the practical requires some resources such as laboratories. The teaching of Control Engineering is quite a challenge because the ideas and phenomena involved in these areas are complex and difficult to understand (Schmid, 2000).

The Proportional–Integral–Derivative (PID) Controller is the most common control algorithm used in Process Control. It is estimated that more than 90% of the control loops use PID control. Most loops are PI type because derivative action is not used very often. PID feedback is based on the present (P), past (I) and future (D) control error. It is amazing how much can be earned with this strategy. It should be the first technique to be implemented when a solution with feedback is required (K. Åström & Hägglund, 1995; K. J. Åström & Hägglund, 2001).

Some types of support devices for the teaching of PID control may be found in the literature. The most common are tank systems (Tepljakov, Petlenkov, Belikov, & Halas, 2013) and furnace systems (Zhao, Sun,

& Wen, 2012). Pedagogical tank systems are very used because they have significant similarities with real-world industrial systems and the results of the applied control are visible. However, they must be filled with fluid, which may be an important limitation. Even if the fluid is just water, it is a fact that classrooms and many laboratories are not equipped with water facilities. Furnace and other thermal systems are quite abstract since the temperature is not a visible physical quantity. Moreover, some thermal systems have large time constants that may not be compatible with the time available for experiments during classes

This paper presents two aero-stabilizer workbenches – each one with one input and one output – that were designed in order to help the teaching of PID controllers without the limitations mentioned above. They are portable, easy to carry to a standard classroom, do not require any fluids to work and respond quickly to changes in the output of the PID controller, giving the students a clear and sharp view of its functioning. The two workbenches differ only on the electronic system that performs the PID control. One of them uses an *Omron CP1L-EM30DT1-D* industrial Programmable Logic Controller (PLC) for that purpose. The other uses an *Arduino UNO* platform. Having both workbenches will allow students to work with two widely used

microcontroller technologies and to compare them.

Some fundamental concepts related to PID control and the main components required to build the workbenches are described in the next sections.

2. PID control

The control signal generated by a PID controller is: (K. Åström & Hägglund, 1995)

$$u(t) = K \left(e(t) + \frac{1}{T_i} \int_0^t e(\tau) d\tau + T_d \frac{de(t)}{dt} \right) \quad (1)$$

Where:

K is the gain;

T_i is the integral time;

T_d is the derivative time.

The input of the PID controller is the control error e , given by the following equation:

$$e = y_{sp} - y \quad (2)$$

Where:

y_{sp} is the set point;

y is process variable .

The transfer function of the PID controller is shown in Figure 1 Figure 1(Ogata, 2002).

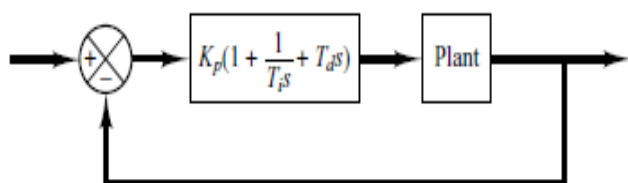


Figure 1 – PID Controller(Ogata, 2002)

2.1. Ziegler-Nichols Rules

Tuning the controller is the process of selecting the controller parameters required in order to meet performance specifications. Ziegler and Nichols suggested rules for the tuning of PID controller based on experimental results(Ogata, 2002).

Ziegler-Nichols rules correspond to two methods (Ogata, 2002). The first one consists of obtaining the response of the plant to a unit-step input. If the result is an S-shaped curve, it is possible apply this method. Drawing a tangent line at the inflection point showed in Figure 2, the delay time L and the time constant T may be obtained. Then, the values of the parameters K_p, T_i and T_d may be computed using the formulas shown in Table 1.

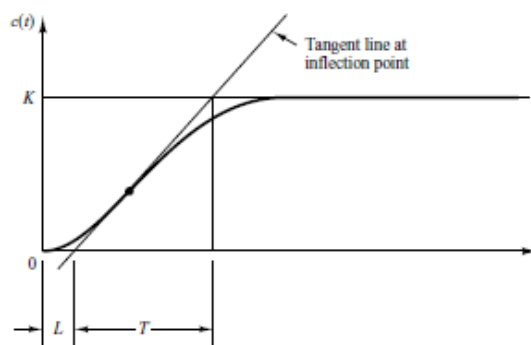


Figure 2 – Unit-step response of a plant (Ogata, 2002)

Table 1 – Ziegler–Nichols tuning rule based on the unit-step response of a plant(Ogata, 2002)

Type of controller	K_p	T_i	T_d
P	$\frac{T}{L}$	∞	0
PI	$0.9 \frac{T}{L}$	$\frac{L}{0.3}$	0
PID	$1.2 \frac{T}{L}$	$2L$	$0.5L$

The second method consists of using only the proportional control, increasing K_p from 0 to a critical value K_{cr} , and setting $T_i = \infty$ and $T_d = 0$. At the critical value, the output first exhibits sustained oscillations and the corresponding period P_{cr} is obtained. If the output does not exhibit sustained oscillations for any value of K_p , this method does not apply. After obtaining the values of K_{cr} and P_{cr} , the values of K_p, T_i and T_d are computed using the formulas showed in Table 2.

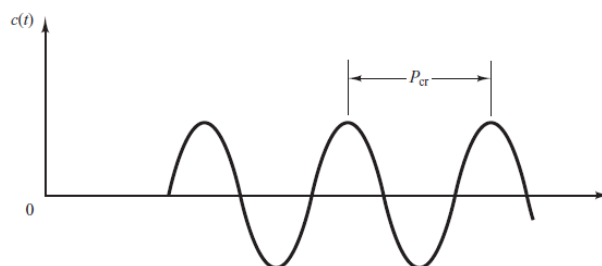


Figure 3 – Sustained oscillation with period P_{cr} (Ogata, 2002)

Table 2 – Ziegler–Nichols tuning rule based on critical gain (Ogata, 2002)

Type of controller	K_p	T_i	T_d
P	$0.5K_{cr}$	∞	0
PI	$0.45K_{cr}$	$\frac{1}{1.2} P_{cr}$	0
PID	$0.6K_{cr}$	$0.5P_{cr}$	$0.125P_{cr}$

After obtaining the values from the two methods, if possible, the system will be tested and a margin for each value will be defined.

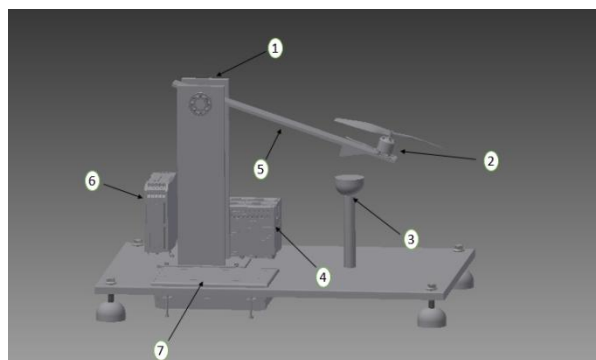
3. The Workbenches

Each workbench (Figure 4) has a bar which is free to rotate about one of its extremities. A motor propeller assembly at the other end of the bar raises it. The desired bar orientation is obtained by controlling the rotation speed of the motor. Bar orientation is measured with a 1024 pulses/revolution optical incremental encoder that sends a feedback signal to a PID controller. Figure 5 shows a block diagram of the bar orientation control system. Each workbench will have a user interface for system control and monitoring. Students will be able to set a reference angle for the bar orientation, define the parameters of the PID controller, verify the oscillations in the system and cause some deliberate disturbances.

The motor-propeller assembly consists of a *Golden Power* A2212-13 brushless motor to which a 23 cm propeller is attached. The weight of the motor is 0,047kg. This kind of motor has a long service life but must be driven by an Electronic Speed Controller (ESC). The 30A ESC used in this project adjusts the motor rotation speed according to a Pulse-Width Modulation (PWM) signal produced by the PID controller. This latter must have at least two digital inputs and one output capable of producing a PWM signal with a minimum switching frequency of 8 kHz.

The PID controller in one of the workbenches will be implemented on *Arduino* (Figure 6), a prototyping platform based on easy-to-use hardware and software, which will be connected to a Personal Computer (PC) via a Universal Serial Bus (USB) port. *Arduino* boards are programmable and have multiple inputs and outputs. An *Arduino UNO* board will be used in this project it has 14 digital inputs / outputs, 6 of which can be used as PWM outputs. *Arduino Software*, an open-source Integrated Development Environment (IDE), allows writing programs on a personal computer and uploading them to an *Arduino* board. Many projects have already been developed with this technology, from everyday devices to complex scientific instruments. (Arduino, n.d.)

To implement its PID controller, the other workbench will use a Programmable Logic Controller (PLC), a microcontroller adapted to industry standards that runs specific functions based on a program. A Human Machine Interface (HMI) for system control and monitoring will be used instead of a PC. The PLC is used in industrial environments to control equipment's and to automate mechanical systems. They are very efficient and reliable in applications involving sequential control and the synchronization of processes. The most used programming languages of a PLC are Function Block Diagram (FBD), Structured Text (ST), Instruction List (IL), Sequential Function Chart (SFC) and Ladder Diagram (LAD) (Huyck et al., 2012), (Qin, 2014). A PLC with relay output – one of the most common types of output – cannot be used in this project because of the given PWM output requirements. Instead, a PLC with at least one transistor sourcing output must be used. The chosen *Omron CP1L-EM30DT1-D* has 18 digital inputs and 12 digital outputs. Four inputs may be used to read the encoder channels A and B. Two outputs are able to produce PWM signals with a switching frequency up to 100 kHz.



- 1 – Encoder
- 2 – Motor propeller assembly
- 3 – Bar support
- 4 – PID controller (PLC or Arduino)
- 5 – Bar
- 6 – Power supply
- 7 – Human Machine Interface (HMI)

Figure 4 – Autodesk Inventor 3D model of a workbench

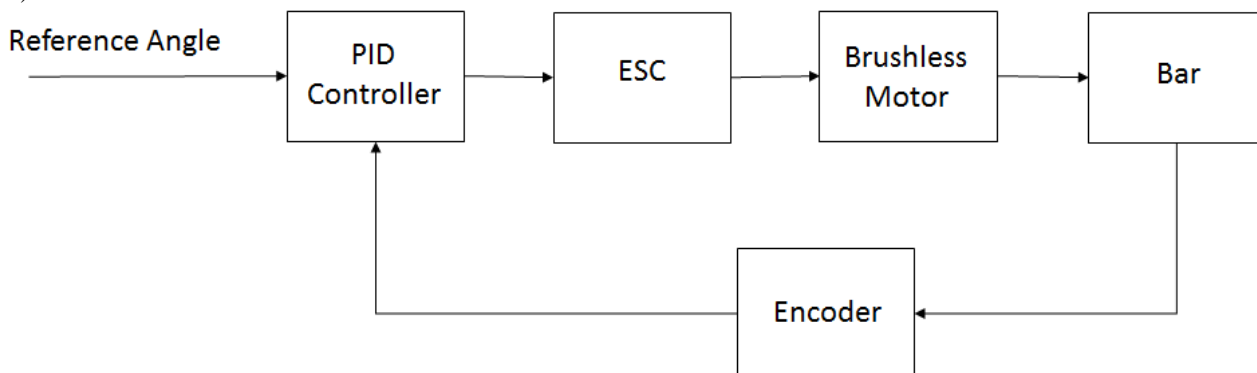


Figure 5 – Block diagram of the bar orientation control system

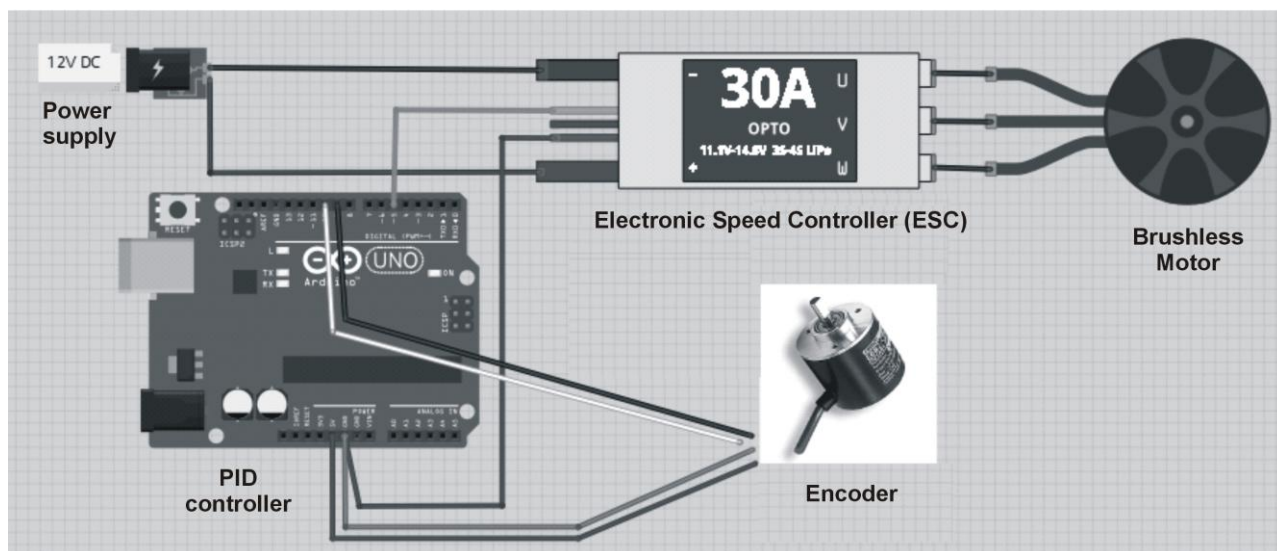


Figure 6 – Bar orientation control system with the PID controller implemented on an Arduino platform [adapted from (Davide Caminati, 2014) and (Motor, 2013)]

Some low-cost laboratory modules, similar to the one presented in this paper but with significant differences, are available. For example, instead of general purpose platforms like *Arduino* boards or PLCs, the systems developed by E. T. Enikov & Campa (2012), Yang & Chou (2009), and Gültekin & Taşcıoğlu (2011) use specific PID controllers. Using general purpose controllers may be an important advantage, since it enables students to experiment and gain knowledge of widely used platforms. The system presented by Gültekin & Taşcıoğlu(2011)use two brushless DC motors, each one able to provide thrust in a single direction. E. T. Enikov & Campa(2012) designed

a portable system with a DC motor and feedback provided by a potentiometer. Yang & Chou (2009)propose a slightly different setup with two bars and a DC motor.

4. Mechanical system model

Students will obtain experimentally the tuning parameters of the PID controller. However, it is useful to have a previous estimate of those parameters, obtained by computations, which requires modelling the mechanical system of the workbenches (Figure 7).

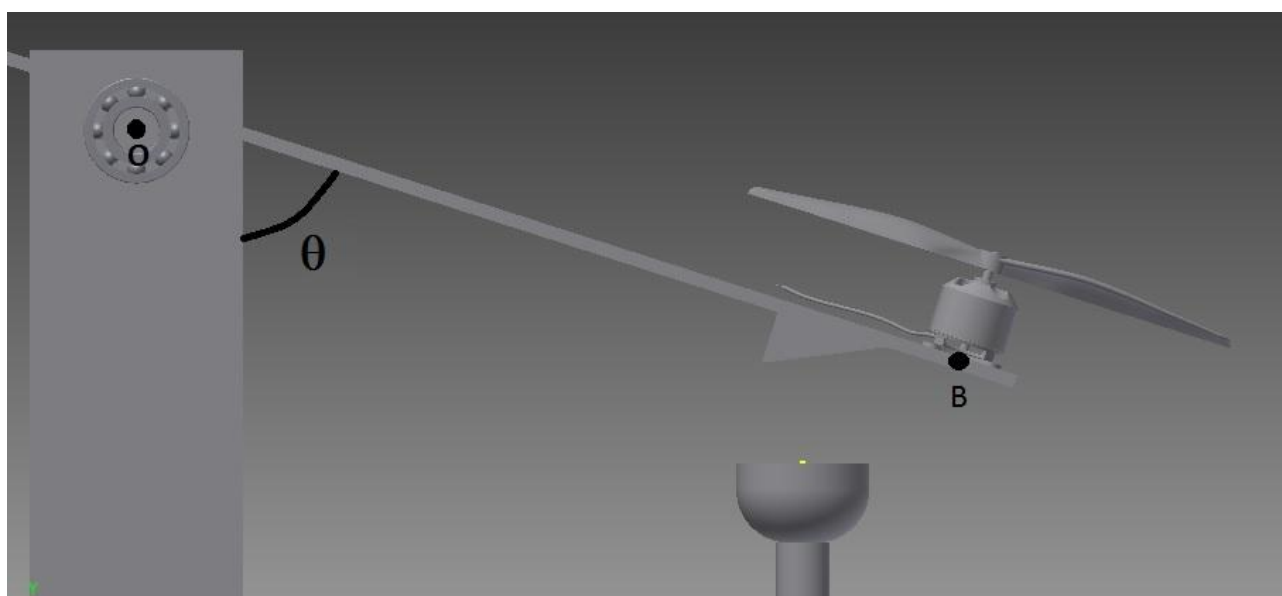


Figure 7 – Mechanical system of the workbenches

Using Newton’s Second Law and D’Alembert Principle, the mechanical system may be modelled as follows(E. Enikov, Polyzoev, & Gill, 2010):

$$mL^2\ddot{\theta} = -mgL\sin\theta - c\dot{\theta} + TL \quad (3)$$

Where

- m = mass of the motor-propeller assembly (kg);
 L = distance from point O to point B (m);
 θ = angle between the bar and a vertical line (rad);
 g = gravitational acceleration (m/s^2);
 c = viscous friction coefficient (Nms/rad);
 T = thrust force produced by the propeller (N).

The thrust force produced by the propeller is given by:

$$T = mg \sin\theta + u \quad (4)$$

Where

u is the control signal.

The transfer function of the resulting linear system is

$$\frac{\theta(s)}{U(s)} = \frac{L}{mL^2s^2 + cs} \quad (5)$$

5. Conclusions

Two aero-stabilizer workbenches designed in order to help the teaching of PID controllers were presented. The two workbenches differ only on the electronic system that performs the PID control used to keep the desired orientation of a bar with the help of motor propeller assembly. One of them uses an industrial PLC and the other uses an *Arduino* platform. Having both workbenches will allow students to work with two widely used microcontroller technologies and to compare them. Some fundamental concepts related to PID control and the main components required to build the workbenches were described.

Acknowledgements

This work has been supported by COMPETE: POCI-01-0145-FEDER-007043 and FCT – Fundação para a Ciência e Tecnologia within the Project Scope: UID/CEC/00319/2013.

6. References

- [4] Arduino. (n.d.). <https://www.arduino.cc/en/Guide/Introduction>. Retrieved June 2, 2016, from <https://www.arduino.cc/en/Guide/Introduction>
- [1] Åström, K., & Hägglund, T. (1995). *PID Controllers: Theory, Design, and Tuning* (2nd ed.).
- [2] Åström, K. J., & Hägglund, T. (2001). The future of PID control. *Control Engineering Practice*, 9(11), 1163–1175. [http://doi.org/10.1016/S0967-0661\(01\)00062-4](http://doi.org/10.1016/S0967-0661(01)00062-4)
- [3] Davide Caminati. (2014). Read Omron Encoder Arduino Mega Interrupt. Retrieved June 3, 2016, from <http://fritzing.org/projects/read-omron-encoder-arduino-mega-interrupt-beta>
- [4] Enikov, E., Polyzoev, V., & Gill, J. (2010). Low-Cost Take-Home Experiment on Classical Control Using Matlab/Simulink Real-Time Windows Target. In *Proceedings of the 2010 American Society for Engineering Education Zone IV Conference*, (May), 322–330. Retrieved from https://nano.arizona.edu/media/education/ASEE2010_Pendulum.pdf
- [5] Enikov, E. T., & Campa, G. (2012). Mechatronic Aeropendulum: Demonstration of Linear and Nonlinear Feedback Control Principles. *Ieee Transactions on Education*, 55(4), 538–545. <http://doi.org/10.1109/TE.2012.2195496>
- [6] Gültekin, Y., & Taşcıoğlu, Y. (2011). Pendulum Positioning System Actuated by Dual Motorized Propellers. *Simulation*, (May), 16–18.
- [7] Huyck, B., Callebaut, L., Logist, F., Ferreau, H. J., Brabanter, J. De, Diehl, M., ... Moor, B. L. R. De. (2012). Implementation and Experimental Validation of Classical MPC on Programmable Logic Controllers. *Proceedings of the 20th Mediterranean Conference on Control and Automation, Barcelona, Spain*, 679–684.
- [8] Motor, D. E. and B. (2013). DJI ESC and Brushless Motor. Retrieved June 3, 2016, from <http://robotic-controls.com/learn/projects/dji-esc-and-brushless-motor>
- [9] Ogata, K. (2002). *Modern Control Engineering. Control Engineering* (Vol. 17). <http://doi.org/10.1109/TAC.1972.1100013>
- [10] Qin, X. (2014). A Model-Integrated Computing based tool prototype for designing Programmable Logic Controllers. *2013 IEEE Conference Anthology, ANTHOLOGY 2013*. <http://doi.org/10.1109/ANTHOLOGY.2013.6784718>
- [11] Schmid, C. (2000). Remote experimentation techniques for teaching control engineering. *Fourth International Scientific-Technical ...*, (June). Retrieved from <http://www.atp.ruhr-uni-bochum.de/publications/upload/Pardubice2000.pdf>
- [12] Tepljakov, A., Petlenkov, E., Belikov, J., & Halas, M. (2013). Design and Implementation of Fractional-order PID Controllers for a Fluid Tank System. *2013 American Control Conference (Acc)*, 0(4), 1777–1782. <http://doi.org/10.1109/ACC.2013.6580093>
- [13] Yang, S. F., & Chou, J. H. (2009). A mechatronic positioning system actuated using a micro DC-motor-driven propeller-thruster. *Mechatronics*, 19(6), 912–926. <http://doi.org/10.1016/j.mechatronics.2009.05.005>
- [14] Zhao, P., Sun, B., & Wen, Y. J. (2012). Experimental teaching system of the assembly line heating furnace temperature control based on LabVIEW. *Proceedings 2012 International Conference on System Science and Engineering, ICSSE 2012*, 578–581. <http://doi.org/10.1109/ICSSE.2012.6257253>

FORECASTING THE DISRUPTIVE SKILLSET ALIGNMENT INDUCED BY THE FORTHCOMING INDUSTRIAL REVOLUTION

Mónica Martins de Andrade Régio¹, Marcelo Rudolfo Calvete Gaspar², Luís Manuel do Carmo Farinha³, Maria Margarida Afonso de Passos Morgado⁴

¹Escola Superior de Educação, Instituto Politécnico de Castelo Branco, monicaregio@ipcb.pt

²Escola Superior de Tecnologia, Instituto Politécnico de Castelo Branco, calvete@ipcb.pt

³Instituto Politécnico de Castelo Branco, luis.farinha@ipcb.pt

⁴Escola Superior de Educação, Instituto Politécnico de Castelo Branco, marg.morgado@ipcb.pt

Abstract - According to the World Economic Forum, in less than five years from now, over one-third of skills that are considered important in today's workforce will have changed. By 2020, a Fourth Industrial Revolution is expected to have promoted an exponential pace of change in every aspect of how we live and how we work. In a near future, the increase of digital interconnectivity will promote the emergence of new business models that have no longer to be limited by geographic borders and constraints. This may represent major opportunities as well as interesting challenges to low density and peripheral territories. In the light of the disruptive changes driven by this set of events, it is important to assess current workers' skills in order to develop dedicated strategies that will foster the envisaged skillset alignment. To this end, a pilot experience was developed in the region of Castelo Branco, classified as a peripheral territory in the Portuguese context. Structured and semi-structured interviews were conducted in diverse industrial and service driven companies in order to assess the local workforce language skills, as well as their intercultural communication abilities. Preliminary findings show that even though labourers are aware of their needs related to the aforementioned communication skills, much work is still needed to promote its widespread increase in local companies.

Keywords: regional ecosystems, peripheral territories, 4th Industrial Revolution, workforce skillsets, intercultural communication

1. Introduction and scope

In the midst of a new Industrial Revolution, a disruptive change of technological, economic and social systems is expected to take place in a near future. As in previous revolutions, work context, social interactions and wealth generation are foreseen to be drastically modified, e.g., the First Industrial Revolution promoted an aggregate shift of employment and incomes from agricultural to industrial activities alongside with a sustained increase in output growths [1]. Unlike the First, which was literally powered by the use of steam in the industry to mechanize production, in the Second Industrial Revolution electricity and new organizational skillsets created conditions to improve even more the high work rates generated with the preceding revolution, consequently enabling a widespread adoption of pre-existing technological systems to create mass-production. The combined effect of electricity as a new energy source with the advances of both production technology and new management tools lead to the upsurge of the Second Industrial Revolution [2].

More recently, the Third Industrial Revolution took place based on the extensive use of electronics and information technology [3], hence allowing current

automation of manufacturing, as well as of related processes. This new revolution came to solve the paradigm of mass-production which was running into difficulties in relation to growth rates, high levels of unemployment and trade imbalances. As such, it allowed a transition from an era of mass-production to one of flexible specialization [4]. It was this flexible specialization that allowed some degree of manufacturing customization - by opposition to large scale mass-production - linked to a new breed of flexible electronics-based automation technologies.

Currently, a Fourth Industrial Revolution is building on the Third and is characterized by the use of cyber-physical system, which results from the fusion of technologies that are blurring the lines between the physical, the digital, and the biological spheres [5]. Even though the mere designation of «Fourth Industrial Revolution» is not consensual among current academia, industry or researchers, they all seem to agree that the envisaged key technologies and associated performances are expected to take place in a relatively near future. However, job losses and a further de-industrialization are feared with the advent of such revolution, whilst current debate focuses on employees regarding ergonomics, integration and cooperation with

these technologies [6].

According to the World Economic Forum [7], in less than five years from now, over one-third of skills that are considered important in today's workforce will have changed. By 2020, the Fourth Industrial Revolution is expected to have promoted an exponential pace of change in every aspect of society and work. In this near future, an increase of digital interconnectivity may promote the emergence of new business models that will no longer be limited to geographic borders and constraints. To this end, as significant changes to business models are forecast to impact the employment landscape over the coming years [7], current investigation aims to find ways of empowering low density and peripheral territories workforce, like the one of the Portuguese Castelo Branco Region.

2. Lifelong learning as empowerment tool

Lifelong learning is the way in which voluntarily and self-motivated professionals constantly seek for knowledge [8] According to Aynur & Bülent [9], lifelong learning can be understood as all learning activities with the purpose of developing knowledge from the individual and social dimension, in order to achieve quality and constant learning in life. Preece [10] has defined lifelong learning as all of the activities of learning from birth to death which can be formal, pervasive and informal. Hursen [11] described the life-long learning competencies as: self-management, learning to learn, initiative and entrepreneurship, information retrieval, digital and decision making. These competencies are closely related to the learner's professional life and his/her competencies at work. They imply to be able by oneself to take decisions for professional development, to be able to motivate oneself for professional development and new learning, determining the existing opportunities for professional development, be able to adapt into information change in professional life or being able to access information and to use internet and computers [12].

Based on the viewpoint of the labour or jobs, the need of new education and new learning models, both for current as for upcoming workers, seem to be the key to adapting to future digital trends. It is this ability of digital technology to change outcomes that can create a more equitable growth. This is true not only for developed state-of-the-art technology savvy countries, but due to the significant increase of interconnectivity, digital technology is becoming progressively available to developing countries and regions. This may create the conditions for such peripheral territories to play a significant role in the forthcoming Industrial Revolution, thus reducing their development gap when compared to current leading countries.

As for every previous Industrial Revolution, disruptive changes are expected to take place cumulatively on technological, economic and social dimensions. New technologies are envisaged as enabling workplace innovations such as remote working, co-working spaces and teleconferencing,

enforcing organizational changes that may lead up to 44% of current workforce having to look for new work environments and accept flexible working arrangements in a near future [7]. In addition, theory related studies show that these technological changes may also cause modifications in mental work demands [13], thus affecting the way workers face and adapt to such disruptive set of events.

It is known that the adoption of new technologies usually comprises a significant effort in terms of learning. As such, skilled labours show to have an advantage at this, as they can more easily adapt to new work arrangements and associated demands. Lifelong learning allows effectively adjusting to such constrains as the foreseen advance in technology will be associated to a new skillset envisaged for future workers. Lifelong learning literally means that learning should take place at all stages of life and, in more recent versions, that it should be life-wide, i.e., during and after schoolyears, as well as in private life [14]. As such, it will become increasingly important for current workforce to be able to educate themselves in order to keep up with the new work environment paradigm of adaptability and change. On the verge of the new Industrial Revolution, an efficient worker should consider the ability to recognize the need of lifelong learning and the skills to self-educate as two of the major requirements to survive and succeed in upcoming demanding work environments.

Considering that future companies are likely to have an ever-smaller pool of core full-time employees for fixed functions, backed up by colleagues in other countries and external consultants and contractors for specific projects [7] a skillset with intercultural communication abilities appears to be key in such context. Considering the envisaged working scenario, companies are most likely to prefer contracting employees that have strong English and inter-culture language skills, thus enabling efficient global communication networks among their workers, suppliers and clients.

3. The role of intercultural skills in the workplace

English has been, in the last few years, chosen as the language of work or the corporate lingua franca. Due to the growing internationalization in the current global market, workers need to be prepared to express themselves in English. Increased globalization implies that countries, companies and also individual business need to collaborate and compete internationally. The internationalization and the increased volume of trade between Europe, the US, and Asian countries are responsible for the growth of non-western research [15]. Mostly the use of English in Portugal, and also in the Castelo Banco region, is due to the fact that English is generally used in companies especially in those with international contacts.

The growing globalization, the presence of foreign companies in the country, Portuguese companies having international contacts and foreign investors buying Portuguese companies (for example

Chinese) suggests the choice of English as communication language. In this context, the lack of foreign-language and intercultural skills is often pointed-out as the cause of a significant lack of opportunities in the corporate world [16]. Considering that in a global competitive market the communication language skills have been proven to be increasingly important, a framework strategy for multilingualism was proposed by the European Union, based on the notion that a lingua franca for communication has to simultaneously support the linguistic identities of those who use it for fear of loss of identity. As a result, a study was commissioned [17] in an attempt to estimate at a European level the cost of not having such foreign language skills (3 foreign languages).

The data of the study was based on a sample of 2.000 small and medium-sized enterprises across Europe and allowed to conclude, e.g., that recruitment of staff with language skills is already a commonplace among major companies, with 73% of respondents referring that they had an established scheme for recruiting language-skilled employees whilst a further 20% said it was common practice. This shows that companies are concerned with adapting to global market's challenges and strategies and that demand from current and future workers' significant levels of intercultural linguistic and communication skills.

To meet and exceed the demands of the ever changing and competitive global market, the effort to investigate ways to help and develop linguistic and communication skills among current and future workforce is key. In the light of the disruptive changes driven by the forthcoming Industrial Revolution, it is important to assess current workers' language and communication skills in order to develop dedicated strategies that may foster the envisaged skillset alignment, especially on low density and peripheral territories. To this end, a pilot experience was developed in the region of Castelo Branco, classified as a peripheral territory in the Portuguese context, based on the following research question: « What is the Portuguese Castelo Branco Region local workforce perception regarding their English intercultural communication abilities? ».

4. Methodology

This study utilized a self-developed survey questionnaire to identify the perception on English language skills as well as the communicative events in which English was mostly used by the Portuguese Castelo Branco Region local workforce. The information for the development of the survey questionnaire was based on structured and semi-structured interview guidelines. These guidelines were supported on previous studies focusing on needs analysis, feedback from informal in-depth interviews and discussions with local employees, as well as on the teaching experiences of the researchers.

The need to know what are the interviewed population's effective intercultural English language

communication skills should definitely help defining strategies to enhance and widespread such abilities. Therefore, the scope of the questionnaires included all four language skills, namely reading, writing, speaking and listening. A strong emphasis was put on the employees' productive skills, namely writing and speaking. Even though several data collection methods may be used in current pilot investigation [18], qualitative research interviews could be more appropriate, considering that the study aims to collect the individual perceptions of a process within a social unit [19]. To support the interviews, taking into account the enquiry purpose, combined structured and semi-structured interviews were preferred, since they traditionally address qualitative research and are recommended for situations where the aim is to collect the interviewees' perception of reality when the interviewer has already identified the issues to address [20].

Data were collected at the interviewees' workplaces and an interview guide was used to ensure that all relevant topics were covered. In order to fulfil the objectives defined by the research question, a questionnaire with both open and close questions was designed and tested with peers [20]. Questions were grouped according to the enquiry objectives and ordered, taking into consideration the data analysis technique and the intended output [21]. A total of 36 interviews were conducted in diverse industrial and service driven companies within the Region of Castelo Branco in Portuguese language. After transcribing the interviews into English, the responses were coded and analysed [22, 23].

5. Preliminary findings and discussion

Considering the skillset alignment envisaged by current digital industrial revolution, English language intercultural communication skills show to be key to allow future workforce adapting to such scenario, considered especially demanding for low density or non-central regions. This exploratory investigation intends to assess current workforce language skills in the region of Castelo Branco, currently classified as a peripheral territory in the Portuguese context.

To this end, a pilot experience was developed in small scale and large local companies, with average workers ranging from 5 to 250 employees. Structured and semi-structured interviews were conducted in a small focus groups of different industrial and service companies in order to assess local workers English language skills, as well as their intercultural communication abilities. To help outline the interviews, several qualitative sub-questions were also derived from the main research question and will be described in this preliminary findings discussion.

• Interviewees' profile

In this pilot investigation, the interviewed population was classified into different categories, considering their role in the company, which ranged

from chief executive officer to regular worker staff. Thus, approximately 3% referred having an upper management role, 11% referred a high-skilled technical job, 17% referred an intermediate management role and 69% were regular workers. These values per category are considered representative of the type of companies studied, maintaining a close correlation to such corporations' worker distribution. In what concerns the gender ratio, 89% were male employees, whilst only 11% were female. The latter index is significantly lower than similar figures published regarding national employability by gender [24], stating that Portuguese employed population in first trimester 2016 presented a 51% male / 49% female gender ratio. Such difference is due to the industrial nature of some of the companies studied, which have a large male working population basis.

In what concerns their academic qualifications, 4% of regular workers referred having a degree, the majority (76%) stated being undergraduate, and the remaining referred having lower academic qualifications. As for the upper level employees, qualifications were distributed according to a 36% graduate / 74% undergraduate proportion. Globally, in the companies at issue, the assessed ratio was of 13.9% - 72.2% - 13.9% for graduate – undergraduate – lower qualifications. Again, such figures differ from national published data [24], where a 25.8% - 25.8% - 48.4% ratio was referred for this year's first trimester on a similar graduate – undergraduate – lower qualifications ratio.

• *English skills and private life*

The focus-group participants filled-in a dedicated self-assessment form to evaluate their English language skills. As a result, 12% of regular workers referred having absolutely no language skills, whilst the remaining were distributed in a 60% - 16% - 12% proportion when referring lower (basic user) – intermediate (independent user) – higher (proficient user) English language skills. For the remaining upper-level employees, such proportion varied by 55% - 27% - 18% proportion regarding the same basic perception on independent – proficient user English language skills. A slightly higher language proficiency of the upper-level employees can be identified when comparing the self-assessments results. The majority of those who claimed having intercultural communication abilities stated that it was easier for them to speak and interact with others in English than reading in such foreign language. Writing in English was perceived by all as the most difficult communication ability.

When asked about the relevance of English in their private life, a large majority of respondents indicated that English was very important in their personal life, using it mostly to communicate and interact with others. Only a minority, approximately 12% of regular workers, referred not having any need for English language skills in their personal life. It should be pointed-out that this proportion is exactly the same of those who claim they have no English

communication abilities, i.e., the ones having absolutely no language skills feel that these are not essential to their private life.

• *Use of English at the workplace*

When referring to the use of English at the workplace, 73% of higher level employees of the focus-group stated that its use was very important, against 27% referring just a moderate importance. For regular workers, such importance ranged in the following ratio scale: 21% - 46% - 25% - 8% (very important - moderately important - slightly important - no use). With such figures, one can conclude that just 8% of the regular workers allocated no significance to the use English language in their workplace. On the contrary, all qualified worker effectively attributed to the use of English a very high, or at least a moderate importance in their workplace. These figures are particularly significant as they refer to current work situations, and not to the envisaged industrial revolution paradigm disruption, where a very high importance of the use of English can be foreseen.

The effective use of English at the workplace on a regular basis was stated by 45% of higher level employees, against almost half (24%) of regular workers. Again, for the 36% of high level employees indicating a sparse use of English, corresponded almost half (20%) of regular workers considering a similar periodicity of its use. Finally, in opposition to 9% of high level workers indicating an occasional use of English in the workplace, more than six times (56%) regular workers pointed-out such seldom use in their work-related tasks.

In what concerned the kind of use of the foreign language at the workplace, most respondents referred its use to communicate and interact with others. Also, almost every local worker, amongst the interviewees stating the relevance of using English at their workplace, emphasised its use to read technical manuals or to talk with foreign visitors, e.g., clients, instructors or suppliers. Local employees also make reference to the use of English on a regular basis when receiving or sending formal e-mails. Finally, most of higher level employees also stated using English language skills to analyse or write companies' proposals or to negotiate with clients or suppliers.

• *Personal viewpoints on English language skills*

In the final part of the interviews, local workers discussed their perceptions regarding personal English language skills in the context of the assignments they carry out in local companies. When asked if they considered having enough language skills to perform their professional tasks, almost one third (27%) of high level employees referred such lack of skills against half of that ratio regular workers (12%) identifying the same gap. Nonetheless, all of the high level employees referred wanting to improve their proficiency in English, against 26% of regular workers stating absolute lack of interest in such skills improvement.

When questioned if they thought that intercultural communication abilities in English could influence their professional future, all of high level workers agreed to such statement, whilst for the regular workers only 12% did not agree to that. Again, this corresponds to the same ratio of workers previously referring not having any English communication abilities, as well as having no need of language skills in their private life.

On the other hand, to the question if they thought that improving English communication skills would enhance their future professional lives, all higher level employees were unanimous in agreeing to that statement, against 8% of regular workers referring having already all the skills needed and other 8% stating no interest in the subject.

Finally, when asked if they were available to improve their current English language skills, 82% of higher level employees showed interest in acquiring further communication skills, even if they had to pay for it. The remaining 18% showed such availability if lecturing was free, or paid by their employing company. In what concerns the regular workers group, 20% would pay for lectures, 36% would attend if it was free and 28% referred availability if the employer would pay, 8% of regular workers referred having already all the skills needed and the last 8% showed no interest in gaining or improving such communications skills.

In what concerns the interviewees referring having absolutely no language skills, most felt that such communication abilities weren't essential to their personal or professional lives. Therefore, these interviewees showed no interest in improving on such lack of skills. As a consequence, these seem to be the most endangered working class types when considering the aforementioned disruptive skillset alignment foreseen by the forthcoming industrial revolution. By doing so, they are not only not aware of the importance of communication skills to their future professional tasks but they may also get excluded of further qualification and adaptation to the new demands foreseen to future workforce in upcoming dynamic and competitive companies.

6. Summary and future research

In order to enhance the development of dedicated strategies which may foster the skillset alignment of low density and peripheral territories, a pilot experience was carried-out focusing on the assessment of Portuguese Castelo Branco Region local workforce perceptions regarding their English intercultural communication abilities. A selected number of interviews was conducted among local companies' workers in the region under analysis. Preliminary findings showed that higher level employees were more sensitive to intercultural communication abilities and needs for work-related tasks and in personal life, when compared to regular workers' expectations and needs perception. Those that feel they have the skills to communicate in English, also highlight their need to continue on-the-job

training in that area, in particular in what concerns writing skills. However, even though a large majority of employees were aware of their needs relating English language communication skills, a significant effort is still needed to promote its widespread increase in local companies, since employees who lack the aforementioned skills fail to recognize its importance for their future employability and work potential.

Further research is needed to validate this pilot investigation, broadening the research to a wider public, *i.e.*, to more companies and to a larger base of activities within local regional economic activity. This research may eventually also bring out into the open the intercultural skills that come from using English as a lingua franca or a language for communication among diverse cultural identities in plurilingual international work settings, as such skills will be particularly useful to prevent work conflicts and mediate between people. In third place, crossing the findings amongst a larger base of results may allow identifying prospective advantages regarding the challenges foreseen to the local entrepreneurial ecosystem by the change of events expected with the forthcoming new industrial revolution.

7. References

- [1] Trew, A., 2014. Spatial takeoff in the first industrial revolution. *Review of Economic Dynamics*, 17(4), pp. 707-725.
- [2] Kanji, K.G., 1990. Total quality management: the second industrial revolution. *Total Quality Management*, 1(1), pp 3-12.
- [3] Greenwood, J., 1997. The third industrial revolution: technology, productivity, and income inequality. *AEI Studies on Understanding Economic Inequality*. The AEI Press.
- [4] Cooper, C., Kaplinsky, R., 1989. *Technology and Development in the Third Industrial Revolution*. Frank Cass & Co. Ltd.
- [5] Schwab, K. 2016. *The Fourth Industrial Revolution*. World Economic Forum.
- [6] Dombrowski, U., Wagner, T. 2014. Mental Strain as Field of Action in the 4th Industrial Revolution. *Procedia CIRP*, 17, pp.100-105.
- [7] WEF-World Economic Forum, 2016. *The Future of Jobs Employment, Skills and Workforce Strategy for the Fourth Industrial Revolution*. Global Challenge Insight Report.
- [8] Myers, J.L. & Greenson, J.K., 2012. Life-long learning and self-assessment. *Archives of Pathology and Laboratory Medicine*, 136(8), pp.851-853.
- [9] Aynur, E. & Bülent, Y., 2009. Lifelong Learning and Public Libraries in Turkey Yaşam Boyu Öğrenme ve Türkiye'de Halk Kütüphaneleri. 23(4).
- [10] Preece, J., 2013. Africa and international policy making for lifelong learning: Textual revelations. *International Journal of Educational Development*, 33(1), pp.98-105.

- [11] Hursen, C., 2014. Are the Teachers Lifelong Learners? *Procedia - Social and Behavioral Sciences*, 116, PP. 5036-5040.
- [12] Ozdamli, F. & Ozdal, H., 2015. Life-long Learning Competence Perceptions of the Teachers and Abilities in Using Information-Communication Technologies. *Procedia - Social and Behavioral Sciences*, 182, pp.718–725.
- [13] Scheer, A., 2013. Industrie 4.0. IMC.
- [14] Laal, M., 2011. Impact of Technology on Lifelong Learning. *Procedia - Social and Behavioral Sciences*, 28, pp. 439-443.
- [15] Bargiela-Chiappini, F. et al., 2003. Five Perspectives on Intercultural Business Communication. *Business Communication Quarterly*, 66(5), pp.73–96.
- [16] Beaven, A., Livatino, L., 2012. CEFcult: Online assessment of oral language skills in an intercultural workplace. *Procedia - Social and Behavioral Sciences*, 34, pp. 25-28.
- [17] CILT-UK National Centre for Languages, 2006. ELAN: Effects on the European Economy of Shortages of Foreign Language Skills in Enterprise.
- [18] Yin, R.K., 2009. *Case Study Research: Design and methods*, London, UK: SAGE Publications.
- [19] Robson, C., 2002. *Real World Research* 2nd ed., London, UK: Blackwell Publisher Ltd.
- [20] Gillham, B., 2000. *Case Study Research Methods*, London, UK: Continuum.
- [21] Oppenheim, A.N., 1992. *Questionnaire Design, Interviewing and Attitude Measurement*, London, UK: Pinter Publisher.
- [22] Miles, M.B. & Huberman, A.M., 1994. *Qualitative Data Analysis: An Expanded Sourcebook*, Thousand Oaks, CA: SAGE Publications.
- [23] Flick, U., 2009. *An Introduction to Qualitative Research*, London, UK: SAGE Publications.
- [24] INE, 2016. *Estatísticas do Emprego - 1.º trimestre de 2016*. Instituto Nacional de Estatística, May 11th 2016.

BRAND:
«SMART MECHATRON - Competitiveness,
performance and high quality through
HIGH-TECH MECHATRONIC PRODUCTS »

THE PORTUGUESE TEXTILE INDUSTRY BUSINESS CO-OPERATION: INFORMAL RELATIONSHIPS FOR INTERNATIONAL ENTRY

Vitor Braga¹, Ana Cristina Gonçalves², Alexandra Braga³

¹*School of Technology and Management of Felgueiras – Porto Polytechnic; CIICESI; CETRAD, vbraga@estgf.ipp.pt*

²*School of Technology and Management of Felgueiras – Porto Polytechnic; CIICESI, crisalvarinho@gmail.com*

³*School of Technology and Management of Felgueiras – Porto Polytechnic; CIICESI; CETRAD, abraga@estgf.ipp.pt*

Abstract—This article discusses the process of cooperation for internationalisation; with special focus on the informal inter-firm cooperation relationships in order to identify how such relationships contribute to the process of internationalization and their permanence in the market. A study with textile SMEs was conducted, providing evidence of the importance of the firms' structural features and, mostly, trust relationships for developing collaborative relationships allowing the exchange of knowledge related to technology, the market and products, as much as on, generally, business management. Data was collected through the administration of surveys to textile production SMEs. Although our results show the existence of inter-organizational informal cooperation mechanisms, the low number of answers by itself is an important result - firms are reluctant with regard to cooperation with scientific research. Although this is a limitation to the data analysis, on the other hand it is an interesting finding, as it demonstrates SMEs willingness to collaborate with higher education institutions.

Keywords: Informal cooperation, Internationalization, International Entrepreneurship, Business Networks, Textile industry, Portugal

1. Introduction

The constant changes observed in the international economic scenario, due to multiple factors such as the globalization of markets, instability in demand and increased competition, triggered new forms of organizing the production. In this context, the emergence of new competitive and more flexible strategies in production processes is inevitable. Therefore, inter – firm relationships, are one of the possible strategies to overcome these difficulties. Firms collaborating with other organizations (customers, suppliers, competitors etc.) aiming to promote an environment conducive to information sharing, new knowledge, new skills and resources essential to the innovation process may become successful actors in the competitive market.

The internationalization process embodies a certain level of difficulties, such as the foreign acceptance of the product / service, cultural and geographic distance and the barriers to trade (standards and regulatory fees). These difficulties depend, mainly, on the quality and availability of resources and the competitive ability of organizations to react to international competition.

Firms, particularly SMEs, in order to be competitive should not act in isolated but, instead, by fostering alliances or entering business networks (Casarotto & Pires, 2001). This is the basis for the need

to develop partnerships with other organizations, so-called inter-organizational ties that need to be lasting and strategically significant for both sides (Zaher, Gulati and Nohria, 2000). These relationships translate into numerous benefits for businesses, however, it requires setting aside some cultural aspects that define the firm as a separate organisation, and the firm is required to know / learn to tolerate, compromise and abandon individualism in favour of a relationship based on partnerships involving trust and commitment (Morgan, 1994). The establishment of inter-firm relationships can provide advantages related to entrepreneurial growth and development.

The main purpose of this article is to understand the role of informal cooperation in business internationalization processes of the Portuguese textile SMEs. It is aimed to study informal cooperation as a strategy and to demonstrate its importance in the international business context. The specific objectives that guided this research are:

- To learn what business activities may work as a barrier to internationalization;
- To know the co-operation mechanisms used by firms, for entering international markets;
- Describe the inter-firm relationships inter-firm aiming to enter and remain in international markets.

2. Literature Review

Business cooperation

In order to overcome certain limitations (size, economic, technological, etc.) and to achieve common goals (expected gains both parties), firms establish relationships based on cooperation, characterized by the existence of interdependent goals and the share of resources (Easton & Araujo, 1992) assuming the independence of the actors. This interaction between firms, over time becomes stronger and competitive.

Thomson and Perry (2006) define collaboration / cooperation as:

"Collaboration is a process in Which autonomous actors interact formally and informally through negotiation, Jointly creating rules and structures governing Their relationships and ways to act or decide on the issues que expreso Them together; it is a process Involving shared norms and mutually beneficial interactions. "

The neoclassical theory considered the economic agent, an isolated individual, lacking social ties. Currently, economic sociology contributed with the perspective that the decisions and economic ties are rooted in a broad system of social relations. The interaction with other organizations, resulting on the firms' ability to accept competitors as partners, brings benefits resulting on organizations finding themselves led to change their mindset (Borba, 2010) becoming more receptive and open to organizational learning.

Cooperation between firms can contribute to the competitiveness of businesses through efficiency gains in customer service, acquisition of new customers, new products, greater knowledge, access to technology, and improving the image and reputation of the firm (Hausman, 2001 and Gadde & Snehota, 2000). In short, firms seek to establish relations of cooperation, in order to share knowledge, information, identity and a common language, or seek to obtain resources, skills and capabilities. In inter - organizational relations, the process of knowledge transfer can be channelled formally or informally, through processes of social interaction and internalization, that may, also, take place in the context of personal and informal networks (Powel et al, 1996).

Formal Vs. Informal co-operation

Cooperation may be formal or informal. Formal cooperation is established when a written agreement between the parties involved in a particular business is necessary. Formal cooperation in the context of internationalization may take the form of operating licenses; franchising; outsourcing; joint ventures; and export consortia. Formal organizations are relatively more bureaucratic because their businesses are based on regulations.

The informal cooperation is based on inter-organizational relationships can be developed independently or jointly with formal cooperation.

The table below shows to some of the differences between the two types of cooperation:

Table 1 - Differences between formal and informal cooperation

Formal cooperation	Informal cooperation
Easy identification of collaborative partners	Difficulty in identifying collaborative partners;
Contract-based (the development process of cooperation progresses rapidly)	Initiated by the interaction (its development requires more time)
Cooperation does not always include a reliable partner (low trust levels may exist);	Trust-based cooperation
Started by senior staff of the administration who do not participate in the relationship	Developed by actors directly involved in the cooperation process (often through manager or other staff)

Source: Hakansson & Johanson (1998)

The fact that there is a written agreement may facilitate the resolution of potential conflicts that may arise during the agreement. However, an agreement on the basis of informal cooperation could contribute to a better relationship between the parties involved, and therefore greater sustainability of the business relationship may be observed.

Informal cooperation within the framework of informal networks is an invisible, but powerful, tool. In organizations, the boundaries of the firms still exist, but co-operation may be the means to add on to the formal channels (Cross & Pruzak, 2002). The possibility of joint understanding between the parties involved in the relationship may contribute positively to the organization and combining the two types of co-operation may behaviour have a positive impact on the results of business co-operation.

Informal cooperation

Despite the potential interest of informal cooperation it has not received much attention, both at the corporate level and academically (Gulati & Gargiulo, 1999); (Galaskiewicz & Mizruchi, 1993); (Uzzi, 1997). It is associated with social networks and social capital, and contributes to reducing information asymmetries and thus reducing also transaction costs (Gulati, Nohria, Zaheer, 2000). In a process of interaction that gives rise to networks, informal and personal relationships become increasingly fundamental to the competitiveness of organizations. Values such as trust, reciprocity, loyalty, commitment will form the basis of lasting informal relationships that promotes strategies based on sharing, thus helping firms to become more competitive and to offer to the market value.

Informal co-operation requires trust between the parties involved in the relationship and trust, on its turn requires the existence of a close relationship based on historical interaction and commitment, aimed at mutually agreed goals. Within informal cooperation, the firms develop relationships of mutual trust that can

provide advantages in terms of stability and security of the business, as well as the level of efficiency and productivity, resulting in a better coordination of activities. Such cooperation allows information and knowledge exchange (Biggiero & Samarra, 2008); provides greater diffusion of innovation (Powell & Grodal, 2005) and further development of social and organisational culture and values; and more efficient management. For Bachmann (2001) trust is considered a key factor in relations within and between organizations. For Phillips & Lawrence (2003) it is elementary that in a confidence building process, the collaboration partners communicate with fairness and sincerity and that are free of representation of their interests devoid of manipulation, coercion and concealment. For Jarillo (1993), trust is developed gradually, aimed to mutually compatible interests, reducing the possible existence of opportunistic behaviour. The existence of such behaviour, as well as the lack of credible commitment, undermine trust, discourages cooperation and negatively affects the business relationship, thus contributing to the existence of risks and threats associated. Confidence assumes, thus, an essential role in the coordination mechanism of social expectations and interaction between the partners (Bradach & Eccles, 1989). For the development of this mechanism, information management needs to be valued, which favours, according to Morrow (1999) sharing information and knowledge, and maximizing co-operation opportunities. Trust can be considered a social institution in creates behavioural patterns, and expectations. This view is very important as it influences institutions in business decisions (Lam, 1997). Thus confidence can be seen as a form of informal institution, which is a detailed set of rules and codes applied within defined limits. These institutions are the result of a set of social conventions and behaviours accepted by society.

So that there is sustainability in informal relationships, management based on loyalty avoiding opportunistic behaviour and power struggles is essential. Associated with power is inherent in the idea of control or influence of one or more of the partners involved in the relationship. Some authors emphasize the role of the reputation of partners in collaborative relationships. Dollinger, Golden & Saxton (1997) argue that the characteristics of decision-makers may overlap the reputation of the organization itself and that reputation affects decisions regardless of the type of partnership. In this sense, a good relationship derives from the reputation of the partners, which besides being a critical factor of success, the cooperation strategies are also a key element in their structure.

The problems related to the loss of trust, reputation and commitment amongst the members of networks can undermine the objectives of their members in terms of equity, efficiency, and adaptation. In a scenario where these characteristics are absent, it is likely that the network is sentenced to failure. Park & Ungson (2001) show that the predominance of competition among firms may be the cause of the failure of the alliance.

Inherent to the potential failure of the network or collaborative relationships may be competition

between the members, which may cause rivalry between firms and consequently the existence of opportunistic behaviours, which is considered by Williamson (1985) the main cause for the existence of market failures . Opportunism results in asymmetric returns, resource ownership by firms and adverse situations that lead to the failure of the alliance. On the other hand, the failure may also arise from the complexity of the relationship management, originated by the cultural differences within the network, which can cause internal conflicts, affecting the creation of synergies. Failure to obtain economic benefits and the lack of common goals could jeopardize the rationale of the networks.

The inter-organisational informal networks have, commonly, their origins on individual relationships rather than on organizational ones. According to Kuipers (1999), there are individuals' actions that may trigger informal networks:

The informal interaction between groups of people;

Individuals who connect to the network frequently and spontaneously because they share the same needs, values and common interests with other network firms;

Interest in communicating, sharing or achieving goals they aim for.

When consolidated informally, networks can lead to improvements on organizations with regards to coexistence and frequent interaction between individuals, as well as easing the access to other organisations. Castilla et al (2001) highlight some organizational benefits of informal networks:

Table 2 - Benefits of informal networks

Organizational benefits of informal networks
Support and social ties;
Support and security;
Cognitive Guide and advice;
Material aid and services;
Access to new contacts (internal and external);
Sharing and information flow;
Bonds of affection;
Regulating access to work;
Improved access to information and distribution opportunities;
Power and status;
Extent to which the individual learns and internalizes the occupational standards.

Source: Castilla et al. (2001)

Strategic alliances for international entry

Cooperation has been a phenomenon of some interest to academics and the business community, where growing popularity is visible through the study of a particular case - strategic alliances. Strategic alliances and other forms of cooperation have been a strategic option increasingly used by firms. They arise from the need to gain competitive advantage, thereby strengthening each member of the network, and will only be obtained if each member views it as an opportunity for learning and not for their own benefit (Hamel et al, 1989).

Strategic alliances, result in the following benefits (Doz & Hamel, 2000):

- Access to new markets;
- New opportunities arising from the combination of complementary skills and resources;
- Construction of new competences associated with the need for a strategic positioning.

Strategic alliances are defined as volunteer organizational arrangements relating to the exchange, sharing and joint development of technologies, products and services (Gulati, 1998). According to Robert & Baden-Fuller (2004) strategic alliances are associated with formalising or contracting strategic cooperation between organizations involved in the relationship, Teixeira & Diz (2005) add to this definition, stating that these agreements are characterized by reciprocity or by the combination of efforts and responsibilities between the firms. A strategic alliance occurs when two or more organizations decide to join their efforts to achieve a common strategic goal. In this context, firms combine resources and activities, maintaining its autonomy (as individual being), but with a certain level of bilateral dependence.

Strategic alliances are, often, used as a synonym for cooperative relations, although in the opinion of Faulker and Easton (1992), a strategic alliance brings together features that cannot be found elsewhere, providing them with greater strategic importance when compared to other forms of cooperation or with regard to operational alliances (non - strategic). These alliances typologies are different, however, they can, sometimes, be confused. According to Hax & Majluf (1988), Johnson & Scholes (1999), alliances are, at an initial stage, operational and they evolve to strategic. It is, however, important that all actors are aware of the objectives in order to avoid mistaking the type of alliance – while some may be expecting an operational alliance and others may be interested in a strategic alliance. The table below identifies some differences between strategic alliances and other types, including the non-strategic or operational ones.

Table 3 - Characteristics of strategic alliances

Differences between strategic alliances and other forms of cooperation / alliances
Result of a coherent set of decisions; It is a means to develop a sustainable competitive advantage It has long-term organizational impact; They are used as a means to respond to opportunities and external threats; They are based on organizational resources that show strengths and weaknesses; Affect the operational decisions; Involve all levels of organizations; Are influenced by the surrounding environment, politics, culture, etc. They involve all the activities of organizations, whether right or indirectly.

Source: Adapted from Hax and Majluf (1988) and Johnson and Scholes (1999)

According Fishmann (2004) strategic alliances can also bring limitations to organisations, such as the high degree of dependence of the relationship, which can be translated in a decrease of corporate efforts in pursuit of perfection.

The literature on the subject covers various types of strategic alliances; Aaker (1995) emphasizes the degree of formalization of the agreements, to demonstrate that alliances can take many forms, from informal arrangements to formal joint ventures. Table below compares two typologies of alliances supported by two theories from two different authors, Faulker (1992) and Root (1988) that can be used to classify strategic alliances and international cooperation agreements, respectively:

Table 4 - Classification of strategies

Classification of strategic		
Faulkner (1992)		
1st dimension	Focused vs. complex	When the actor uses activities developed by the partners.
2nd dimension	Joint ventures vs. non joint ventures	It is related to the capital and the legal form of the alliance.
3rd dimension	Two partners vs. consortium	It is related to the number alliance partners
Root (1988)		
1st dimension	The nationality	Agreements can be made within one country (national); between two countries (binational); or include several countries (multinational)
2nd dimension	Type of developed cooperation	The agreements may involve open market transactions, or intra and inter-organisational cooperation agreements

Source: Faulker, (1992) & Root, (1988)

For their expansion to international markets, firms, often, struggle to deal with foreign laws and difficulties inherent to understanding the host markets. Under such circumstances, strategic alliances, named as joint ventures, may be critical. This type of strategy is very common for firms pursuing commercial or production goals. They are attractive given their limited legal regulation and they are considered a low - risk strategy allowing firms to enter markets difficult to access. Firms see in international joint ventures a success mechanism, due to its flexibility, adaptability to different situations and the possibility of achieving the goals. According to Lorange & Johan (1996) joint ventures provide greater freedom of resource allocation and the resources generated tend to be kept within the strategic alliance. Some of the advantages of joint ventures are generating synergies, entry into different markets, strengthening the firm positioning and access to specialized know-how. It is a cooperative strategy

that can be conceived as a mechanism to achieve goals through cooperation (Child & Faulkner, 1998) contributing, thus, to improve the competitiveness of firms in domestic markets, to facilitate the entry of foreign firms in the domestic markets as well as expanding their business on a global scale. However, problems with certain aspects of regulation and competition may be a result of this strategy as there are a some unsuccessful joint-ventures attempts, resulting in a poor performance given the cross-country, cross-cultural, and economic conditions (Beamish, 2003).

Barriers to SME's International Entry

The internationalization process requires rational decision-making and objective goals definition (Schmitt Neto, 2005) In this sense the classical economic literature focuses on large firms (usually multinational companies – MNCs) as the object of analysis (Rowden, 2001); (Hollenstein, 2005); (Buckley & Ghauri, 1999), and these are better able to overcome market, commercial and political risks. By contrast, SMEs find certain difficulties such as the lack of human, financial, technological and information resources (Hollenstein, 2005); (Gemser & Brand, 2004). For Hollenstein (2005), in addition to severe limitations in terms of resources, there are also barriers associated to the international regulations, national laws and market needs, due to the uniqueness of different cultures.

The internationalization of large firms motivates small-scale ones, to strive and to overcome the difficulties associated to the expansion of their activities into international markets. Furthermore, technological advances, supported internationalization of firms regardless of their size, industry and location enabling SMEs to access new markets, strategically deciding upon forming cooperative alliances (Freeman & Schroder, 2006).

It should be noted that SMEs have had a growing performance in the contribution to the trade balance contribution of their countries, and that the SME niche exports were not affected by the size, whereas Chiara & Minguzzi (2002), refer to the firm size as a secondary aspect for external competitiveness. According to Naisbitt (1998) SMEs are contributing more to the creation of the global economy than large firms.

In order to access other markets, SMEs define strategies that take into account the degree of involvement and type of control they aim to take to the international market.

3. Methodology

As commonly found in research a literature review was made on the issues related to the informal cooperation, in order to provide a theoretical framework for the research. References were sought for internationalization, networks, formal and informal cooperation and the barriers to international entry faced by SMEs. After such analysis, a survey was prepared to

be administered to firms operating in the textile industry. This survey was developed to meet the research objectives but supported in the literature reviewed earlier.

The results were generated using SPSS, where it was possible to carry out a descriptive analysis of the sector of activity. The information obtained allowed to draw conclusions about the role of informal cooperation for internationalization in the sector of firms in the study. Initially, the aim was to perform a factorial analysis, but the limited number of responses did not allow performing the statistical analysis.

In order to prepare the survey, several studies on the methods of preparing questionnaires were reviewed. The questionnaire administration process was divided into four parts:

Identification of firm – particular industry, main activity, legal form, turnover, location of activities, and number of employees;

Identification of the interviewee - sex, age, academic background, position within the firm;

Internationalisation process – international markets operations, motivations for international entry, country selection criteria, entry forms, product types strategies for international entry, external support provided, difficulties and aims for international entry;

Informal Co-operation – Partnerships and feelings associated, process and forms of partners' selection, motivations for informal co-operation, and advantages and outcomes.

Sample

For this study, the population considered was retrieved from database provided by ATP – Portuguese Textile Associated with all the firms located in the north of Portugal, where there is a very significant share of firms within the industry.

The data was obtained by questionnaire survey, which allowed determining the internationalisation stage that firms, within the industry, can be found. In the case where the internationalisation processes had already been triggered, it was also possible to assess if agreements based on informal cooperation were used. It has also allowed investigating the circumstances of internationalized firms, their motivations, as well as the strategies used to internationalize.

Regarding the inquiry process, an online survey and e-mailed to firms, explaining the context, objectives and process of the research. This survey was sent by email to a total of 544 firms (n = 544) of the various sub-sectors of the industry. It has been sent twice. Initially, emails were sent to firms included in the ATP database without the identification of the person expected to respond. Since only 10 responses were obtained, in the first stage (of which 1 was invalid), emails were re-sent, with an identification of the person that expected to provide the information (data was also obtained in the database). In the second stage, 487 firms were contacted questionnaires, 57 less than on the previous stage, as no information regarding the

respondent could be retrieved. At this stage 27 responses were obtained, of which one of them invalid. In total 37 responses were gathered, 35 valid 2 invalid, which is equivalent to a percentage of 6,43% response rate. In order to increase the response rate of the questionnaire some telephone contacts were made, to randomly selected firms. In addition, the researchers' network of contacts was also approached in order to gain access, directly, to managers and such a network of contacts was used as respondents' gatekeepers.

Table 5 - Methodological aspects

Geographical area	North of Portugal
Activity Sector	Textile industry
Firm size	SMEs (small and medium enterprises)
Sample / Population	Sample (ATP data)
Population size	544 Firms in operation
Data collection	Questionnaire survey (online survey)
Response rate	Questionnaires sent 544 (1 st stage); 487 questionnaires sent (2 nd stage); 37 responses obtained; 2 Invalid answers; Response rate: 6.80%; valid response rate: 6:43%
Respondents	Administrator, commercial, foreign market manager, accountant, Financial, Administrative
Data Analysis	Descriptive statistics

Source: Elaborated by the authors

4. Results

The Presence in international markets

In order to provide the context to the main topic of this paper - informal cooperation for international entry – it is important to provide an overview of the internationalisation stage of the respondent firms. In particular it was sought to find out about their motivations and strategies, which led the firms to engage into such a process. The analysis of the data reports that 84.38% of the firms are, already, operating in foreign markets, and the remaining (15.63%) are not internationalised. In addition, firms operating in firms choose several destination countries, although the majority relies on European markets (65%), with America (17%) and Asia (10%) coming in second and third, respectively

Within the criteria above mentioned, the possibility of strategic partnerships is the main motivation for entering particular international markets, followed by the geographical proximity, less risk markets and the possible of accessing to specialized agent. Therefore, entering a particular international market is, to some extent, result of the existing partnerships and firms seem to follow their network. This result confirms the relevance of the topic, since stresses the role of cooperation in the internationalization process.

In order to internationalize, firms need to choose the entry strategies in foreign markets. The questionnaire listed a number of possible entry forms, namely, exports, direct investment, strategies joint-ventures, franchising, subcontracting, licensing, and via agents. However, respondents identified only three ways to enter foreign markets: exporting, agents, and foreign direct investment.

In combination with the analysis of the host country, one can suggest that the theory of Uppsala School is confirmed, as firms tend to go, initially, for culturally closer markets and adopt the ways of easier entry.

In addition to the markets firms are willing to enter, the Uppsala theory also refers to the entry modes. The data shows that the most common entry mode (which is also the less compromising one) is exporting; followed by investment through agents and, finally, Foreign Direct investment. No other entry modes have been identified.

In what regards the promotion of products internationally, the most commonly found options are Online presence (websites social media, etc.) in first place; industry exhibitions represents the second most important entry mode; followed by partnerships; and finally merchandising. When in international markets, most firms choose, strategically, to adapt their products to the host market, with some of the products and services being sold with no differences to the domestic market.

The International Entry process

In addition to characterise the international presence of firms, it is also important to know how businesses have started the expansion into new markets. However, it is important to distinguish firms, which have entered the markets alone, from those which process has been supported by partners, in order to overcome potential difficulties to access international firms.

Within the respondents 60% refer to difficulties to internationalize but the remaining agree that it is a difficult process. Most of the respondents who have not faced difficulties to internationalize were also able do it alone, with only a small percentage being supported in co-operation processes. The remaining (who found internationalisation a difficult process) did not rely on partnerships. Overall, there were few firms that used partnerships to internationalize.

However, since the majority of the respondents was, already, with an internationalization processes in progress, strengthening their presence in international markets was also important to analyse, from a co-operation perspective.

Based on the table below, it is possible to explore the role of partnerships on entering or expanding international presence.

Table 6 – The role of partnerships international contacts

		Have you ever been contacted by other firms in order to establish informal cooperation partnerships?			Total
		No	Yes		
International market share	Up to 10%	0	2	0	2
	10% to 30%	0	1	0	1
	30% to 50%	0	3	1	4
	50% to 70%	0	0	1	1
	70% to 90%	2	1	6	9
	Greater than 90%	1	2	1	4
Total		3	9	9	21

Source: Elaborated by the authors

Of the 21 responses received on this question, 12 firms refer that they had never been contacted in order to establish informal partnerships with 9 being contacted. It is important to note that, for 7 of the 9 firms who have been contacted for establishing partnerships international markets represent more than 70% of their total turnover, i.e., as firms increase their presence in international markets they also become more attractive for other firms to engage into partnerships.

With regards to the future of firms in the international market context, it is found that 95.24% plan to increase their international market share, in the subsequent year. Based on an open question for exploring firms goals for the subsequent year, respondents refer to sales growth; new products; new markets; increasing exports; expanding the networks of agents / importers in markets where they already operate and in new markets; increasing the number of markets; and exploring new opportunities.

The Selection of Partners and forms of partnerships

Cooperation involves the existence of partnerships. The economic actors with whom such partnerships are possible varies, as firms, on their daily routines interact to a number of potential partners. In order to know which are the most important actors for establishing partnerships, respondents have identified gatekeepers to contacts that may become future partners. The respondents consider customers as the main actors that assist on the process of introducing partners, followed by, with the same importance, suppliers, associations and the family. While the gatekeepers may put the firm in contact with potential partners, the subsequent process refers to selecting the actual partners, among those that are available. In order to investigate this process, the respondents have identified what are the most important forms of selecting the partners. The personal relationships of the entrepreneur seem to be the most commonly adopted form (representing the vast majority of the responses). The data reveals that the selection of partners occurs

through personal knowledge (77.8%), interest shown by other organizations (22.2%) and by previous studies to businesses, market research and social networks. It is in general partnerships that last for many years and are mostly informal partnerships. It is also noted that entrepreneurs live (in their personal and social life) informally, sometimes with partners.

Firms opt for informal cooperation between enterprises in order to access the new knowledge (53.3%), new markets (53.3%) and resources. The capacity for innovation and responsiveness are also considered factors that contribute to informal cooperation (20%). The firms have been aware of this type of strategy, through informal conversations.

Contribution of collaborative partnerships for the development of firms

The inter-relationships may promote the growth and development of enterprises. In this sense, we aim to find out if the business environment of the industry reinforces of informal cooperation as a catalyst for entrepreneurial development and growth.

In line with the fundamentals of informal co-operation, respondents were asked about the frequency of ideas exchange with other entrepreneurs, with 72.7% acknowledging such process. However, only a very small part of the respondents did not consider the informal co-operation as a means for entrepreneurial growth. In addition to such insights, 83.3% of the respondents agree that they would, again, be engaged in to collaborative relationships, as they recognise the resulting advantages. Such advantages are, according to the respondents the knowledge exchange about new business opportunities; finding new business partners and customers; trust levels developed throughout the process; and the access to new markets allowing, in some cases, firms to enter markets different from their domestic one.

In addition to the internationalization process it is also important to assess what motivates firms to enter such internationalization process, as displayed in the figure below.

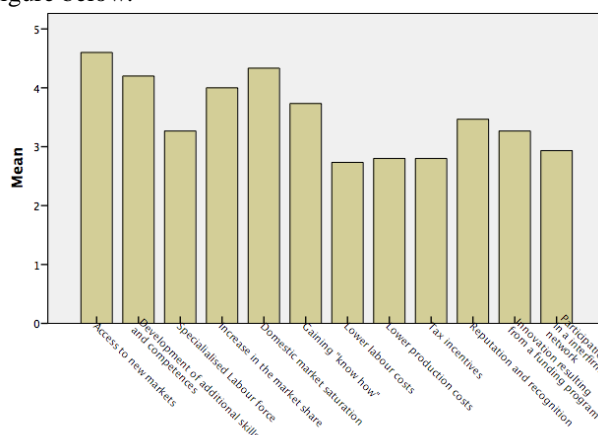


Figure 1 - Reasons motivating firms to international entry

Source: Elaborated by the author

There are several reasons that motivate firms to enter international markets. However, taking into account the chart above, access to new markets, market saturation, developing new skills and increased market share are those that influence the decision of firms.

At the same time it is also important to assess barriers that firms face in the internationalization process. These factors can be overcome by establishing partnerships, but for this it is necessary to identify these barriers and ensure that firms are willing to share the process of internationalization.

The data shows that, high competition, the price, the financing difficulties and the lack of information, they are considered the major barriers and / or difficulties encountered by enterprises to enter international markets.

The feeling of the firms before the entry into new markets with informal partners, gives an idea of the results of informal partnerships with the goal of internationalization.

In addition, the results obtained show which is the sense when firms resort to informal partnerships to internationalize. Responses with more emphasis on this issue were in particular: enter into partnerships with people or institutions I trust a lot and the importance of shared goals. This process is also important to choose one or more partners with whom there is a close values. In this context, firms were asked about what factors are decisive in the choice of partners for the process of internationalization, as the chart below.

Taking into account our results it can be concluded that most of the figures are essential for a partnership works well, however stand out, confidence, respect, common sense and collaboration, as those who most important is. On the other hand, there are factors, which are seen as barriers to establishing partnerships.

Apart from the advantages inherent in the proper functioning of a partnership, there may be less favourable situations detrimental to the relationship. According to the respondents, concerning situations are the opportunistic behaviour, dishonesty, abuse of power and convenience.

5. Conclusions

Based on the results obtained it is possible to identify the firms that are more open to informal cooperation. These are, mostly, mature SMEs, with more than 50 employees, and mostly managed by administrators (owners), aged between 40 and 54 years old and with a degree of training at the undergraduate level.

Firms are mostly, internationalized and have future goals of expansion and consolidation of markets. They began the process of internationalization, alone, without the support of partners. The form mostly used, in industry, to internationalize is exporting. The motivations that led to internationalize were related to the access to new markets, development of new skills, increased market share and the saturation of the

domestic market. The main barriers were particularly high competition and price.

With regards to informal cooperation, the respondents identified mechanisms to share ideas and business with other entrepreneurs, partnerships that occur based on personal knowledge and that are established, mainly, with clients that engage in enduring informal agreements. Our results also suggest that the use of informal cooperation arises from their necessity to access new knowledge and new markets, and it is based, primarily, on the values trust, common sense, respect, cooperation and honesty. However, not all relationships operate as expected and the lack of honesty and opportunistic behaviour may be the cause of misunderstandings between the parties and as a result the end of the relationship.

With regard to performance, most firms consider the use of informal cooperation may leverage the industry needs to allow growth and development. Respondents believe the informal cooperation benefits them and, as a consequence, they recommend such practices

It corroborates the importance of informal relationships regarding collaborative partnerships. The small number of observations is also explained by the absence of a personal relationship between the researchers and the potential respondents. In fact, it shows a reluctance of firms in the industry to collaborate with higher education institutions and, therefore our results are unable to characterise the industry, but rather our results are valid to characterise a group of firms, which are willing to collaborate with scientific research. Accessing to different groups, within the industry, could reveal different perspectives on informal co-operation; however access to such groups could provide different results.

6. References

- [1] Aaker. D. (1995). *Strategic Management Market*. New York: John Wiley & Sons.
- [2] Bachmann. R. et al (2001). *Trust and control in organizational relations*. *Organization Studies*. Ed 2, Vol. 22).
- [3] Baden-Fuller., Robert. M. Grant., Charles. (2004). *The Theory of Knowledge Accessing Journal of Management Studies*. Vol. 41.
- [4] Beamish. P. (2003). *The design and management of international joint ventures*. Burr Ridge, Illinois: Irwin.
- [5] Biggiero.L., Samarra. A. (2008). *Heterogeneity and specificity of inter-firm knowledge flows in innovation networks* . *Journal of management studies*. 4 Ed, Vol. 45
- [6] Borba. . A. (2010) *Cooperates networks tio o: Reflections perceived by the participating firms*. Novo Hamburgo : Feevale.
- [7] Bradach. . J. (1989) *Rice, authority, and trust: From ideal types to plural forms* . *Annual Rev. Socio Ed* 15 .
- [8] Buckley. P. Ghauri, P. (1999). *The internationalization of the Firms*. Oxford.

- [9] Casarotto Son., Pires. . (2001) of small and medium enterprises and local development networks: strategy is gies for achieving global competitiveness based on the Italian experience. S ã o Paulo: Atlas.
- [10] Castilla. E., Choong Moon. L. Miller. W., Hancock. M. (2001). The Silicon Valley Edge. Stanford University.
- [11] Chiara A., Minguzzi. A. (2002). Success Factors in SMEs' Internationalization Processes: An Italian Investigation . Ed 2, Vol. 40.
- [12] Child. J. Faulkner. . D. (1998) Strategies of cooperation: Managing Alliances Networks, and Joint ventures. Oxford University press.
- [13] Cross. R., Pruzak. L. (2002). The people que make organizations stop - or go . Harvard business review. Vol. 80
- [14] Dollinger. M., Golden. P. Saxton. (1997). The effect of reputation on the decision to join venture. . Strategic Management Journal. 2nd Ed, Vol. 18.
- [15] Doz. . H. (2000) The advantage of alian ç as: the art of creating value through partnerships. Rio de Janeiro: Qualitymark.
- [16] Easton. G., Ara ú jo L. (1992). Non-economic exchange in industrial networks in Industrial. London: A New View of Reality Axelsson, B. & Easton, G. (eds) Routledge
- [17] Gadde. L. E. Snehota. I. (2000). Makind the most of industrial supplier relationship . Marketing management. Vol. 29.
- [18] Hakansson. H. Johanson. J. (1998). Formal and informal cooperation strategies international industrial networks. (FJCo ntractor, Ed.) Toronto: Cooperative strategies in international bussiness.
- [19] Hamel et al. . (1989) Collaborate with your competitors: And Win . Harvard Business Review. 1 Ed, Vol. 89.
- [20] Hausman. A. (2001). Variation in relationship strength and its impact or performance and satisfaction in bussiness relationship.
- [21] Hax. A. Majluf N. (1988). The concept of strategy and the strategy formation process . Ed 3, Vol. 18.
- [22] Hollenstein. . H. (2005) Determinants of international activities: Are sme's different? Small Business Economics. Ed 24
- Jarillo. J. (1993). Strategic Networks:.. Creating the borderless organization Oxford: Butterworth & Heinemann.
- [24] Johnson, Scholes, K. (1999).. Exploring corporate strategy . New York: Prentice Hall. Ed 5.
- [25] Kuipers. . K. (1999) Formal and Informal network in the workplace. Stanford: stanford university.
- [26] Lam A. (1997).. Embedded Firms, embedded knowledge: Problems of collaboration and knowledge transfer in global ventures cooperative . Organization Studies, 18 (6).
- [27] Lorange. P. Roos. . J. (1996) Alian ç the strategy is gicas: way tio the implements ction oe evolution ction it. S.Paulo: Atlas.
- [28] Maximiano. . A. (2000) General Theory manages tio the scienti school í is: Competitiveness in the global economy. S ã o Paulo: Atlas.
- [29] Morgan., Hunt, S. (1994). The commitment- trust theory of relationship maketing. Journal of Marketing. 3 Ed, Vol. 58 , pp. 20-38.
- [30] Morrow. B. (1999). Identifying and mapping community vulnerability disasters . Ed 23, Vol. 1.
- [31] Naisbitt. J. (1998). Macrotend is stances - Ten new guides tio . Es that transform our lives (E. Presen ç a, Ed.)
- [32] Park. S., UNGSON. . G. (2001) interfirm rivalry and managerial complexity: the conceptual framework of alliance failure . Organization science. Vol. 12.
- [33] Powel. W., Koput. K. Smith. D. (1996). Interorganizational collaboration and the locus of innovation: Networks mp learning in biotechnology . Administrative Science Quarterly. (Vol. 41)
- [34] Root. . F. (1988) Some taxonomies of international cooperation arrangements In: Contractor, FJ, Lorange P. (eds) Cooperative strategies in international business: join ventures and technology partnerships between Firms. New York: Lexington Books.
- [35] Rowden. . R. (2001) Research note: How a small business enters the international market . Vol. 43.
- [36] Schimitt Neto., Cesar. J. (2005). The process of internationalizing tio the firms under an optical contextualist: a case study cer â mica Portobello.
- [37] Teixeira. S., said. H. (2005). Strategy is gies internationalized tio the. Publisher touch Lisbon .
- [38] Uzzi. . B. (1997) Social structure in interfirm networks: The paradox ob embeddedness . Administrative Science Quarterly. Ed 42
- [39] Williamson. . O. (1985) The economic Institutions of Capitalism. New York: Free pass.
- [40] Zaher, Gulati, Nohria (2000). Strategic Networks . Strategic Management Journal, 21